Universidade do Minho
Escola de Engenharia

Carla Andreia Freixo Portela

In vivo metabolic pathway analysis of *Enterococcus faecalis* for uncovering key pathogenicity factors

November 2013

In vivo metabolic pathway analysis of *Enterococcus faecalis* for uncovering key pathogenicity factors
Carla Andreia Freixo Portela
UMinho | 2013

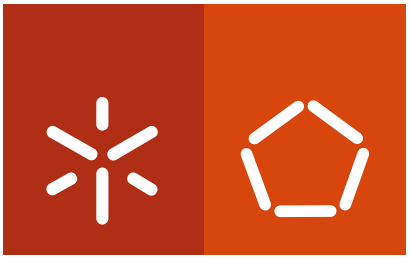

Universidade do Minho
Escola de Engenharia

Carla Andreia Freixo Portela

In vivo metabolic pathway analysis of *Enterococcus faecalis* for uncovering key pathogenicity factors

Doctoral Dissertation for PhD degree in Chemical and Biological Engineering

Supervisors of the thesis:
Eugénio Manuel de Faria Campos Ferreira
Isabel Cristina de Almeida Pereira da Rocha
Silas Granato Villas-Boas

November 2013

Autor: Carla Andreia Freixo Portela

E-mail: portela.carla@deb.uminho.pt / portela.carla@gmail.com

Título da tese:

***In vivo* metabolic pathway analysis of *Enterococcus faecalis* for uncovering key pathogenicity factors**

Orientadores:

Doutor Eugénio Manuel de Faria Campos Ferreira

Doutora Isabel Cristina de Almeida Pereira da Rocha

Doutor Silas Granato Villas-Boas

Ano de conclusão: 2013

Doutoramento em Engenharia Química e Biológica

Universidade do Minho, 15 de Novembro de 2013


DO YOU HAVE AN IDEA FOR YOUR PROJECT YET?
NO, I'M WAITING FOR INSPIRATION.
YOU CAN'T JUST TURN ON CREATIVITY LIKE A FAUCET. YOU HAVE TO BE IN THE RIGHT MOOD.
WHAT MOOD IS THAT?
LAST-MINUTE PANIC.

Acknowledgments

This is probably the longest acknowledgements ever wrote, so please be patient, it does get interesting. First, I would like to thank my supervisors and co-supervisor for their support during this very long and exhausting journey. To Prof. Dr. Eugénio Ferreira, for the wisdom that only a long and brilliant professional career could offer, to Prof. Dr. Isabel Rocha, not only for her exceptional scientific intellect but also for being an inspiration for all women in science and finally to Prof. Dr. Silas Villas-Bôas for the warm welcome in New Zealand, the support and motivation and excellent academic background.

Next, I would like to thank to all my co-workers from New Zealand. In particular to Dung Nguyen for her help in data analysis, Francesca Casu for her help with my samples after I was gone, to Sergey Tumanov for fatty acid analysis and Leandro Ladvanszky for helping me with sample derivatisation. To Farhana Pinu for never let me starve and always save the lab "hairy" situations with her wisdom and to Raphael Aggio, for his help with the model and data analysis. To Tim Liu, the other "*faecalis*" guy, for the interesting discussions and his help setting up the fermenters. To Michael Yap for his help in the lab and for being my badminton buddy. To Morgan Han for simply being the person that always admires whatever you do. To me dearest friends Fathima Iftikar, Francesca Casu, Indika Koggalahewa, Kris Montrose, Rita Malcata for being my family in New Zealand. You were truly special during this journey.

To all my co-workers in Portugal for the great lab environment and for supporting me especially during this last year. To Ana Alão, André Sousa, Daniela Correia, Hugo Costa, Joana Xavier, João Saraiva, Óscar Dias, Pedro Barbosa, Rafael Pereira, Rui Pereira, Sónia Carneiro, Sophia Santos and Tiago Resende. On a particular note, to Daniel "Lagares" Gomes, for that constant silliness inspiration, to Pedro Barbosa for the everyday grumpy answers that made me learn how grumpiness is sometimes disguised of kindness and to Tiago Resende for showing me all the websites that will surely distract you from work but will always teach you something new and you never know when it might come handy, right?

A special thank to Cristiana Faria, Daniel "Cenouria" Machado, Paulo Vilaça, Sara Correia and Simão Soares for being brilliant co-workers but also amazing friends whose support to my project was endless. Your friendship, the long talks about all and about nothing, the late night (horrible) pizzas at work, the super fancy R scripts, the formatting and editing and re-formatting with freshly baked bread at 4 a.m made those crazy late working nights memorable. Thank you.

To all my other friends who have heard me whining non-stop for this last year. Ana Catarina Castro, Bárbara Lourenço, Bruno Fernandes, Gustavo André, João Marco, Marlene Lopes, Paula Ferraz, Paula Ribeiro, Rita Torres, Tânia Miranda, my indoor soccer team friends from "ladies DEB" and "Maria da Fonte" and my squash buddy Héctor Ruiz. Your friendship is a blessing.

To Cristiana Castro, with whom, for the last year and half, I have shared a common goal: to finish the PhD thesis. I can truly say that finishing this thesis without going totally insane was only possible because we were together in this "sinking boat". Thank you for the week after week after week of late working nights, the scientific discussions, the support in R programming, the "laughing-so-we-don't-cry" moments, the photo shooting that should be considered street art, the pancake breaks and the healthy diet milkshakes. You are also responsible for me being able to hand in this thesis. And maybe, Luna (the cat!) has also contributed for both of us being able to finish it with some sanity. HURRAY!

Finally, I would like to thank my family for being there supporting me even if they did not understand why I was working so hard. You are my safe harbour where I can always return for support.

To do a PhD project demands a lot of effort and some sacrifices', but it is also the only moment of our lives where we are free to learn and create. To finish something so big like a PhD was one of the toughest challenges of my life.

Therefore, I would like to dedicate this thesis to my beloved mother who despite not being among us anymore, I am sure would be proud of me. I love you and I miss you.

The work presented in this thesis was only possible thanks to the finantial support from different entities. In particular from the research grant SFRH/BD/47016/2008 financed by FCT (fundação para a Ciência e a Tecnologia).

ABSTRACT

In spite of the increasing progress in the fight against prokaryotic pathogens, numerous bacteria play a significant concern for human health. Most of the current knowledge has been on isolated biochemical reactions or pathways exposed to a potential stress likely to be encountered in the host. Enterococci are equipped with a variety of intrinsic (i.e., naturally occurring) antibiotic resistances, but are also capable of acquiring new resistance genes and / or mutations.

The present thesis aimed to gather knowledge on the pathogenic bacterium *Enterocccus faecalis* using genomics and post-genomics technologies and continuous culture techniques to study the behaviour of the complete biological system (bacterial cell) *in vivo* under different environmental perturbations.

The knowledge obtained, together with the annotated genome sequence of *E. faecalis* was used to develop the first genome-scale mathematical model that will hopefully serve as a valuable tool to explore the metabolism of the organism and help unravel hidden metabolic pathways essential for bacterial growth and survival.

The experiments carried out allowed testing two *Enterococcus faecalis* strains against the oxidative stress imposed in the form of oxygen and hydrogen peroxide while varying the dilution rate. The first line defence was observed to be a shift in the glycolytic pathway, the pentose phosphate pathway and glutathione production while the downstream response was imposed on the fatty acid metabolism and demethylmenaquinone biosynthesis.

The first genome-scale reconstruction of this organism involved a pipeline of extremely laborious tasks that comprised the assembly of all the metabolic reactions encoded on the annotated genome sequence, the manual curation of the information collected and the refinement of the network to allow the model to simulate and further test the capabilities of the network. This model aimed to predict *in silico*, the capabilities expressed by this organism *in vivo*. Indeed, the simulations carried out were able to accurately predict the qualitative behaviour of this organism evidenced by the metabolic

distribution shift observed in the simulations of homolactic and heterolactic metabolism or under aerobic and anaerobic environment.

RESUMO

Apesar do crescente progresso na luta contra agentes patogénicos, são inúmeras as bactérias que desempenham um papel significativo na saúde humana. O atual conhecimento tem sido obtido através da análise de reações bioquímicas isoladas ou das vias expostas a uma condição de estresse passível de ser encontrada no hospedeiro. O género enterococos está intrinsecamente equipado com uma grande variedade de resistências a antibióticos, mas é igualmente capaz de adquirir novos genes de resistência e / ou mutações

A presente tese teve como objetivo explorar o metabolismo do patogénico *Enterococcus faecalis*, utilizando para o efeito tecnologias na área da genómica e pós-genómica acopladas a técnicas de cultura contínua para estudar o comportamento do sistema biológico completo (célula bacteriana) *in vivo* sujeito a diferentes perturbações. O conhecimento obtido, juntamente com o recurso à sequência anotada do genoma da *E. faecalis* permitiu desenvolver o primeiro modelo à escala genómica que pretende ser uma ferramenta valiosa para explorar o metabolismo do organismo e ajudar a revelar novas vias metabólicas essenciais para o crescimento bacteriano e a sua sobrevivência.

As experiências levadas a cabo com duas estirpes de *Enterococcus faecalis* analisaram a resposta metabólica ao estresse oxidativo, aplicada sob a forma de oxigénio e de peróxido de hidrogénio conjuntamente com uma variação da taxa de diluição. Observou-se que a primeira linha de defesa em resposta ao estresse foi uma mudança na via glicolítica, a via das pentoses fosfato e da produção de glutationa, enquanto a resposta a jusante foi imposta sobre o metabolismo dos ácidos gordos e biossíntese de demetilmenaquinona.

A reconstrução do primeiro modelo à escala genómica deste organismo envolveu tarefas laboriosas e complexas num processo iterativo. Todas as reações metabólicas codificadas na sequência genómica foram recolhidas, seguida da sua curação manual e posterior refinamento da rede para obter um modelo simulável capaz de testar as capacidades da rede. Este modelo pretende prever *in silico* as capacidades expressas *in vivo* por este organismo. As simulações realizadas foram capazes de prever com

precisão o comportamento qualitativo deste organismo evidenciando uma distribuição metabólica característica de um metabolismo homolático e heterolático ou em ambiente aeróbio e anaeróbio.

INDICE

1 Motivation and outline 1

1.1 Thesis Motivation 3

1.2 Thesis Outline 4

1.3 References 6

2 State of the art 7

2.1 Gut Microbiota 9

2.2 Enterococcus faecalis 13

2.2.1 Physiology of *E. faecalis* 15

2.2.2 Antibiotic resistance in *E. faecalis* 22

2.2.3 Oxidative stress in *E. faecalis* 23

2.3 Systems Biology 27

2.3.1 integration of SB within the pathogenic bacterial panorama 28

2.4 Genome scale metabolic network reconstruction 35

2.5 Model Validation 39

2.5.1 Continuous culture 39

2.5.2 Metabolomics 40

2.5.3 Metabolomics and pathogens 51

2.5.4 Fluxomics 53

2.6 References 55

3 A metabolomics analysis of *Enterococcus faecalis* response to oxidative stress – the effect of hydrogen peroxide, oxygen and dilution rate 69

3.1 Introduction 71

3.2 Material and methods 74

3.2.1 Chemicals 74
3.2.2 Bacterial strain and culture conditions 74
3.2.3 Experimental design 74
3.2.4 Fermentation 75
3.2.5 Sampling and extraction procedure for intracellular metabolite analysis 76
3.2.6 Extracellular metabolite analysis 77
3.2.7 Hydrolysis of protein biomass for amino acid composition analysis 77
3.2.8 Chemical derivatisation of metabolites and GC-MS analysis 78
3.2.9 Metabolite identification and data analysis 78
3.2.10 ^{13}C-labelling distribution analysis 79
3.3 Results 79
3.3.1 Multivariate analysis 79
3.3.2 Intracellular metabolomics 87
3.3.3 Extracellular metabolomics 92
3.3.4 ^{13}C labelling experiments 100
3.4 Discussion 105
3.4.1 overall impact observed from the multivariate analysis 105
3.4.2 Metabolic response of *E. faecalis* to H_2O_2 106
3.4.3 Metabolic response of *E. faecalis* to O_2 109
3.4.4 Metabolic response of *E. faecalis* to the dilution rate 111
3.5 Conclusions 112
3.6 References 115
4 The global metabolic response of a vancomycin-resistant *Enterococcus faecalis* strain to oxygen 119
4.1 Introduction 121
4.2 Material and Methods 122

4.2.1 Chemicals 122
4.2.2 Bacterial strain and culture conditions 122
4.2.3 Sampling and extraction procedure for intracellular metabolite analysis 124
4.2.4 Extracellular metabolite analysis 124
4.2.5 Hydrolysis of protein biomass for amino acid composition analysis 125
4.2.6 Chemical derivatisation of metabolites and GC-MS analysis 125
4.2.7 Acetate quantification 125
4.2.8 Demethylmenaquinone extraction and quantification 125
4.2.9 Fatty acid composition of cell envelopes 126
4.2.10 Metabolite identification and data analysis 126
4.2.11 ^{13}C-labelling distribution analysis 127
4.3 Results 127
4.3.1 Growth of *E. faecalis* in continuous culture 127
4.3.2 Metabolite profile during the transition between anaerobic and aerobic growth conditions 128
4.3.3 Metabolite profiles at steady-state 129
4.3.4 Response of metabolic pathways to oxygen tension 131
4.3.5 ^{13}C-labelled distribution 133
4.3.6 Demethylmenaquinone levels in *E. faecalis* membrane 135
4.3.7 Fatty acid composition of *E. faecalis* cells 135
4.4 Discussion 137
4.4.1 Sulphur + glutathione metabolism 139
4.4.2 Increased glycolytic flux 140
4.4.3 Benzoate metabolism 141
4.4.4 Fatty acid metabolism 143

4.5 Conclusions 144
4.6 References 146
5 Genome scale metabolic model reconstruction of *Enterococcus faecalis* V583 .. 151
5.1 Introduction 153
5.2 Methodology 155
5.2.1 Network reconstruction 155
5.3 Results 159
5.3.1 Basic network characteristics 159
5.3.2 Substrate utilisation 162
5.3.3 Amino Acids requirements 163
5.3.4 Prediction of physiological parameters 166
5.3.5 Modelling the shift from homolactic to heterolactic fermentation 172
5.3.6 Modelling the shift from anaerobic to aerobic environment 177
5.3.7 Essentiality analysis 180
5.4 Conclusions 180
5.5 References 184
6 General Conclusions and Future work 187
Scientific Output 193
Supplementary material 195

LIST OF FIGURES

Figure 2.2. Intestinal flora composition. Variation of bacterial numbers across the length of the GI tract and across the different intestine layers. 11

Figure 2.3. Fermentation pathways of glucose by lactic acid bacteria 16

Figure 2.4. Pyruvate metabolism.. 18

Figure 2.5. Schematic model of the adapted respiratory chain of *E. faecalis* 21

Figure 2.6. Mechanism of oxidative damage of an iron sulphur-cluster by $O_2^{\cdot -}$. 24

Figure 2.7. Iterative process for metabolic network reconstruction. 37

Figure 2.8. Schematic representation of a toy cell where reactions of degradation and production of compounds occur simultaneously. 38

Figure 2.9. Representation of the mass balances under steady-state in a matrix format. 39

Figure 2.10. General steps for metabolomics sample preparation. 42

Figure 2.11. GC-MS components for the metabolome analysis. 51

Figure 2.12. Central carbon metabolism and biosynthesis of amino acids. 54

Figure 3.1. Peptidoglycan structure and mechanism of action of vancomycin 73

Figure 3.2. Overview of the experimental design. Continuous culture was defined by two variables: aeration and dilution rate. 75

Figure 3.3. Biplot principal component analysis of the intracellular metabolites dataset 80

Figure 3.4. Biplot principal component analysis of the extracellular metabolites dataset. 83

Figure 3.5. Hierarchical cluster (hclust) of the intracellular dataset with a cut-off of 0.8 and a cut tree of 5 clusters. 84

Figure 3.6. Hierarchical cluster (hclust) of the extracellular dataset with a cut-off of 0.8 and a cut tree of 5 clusters. 86

Figure 3.7. Intracellular response of *E. faecalis* to H_2O_2. 89

Figure 3.8. Intracellular response of *E. faecalis* to O_2. 90

Figure 3.9. Intracellular response of *E. faecalis* to the dilution rate. 91

Figure 3.10. Extracellular response of *E. faecalis* to H_2O_2. 94

Figure 3.11. Extracellular response of *E. faecalis* to O_2. 97

Figure 3.12. Extracellular response of *E. faecalis* to the dilution rate.. 99

Figure 3.13 Fraction of ^{13}C-labelling in amino acids derived from hydrolysed biomass in each of the conditions analysed.....101

Figure 3.14. Tracking of ^{13}C atom from U-^{13}C glucose to ^{13}C-lactate through glycolysis 103

Figure 3.15 Isotope labelling patterns of lactic acid when grown under anaerobic conditions and high dilution rate. 104

Figure 3.16 Isotope labelling patterns of lactic acid when grown under a high dilution rate in the absence of H_2O_2 treatment.. 104

Figure 4.1. Changes in metabolite levels over time during transition from anaerobic-to-aerobic steady-states.....128

Figure 4.2. Extracellular metabolite levels of *E. faecalis* cultures grown under anaerobic and aerobic conditions.....130

Figure 4.3. Intracellular metabolite levels of *E. faecalis* cells detected at significant different levels (p<0.05) when comparing anaerobic and aerobic growth conditions.. 131

Figure 4.4. Pathway activity profiling (PAPi) analysis based on extracellular metabolite data from *E. faecalis* grown under different environmental conditions (anaerobic and aerobic).....132

Figure 4.5. Pathway activity profiling (PAPi) analysis based on intracellular metabolite data from *E. faecalis* grown under different environmental conditions (anaerobic and aerobic).....133

Figure 4.6. Isotope labelling patterns of A – lactate, B – glutamate, C – pyroglutamate, D – glycine.. 134

Figure 4.7. Membrane fatty acid composition of *E. faecalis* cells grown under different environment conditions. 136

Figure 4.8. Overall metabolic response of *E. faecalis* to oxygen.....138

Figure 5.1. Venn diagram where the intersection of information available in the KEGG database and the significant information added to the model is depicted. 160

Figure 5.2. Arginine deiminase pathway. 171

Figure 5.3. Effect of increased glucose concentration on the metabolism of *E. faecalis*. 175

LIST OF TABLES

Table 2.1. Proteins involved in the oxidative stress of *E. faecalis*. 25

Table 2.2. Genome-scale models published by the Systems Biology Research Group at the University of California for pathogenic or related bacteria [101]. 30

Table 2.3. Main applications of GEM of important pathogenic or related bacteria. 32

Table 2.4. Quenching protocols published for several bacteria and *S. cerevisae* 45

Table 2.5. Compilation of extraction methods depending on the metabolites of interest 48

Table 5.1. Basic network properties of *E. faecalis'* genome-scale model 160

Table 5.2. Different sources of information and confidence levels to support the inclusion of the reactions in the metabolic network. 161

Table 5.3. Essential amino acids for each strain tested in different published studies and *in silico* simulation. 164

Table 5.4 – Simulation A. Minimal medium and the phenotypic response of *E. faecalis*.. 166

Table 5.5. Simulation B. Chemically defined medium and the phenotypic response of *E. faecalis*. 168

Table 5.6. Simulation C. Fitting of the specific growth rate and the phenotypic response of *E. faecalis*. 170

Table 5.7. Simulation D. Homolactic fermentation. 173

Table 5.8. Reactions involved in the adapted respiratory system of *E. faecalis* 177

Table 5.9. Simulation E. The effect of oxygen in the phenotypic response of *E. faecalis*.. 178

Table 5.10. *In silico* prediction of essential reactions for model viability in terms of the pathways involved. 180

Table 5.11 Growth yields of each end product for *E. faecalis* in each of the conditions analysed. 181

ABBREVIATIONS

Abbreviations of the International System of Units (SI), SI derived units, and standard notations for chemical elements and IUPAC amino acids codes are used in this thesis. Other abbreviations used in the text are defined below.

1,3BPG	glycerate 1,3-biphosphate
2PG	glycerate 2-phosphate
3PG	glycerate 3-phosphate
6PG	6-phosphogluconate
AHF	aerobic, high dilution rate, H_2O_2 negative
AHS	aerobic, high dilution rate, H_2O_2 positive
AMDIS	automated mass spectral deconvolution and identification system
AMP	adenosine monophosphate
AnHF	anaerobic, high dilution rate, H_2O_2 negative
AnHS	anaerobic, high dilution rate, H_2O_2 positive
AnLF	anaerobic, low dilution rate, H_2O_2 negative
AnLS	anaerobic, low dilution rate, H_2O_2 positive
ATP	adenosine triphosphate
CAP	community-acquired pneumonia
CBS	centraalbureau voor schimmelcultures
CR	catabolite repression
CuZnSOD	copper-zinc superoxide dismutase
DHAP	dihydroxyacetone-phosphate
DMK	demethylmenaquinone
DMKH2	demethylmenaquinol
DNA	deoxyribonucleic acid

DNS	3,5-dinitrosalicylic acid
DO	dissolve oxygen
EDTA	ethylenediaminetetraacetic acid
EI	electron ionisation
ETC	electron transport chain
FBA	flux balance analysis
FBP	fructose-1,6-diphosphate
FeSOD	iron superoxide dismutase
GAP	glyceraldehyde-3-phosphate
GC-MS	gas chromatography-mass spectrometry
GEM	genome-scale model
GENRE	genome-scale network reconstruction
GI	gastro-intestinal
GSH	glutathione
GSSH	glutathione disulfide
HDR	high dilution rate
HO^-	hydroxyl radical
ICE	integrative conjugative element
KDPG	2-keto-3-deoxy-6-phosphogluconate
KEGG	kyoto encyclopedia of genes and genomes
LDH	lactate dehydrogenase
LDR	low dilution rate
m/z	mass to charge ratios
MCF	methyl chloroformate
MnSOD	manganese superoxide dismutase
NADH	nicotinamide adenine dinucleotide
NADPH	nicotinamide adenine dinucleotide phosphate

NCBI	national center for biotechnology information
NMR	nuclear magnetic resonance
O_2^-	superoxide
OD	optical density
ORF	open reading frame
PAI	pathogenicity island
PAPi	pathway activity profiling
PCA	principal component analysis
PEP	phosphoenolpyruvate
PFL	pyruvate formate lyase
PTS	phosphotransferase system
RNA	ribonucleic acid
ROS	reactive oxygen species
rpm	revolutions per minute
SB	systems biology
SEM	standard error of the mean
SOD	superoxide dismutase
SODA	manganese superoxide dismutase
SODB	iron superoxide dismutase
SODC	copper-zinc superoxide dismutase
TCA	tricarboxylic acid
TOF	time-of-flight
TPA	tryptone phosphate agar
v/v	volume by volume
VRE	vancomycin resistant enterococci
w/v	weight by volume
w/w	weight by weight

CHAPTER 1

MOTIVATION AND OUTLINE

ABSTRACT

This chapter introduces the aim of this PhD project. To understand the metabolism of an opportunistic pathogen such as *Enterococcus faecalis* and its mechanisms of action to cope with oxidative stress is of paramount importance, as this organism is responsible for several diseases in the medical field. From bacteraemia, surgical wound infections, urinary tract infections, and endocarditis, enterococci are intrinsically resistant and have the extraordinary ability to acquire resistance to many useful clinical antimicrobials. In this chapter a more detailed motivation for the study conducted with this organism is provided, together with the main objectives. We also outline the thesis chapters in order to provide a clear layout of the project.

1.1 *THESIS MOTIVATION*

Enterococci are versatile Gram-positive, lactic acid producing bacteria that can survive under harsh conditions. Enterococcal infections are predominantly caused by *Enterococcus faecalis*. Over the past two decades, the proportion of *E. faecalis* infections has steadily increased. Vancomycin resistant enterococci (VRE) gained a particular interest in the field as vancomycin has been considered a last resort antibiotic. High-level vancomycin resistance is particularly problematic as it often appears in strains already highly resistant to ampicillin. The incidence of VRE in Europe was mainly a consequence of the use of glycopeptides, including avoparcin as a food additive for growth promotion in farm animals which was subsequently banned by the European Union. In North America, VRE followed Europe but due to multiple epidemics of VRE infection that have been described in diverse hospital settings [1,2]. The use of multiple antibiotics gave raise to increased multi-resistant strains.

Although various bactericidal antibiotics have different cellular targets, recent studies have demonstrated that the mechanism of action of antibiotics is similar to the stress imposed by oxidative stress. The ability of enterococci to cope with oxidative stress is important in their transmission capacity and the likelihood of exchanging genetic material with other pathogens. Hence, the aim of this study was to generate knowledge on the *in vivo* metabolism of VRE strains and determine how the bacterial cell responds to switches between aerobic and anaerobic conditions, as well as in the presence and absence of hydrogen peroxide. The information gathered from *in vivo* experiments supported the reconstruction of the first genome-scale metabolic model of *E. faecalis*.

To understand biology at the system-level, it is mandatory to analyse the structure and the dynamics of the cellular functions, rather than the characteristics of isolated parts of a cell or organism. Systems biology aims to fill that gap by allowing the interaction between biological systems and computational tools [3]. Mathematical modelling and network reconstructions are increasingly gaining more importance due to the possibility offered in understanding high-throughput experimental data and the metabolism of the organism of study. There is nowadays a golden opportunity for system-level analysis to be grounded in a molecular-level understanding, resulting in a continuous spectrum of

knowledge [3]. The prospect of understanding massive amounts of biological data using mathematical models to describe a system and its response to external perturbations is extremely appealing and could allow researchers to answer a new level of questions.

Ultimately, this project aims to facilitate the identification of new metabolic targets for the development of new antibacterial drugs

1.2 *THESIS OUTLINE*

The main goals of this thesis were to understand how oxidative stress influences and changes the metabolism of *Enterococcus faecalis* using metabolomics approaches and to develop a genome-scale model reconstruction that could mimic the metabolic behaviour of the organism. Finally, the integration of the information generated *in vivo* from metabolomic data with *in silico* simulations was also foreseen. For that, the main tasks carried out comprised:

- Oxidative stress experiments:
    - Chemostat experiments with different dilution rates
    - Switch from anaerobic to aerobic environment
    - Introduction of hydrogen peroxide
    - Metabolomic techniques (quenching, extraction, derivatisation)
    - Carbon labelled experiments
    - Data analysis and interpretation

- Genome-scale network reconstruction
    - Collection of literature info
    - Annotation evaluation and validation
    - Manual curation of the reactions and pathways
    - Analysis of the network
    - Gap filling
    - Connectivity of the network to an objective function
    - Test the capabilities and robustness of the network

- Combining experimental data with genome scale model
    - Data interpretation
    - Simulations

Based on the main objectives, this thesis was organized in 6 chapters. Chapter 2 gives an overview of the state of the art of *E. faecalis* as a member of the lactic acid bacteria group whose natural environment is the human microbiota; the effect of oxidative stress and increasing antibiotic resistance; *E. faecalis* metabolism under different environmental conditions; the state of the art of metabolomics and different metabolomic techniques, and finally the state of the art of genome-scale reconstructions.

Chapters 3 presents a study that aimed to understand how different forms of oxidative stress (in the form of hydrogen peroxide and oxygen) can influence the metabolism of *E. faecalis*, while also submitted to different growth rates, which could by itself act as a form of stress.

Chapter 4 on the other hand, focuses on the oxidative stress in the form of oxygen and its effects on a strain resistant to vancomycin and grown under the presence of the antibiotic. The main goal was to analyse if the metabolic response of a resistant strain is similar to a sensitive strain and understand if vancomycin originates an oxidative stress response as postulated or if its mode of action relies solely on the inhibition of the cell wall synthesis.

Chapter 5 presents the reconstruction of the first genome-scale metabolic model of *E. faecalis* while combining some valuable data obtained from the previous chapters. This model hopes to be used to elucidate the metabolism of *Enterococcus faecalis* V583 and serve as a valuable tool to further explore new interesting targets to design more efficient drugs.

Chapter 6 presents the overall conclusions, recommendations and future work.

1.3 *REFERENCES*

1. Rubinstein, E. & Keynan, Y. Vancomycin-Resistant Enterococci. *Crit. Care Clin.* **29,** 841–852 (2013).

2. Cetinkaya, Y., Falk, P. & Mayhall, C. G. Vancomycin-Resistant Enterococci. *Clin. Microbiol. Rev.* **13,** 686–707 (2000).

3. Kitano, H. Systems biology: a brief overview. *Science* **295,** 1662–4 (2002).

CHAPTER 2

STATE OF THE ART

ABSTRACT

Enterococcus faecalis is a gram positive commensal bacterium, from the lactic acid bacteria group that colonises the gut of humans and mammals. Once known only as a prominent constituent of the human microbiome and a popular agent used in industrial fermentation processes, it is nowadays seen as an important opportunistic pathogen, particularly in the nosocomial context, due to its proficient acquisition of resistance to a large repertoire of antibiotics. Understanding how this bacterium responds to oxidative stress is paramount in gaining insights into its pathology; as the tolerance to oxidative stress plays a vital role in its survival under oxygen-rich environments and in the presence of bactericidal antibiotics. Here we revise the main aspects regarding *E. faecalis'* natural environment and its role on the human microbiota. An overview of its metabolism and physiology is explored, as well as their link towards the stress caused by antibiotics and oxidative stress. The growing field of systems biology is also addressed in this chapter with a review over the process of genome scale reconstruction, the application of these models in pathogenic bacteria and also the role of metabolomics techniques in uncovering physiological behaviour, discovering new metabolites or yet unknown pathways essential for the improvement of genome scale reconstructions.

2.1 *GUT MICROBIOTA*

The human microbiome contains a broad spectrum of microorganisms in a mutualistic relationship that guarantees the survival of the bacteria and the human well-being. Nevertheless, the disturbance of this delicate balance can cause many bacterial infections.

The human intestinal habitat contains 300 to 500 different species of bacteria and the number of microbial cells within the gut lumen is about 10 times larger than the number of eukaryotic cells in the human body [1].

In order to better understand and control diseases, it is necessary to understand the bacteria-bacteria and the bacteria-host interactions that occur in the human gut.

It is generally assumed that humans are born with a sterile gut. However, recent studies suggest that the colonization of the gastrointestinal tract may start before birth as some studies have demonstrated the presence of microbes in the amniotic fluid with no evidence of rupture of the membrane [2]. The abundance of oxygen in the neonatal gut limits the expansion of anaerobes and reduces the colonization to facultative and aerotolerant bacteria. When facultative anaerobic bacteria populations expand, they consume oxygen, creating an anaerobic environment adequate to the growth of obligate anaerobes [3].

In a mature adult gut, the prevailing divisions that constitute the intestinal flora are the Firmicutes and *Bacteroides*. Each one of them represents approximately 30% of the bacteria present in our faeces and the mucus overlying the intestinal epithelium. Proteobacteria are also common but usually not dominant [4].

However, the distribution of the microbiota throughout the Gastro-Intestinal (GI) tract is not homogeneous. In the stomach and duodenum the number of bacteria varies from 10^1 to 10^3 cells/gram, progressing to 10^4 to 10^7 cells/gram in the jejunum and ileum and reaching its highest value in the colon with values up to 10^{12} cells/gram [5,6] (Figure 2.1). The upper tract has lower bacterial densities due to the fact that the acids, bile and pancreatic secretions present in this organ are toxic for many microorganisms.

Additionally, the microbial composition varies between these sites. Frank *et al.* (2007) have compared different biopsy samples of the small intestine and colon from healthy individuals and observed different bacterial groups in the different areas. In this study, the small intestine was predominantly populated by the Bacilli class of the Firmicutes and Actinobacteria while Bacteroidetes and the Lachnospiraceae family of the Firmicutes were more prevalent in samples from the colon [7]. In addition to the heterogeneity displayed along the intestinal microbiota, there is also a great radial variation in the microbiota composition of the intestine. The mucus layer separates the epithelium surface from the lumen [8] and the microbiota present in each of these areas differs significantly. Species present in the intestinal lumen do not access the mucus layer and epithelial crypts. For instance, *Bacteroides, Bifidobacterium, Streptococcus*, members of Enterobacteriaceae, *Enterococcus, Clostridium, Lactobacillus,* and *Ruminococcus* were all found in faeces, whereas only *Clostridium*, *Lactobacillus*, and *Enterococcus* were detected in the mucus layer and epithelial crypts of the small intestine [8].

Metabolic functions and barrier protection

Metabolic functions of the gut microbiota include the production of different vitamins, amino acids and bile acid biotransformation, which have important implications in terms of glucose and cholesterol metabolism [9].

Another important metabolic role occurs throughout the fermentation process, where short-chain fatty acids (SCFA) and gases are produced as a consequence of the bacterial metabolism. The major short-chain fatty acids produced are acetate, butyrate, and propionate. Wong *et al.* (2006) have demonstrated that acetate is the main SCFA in the colon, and is involved in cholesterol synthesis, while propionate supplementation in the diet was shown to reduce cholesterol levels *in vivo*. Butyrate has been studied for its role in nourishing the colonic mucosa and in the prevention of colon cancer. Clinical trials have yet to confirm these data, but there are strong evidences that the metabolic activities driven by gut microbiota are important for the host metabolism [10].

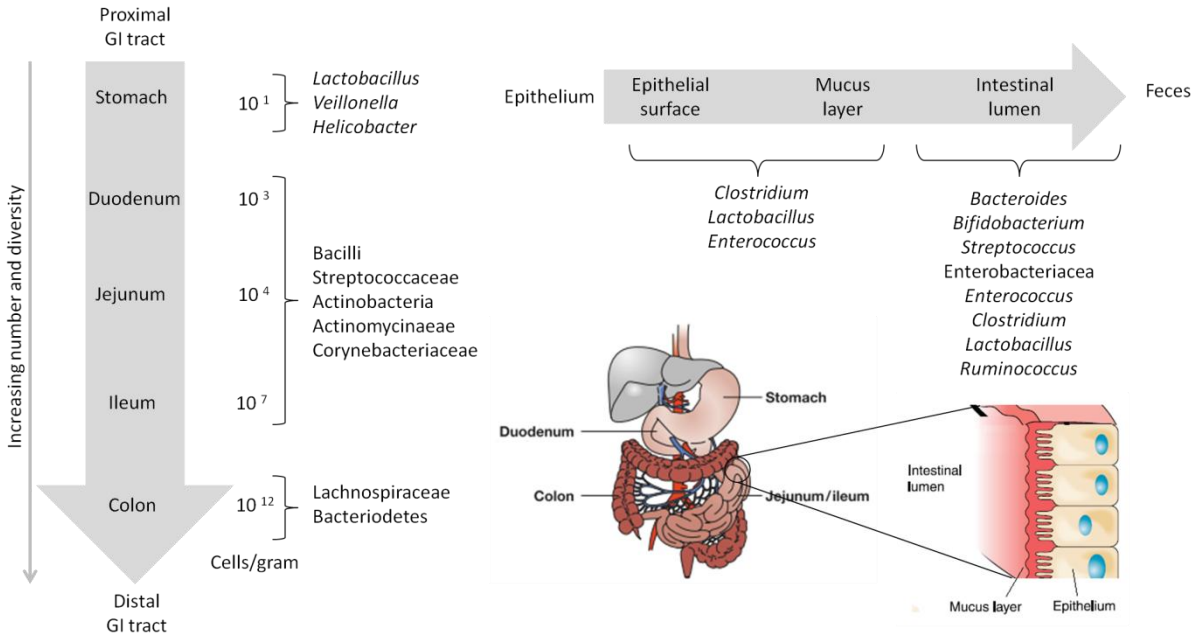

Figure 2.1. Intestinal flora composition. Variation of bacterial numbers across the length of the GI tract and across the different intestine layers. Adapted from work from Sekirov *et al.* (2010) [11].

The gut microbiota also play a role in protecting the host, as commensal organisms create a physical barrier to incoming pathogens by competing for attachment sites, consumption of nutrients and also through the production and secretion of antimicrobials. Those mechanisms are relevant to reduce the level of lipopolysaccharides, peptidoglycans and superantigens, which decreases the risk of infection [12,13]. Therefore, commensal bacteria of the gastrointestinal tract play an active role in the development and maintenance of a strong immune system [12].

Auto-immune and allergic diseases

Although the intestinal microbiome acts in synergy with the host to maintain homeostasis, many factors can alter the gastrointestinal ecosystem, including antibiotics, stress, dietary changes, among others. These alterations may lead to a change in the composition of the microbiota or a modification in the bacterial metabolic activity, named Dysbiosis [14]. Unbalanced intestinal flora may have some consequences, as described next.

An autoimmune disease arises when the immune system targets healthy cells and tissues as strange agents and attacks them. That is the case of type 1 diabetes mellitus, celiac disease, and inflammatory bowel diseases. Most often, the immune response is initiated by unknown factors. Alteration of the gut microbiota as a result of modern lifestyles became an attractive hypothesis to explain the escalating number of patients with those conditions[15–19].

In the same line of study, correlations between the gut microbiota and the prevalence of allergies have been made [20,21]. A study reported that children who suffer from allergies were significantly less colonized with *Lactobacilli* and *Bifidobacteria* in comparison with non-allergic children [20]. Also, in a different study it was reported that the supplementation of prebiotics oligosaccharides was effective as a primary prevention of atopic dermatitis in infants [21].

Hence, it is possible to establish a correlation between the differential gut microbial communities and the development of allergies. Although these studies confirm the positive effect of a healthy microbiome, additional studies need to be made to fully characterise the balance within this mutualistic relation.

Metabolic diseases

The impact of the modulation of the gut microbiota on obese mice is well documented. It has been reported that mice genetically predisposed to develop obesity have a gut microflora richer in Firmicutes and Bacteroidetes [22].

Turnbaugh *et al.* (2009) have characterised the faecal microbial communities of obese and lean twins to address the changes in the microbiota. Obesity was associated with changes in microbiota, reduced bacterial diversity and altered representation of bacterial genes [23].

Moreover, Kalliomaki *et al.* (2008) have also determined that aberrant compositional development of the gut microbiota precedes overweight and that bifidobacterial numbers in faecal samples during infancy were lower in overweighed children, while the number of *S. aureus* colonies was higher [24].

Colorectal cancer

In the new industrialized world, cancer has become a huge scourge and a present element of our lives. Although important achievements have been made, it is still very difficult to cure cancer patients. Cancer cells can develop from the majority of body tissues and colorectal cancer is one of the most prevalent and represents the second most fatal malignancy after lung cancer [25].

Uronis *et al.* (2009) demonstrated how the manipulation of the intestinal microbiota alters the development of colitis-associated cancer along with a correlation of chronic colitis to colorectal tumour development [26].

In addition, colorectal cancer patients demonstrate decreased levels of *Eubacterium rectale* and *Faecalibacterium prausnitzii* and higher populations of *E. faecalis* in comparison with healthy individuals [27].

How do pathogens overcome in the microbiome?

Pathogenic bacteria can invade the gastrointestinal tract and infect the body, producing sepsis, shock, multisystem organ failure and death of the host. The mechanisms by which pathogens overcome obstacles to achieve a successful infection are uncertain [28]. Pathogenic infections might be facilitated by disruption of the intestinal ecosystem by environmental factors. A mechanism that explains how hosts' immune defences are triggered was elucidated using models of *C. rodentium* (mimicking diarrheal pathogen-associated inflammation) and *Campylobacter jejuni* infections, observing an overgrowth of Enterobacteriaceae, along with an increase of *E. faecalis*, indicating that inflammation induced by microbiota changes, supports colonization by aerotolerant bacteria. The inflammatory response, triggered by the invading pathogen, may function to enhance its colonization, further facilitating its virulence [29].

2.2 *ENTEROCOCCUS FAECALIS*

E. faecalis is a Gram-positive coccus, non-spore forming, non-motile and facultative anaerobe that belongs to the lactic acid bacteria (LAB) group. For a long time, *E.*

faecalis has been considered to be catalase negative because the organism is not able to synthesise haemin [30]. Haemin is a prosthetic group present in a variety of proteins, such as cytochromes and catalases. However, it was later observed that when haemin was supplied to the medium, synthesis of hemoproteins can take place [31].

The LAB clade in which e*nterococci* are grouped are identified by a low G+C content and are able to grow in a broad range of temperatures ranging from 5 to 60ºC [32].

Until 1984, *E. faecalis* and *E. faecium* were classified as *Streptococcus faecalis* and *Streptococcus faecium,* belonging to the *Streptococcus* genus, but new data collected from DNA-DNA hybridisation and 16S rRNA sequencing techniques revealed their close relation to the *Enterococcus* genus and were therefore classified as *E. faecalis* and *E. faecium* [33].

E. faecalis was once considered to be harmless to humans and with no medical relevance, but became a problem in the 70-80's as a leading cause for hospital-acquired infections, urinary tract infections, surgical wounds and other conditions [34]. Last available data comprising all web and hospital numbers on enterococcal infections, identified that 20.6% of the infections were caused by vancomycin resistant isolates and from those, 76% were from *E. faecalis* [34]. Another source of contamination by *enterococci* takes place when the meat is processed in slaughterhouses and no care is taken to separate the gastrointestinal tract of the animals (where *enterococci* live) from the rest of the body. This way, there is an increased risk of contamination of the meat that can play a role in the spread of *enterococci* virulent traits to humans [35,36]. In addition, *E. faecalis* plays a problematic role in endodontic diseases. Endodontics is the dental speciality focused on the study and treatment of the dental pulp. Although *E. faecalis* occurs in small proportions of the flora of untreated teeth [37], they have been found in 70% of the positive cultures of scrubs collected from the dental pulp [38].

Nevertheless, *enterococci* also play a positive role in many areas. Although its use is very controversial, some strains of the *Enterococcus* genus have been successfully used as probiotics, due to its ability to produce bacteriocins [32,39,40] and as enhancers of flavour and ripening of cheese [41].

2.2.1 PHYSIOLOGY OF *E. FAECALIS*

Due to its natural habitat, *E. faecalis* encodes pathways for the uptake of several different sugars, which is consistent with its transport capabilities. All *enterococci* are able to metabolise the following carbohydrates: D-glucose, D-fructose, D-mannose, ribose, galactose, N-acetyl-glucosamine, amygdalin, arbutin, salicin, cellobiose, maltose, lactose and β-gentiobiose. With exception of ribose, galactose, amygdalin and β-gentiobiose, those sugars are uptaken via the phosphotransferase system (PTS). In addition to that list, *E. faecalis* can also metabolise trehalose, mannitol, gluconate, D-glucosamine, N-acetyl-muramic acid, sorbitol, galactitol, L-ascorbate and sucrose via PTS [42]. The absence of a complete tricarboxylic acid (TCA) cycle suggests that energy production occurs mostly *via* glycolysis or the pentose phosphate [43].

During growth on glucose, *E. faecalis* is able to expel other sugars, an effect called inducer expulsion. In this process, sugars are dephosphorylated and then transported to the extracellular space to avoid their accumulation [44]. This process is achieved by catabolite repression (CR), the global control system used by *E. faecalis* to quickly adapt to a preferred carbon and energy source [45].

2.2.1.1 Sugar metabolism

Sugar degradation occurs mainly *via* the Embden-Meyerhof Parnas (Glycolysis) pathway with the final product being pyruvate (Figure 2.2). In short, glucose 6-phosphate is converted in fructose-1,6-diphosphate (FBP) at the expense of 2 mol of ATP, which is then split into dihydroxyacetone-phosphate (DHAP) and glyceraldehyde-3-phosphate (GAP). GAP (and DHAP *via* GAP) is further converted to pyruvate in a metabolic sequence including substrate-level phosphorylation [46]. The overall sums of the conversion yields 2 mol of ATP and 2 mol of NADH per mol of glucose consumed.

Sugar degradation may also occur *via* the Entner-Doudoroff pathway (Figure 2.2). In fact, *E. faecalis* is one of the few gram positive bacteria to be able to use this pathway. However, it plays a peripheral role in central metabolism as it is only induced by certain carbohydrates such as gluconate [47]. The Entner-Doudoroff pathway begins with the formation of glucose 6-phosphate, which is then converted to 6-phosphogluconate with NADPH formation. Next, 6-phosphogluconate is dehydrated to form 2-keto-3-deoxy-6-

phosphogluconate (KDPG), the key intermediate of the pathway. KDPG is then cleaved by KDPG aldolase to pyruvate and GAP. The GAP is converted to pyruvate in the Embden-Meyerhof pathway and the energetic balance is: 1 mol ATP, 1 mol NADH and 1 mol NADPH per glucose metabolised [48]

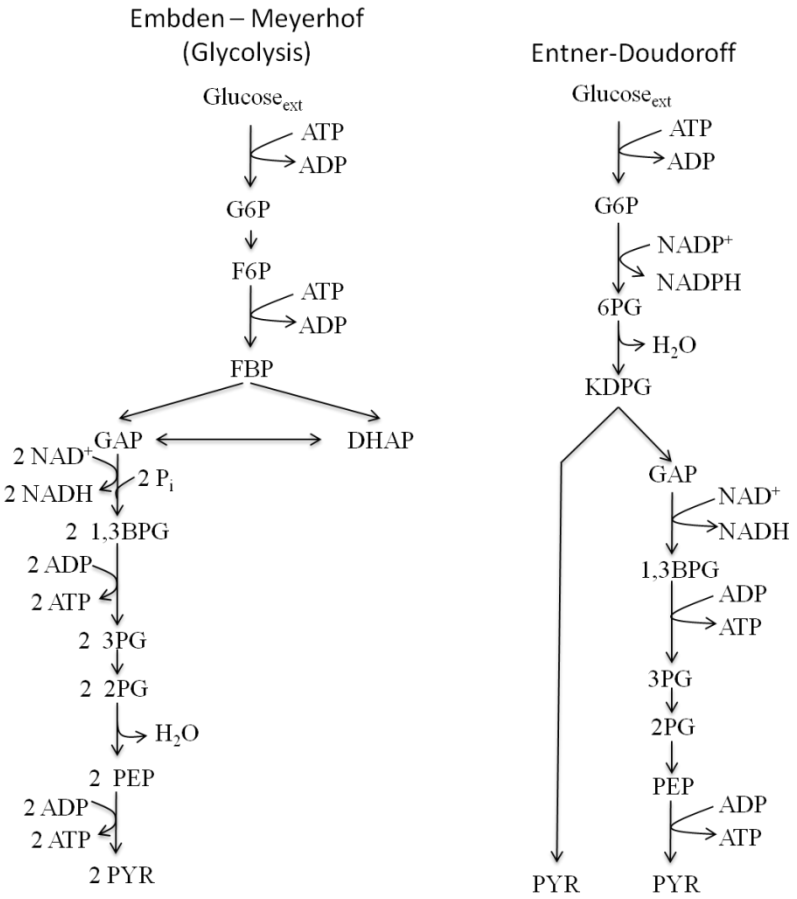

Figure 2.2. Fermentation pathways of glucose by lactic acid bacteria: G6P, glucose 6-phosphate; F6P, fructose 6-phosphate; FBP, fructose-1,6-biphosphate; DHAP, dihydroxyacetone-phosphate; GAP, glyceraldehyde-3-phosphate; 1,3BPG, glycerate 1,3-biphosphate; 3PG, glycerate 3-phosphate; 2PG, glycerate 2-phosphate; PEP, phosphoenolpyruvate; PYR, pyruvate; 6PG, 6-phosphogluconate; KDPG, 2-keto-3-deoxy-6-phosphogluconate. Adapted from Salminem *et al.* (2004) [46] and from Willey *et al.* (2009) [48].

2.2.1.2 Fates of pyruvate

The alternative fates of pyruvate are depicted in Figure 2.3 The reactions do not necessarily occur simultaneously but depend on the growth conditions and the enzymatic capacity.

Under conditions of excess of sugar and limited oxygen availability (which are the common environmental conditions of this bacterium), glycolysis is the main pathway of sugar catabolism and pyruvate formation. Typically 2 mol of pyruvate are further reduced to lactic acid (1) by a NAD^+-dependent lactate dehydrogenase (LDH), thus reoxidizing the NADH formed during the earlier glycolytic steps [49]. A redox balance is obtained and lactic acid is basically the only end product. This pathway yields 2 mol of ATP and 2 mol of lactate per mol of glucose. Such a metabolism is referred to as homolactic fermentation.

However, when cells experience certain growth conditions, the metabolism tends to shift from homolactic to mixed acid fermentation (heterolactic fermentation). In that case, the pyruvate produced in glycolysis follows different catabolic routes diminishing the flux through LDH and lactic acid formation. That could be mainly caused by the positive correlation observed between the concentration of FBP and the LDH activity. In fact, a high glucose concentration leads to high concentrations of FBP, which activate LDH, and the opposite is equally true [49].

Under anaerobic glucose-limited conditions or aerobic conditions, *E. faecalis* switches to different fermentation products. In an anaerobic environment with low concentration of sugars, the carbon metabolism flows to the production of acetate, ethanol, lactate and formate (mixed acid fermentation) [50] while in the presence of oxygen, the main end-products of the fermentation are acetate and CO_2. The formation of acetate increases the global energy to 4 ATP per glucose consumed [51]. The shift towards acetate production is related to the induction of various enzymes able to oxidise NADH (NADH oxidase, NADH peroxidase) in aerated cultures [52,53]. These enzymes are able to regenerate cofactors directly without recourse to carbon compound redox reactions Table 2.1) therefore favouring acetate and ATP production. This metabolic response should not be confused with respiration since no phosphorylation coupled with electron transport is involved though an effective but indirect energetic gain is achieved due to the increased production of acetate.

The pathway leading to acetoin formation (2) occurs if there is a pyruvate surplus in the cell relative to the need for NAD^+ regeneration

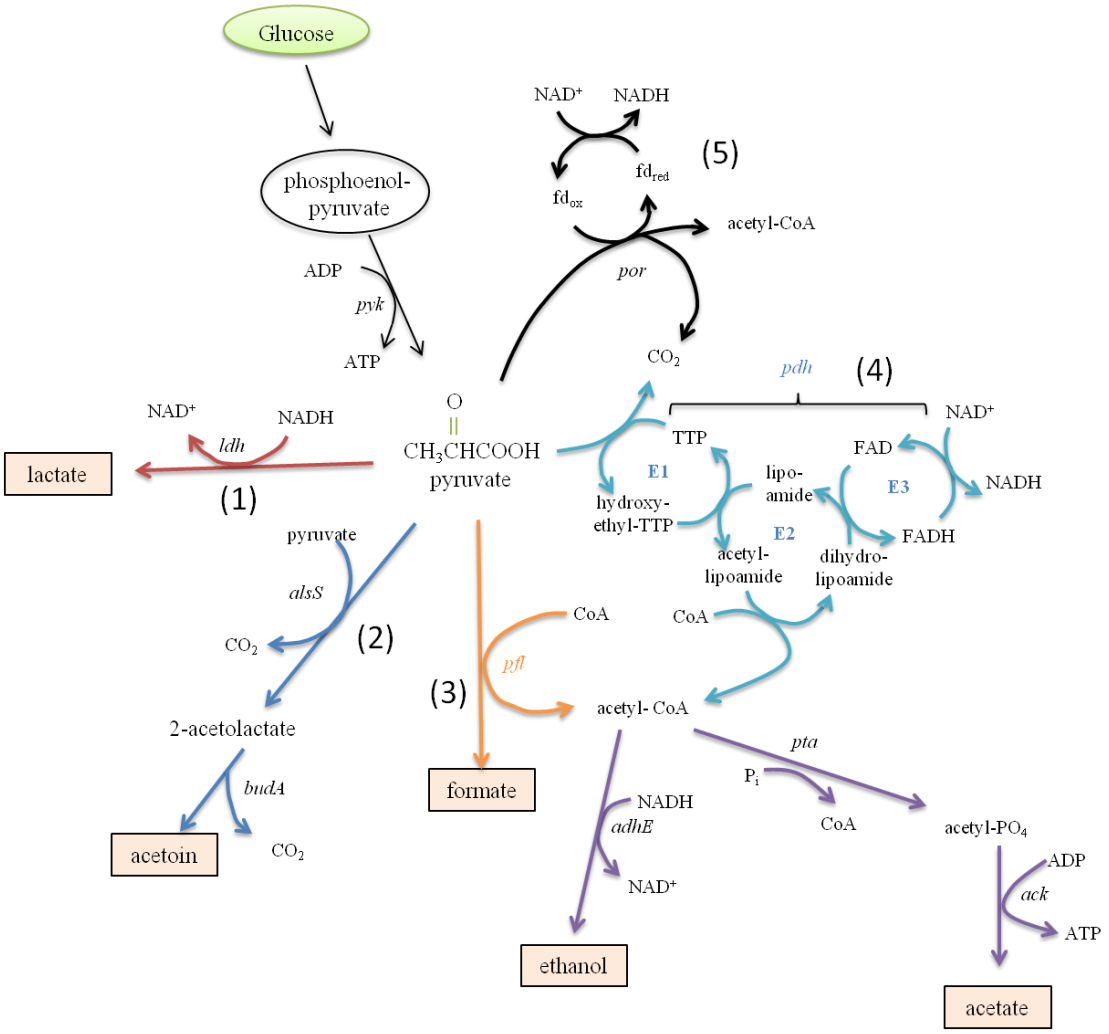

Figure 2.3. Pyruvate metabolism. *E. faecalis* genes coding for enzymes are shown: *pyk*, pyruvate kinase; *por*, pyruvate decarboxylase; fd_{red}, reduced ferredoxin; fd_{ox}, oxidized ferredoxin; *pdh*, pyruvate dehydrogenase complex with E1, E2, E3 subunits; TTP, thiamine pyrophosphate; *ldh*, lactate dehydrogenase; *alsS*, α-acetolactate synthase; *budA*, α-acetolactate decarboxylase; *pfl*, pyruvate-formate-lyase; *adhE*, aldehyde-alcohol dehydrogenase; *ack*, acetokinase; *pta*, phosphoacetyltransferase. Stoichiometric values are not presented for simplification purposes. Adapted from Gilmore (2002) [42].

A pyruvate surplus can be created if there is a source of pyruvate in the growth medium other than the fermented carbohydrate (such as citrate which can be converted into pyruvate *via* oxaloacetate decarboxylation) [54] which causes an overproduction of pyruvate that can be directed to the synthesis of acetoin.

Pyruvate formate lyase (PFL) converts pyruvate and CoA into formate and acetyl-CoA when the organism is grown under glucose limited concentrations and in the absence of oxygen (3). In fact, this enzyme is extremely sensitive to oxygen and can be irreversibly inactivated with this compound. Therefore, cells only activate PFL if grown under anaerobic conditions [55]. Also, PFL is inhibited by increased levels of GAP and DHAP. The intracellular levels of these compounds are proportional to the glucose concentration. As PFL is inhibited, a higher flux is channelled towards LDH and lactate formation.

The pyruvate dehydrogenase complex (PDH) is a system of enzymes that occupy a key position between glycolysis and the citric acid cycle (4). The enzyme complex is an important point of regulation and contrary to what is observed in other organisms, in *E. faecalis* it functions both under aerobic and anaerobic conditions [56]. The PDH complex is a collection of multiple copies of the three enzymes: pyruvate dehydrogenase (E1 subunit, *pdhA* and *phdB*, 1.2.4.1), dihydrolipoyl acyl-transferase (E2 subunit, *aceF*, 2.3.1.12) and dihydrolipoamide dehydrogenase (E3 subunit, *bkdD*, 1.8.1.4) which catalyses the oxidative decarboxylation of pyruvate into acetyl-CoA and CO_2 [56].

The significant difference between PDH and PFL reactions is that a CO_2 rather than formate is produced with additional NADH generation in PDH.

Irrespective of the enzyme involved in acetyl-CoA formation, further metabolism of this intermediate will generate acetate, *via* phosphoacetyltransferase (*pta*)/acetatokinase (*ack*) or ethanol *via* alcohol dehydrogenase (*adhE*). As mentioned above, acetate formation generates a supplementary ATP while ethanol production regenerates 2 NAD^+. When pyruvate formate-lyase is employed, the equilibrium in reducing equivalents can be maintained by an equimolar partition of acetyl-CoA between acetate and ethanol with a net increase in ATP. No obvious gain seems to occur from using the PDH, since the additional NADH synthesised requires that all acetyl-CoA is converted to ethanol to maintain the redox equilibrium [57]. Nevertheless, the PDH complex is continuously used as it is able to function both in aerobic and anaerobic conditions.

A distinctive pyruvate dehydrogenation (5) has been reported only for *E. faecalis* and converts pyruvate directly to acetyl-CoA under reduced conditions. It is carried out by pyruvate:ferredoxin oxireductase [58].

It can be stated that the mixed acid fermentation predominates when sugar consumption is rate limiting under anaerobic conditions, i.e., when the rate of formation of new cell material is limited by the availability of ATP rather than the availability of anabolic carbon metabolites.

The impact of oxygen on a cell is strongly dependent on the mechanisms the organism has developed to cope with this environment. The survival of *E. faecalis* (best known as a fermenting, acidifying bacterium), in a rich aerated environment is generally poor. However, if haemin is present, *E. faecalis* (similarly to other LAB such as *L. lactis*) uses oxygen to switch from fermentation to a respiration metabolism, resulting in an improved long-term survival. Oxygen is thus beneficial rather than detrimental for survival, if haemin is provided [59].

Several enterococcal species express an electron transport chain that couples fermentation to oxidative phosphorylation with a net energy gain for the cell.

A conceptualized model for the *E. faecalis* respiratory chain, which is dependent on different components to work, is represented in Figure 2.4. The respiratory chain pathway starts with the transport of haemin by the putative haematin transporter. This step is crucial since it is the haemin that activates the cytochrome *bd*. Haemin groups are present as prosthetic groups in a variety of proteins, including, for example, catalases, cytochromes and hemoglobins. *E. faecalis* strain V583 is not able to synthesize these groups, a fact confirmed by the absence of genes encoding known porphyrin biosynthetic enzymes [31]. Therefore, external haemin needs to be provided to activate the respiratory chain.

Cytosolic reducing equivalents produced by sugar fermentation are transferred to demethylmenaquinone (DMK) through a putative NADH:quinone oxireductase. Reduced DMK.(i.e., demethylmenaquinol, $DMKH_2$) binds to terminal quinol oxidase fumarate reductase (Frd).

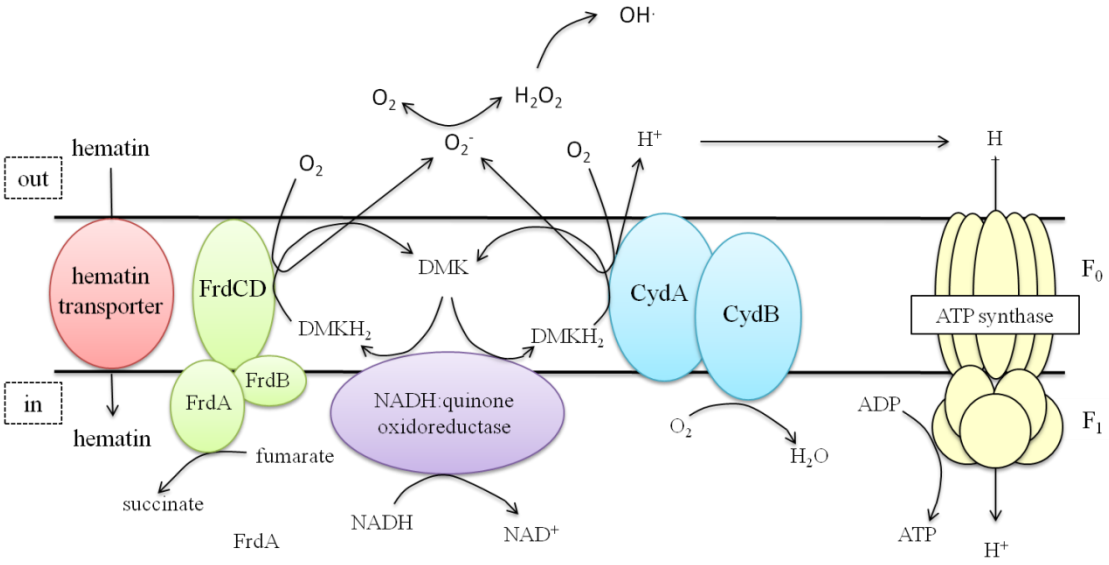

Figure 2.4. Schematic model of the adapted respiratory chain of *E. faecalis*. The elements that constitute the respiratory chain are: cytochrome *bd* (CydAB); fumarate reductase (FrdABCD); demethylmenaquinone (DMK); demethylmenaquinol ($DMKH_2$). Picture adapted from Gilmore 2002 [42] and from Huycke *et al.* (2001) [60].

This enzyme is constitutively expressed and facilitates anaerobic respiration by catalysing the conversion of fumarate to succinate using $DMKH_2$ as an electron donor. Alternatively, $DMKH_2$ can be oxidized by a second terminal quinol oxidase in the form of cytochrome *bd* that can be activated if exogenous haemin has been incorporated into the cytosol. The reduction by cytochrome *bd* is accompanied by oxygen reduction to water with simultaneous release of protons into the extracellular compartment establishing a proton motive force. In the absence of fumarate and haemin, extracellular superoxide (O_2^-) is generated through the univalent reduction of oxygen on the two terminal quinol oxidases. Under neutral or acidic conditions, superoxide is readily dismuted into hydrogen peroxide (H_2O_2) and, in the presence of transition metals like iron, will be catalytically converted into hydroxyl radical (OH^-) [60].

Compared to fermentation, respiration provides a growth advantage which can be observed by the size of the colonies grown on solid media under aerobic conditions [42].

Interestingly, this adapted system not only allows respiration to occur but it has also been implicated in the ability for *E. faecalis* to generate extracellular superoxide. Superoxide, along with hydroxyl radical (HO^-) and, H_2O_2 constitute a group of reactive

oxygen species (ROS). These species result from the partial reduction of oxygen into highly reactive agents that can be deleterious to the cells. A study by Huycke *et al.* (2001), found that the formation of superoxide and its derivatives hydroxyl radicals are dependent on the presence of demethylmenaquinone but also on the inactivity of the terminal oxidase, cytochrome *bd*. In fact, when supplying exogenous haemin, the cytochrome restored its functionality and attenuated extracellular superoxide production [60]. The other quinol oxidase, fumarate reductase, converts fumarate to succinate using menaquinol as an electron acceptor. The availability of fumarate also influences the extracellular superoxide production. Overall observations from Huycke *et al.* (2001) work suggested that fumarate, like haemin, had a suppressive effect on the production of extracellular superoxide, reducing it by 75.0% [60]. Nevertheless, the production of extracellular superoxide by *E. faecalis* has recently been proposed to exert damages in host-cell DNA and to be a potential trigger for severe conditions as colorectal cancer [27,61].

2.2.2 ANTIBIOTIC RESISTANCE IN *E. FAECALIS*

E. faecalis' antibiotic resistance has been well documented over the past years. It is established that *E. faecalis* is inherently resistant to many antimicrobial drugs, namely cephalosporins, antistaphylococcal penicillins, low concentrations of clindamycin and aminoglycosides, and trimethoprim. In addition, it has also developed resistance to gentamycin and streptomycin [62]. *E. faecalis* is able to quickly and efficiently acquire antibiotic resistance, namely by horizontal transfer of genes. In a study from Manson *et al.* (2010), *E. faecalis* pathogenicity island (PAI) encoding 129 ORF (open reading frame) was on focus in order to understand the evolution of horizontal gene transfer in *E. faecalis* strains. They observed chromosome-chromosome transfer through plasmid mobilization that occurs as an integrative conjugative element (ICE) [63].

This problem acquires a new dimension when pathogens can not only transfer the resistance genes among themselves but also into other species. Population genetics studies revealed that recombination prevails as a driving force of genetic diversity in *E. faecalis, E. faecium, S. pneumonia* and *S. pyogenes* and, more importantly, horizontal acquisition of resistance and virulence genes play a key role in the emergence of new clinically relevant clones [64].

Vancomycin is a glycopeptide antibiotic used to treat infections caused by gram positive bacteria. High-level vancomycin resistance is the most problematic resistance of *enterococci*, because it often appears in strains already highly resistant to ampicillin. Vancomycin inhibits e*nterococci* by binding to the D-alanyl-D-alanine (D-Ala-D-Ala) terminus of cell wall precursors, compromising the subsequent enzymatic steps in the synthesis of the cell wall [65].

Among *enterococci* there are six types of glycopeptide resistance that confer vancomycin resistance which are encoded by different gene clusters (*vanA, vanB, vanC, vanD, vanE and vanG*,), although the major vancomycin determinants are VanA and VanB [66]. VanA-type resistance is characterised by high-level resistance to both vancomycin and teicoplanin, whereas VanB-type strains are resistant to variable levels of vancomycin but susceptible to teicoplanin [66]. Both antibiotics (vancomycin and teicoplanin) inhibit the bacterial cell wall synthesis [68].

Faecal vancomycin-resistant *enterococci* are important as a source of infection and nosocomial spread and have hardly ever been eliminated or their reintroduction prevented; therefore, the development of additional therapies and the comprehension of their metabolism must be a priority.

2.2.3 OXIDATIVE STRESS IN *E. FAECALIS*

In a homeostatic environment, the microorganisms tend to keep a reduced state within their cell wall. It is considered that an organism is under oxidative stress when there is an imbalance between the production of ROS and the cell's ability to neutralize them. ROS represent natural by-products of the oxygen metabolism and, in the particular case of humans, represents a key signal to eliminate defective cells through a process called apoptosis. Furthermore, a specific type of immune system cells called phagocytic cells, take advantage of the destructive characteristics of ROS to kill harmful agents that attack the human body [69]. On the other hand, for bacteria, the production of ROS can be extremely destructive especially for DNA, RNA, lipids and proteins. These reactive by-products of oxygen, such as the anion radical or superoxide ($O_2^{\cdot-}$), hydrogen peroxide (H_2O_2) and hydroxyl radicals (OH^-) are continuously generated in cells growing aerobically or in microaerophily [70]. The exposure to radiation or the presence of metal

ions also triggers the formation of ROS and therefore, a state of oxidative stress within the cell [70]. Several studies have also suggested that the production of $O_2^{\cdot-}$ triggers the Fenton reaction. In particular, molecules containing [4Fe-4S] clusters are more susceptible to release the iron due to oxidation which destabilises the cluster and causes enzyme inactivation Figure 2.5).

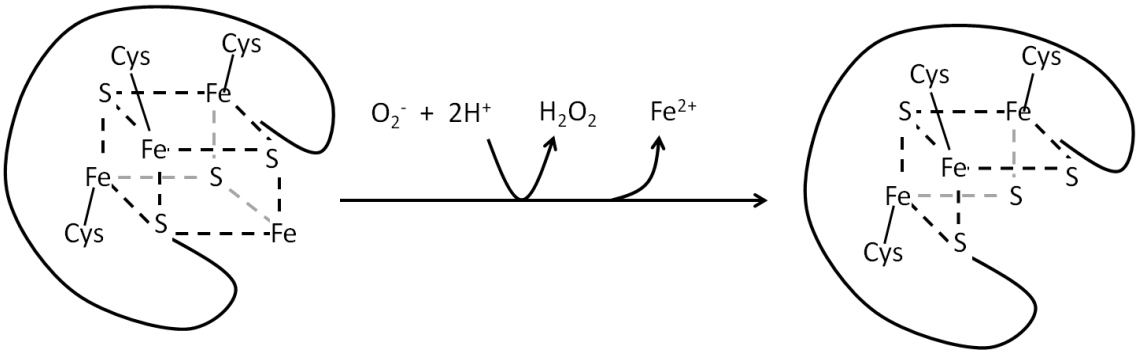

Figure 2.5. Mechanism of oxidative damage of an iron sulphur-cluster by $O_2^{\cdot-}$. Adapted from Imlay (2003) [72].

The implication of this is the accumulation of "free iron" which promotes the conversion of H_2O_2 into hydroxyl radicals: $H_2O_2 + Fe^{2+} \rightarrow O_2^{\cdot-} + F3^{3+} + OH^{-}$. These radicals damage DNA, proteins and lipids leading to cell death [71,72].

ROS species can damage DNA by generating apurinic and apyrimidic sites and by breaking the double strand. Furthermore, oxidation of amino acids converts them into various derivatives that generally, if incorporated, inactivate enzymes [73]. Lipids are a major target for oxidative stress as free radicals can directly attack the fatty acids present in the membrane and elicit lipid peroxidation, which changes membrane fluidity and interferes with membrane properties and membrane-bound protein functions. This process falls into a spiral of further production of free radicals that are finally degraded into "secondary toxic messengers", especially the aldehydes that are very reactive and can damage molecules such as proteins [70].

E. faecalis possesses an arsenal of strategic responses to fight oxidative stress, which gives this organism an advantage towards its host and other bacteria. Table 2.1 lists the proteins that play or are suspected to play a role in oxidative stress resistance in *E. faecalis.*

Table 2.1. Proteins involved in the oxidative stress of *E. faecalis*. Adapted from Riboulet *et al.* (2007) [74].

Protective proteins	Gene	*E. faecalis* gene[a]	Enzymatic reactions or regulated genes	Reference
Superoxide dismutase	sodA	EF0463	$2H^+ + 2O^- \rightarrow H_2O_2 + O_2$	Poyart *et al*., 2000 [75]
Catalase	katA	EF1597	$2H_2O_2 \rightarrow 2H_2O + O_2$	Frankenberg *et al*., 2002 [31]
Glutathione reductase	gor	EF3270	$NADPH + H^+ + GSSG \rightarrow NADP^+ + 2\ GSH$	Paulsen *et al*., 2003 [43]
NADH peroxidase	npr	EF1211	$NADH + H^+ + H_2O_2 \rightarrow NAD^+ + 2H_2O$	Ross and Claiborne, 1991 [76]
NADH oxidase	nox	EF1586	$2NADH + O_2 + 2H^+ \rightarrow 2NAD^+ + 2H_2O$ (NADH:H_2O oxidase) $NADH + O_2 + H^+ \rightarrow NAD^+ + H_2O_2$ (NADH:H_2O_2 oxidase)	Paulsen *et al*., 2003 [43]
Thioredoxine reductase	trx	EF1338; EF1405	$Trx(S\text{-}S) + NAD(P)H + H^+ \rightarrow Trx(SH)_2 + NAD(P)^+$	Paulsen *et al*., 2003 [43]
Organic hydroperoxide resistance protein	ohr	EF0453	$ROOH + Ohr(SH)_2 \rightarrow ROH + Ohr(S\text{-}S) + H_2O$	Rincé *et al*., 2005 [77]
DNA-binding protein	dps	EF3233; EF0606[b]	Bind and protect DNA from the oxidative stress	Paulsen *et al*., 2003 [43]
Peptide methionine-S-sulfoxide reductase	msrA	EF1681	Met-(S)-SO → Met	Paulsen *et al*., 2003 [43]
Peptide methionine-R-sulfoxide reductase	msrB	EF3164	Met-(R)-SO → Met	Laplace *et al*., 2000 [78]

[a] – According to the annotation by TIGR (http://cmr.tigr.org/tigr-scripts/CMR/CmrHomePage.cgi).

[b] – Orf present in the PAI of *E. faecalis*.

Some of these proteins have been studied in greater detail. Superoxide dismutases (SOD) are metalloenzymes that catalyse the conversion of O_2^- to H_2O_2 and molecular oxygen (O_2). There are three main classes of SOD in bacteria, manganese SOD (MnSOD or SODA), iron SOD (FeSOD or SODB) and copper-zinc SOD (CuZnSOD or SODC) [79], although for *E. faecalis* only MnSOD is available and has been characterised [80]. Further dismutation of H_2O_2 to H_2O and O_2 is undertaken by catalase [31] or to H_2O and NAD^+ by NADH peroxidase [76].

Glutathione (GSH) is a tripeptide radical scavenger that prevents damage of important cellular components caused by ROS.

Glutathione exists in both reduced (GSH) and oxidized (GSSG) states. In the reduced state, the thiol group of cysteine is able to donate reducing equivalents to other unstable molecules, such as ROS. In donating an electron, glutathione itself becomes reactive, but readily reacts with another reactive glutathione to form glutathione disulfide (GSSG) [81]. GSH is possibly the most abundant redox scavenging molecule in the cells [70]. Consequently, its role in maintaining cellular redox state is very important. GSH is usually synthesised in a two-step reaction catalysed by γ-glutamylcysteine synthase (orf EF3089, 6.3.2.2) and glutathione synthetase. Although glutathione synthetase has not been identified for *E. faecalis*, a study conducted by Janowiak *et al.* (2005) identified a novel bifunctional enzyme that would be able to catalyse both steps of GSH synthesis in *Streptococcus agalactiae*. The sequence of this bifunctional enzyme was blasted against the NCBI database and homology data have been found for *E. faecalis* [82].

Glutathione reductase is a member of the family of flavoprotein disulfide oxireductases, which catalyses the NADPH-dependent reduction of glutathione disulfide (GSSH).

$$NADPH + H^+ + GSSG \rightarrow NADP^+ + 2\ GSH$$

Glutathione reductase is involved in a variety of cellular functions, including antioxidant defence mechanisms. This enzyme has been identified in *E. faecalis* (*gor*, 1.8.1.7) and purified to homogeneity [83].

Regarding peroxides, a comparative study from Hartke *et al.* (2007) analysed the presence of three types and their impact in oxidative stress, survival inside macrophages

and virulence of *E. faecalis*: NADH peroxidase, Alkyl hydroperoxidase reductase and thiol peroxidase. The three of them constitute important defence barriers against exogenous H_2O_2 [84].

In 1998, Flahaut *et al.* performed some physiological studies to test the concentration of H_2O_2 required to kill 99.8% of *E. faecalis* cells harvested in the exponential growth phase. The study indicated that 45 mM of H_2O_2 during a 30-min treatment revealed to be necessary. Additionally, an adaptation study was performed by the same group. A sublethal assay was carried out using a lower concentration of 2.4 mM H_2O_2 during a 30-min treatment and it was observed that afterwards, the resistance against higher concentrations further increased by two orders of magnitude. Other treatments using acid pH (4.8), osmotic pressure (NaCl 6.5%) or heat shock (50ºC) during 30 min revealed the same cross-protection over stress [73].

Interesting to note is that *E. faecalis* is particularly well provided with oxidative stress protective enzymes and those enable the organism to persist longer in the host, increasing its likelihood to survive and cause harm [74].

2.3 *SYSTEMS BIOLOGY*

In a world where scientific knowledge and data generation increase by the hour, it becomes more relevant to develop new tools to deal with all that information wisely. For a long time now, cells are seen as systems that work for a common purpose. Therefore, the progress of biology is likely to be supported by computer technology (*in silico* simulations) and mathematical modelling. There is nowadays a golden opportunity for system-level analysis to be grounded in a molecular-level understanding, resulting in a continuous spectrum of knowledge [85].

The range of applications of system biology is unlimited. A quick search on Pubmed will retrieve innumerous references of application of systems biology (SB) in very different areas like medicine [86–89], plant biology [90–93], metabolic engineering [94–97] or synthetic biology [98–100].

2.3.1 INTEGRATION OF SB WITHIN THE PATHOGENIC BACTERIAL PANORAMA

The prospect of understanding the massive amount of biological data using mathematical models to describe the structure of a system and its response to external perturbations is extremely appealing and could allow researchers to answer a new level of questions. Some authors ambitiously stated that "model organisms are the Rosetta stone for deciphering biological systems" when it became clear that some informational pathways are remarkably similar between yeast, fly, worm and humans with many orthologous genes being identified across these species [90].

After genome sequence and genome annotations became available, metabolic models developed into a new level of specificity and capabilities and started to be used as powerful tools.

A Genome-scale Network Reconstruction (GENRE) is a collection of reactions that translate all the chemical transformations known to take place in a specific organism [101]. When annotated genomes were not available, smaller network reconstructions were based on literature and biochemical characterization of enzymes known to exist in the organisms [102,103]. A Genome-scale Model (GEM), on the other hand, comprises a genome scale network reconstruction that allows performing simulations using e.g., constraint-based methods such as flux balance analysis (as will be discussed later).

The field of genome-scale reconstructions has expanded rapidly over the years and currently counts with more than 60 GENRE for bacterial species alone. When considering archea and eukaryotes the total number of GENREs raises up over 100. An updated website hosting many of the available *in silico* models of different organisms is maintained by the Systems Biology Research Group at the University of California, San Diego (http://gcrg.ucsd.edu/InSilicoOrganisms) [101].

Genome scale reconstructions of pathogenic bacteria can serve as a valuable tool to allow understanding how the metabolism of these organisms changes in different environments and stress conditions. In fact, from the total of 64 bacteria models listed in the repository mentioned above, at the moment (August 2013), 16 correspond to

pathogenic bacteria. Additionally, if considering the updated versions of previously published models, the total sums up to 26 models, which is translated to 40% of the total bacterial models.

That number demonstrates the impact GENREs may have as tools to support the development of new techniques and strategies to control pathogens. Table 2.2 summarises the metabolic models so far published for pathogenic bacteria, while Table 2.3 details about their applications.

As depicted in Table 2.3, most GEMs for pathogens have been reconstructed to fundamentally gain a deeper knowledge on the physiology of the organisms and further explore their capabilities.

Some of the organisms studied are extremely dangerous and the deadliest pathogens known nowadays such as, *Salmonella typhimurium* and *Yersinia pestis*, respectively [128,130]. Others are even referred to be involved in the development of biological weapons, namely *Francisella tularensis.*[106] The importance of developing strategies to fight these organisms or develop new drug targets is therefore fundamental.

Haemophilus influenzae earned the status of being the first living sequenced organism but its pathogenesis is still not fully understood. The developed GEMs have sustained and supported that task by testing different metabolic phenotypes [107].

Helicobacter pylori, a human pathogen that has been associated with gastric cancer, had its GEM reconstructed to simulate growth in minimal medium and for an *in silico* deletion study, being able to predict with accuracy the experimental data. Later, the updated version also included prediction of several essential genes [109,110].

Table 2.2. Genome-scale models published by the Systems Biology Research Group at the University of California for pathogenic or related bacteria [101].

Organism	Model id	Genes	Metabolites	Reactions	References	Comments
Acinetobacter baumannii	AbyMBEL891	650	778	891	Kim *et al.* (2010) [104]	
Bacillus subtilis	iBsu1103	1103	1138	1437	Henry *et al.* (2009) [105]	Similarities with some pathogenic organisms
Francisella tularensis	iRS605	683	586	605	Raghunathan *et al.* (2010) [106]	
Haemophilus influenzae	iJE296	296	343	488	Edwards, (1999) [107]	
Haemophilus influenzae	iCS400	400	451	561	Schilling & Palsson (2000) [108]	
Helicobacter pylori	iCS291	291	340	388	Schilling *et al.* (2002) [109]	
Helicobacter pylori	iIT341	341	485	476	Thiele *et al.* (2005) [110]	
Klebsiella pneumoniae	YL1228	1228	1685	1970	Liao *et al.* (2011) [111]	
Mycobacterium tuberculosis	iNJ661	661	828	939	Jamshidi & Palsson (2007) [112]	
Mycobacterium tuberculosis	GSMN-TB	726	739	849	Beste *et al.* (2007) [113]	
Mycobacterium tuberculosis	iNJ661m	663	838	1049	Fang *et al.* (2010) [114]	
Mycoplasma genitalium	iPS189	189	274	262	Suthers *et al.* (2009) [115]	
Neisseria meningitidis	na	555	471	496	Baart *et al.* (2007) [116]	
Porphyromonas gingivalis	iVM679	na	564	679	Mazumdar *et al.* (2009) [117]	
Pseudomonas aeruginosa	iMO1056	1056	760	883	Oberhardt *et al.* (2008) [118]	
Salmonella typhimurium	iRR1083	1083	774	1087	Raghunathan *et al.* (2009) [119]	
Salmonella typhimurium	iMA945	945	1036	1964	AbuOun *et al.* (2009) [120]	
Salmonella typhimurium	STM_v1.0	1270	1119	2201	Thiele *et al.* (2011) [121]	
Staphylococcus aureus	iSB619	619	571	641	Becker & Palsson (2005) [122]	
Staphylococcus aureus	iMH551	551	604	712	Heinemann *et al.* (2005) [123]	
Staphylococcus aureus	na	546	1431	1493	Lee *et al.* (2009) [124]	
Streptomyces coelicolor	na	700	500	700	Borodina *et al.* (2005) [125]	ability to produce antibacterial compounds
Streptomyces coelicolor	na	798	759	1015	Alam *et al.* (2010) [126]	
Vibrio vulnificus	VvuMBEL943	673	792	943	Kim *et al.* (2011) [127]	

Yersinia pestis	iAN818m	815	963	1678	Navid & Almaas (2009) [128]
Yersinia pestis	iPC815	347	579	601	Charusanti *et al.* (2011) [129]

Table 2.3. Main applications of GEM of important pathogenic or related bacteria.

Organism	Model id	Comments & applications	References
Acinetobacter baumannii	AbyMBEL891	Isolated from soil and water but also humans. Its infection and resistance rates rapidly increase in hospitals. GEM used for gene/reaction essentiality prediction and phenotype comparison under different environmental conditions.	Kim *et al.* (2010) [104]
Bacillus subtilis	iBsu1103	Used as a model organism of gram + and sporulating bacteria. Has important industrial applications and similarities with pathogenic organisms.	Henry *et al.* (2009) [105]
Francisella tularensis	iRS605	Highly lethal pathogen that can be used as a biological weapon. GEM predicts experimental phenotypes and growth profile in defined minimal medium with 80% accuracy. Allows the identification of lethal genes that can be used as potential drug targets.	Raghunathan *et al.* (2010) [106]
Haemophilus influenzae	iJE296 and iCS400	First free-living organism sequenced. GEM used to study systematic characteristics including different optimal metabolic phenotypes.	Edwards (1999) [107] Schilling & Palsson (2000) [108]
Helicobacter pylori	iCS291 and iIT341	Human pathogen that colonizes the gastric mucosa and is responsible for several diseases including gastric cancer. GEM was used to simulate growth in minimal medium and an *in silico* deletion study was performed with high accuracy when compared with experimental data.	Schilling *et al.* (2002) [109] Thiele *et al.* (2005) [110]
Klebsiella pneumoniae	iYL1228	Human pathogen that often infects people in hospitals with a high rate of resistance to multiple antibiotics. Also, it is used to produce valuable chemicals. GEM was curated and validated to simulate growth on different substrates.	Liao *et al.* (2011) [111]

Mycobacterium tuberculosis	iNJ661, GSMN-TB and iNJ661m	Major pathogen in underdeveloped countries. Concern is also arising with the emerging multi-resistant strains in developed countries. Simulations with the first versions in respect to growth rates on different media were satisfactory but further improvement needed to be made concerning the identification of essential genes and consequent drug targets. The first updated version of Beste *et al*. simulated growth properties and gene essentiality with high accuracy. In addition, drug targets and single knock-outs phenotypes were identified, while the updated version of Fang *et al*. increased accuracy towards the identification of essential genes during the host infection.	Jamshidi & Palsson (2007) [112] Beste *et al.* (2007) [113] Fang *et al.* (2010) [114]
Mycoplasma genitalium	iPS189	Is the smallest organism known that can be grown in pure cultures. GEM increased the accuracy in identifying essential and non-essential genes.	Suthers *et al.* (2009) [115]
Neisseria meningitidis		Human pathogen that causes death and disability especially in young infants. GEM is reduced to the central metabolism. Nevertheless, a minimal medium for growth was successfully designed.	Baart *et al.* (2007) [116]
Porphyromonas gingivalis	iVM679	Gram - anaerobe pathogen that causes periodontitis. GEM simulates the growth profile on rich media and provides useful information to the development of drug targets by simulating single-knockouts.	Mazumdar *et al.* (2009) [117]
Pseudomonas aeruginosa	iMO1056	Life-threatening bacteria for immune-compromised patients. GEM provides a basic modelling framework to identify growth yields, nutrient requirements and genetic constraints for this pathogen.	Oberhardt *et al.* (2008) [118]
Salmonella typhimurium	iRR1083, iMA945, STM_v1.0	Human pathogen that causes death and morbidity worldwide. GEM identified gene essentiality and predicted growth profiles under a wide range of conditions that mimic the environment surrounding the host infection. The first updated GEM from AbuOun *et al.*, was compared with the commensal *E. coli* providing an interesting insight between the differences of a pathogen and its close but non-pathogen relative. The second updated GEM, from Thiele *et al*, included the development of a common workflow, implementation of thermodynamic data and usage of the GEM to identify multi-target drug therapy approaches.	Raghunathan *et al.* (2009) [119] AbuOun *et al.* (2009) [120] Thiele *et al.* (2011) [121]

Staphylococcus aureus	iSB619 , iMH551	Antibiotic resistant pathogen that represents a concern to the health authorities. The first GEM was used to predict cellular growth and phenotypes on different carbon sources and potential drug targets. The GEM from Heinemann *et al.* comprised genomic data, literature and physiological information and was curated against experimental observations including aerobic and anaerobic fermentation. An *in silico* gene deletion study was made to identify essential reactions. Later, Lee *et al.* published another GEM with the analysis of single and double deletion experiments that led to the identification of new reactions essential for growth	Becker & Palsson (2005) [122] Heinemann *et al.* (2005) [123] Lee *et al.* (2009) [124]
Streptomyces coelicolor		Antibiotic producer. GEM simulates the wild-type and mutants growth on different carbon and nitrogen sources. The essential reactions were also identified. Updated GEM from Alam *et al*. incorporated the switch between growth and antibiotic production.	Borodina *et al.* (2005) [125] Alam *et al.* (2010) [126]
Vibrio vulnificus	VvuMBEL943	Opportunistic human pathogen found in estuarine waters and coastal areas. GEM was validated and employed to identify key-metabolites that are critical for growth. Drug targeting strategies can be developed based on these discoveries.	Kim *et al.* (2011) [127]
Yersinia pestis	iAN818m , iPC815	One of the deadliest known pathogens. This GEM allows to simulate the phenotype on different environments and identify essential steps that can lead to the formulation of broad therapeutics. The updated GEM from Charusanti *et al*., simulates growth on different carbon sources and nutritional requirements of the strain CO92	Navid & Almaas (2009) [128] Charusanti *et al.* (2011) [129]

Most of the remaining published models are industrially relevant for metabolic engineering projects whose aim is to improve a strain to produce a compound of interest. Overall, GEMs are powerful tools that allow the prediction of the phenotypic behaviour under different sets of conditions and can thus be valuable to predict and improve microbial cell factories to produce relevant industrial products.

Additionally, GEMs can be the support basis to develop other more robust models that include regulatory data.

The reconstruction of GEMs created the need to develop tools to support the reconstruction process, as well as to explore the capabilities of the models. Some tools that support this task are OptKnock [131], OptGene [132] and Optflux [133].

The OptKnock and OptGene frameworks can be used to suggest gene deletion strategies leading to the overproduction of chemicals or biochemicals coupling biomass formation with the production of a chemical of interest. They aim at a growth selection/adaptation for indirectly evolving overproducing mutants [131,132].

Optflux is an open-source and modular software that aims to support strain optimization tasks, i.e., the identification of metabolic engineering targets, and a multitude of simulations to support the interpretation of the model capabilities with different algorithms implemented, included the ones from OptGene [132] and OptKnock [133].These tools allow the user to explore the overall network and design directed experiments based on the *in silico* resulting simulations.

2.4 *GENOME SCALE METABOLIC NETWORK RECONSTRUCTION*

To reconstruct a genome scale metabolic model, is it fundamental to have a well-known set of all the biochemical reactions and the corresponding stoichiometry. Hence, metabolic models tend to be organism-specific.

The reconstruction of a GEM is very laborious and time consuming and requires a fully annotated genome to start with. Efforts have been made in order to standardize a

reconstruction pipeline [134] but each reconstruction tends to be organism-specific and therefore unique.

A brief description of a genome scale reconstruction, based on available literature [135], is given in Figure 2.6.

A genome scale reconstruction starts with an annotated genome. This information, combined with the biochemical knowledge, can be used to support the construction of a first draft metabolic network. That information can be found in numerous databases which contain data about the genome sequence, enzymes and metabolic reactions, proteins, etc. The first bottleneck appears when trying to merge the content of different databases. The information is sometimes contradictory, which can mislead the reconstruction process. To overcome this problem, manual curation is required and literature validation essential.

A genome scale reconstruction is primarily focused on the reactions involved in metabolic pathways, hence, reactions catalysed by enzymes. To speed up the process, the modeller can initially focus on checking the genes that code for enzymes with EC numbers assigned. After, the stoichiometry and cofactors requirements need to be assigned and each reaction needs to be allocated to a compartment. For prokaryotic microorganism the task is easier, as the compartments are limited to cytosol and, in some cases, to the periplasmic space, whereas in eukaryotic microorganisms the metabolic reactions can occur in different compartments inside the cell.

The energy requirements in terms of ATP molecules per gram of biomass synthesized also needs to be included, as these molecules are related to amino acid and nucleotide polymerization, among others. ATP consumption for maintenance also needs to be specified, representing phenomena such as the maintenance of the membrane potential and turnover of macromolecules.

Other constraints are also important inputs to the model, including information related with the reversibility of reactions or flux values for nutrients present in the medium. Physiologically, these values represent the substrate availability or maximal uptake rates [136].

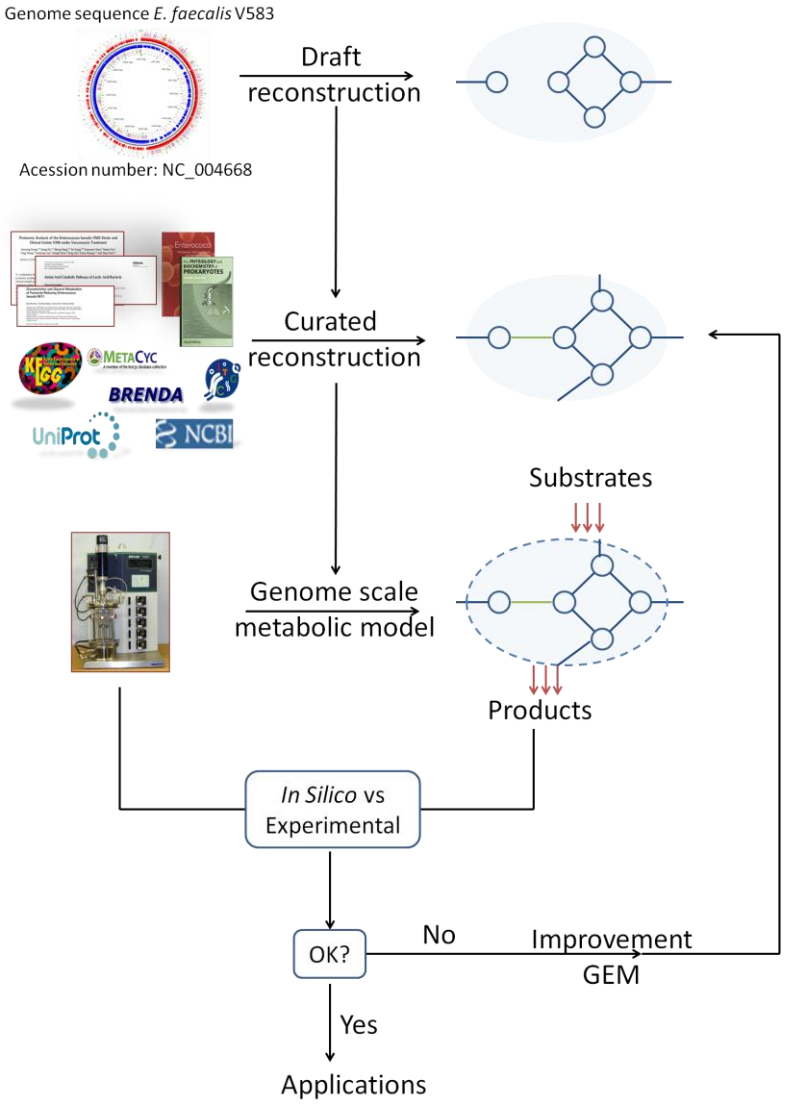

Figure 2.6. Iterative process for metabolic network reconstruction.

Once the model is assembled and debugged, it is necessary to translate that information into mathematical equations to represent the system.

In Figure 2.7 simplified toy model of a cell is presented. When analysing the cell dynamics, multiple reactions happen simultaneously for the production and consumption of different compounds and generation of biomass.

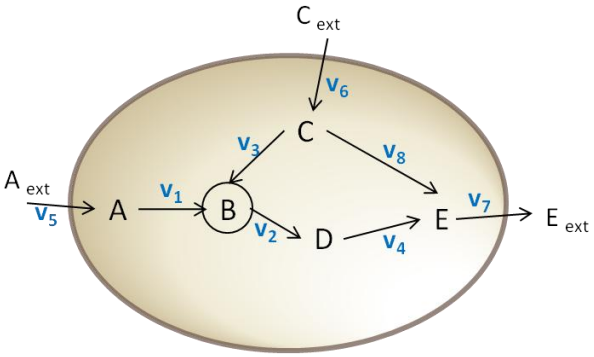

Figure 2.7. Schematic representation of a toy cell where reactions of degradation and production of compounds occur simultaneously.

The mathematical representation starts with a mass balance equation for each compound. The mass balance equation defines the dynamics between the rate of consumption and production for a given compound. As an example, the mass balance of compound B from Figure 2.7 would be:

$$\frac{dB}{dt} = v_1 + v_3 - v_2$$

However, the usual lack of kinetic expressions and parameters does not allow the simulation of the dynamic behaviour of the overall model. Nevertheless, it is generally accepted that cells tend to maintain their equilibrium and therefore, a steady state approximation can be applied [136]:

$$0 = v_1 + v_3 - v_2$$

This assumption reduces the mass balances equations of the system to a set of linear homogeneous equations. For the example given above in Figure 2.8:

For most of the metabolic networks, the number of mass balance equations is much smaller than the number of variables known, and therefore the system in underdetermined.

The set of additional constraints helps to reduce the space of potential solutions of the matrix; yet, the most common methodology used to calculate a single solution of the metabolic model is Flux Balance Analysis (FBA) [137].

$$\begin{bmatrix} -1 & 0 & 0 & 0 & 1 & 0 & 0 & 0 \\ 1 & -1 & 1 & 0 & 0 & 0 & 0 & 0 \\ 0 & 0 & -1 & 0 & 0 & 1 & 0 & -1 \\ 0 & 1 & 0 & -1 & 0 & 0 & 0 & 0 \\ 0 & 0 & 0 & 1 & 0 & 0 & -1 & 1 \end{bmatrix} \begin{bmatrix} v1 \\ v2 \\ v3 \\ v4 \\ v5 \\ v6 \\ v7 \\ V8 \end{bmatrix} = \begin{bmatrix} 0 \\ 0 \\ 0 \\ 0 \\ 0 \end{bmatrix}$$

Figure 2.8. Representation of the mass balances under steady-state in a matrix format.

Flux balancing methods provide estimation of metabolic fluxes based on the stoichiometric coefficients and knowledge of relevant biological functions [138].

The resulting flux distribution is the optimal solution for a given linear objective function and can be used to examine the metabolic network and compare with experimental data to validate the model.

The validation process is essential and requires the use of data generated in the laboratory. Usually, continuous fermentation is performed with the organism of interest to collect information about growth rates, yields on substrate, end-products, etc.

2.5 *MODEL VALIDATION*

2.5.1 CONTINUOUS CULTURE

Continuous culture consists in cultivating an organism in which the environmental conditions are maintained at a constant state. When cultivating microorganisms, initially a batch phase is required to reduce the lag phase of the growth and proceed quickly to the exponential phase. Since the inflow of nutrients and removal of waste is constant, the cells can maintain exponential growth indefinitely, ensuring that the population is continuously directing substrate utilisation for growth and primary metabolism [139].

Furthermore, environmental factors such as pH, nutrient concentration, and metabolic products can be controlled by the researcher and analysis of the effects of external factors (such as induction of stress conditions) can be measured.

During steady state operation, the specific growth rate of the microbial cell is equivalent to the dilution rate of the chemostat [140], thus a higher dilution rate confers a faster cell generation time. This dilution rate, which describes the rate in which the culture volume is being replaced by the inflow feed (culture medium), has been recognised to be highly influential on the metabolic activities of cell cultures [141–143].

Experimental design can be planned in order to validate the reconstructed model in terms of the effect of dilution rate, stress conditions or nutrient requirements.

2.5.2 METABOLOMICS

Metabolomics describes the approaches that aim to analyse the metabolome. The metabolome of an organism covers the complete set of all metabolites used or formed by the cell during its metabolism. This list can be extremely diverse and include chemical compounds from ionic inorganic species to hydrophilic carbohydrates, volatile alcohols and ketones, amino and non amino organic acids and hydrophobic lipids.

A metabolome analysis comprises both the endometabolome (the complete set of intracellular metabolites) and the exometabolome (the set of metabolites excreted into the broth or extracellular fluid) [144]. Distinguishing these two sets is important, as the exometabolome often exert a different physiological role in comparison to the endometabolome. In correspondence to the analysis performed, the exometabolome has been given the term metabolic footprint, while analysis of the endometabolome is known as metabolic fingerprint [145].

Metabolomics techniques are considered particularly useful in understanding cellular systems due to the fact that metabolites are the end-products of not only gene expression, but also regulatory responses to the surrounding environment [146]. Thus, metabolomics is increasingly being used in studies involving the phenotypic characterization of microbial strains [147], growth medium optimization [148], environmental stress responses [149] and drug discovery [150]. In the particular context of genome scale metabolic models, metabolomics provides the information to link the different metabolites to the metabolic network. Additionally, it is possible to determine the fluxes through different pathways, and through combination with metabolome analysis, it is

possible to correlate metabolite levels and fluxes, which enables identification of key control points in the metabolism [144].

Metabolomics is hence a growing field with the potential to interpret cellular systems, as metabolites levels can be regarded as the ultimate response of biological systems to genetic or environmental changes [146].

2.5.2.1 Sampling in metabolomics

Sampling for metabolomics is like taking a 'snapshot' of the moment, which reflects the *in vivo* phenotype in response to a genetic or environmental perturbation.

Since cellular metabolism is dynamic, it is imperative that the sampling process is fast and precise in order to obtain a true representation of the cellular metabolism. The sampling preparation is generally considered the limiting step in metabolome analysis because it is an important source of variability. The general steps in sample preparation for metabolome analysis are depicted in Figure 2.9.

After harvesting the cells, a rapid quenching (i.e., inactivation of the cellular metabolism and enzymatic activities) is mandatory to minimize the fact that metabolites concentration change very rapidly. The turnover of metabolites depends on whether they are primary or secondary metabolites and if they are located intracellularly or extracellularly. Primary metabolites (which are metabolites related to biochemical reactions involved in cellular synthesis) have usually high turnover rates. Glucose is converted into glucose 6-phosphate at an approximate rate of 1 mM/s and ATP, a metabolite involved in several reactions, is converted at a rate of 1.5 mM/s [144]. Intracellular metabolites, although present in higher concentrations, also have a much faster turnover than that of extracellular metabolites, essentially because intracellular metabolites are involved in several reactions and are therefore more demanded. Extracellular samples are more diluted and much less susceptible to turnover if rapidly separated from the living cells in the medium [144].

Following quenching, intracellular metabolites need to be extracted from the interior of the cells. The extraction of metabolites involves the disruption of the cell envelop and

subsequent separation of the low molecular mass metabolites from the biological matrix [144].

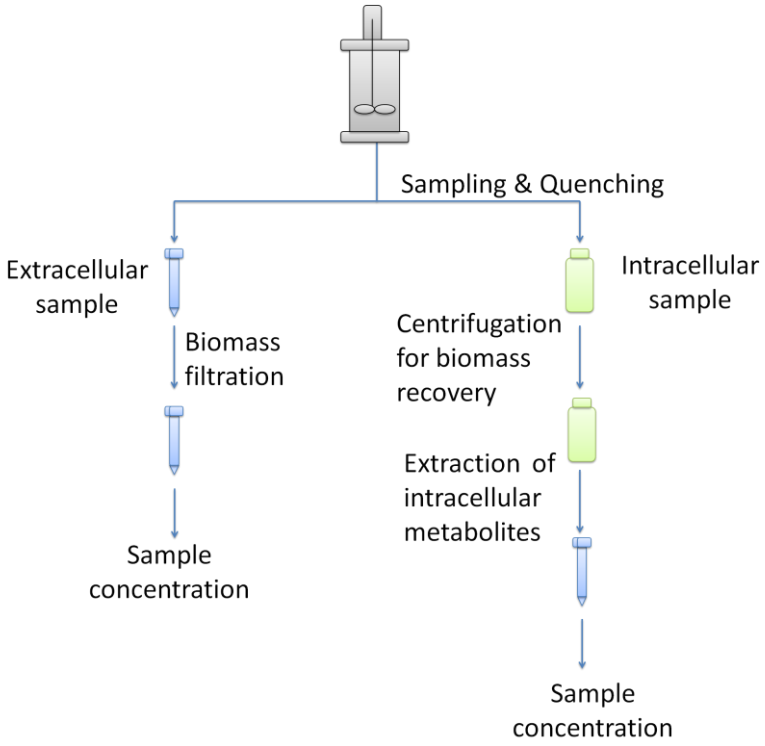

Figure 2.9. General steps for metabolomics sample preparation.

Next, sample concentration is advisable since several metabolites are present at fairly low levels.

Minimization of losses should be taken into account, as they are inevitable. To date no method has been so far reported to avoid losses and much less applicable to different microbial species; therefore, the quenching and extraction methods should be chosen considering the purpose of study as well as the organism involved [151].

2.5.2.2 Quenching methods

Many quenching methods are not able to overcome the leakage of intracellular metabolites due to the disruption of the cell integrity caused by either the drastic change in temperature or pH or even due to contact with the quenching solution that permeabilizes the membrane [144,151,152].

Another important characteristic common to all quenching methods is the speed at which this step must take place in order to avoid changes in metabolite levels. Ideally, the time window should be of seconds.

Most common quenching methods combine the usage of organic solvents (usually methanol or ethanol), buffered or non-buffered, set to an extreme temperature (either very cold or very hot) or an acidic solution, typically perchloric acid ($HClO_4$).

Typically, quenching procedures can be divided in two main groups, namely those where biomass and supernatant are separated and those in which this separation does not occur. For the last category it is important to keep in mind that the method is only suitable to measure compounds for which the total amount present in the supernatant is negligible compared to the total intracellular amount [151].

One popular quenching method is the cold methanol/water developed by De Koning and Van Dam (1992) [153]. With this method, a methanol:water solution (3:2) at -40ºC was used to quench yeast cells. 15 mL of culture broth were poured into the cold solution and left to acclimatize for 5 minutes and, afterwards, the sample/solution mixture was centrifuged to separate the cell pellet from the supernatant. The pellet was subsequently extracted.

This procedure, however, has shown to cause losses due to leakage of metabolites into the methanol solution both for yeast and bacteria [154,155]. This leakage was particularly significant in prokaryotes, as observed in the study by Bolten *et al.* (2007) [152].

Continuous attempts to try to develop new or improved techniques have been undertaken and are summarized in Table 2.4. Most of the methods present good results when designed for a specific strain. However, when applied by other researchers, the results achieved are constantly divergent and therefore, as mentioned before, the best method should be decided in accordance to the purpose of the study.

Villas-Bôas and Bruheim (2007) proposed a method that significantly prevented leakage of intracellular metabolites by the usage of a cold glycerol-saline quenching agent when tested with different gram positive and gram negative bacteria, as well as yeast cells [156].

This method has been shown to produce positive results within our laboratory experiments; therefore, this methodology was adopted throughout the chapters.

2.5.2.3 Extraction of metabolites

Metabolites present in biological samples are generally grouped in three major classes, namely, (1) water soluble metabolites or polar compounds, (2) water insoluble metabolites or non polar compounds, and (3) volatile metabolites [144]. Since it is not possible to extract and group all classes simultaneously, different techniques and different extraction agents are usually applied, depending on the purpose of the study. The extraction procedure aims to disrupt the cell structure liberating the maximum number of metabolites to a defined extraction matrix.

It is important to keep in mind that no extraction procedure to date can keep the metabolites in their original state and that changes in the initial intracellular ratio of the metabolites can occur. That is caused by the dilution inherent to extraction procedures, to incomplete extraction, chemical modification or partial degradation or even the addition of artefacts such as chemical contaminants from solvents.

The cell envelope of the organisms is the main barrier to be broken in order to reach to the metabolites. Due to the nature of the different organisms, the strength and rigidity of the wall matrix will offer more or less resistance to rupture following the general order of ease of disruption: gram negative bacteria > gram positive bacteria > yeast cells.

Generally, chemical agents (organic solvents, methanol, chloroform, boiling ethanol, boiling water) are used for extraction purposes; however, there are other methods that can be used independently or in combination with the chemical agents, namely the enzymatic (lysozyme), which are not very common for metabolomic analysis, and the physical (osmotic shock, freeze/thaw, heating) which are not very efficient *per se*, but that, when coupled with chemical extraction, exert a significant effect.

Table 2.4. Quenching protocols published for several bacteria and *S. cerevisiae*. Table adapted from Villas-Bôas *et al.* (2007) [144].

Quenching agent	Main conditions	Organism quenched	Reference
$HClO_4$	0.85 M in water 1:2 sample:$HClO_4$ sol. room temperature	*Alcaligenes eutrophus*	Cook *et al.* (1976) [157]
Hot NaOH	0.25 M in water 4:1 sample:NaOH sol. 85ºC	*Alcaligenes eutrophus*	Cook *et al.* (1976) [157]
Cold MeOH	60% (v/v) in water 1:4 sample:methanol sol. -40ºC	*Saccharomyces cerevisiae*	De Koning and van Dam (1992) [153]
$HClO_4$	0.66 M in water 1:1 sample:HClO4 sol. room temperature	*Saccharomyces cerevisiae*	Larsson and Törnkvist (1996) [158]
Boiling EtOH	75% (v/v) in buffer 1:4 sample:ethanol sol. 80ºC	*Saccharomyces cerevisiae*	Gonzales *et al.* (1997) [159]
Cold $HClO_4$	35% (w/w) in water 1:1 sample:$HClO_4$ sol -40ºC	*Zymomonas mobilis*	Weuster-Botz (1997) [160]
Cold MeOH	60% (v/v) in water 1:3 sample:methanol -50ºC	*Escherichia coli*	Schaefer *et al.* (1999) [161]
Cold MeOH	60% (v/v) in buffer 1:3 sample:methanol -35ºC	*Lactococcus lactis*	Jensen *et al.* (1999) [162]
Cold MeOH	75% (v/v) in buffer 1:5 sample:ethanol sol. -75ºC	*Xanthomonas campestris*	Letisse and Lindley (2000) [163]

Liquid nitrogen	~1:3 sample:liquid N_2 -196ºC	*Escherichia coli*	Buziol *et al.* (2002) [164]
Liquid nitrogen	-196ºC	*Saccharomyces cerevisiae*	Mashego *et al.* (2003) [165]
Cold NaCl solution	0.9% (w/w) in water 1:40 sample:saline -0.5ºC	*Corynebacterium glutamicum*	Wittmann *et al.* (2004) [155]
Cold MeOH	75% (v/v) in water/buffer 1:2 sample:methanol sol. -40ºC	*Saccharomyces cerevisiae*	Villas-Bôas *et al.* (2005a,b) [166,167]
Cold glycerol saline	3:2 (v/v) glycerol:saline 1:4 sample:solution -23ºC	*Saccharomyces cerevisiae* *Pseudomonas fluorescens* *Streptomyces coelicolor*	Villas-Bôas *et al.* (2007) [156]
Cold MeOH	60% (v/v) methanol buffered with 0.85% (w/v) $(NH_4)_2CO_3$ or 70 mM HEPES 1:3 sample:methanol sol. -40ºC	*Lactobacillus plantarum.*	Faijes *et al.* (2007) [168]
Cold MeOH	60% (v/v) in water 1:4 sample:methanol sol. -40ºC	*Saccharomyces cerevisiae*	Canelas *et al.* (2008) [154]
Cold MeOH	3:2 (v/v) methanol:glycerol -50ºC	*Escherichia coli*	Link *et al.* (2008) [169]
Cold EtOH	40% (v/v) ethanol:NaCl (0.8%, w/v) 1:1 sample:solution -20ºC	*Saccharomyces cerevisiae* *Corynebacterium glutamicum* *Escherichia coli*	Spura *et al.* (2009) [170]

Polar solvents like methanol, methanol-water mixtures, or ethanol are used to extract polar metabolites, and non polar solvents like chloroform, ethyl acetate, or hexane are used to extract lipophilic compounds. Table 2.5 summarises the different techniques and chemical extraction agents most commonly used.

Methanol is a powerful organic solvent that can be used alone or mixed with water to efficiently extract intracellular metabolites from both bacteria [161,169] and yeast [166,167]

A technique that has been shown to minimize destructive effects on metabolites and to be overall effective is described in the work of Smart *et al.* (2010). This protocol combines the effort of cold methanol-water solution as the chemical extraction agent with a mechanic action of freeze-thaw cycles [171].

However, the process has to be performed under low temperatures (< -20ºC) to devoid further biochemical reactions to occur and degradation of compounds. Freeze-thaw cycles enhance the permeability of cells, as water expands when it is frozen, and therefore, subsequent thawing disrupts or damages cell envelopes, enhancing the chemical extraction of metabolites by the cold methanol-water solution [171]. This protocol has been shown to efficiently recover polar and mid-polar metabolites and was also used throughout the studies in the present work, along with the quenching method mentioned previously.

2.5.2.4 Analytical methodologies

From previous sections, it is possible to understand that the complexity of the metabolome is very high in terms of chemical diversity and levels of metabolites. With the analytical technologies currently available, it is still not possible to detect the complete metabolome in a single analysis. Nevertheless, a combination of Mass Spectrometry with gas chromatography (GC-MS) has been the most used methodology for metabolome analysis.

Table 2.5. Compilation of extraction methods depending on the metabolites of interest. Adapted from Villas-Bôas *et al.* (2007) [144].

Method	Extraction of	Advantages	Disadvantages	Reference
Methanol-water-chloroform	Polar compounds (methanol–water phase) Non polar compounds (chloroform phase)	- Chloroform avoids further reactions by denaturating enzymes. - Allows separation of polar and non polar compounds. - Good recovery of phosphorylated metabolites and thermolabile compounds	- Tedious and time consuming - Toxic effects of chloroform - Presence of buffer may pose problems for many analytical techniques	De Koning and van Dam (1992) [153] Cremin *et al.* (1995) [172] Smits *et al.* (1998) [173] Le Belle *et al.* (2002) [174] Maharjan and Ferenci (2003) [175] Villas-Bôas *et al.* (2005a,b) [166,167] Sánchez *et al.* (2010) [176] Meyer *et al.* (2012) [177] Kawase *et al.* (2013) [178]
Boiling ethanol	Polar thermostable metabolites	- Simple and fast - Denaturation of enzymes by hot ethanol - Enhanced cell disruption by heating - Good reproducibility	- A number of metabolites are not stable at high temperatures for extraction	Gonzalez *et al.* (1997) [159] Hans *et al.* (2001) [179] Castrillo *et al.* (2003) [180] Maharjan and Ferenci (2003) [175] Villas-Bôas *et al.* (2005a) [131] Sánchez *et al.* (2010) [176] Meyer *et al.* (2010) [181] Tredwell *et al.* (2011) [182]
Cold methanol	Polar and mid-polar metabolites	- Simple and fast - Easy removal of solvent by evaporation - Excellent recovery of metabolites - Excellent reproducibility - Broad range of metabolites extractable	- Incomplete denaturation of enzymes - Low recovery of non-polar compounds	Shryock *et al.* (1986) [183] Maharjan and Ferenci (2003) [175] Villas-Bôas *et al.* (2005a,b) [166,167] Villas-Bôas *et al.* (2007) [156] Tremaroli *et al.* (2009) [184] Sánchez *et al.* (2010) [176] Smart *et al.* (2010) [171]

Acidic extraction	Polar and acid-stable metabolites	- Simple - Excellent recovery of amines and polyamines - Denaturation of enzymes by extreme low pH	- Bad recovery of the remaining metabolites - Hydrolysis of proteins and polymers	Shryock *et al.* (1986) [183] Kopka *et al.* (1995) [185] Buziol *et al.* (2002) [164] Villas-Bôas *et al.* (2005a) [131]

In gas chromatography, the compounds are separated before detection. The mobile phase is usually an inert gas like helium or nitrogen while the stationary phase is an inert (silicone polymers) solid support located inside of the chromatograph column. Usually the column is a long tube of fused silica, where the stationary phase is bound to the inner surface. The samples are injected through the sample injector that is connected to the column and compounds migrate along the column at different rates depending on the adherence to the stationary phase, until they are eluted at a specific retention time. Linked to the chromatograph equipment is the MS that is composed by an ion source where the analytes are ionized and transferred to the mass analyser, where ions are separated according to mass to charge ratios (m/z). Next, a detector measures the ion current, which is translated into a signal and measured by a data system to control and process the data. Finally, vacuum pumps are extremely important to maintain the high vacuum of the system (Figure 2.10).

Different mass analysers are available in the market, such as: quadrupole, ion trap or TOF analyser. For the purposes of this thesis a quadrupole mass analyser was used. This analyser is widely used particularly for GC-MS and is one of the simplest and most versatile components. 4 metal rods compose this apparatus and a voltage current is supplied, creating an electric field between the rods. The charged molecules are continuously injected and spin within the four metal cylinders until they reach the detector [144].

The ion trap, also called quadrupole ion trap is part of the quadrupole mass analyser family but instead of continuously transmitting ions through the quadrupole, the ion-trap can store ions and eject these when required.

Finally, the TOF (time-of-flight) mass spectrometer gives the ions a "push" to measure the time the ions take to travel a flight tube and store that time in the spectrum. The mass-to-charge ratio is proportional to the squared flying time [144].

Prior to inject the samples in the equipment, an extra step of derivatisation is required for most compounds. That step is important as samples need to be sufficiently volatile to be evaporated in the injector. Most of these metabolites are in their normal non-volatile form, but they can be made volatile by "covering", e.g., the carboxylic,

hydroxylic, and amino groups with an apolar functionality, thus making them more volatile to be analysed by gas chromatography [144].

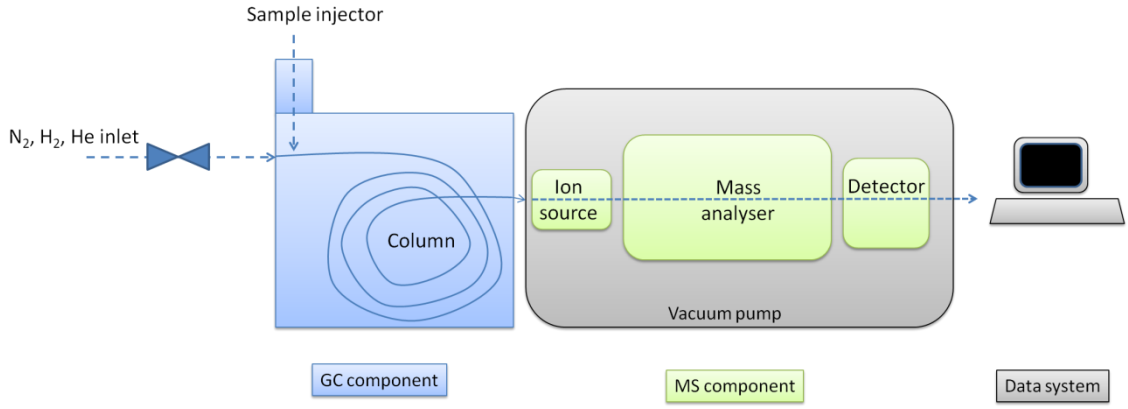

Figure 2.10. GC-MS components for the metabolome analysis.

2.5.3 METABOLOMICS AND PATHOGENS

Among other applications, metabolomics has been useful in characterising metabolic profiles of pathogenic bacteria.

Staphylococcus aureus is a versatile pathogen that causes different disease patterns because of its physiological adaptation capacity. The metabolite profile during transition from exponential growth phase to glucose starvation was analysed by Liebeke and co-workers using a combined metabolomics and proteomics approach [186].

Pseudomonas syringae's interaction with *Arabidopsis thaliana* has been studied by analysing the cellular metabolome of the host and the pathogen after co-culture to model the individual responses [187].

Another study from Henderson *et al.* (2009) has developed a novel quantitative metabolomic approach based on stable isotope dilution to compare siderophores production in *E. coli* strains associated with intestinal colonization or urinary tract disease [188].

The complex morphological changes that occur during sporulation of *Bacillus subtilis* when submitted to nutritional limitation or high cell densities are thought to be controlled by metabolic networks. Metabolite profiles of *B. subtilis* cells before and

during spore formation were analysed using capillary-electrophoresis mass spectrometry (CE-MS). Metabolites are first separated by CE based on charge and size and then selectively detected by coupling an MS equipment [189].

Mycobacterium tuberculosis, the causative agent of tuberculosis, is one of main causes of infectious diseases worldwide. Its pathogenicity results from an adaptation to very specific niches within the human body. Untargeted metabolite profiling of *M. tuberculosis* growing on ^{13}C labelled carbon revelled that this pathogen can co-metabolise multiple carbon sources simultaneously to enhance its growth. Additionally, the authors also observed that the organism has the ability to simultaneously channel carbohydrates and fatty acids to distinct metabolic fates reshaping the basic understanding of this pathogen capacity to adapt to the host niche [190].

Recently, metabolomics using nuclear magnetic resonance (NMR) spectroscopy has been applied both in biofilm and planktonic bacterial cells of *Acinetobacter baumannii* to gain insight into the metabolic changes of this multidrug resistant organism. The ability to form biofilms gives the organism an increased resistance to various stresses, especially antibiotics, relative to its planktonic counterparts. Metabolites such as acetate, pyruvate, succinate, UDP-glucose, AMP, glutamate, and lysine were increasingly involved in the energy metabolism of biofilm formation [191].

Pneumonia, also known as community-acquired pneumonia (CAP) is caused by a number of organisms such as, bacteria, viruses or parasites and is responsible for a significant number of deaths worldwide. A study carried by Slupsky *et al.* (2009), using NMR technology, collected urinary samples from infected patients and was able to identify distinguishing metabolomic profiles between organisms involved in CAP (namely *Streptococcus pneumoniae* from other organisms), in an attempt to find patterns of metabolic recognition between organisms causing pneumonia [192].

In this thesis we will also explore the role of metabolomics to understand the impact that different stress conditions have on the metabolism of *E. faecalis*. Whenever possible, generated data will be further explored with the support of the reconstructed genome scale model of the organism.

2.5.4 FLUXOMICS

As described in the previous section, metabolomics aims to identify and describe all metabolites present in a system. However, it is important to realise that metabolism is a dynamic process, where metabolites are continuously being transformed during cellular processes. Understanding metabolic fluxes, the rates at which these transformations occur, is a vital element in the study of cellular metabolism. Fluxome describes the complete set of metabolic fluxes of a biological system, and together with the metabolome, integrate all metabolic pathways to compose the metabolic network [193]. Similarly to the metabolome, fluxome output changes in response to cellular perturbations caused by environmental alterations [194].

Several techniques have been developed to assist in the quantification of metabolic fluxes, with flux balance analyses being the most popular approaches, as mentioned before. However, previous studies have indicated that the most reliable of these methods work in conjunction with labelling experiments involving isotope-labelled precursors of metabolic pathways, particularly ^{13}C-labelled substrates [195]. During ^{13}C-labelling experiments the growth medium utilised contains ^{13}C-labelled substrates, such as glucose, thereby allowing the labelled carbon to be distributed along the network to related metabolites of the cellular system. Depending on the metabolic pathways that are driven by the environmental setup conditions, the introduction of the labelled substrate will allow retrieval of specific flux information by examining the labelling patterns of downstream compounds [193]. However, this process requires prior knowledge of the possible distribution of the labelled atoms within the network. Thus, at this stage, analysis of metabolic fluxes focuses mainly within the central carbon metabolism [196].

A well-established method to obtain microbial fluxomic information regarding the central carbon network is to utilise the labelling patterns of amino acids from hydrolysed biomass [195]. Since biosynthesis of amino acids relies essentially on key compounds from the central carbon network (Figure 2.11), during metabolic steady state (such as one established by continuous cultures), the labelling patterns will be reflected on the amino acids. Examining amino acids instead of central metabolites themselves is overall a more advantageous approach when trying to infer central

metabolic fluxes as amino acids incorporated into biomass are more abundant and a more stable source for labelling patterns [197].

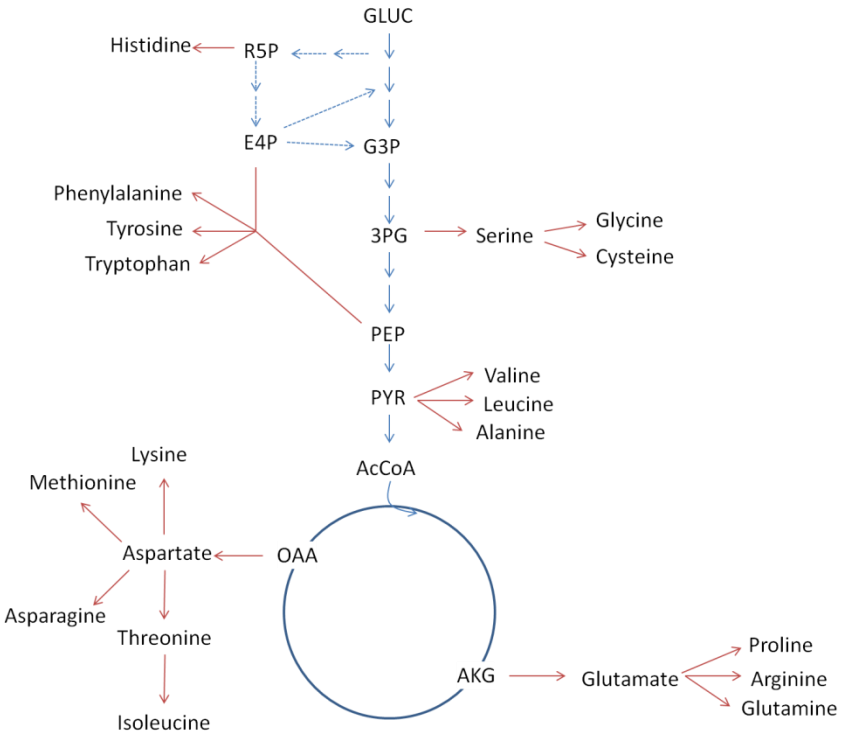

Figure 2.11. Central carbon metabolism and biosynthesis of amino acids. Adapted from Akashi & Gojobori (2002) [198].

2.6 *REFERENCES*

1. Guarner, F. & Malagelada, J.-R. Gut flora in health and disease. *Lancet* **361,** 512–9 (2003).

2. Mshvildadze, M. & Neu, J. The infant intestinal microbiome: friend or foe? *Early Hum. Dev.* **86,** 67–71 (2010).

3. Adlerberth, I. & Wold, a E. Establishment of the gut microbiota in Western infants. *Acta Paediatr.* **98,** 229–38 (2009).

4. Bäckhed, F., Ley, R. E., Sonnenburg, J. L., Peterson, D. a & Gordon, J. I. Host-bacterial mutualism in the human intestine. *Science* **307,** 1915–20 (2005).

5. Ley, R. E., Peterson, D. a & Gordon, J. I. Ecological and evolutionary forces shaping microbial diversity in the human intestine. *Cell* **124,** 837–48 (2006).

6. O'Hara, A. M. & Shanahan, F. The gut flora as a forgotten organ. *EMBO Rep.* **7,** 688–93 (2006).

7. Frank, D. N. *et al.* Molecular-phylogenetic characterization of microbial community imbalances in human inflammatory bowel diseases. *Proc. Natl. Acad. Sci. U. S. A.* **104,** 13780–5 (2007).

8. Swidsinski, A. *et al.* Spatial organization of bacterial flora in normal and inflamed intestine: A fluorescence in situ hybridization study in mice. *world J. Gastroenterol.* **11,** 1–19 (2004).

9. Lefebvre, P., Cariou, B., Lien, F., Kuipers, F. & Staels, B. Role of bile acids and bile acid receptors in metabolic regulation. *Physiol. Rev.* **89,** 147–191 (2009).

10. Wong, J. M. W. ., de Souza, R., Kendall, C. W. C. ., Emam, A. & Jenkins, D. J. A. Colonic Health: Fermentation and Short Chain Fatty Acids. (2006).

11. Sekirov, I., Russell, S. L., Antunes, C. M. & Finlay, B. B. Gut microbiota in health and disease. *Physiol. Rev.* **90,** 859–904 (2010).

12. Tlaskalová-Hogenová, H. *et al.* Commensal bacteria (normal microflora), mucosal immunity and chronic inflammatory and autoimmune diseases. *Immunol. Lett.* **93,** 97–108 (2004).

13. Hooper, L. V. Do symbiotic bacteria subvert host immunity? *Nat. Rev. Microbiol.* **7,** 367–74 (2009).

14. Hawrelak, J. A. & Myers, S. P. The causes of intestinal dysbiosis: A review. *Altern. Medine Rev.* **9,** 180–197 (2004).

15. De Palma, G. *et al.* Intestinal dysbiosis and reduced immunoglobulin-coated bacteria associated with coeliac disease in children. *BMC Microbiol.* **10,** 63 (2010).

16. Nadal, I. *et al.* Imbalance in the composition of the duodenal microbiota of children with coeliac disease. *J. Med. Microbiol.* **56,** 1669–74 (2007).

17. Walker, A. W. *et al.* High-throughput clone library analysis of the mucosa-associated microbiota reveals dysbiosis and differences between inflamed and non-inflamed regions of the intestine in inflammatory bowel disease. *BMC Microbiol.* **11,** 7 (2011).

18. Roesch, L. F. W. *et al.* Culture-independent identification of gut bacteria correlated with the onset of diabetes in a rat model. *ISME J.* **3,** 536–48 (2009).

19. Brugman, S. *et al.* Antibiotic treatment partially protects against type 1 diabetes in the Bio-Breeding diabetes-prone rat. Is the gut flora involved in the development of type 1 diabetes? *Diabetologia* **49,** 2105–8 (2006).

20. Sjögren, Y. M., Jenmalm, M. C., Böttcher, M. F., Björkstén, B. & Sverremark-Ekström, E. Altered early infant gut microbiota in children developing allergy up to 5 years of age. *Clin. Exp. Allergy* **39,** 518–26 (2009).

21. Grüber, C. *et al.* Reduced occurrence of early atopic dermatitis because of immunoactive prebiotics among low-atopy-risk infants. *J. Allergy Clin. Immunol.* **126,** 791–7 (2010).

22. Ley, R. E. *et al.* Obesity alters gut microbial ecology. *Proc. Natl. Acad. Sci. U. S. A.* **102,** 11070–5 (2005).

23. Turnbaugh, P. J. *et al.* A core gut microbiome in obese and lean twins. *Nature* **457,** 480–4 (2009).

24. Kalliomaki, M., Collado, M. C., Salminen, S. & Isolauri, E. Early differences in fecal microbiota composition in children may. 534–538 (2008).

25. Snover, D. C. Update on the serrated pathway to colorectal carcinoma. *Hum. Pathol.* **42,** 1–10 (2011).

26. Uronis, J. M. *et al.* Modulation of the intestinal microbiota alters colitis-associated colorectal cancer susceptibility. *PLoS One* **4,** e6026 (2009).

27. Balamurugan, R., Rajendiran, E., George, S., Samuel, G. V. & Ramakrishna, B. S. Real-time polymerase chain reaction quantification of specific butyrate-producing bacteria, Desulfovibrio and *Enterococcus faecalis* in the feces of patients with colorectal cancer. *J. Gastroenterol. Hepatol.* **23,** 1298–1303 (2008).

28. Prakash, S., Rodes, L., Coussa-Charley, M. & Tomaro-Duchesneau, C. Gut microbiota: next frontier in understanding human health and development of biotherapeutics. *Biologics* **5,** 71–86 (2011).

29. Lupp, C. *et al.* Host-mediated inflammation disrupts the intestinal microbiota and promotes the overgrowth of Enterobacteriaceae. *Cell Host Microbe* **2,** 119–29 (2007).

30. Sneath, P. H. A., Mair, N. S., Sharpe, M. E. & Holt, J. G. *Bergey's manual of systematic bacteriology*. (Williams and Wilkins, Baltimore, Md, 1986).

31. Frankenberg, L., Brugna, M. & Hederstedt, L. *Enterococcus faecalis* Haem-Dependent Catalase. **184,** (2002).

32. Fisher, K. & Phillips, C. The ecology, epidemiology and virulence of Enterococcus. *Microbiology* **155,** 1749–57 (2009).

33. Schleifer, K. H. & Kilpper-Balz, R. Transfer of *Streptococcus faecalis* and Streptococcus faecium to the Genus Enterococcus nom. rev. as *Enterococcus faecalis* comb. nov. and *Enterococcus faecium* comb. nov. *Int. J. Syst. Bacteriol.* **34,** 31–34 (1984).

34. Gilmore, M. S., Lebreton, F. & van Schaik, W. Genomic transition of enterococci from gut commensals to leading causes of multidrug-resistant hospital infection in the antibiotic era. *Curr. Opin. Microbiol.* 1–7 (2013).

35. Klibi, N. *et al.* Species distribution, antibiotic resistance and virulence traits in enterococci from meat in Tunisia. *Meat Sci.* **93,** 675–80 (2013).

36. Koluman, A., Akan, L. S. & Çakiroğlu, F. P. Occurrence and antimicrobial resistance of enterococci in retail foods. *Food Control* **20,** 281–283 (2009).

37. Sundqvist, G. Associations between microbial species in dental root canal infections. *Oral Microbiol. Immunol.* **7,** 257–262 (1992).

38. Kayaoglu, G. & Orstavik, D. Virulence Factors of *Enterococcus faecalis*: Relationship To Endodontic Disease. *Crit. Rev. Oral Biol. Med.* **15,** 308–320 (2004).

39. Franz, C. M. A. P., Huch, M., Abriouel, H., Holzapfel, W. & Gálvez, A. Enterococci as probiotics and their implications in food safety. *Int. J. Food Microbiol.* **151,** 125–140 (2011).

40. Balciunas, E. M. *et al.* Novel biotechnological applications of bacteriocins: A review. *Food Control* **32,** 134–142 (2013).

41. Foulquié Moreno, M. R., Sarantinopoulos, P., Tsakalidou, E. & De Vuyst, L. The role and application of enterococci in food and health. *Int. J. Food Microbiol.* **106,** 1–24 (2006).

42. Gilmore, M. S. *The Enterococci: pathogenesis, molecular biology, and antiobiotic resistance*. *ASM Press* 133–175 (ASM Press, 2002).

43. Paulsen, I. T. *et al.* Role of mobile DNA in the evolution of vancomycin-resistant *Enterococcus faecalis*. *Science (80-.).* **299,** 2071–4 (2003).

44. Ye, J., Minarcik, J. & Saier, M. H. Inducer expulsion and the occurrence of an phosphatase in *Enterococcus faecalis* and Streptococcus pyogenes. 585–592 (1983).

45. Leboeuf, C., Auffray, Y. & Hartke, a. Cloning, sequencing and characterization of the ccpA gene from *Enterococcus faecalis*. *Int. J. Food Microbiol.* **55,** 109–13 (2000).

46. Salminem, S., Wright, A. von & Ouwehand, A. *Lactic Acid Bacteria: Microbiological and Functional Aspects*. 629 (Marcel Dekker, Inc., 2004).

47. Goddard, J. L. & Sokatch, J. R. 2-ketogluconate fermentation by *Streptococcus faecalis*. *J. Bacteriol.* **87,** 844–851 (1963).

48. Willey, J. M., Sherwood, L. M. & Woolverton, C. J. *Prescott's principles of microbiology*. 969 (2009).

49. Snoep, J. L., de Graef, M. R., Teixeira de Mattos, M. J. & Neijssel, O. M. Pyruvate catabolism during transient state conditions in chemostat cultures of *Enterococcus faecalis* NCTC 775: importance of internal pyruvate concentrations and NADH/NAD+ ratios. *J. Gen. Microbiol.* **138,** 2015–20 (1992).

50. Snoep, J. L. *et al.* Differences in sensitivity to NADH of purified pyruvate dehydrogenase complexes of *Enterococcus faecalis*, *Lactococcus lactis*, *Azotobacter vinelandii* and *Escherichia coli*: implications for their activity in vivo. *FEMS Microbiol. Lett.* **114,** 279–83 (1993).

51. Ward, D. E. *et al.* Catabolism of Branched-Chain α-Keto Acids in *Enterococcus faecalis*: the bkd Gene Cluster , Enzymes and Metabolic Route. *J. Bacteriol.* **181,** 5433–5442 (1999).

52. Schmidt, H. L., Stöcklein, W., Danzer, J., Kirch, P. & Limbach, B. Isolation and properties of an H2O-forming NADH oxidase from *Streptococcus faecalis*. *Eur. J. Biochem.* **156,** 149–55 (1986).

53. Smart, J. B. & Thomas, T. D. Effect of oxygen on lactose metabolism in lactic Streptococci. *Appl. Environ. Microbiol.* **53,** 533–541 (1987).

54. Sarantinopoulos, P., Kalantzopoulos, G. & Tsakalidou, E. Citrate Metabolism by *Enterococcus faecalis* FAIR-E 229. **67,** 5482–5487 (2001).

55. Lindmark, D., Paolella, P. & Wood, N. P. The Pyruvate Formate-lyase System of *Streptococcus faecalis*. **244,** (1969).

56. Snoep, J. L. *et al.* Isolation and characterisation of the pyruvate dehydrogenase complex of anaerobically grown *Enterococcus faecalis* NCTC 775. *Eur. J. Biochem.* **203,** 245–50 (1992).

57. Cocaign-bousquet, M., Garrigues, C., Loubiere, P. & Lindley, N. D. Physiology of pyruvate metabolism in *Lactococcus lactis*. *Antonie Van Leeuwenhoek* **70,** 253–267 (1996).

58. Yamazaki, A., Watanabe, R., Nishimura, Y. & Kamihara, T. Mutants of *Streptococcus faecalis* concerning pyruvate dehydrogenation. in **64,** 364–368 (1976).

59. Winstedt, L., Frankenberg, L., Hederstedt, L. & von Wachenfeldt, C. *Enterococcus faecalis* V583 contains a cytochrome bd-type respiratory oxidase. *J. Bacteriol.* **182,** 3863–6 (2000).

60. Huycke, M. M. *et al.* Extracellular superoxide production by *Enterococcus faecalis* requires demethylmenaquinone and is attenuated by functional terminal quinol oxidases. *Mol. Microbiol.* **42,** 729–40 (2001).

61. Wang, X. *et al. Enterococcus faecalis* induces aneuploidy and tetraploidy in colonic epithelial cells through a bystander effect. *Cancer Res.* **68,** 9909–17 (2008).

62. Murray, B. E. Vancomycin-resistant enterococcal infections. *N. Engl. J. Med.* **342,** 710–21 (2000).

63. Manson, J. M., Hancock, L. E. & Gilmore, M. S. Mechanism of chromosomal transfer of *Enterococcus faecalis* pathogenicity island, capsule, antimicrobial resistance, and other traits. *Proc. Natl. Acad. Sci. U. S. A.* **107,** 12269–74 (2010).

64. Willems, R. J. L., Hanage, W. P., Bessen, D. E. & Feil, E. J. Population biology of Gram-positive pathogens: high-risk clones for dissemination of antibiotic resistance. *FEMS Microbiol. Rev.* **35,** 872–900 (2011).

65. Rubinstein, E. & Keynan, Y. Vancomycin-Resistant Enterococci. *Crit. Care Clin.* **29,** 841–852 (2013).

66. Depardieu, F., Perichon, B. & Courvalin, P. Detection of the van alphabet and identification of enterococci and staphylococci at the species level by multiplex PCR. *J. Clin. Microbiol.* **42,** 5857–5860 (2004).

67. Boyd, D. a, Willey, B. M., Fawcett, D., Gillani, N. & Mulvey, M. R. Molecular characterization of *Enterococcus faecalis* N06-0364 with low-level vancomycin resistance harboring a novel D-Ala-D-Ser gene cluster, vanL. *Antimicrob. Agents Chemother.* **52,** 2667–72 (2008).

68. Wood, M. J. The comparative efficacy and safety of teicoplanin and vancomycin. *J. Antimicrob. Chemother.* **37,** 209–222 (1996).

69. Devasagayam, T. P. A., Tilak, J. C., Boloor, K. K. & Sane, K. S. Free Radicals and Antioxidants in Human Health : Current Status and Future Prospects R ESEARCH. **52,** (2004).

70. Cabiscol, E., Tamarit, J. & Ros, J. Oxidative stress in bacteria and protein damage by reactive oxygen species. *Int. Microbiol.* **3,** 3–8 (2000).

71. Kohanski, M. A., Dwyer, D. J., Hayete, B., Lawrence, C. A. & Collins, J. J. A common mechanism of cellular death induced by bactericidal antibiotics. *Cell* **130,** 797–810 (2007).

72. Imlay, J. A. Pathways of oxidative damage. *Annu. Rev. Microbiol.* **57,** 395–418 (2003).

73. Flahaut, S., Laplace, J. M., Frère, J. & Auffray, Y. The oxidative stress response in *Enterococcus faecalis*: relationship between H2O2 tolerance and H2O2 stress proteins. *Lett. Appl. Microbiol.* **26,** 259–64 (1998).

74. Riboulet, E. *et al.* Relationships between oxidative stress response and virulence in *Enterococcus faecalis*. *J. Mol. Microbiol. Biotechnol.* **13,** 140–6 (2007).

75. Poyart, C., Quesnes, G. & Trieu-Cuot, P. Sequencing the gene encoding manganese-dependent superoxide dismutase for rapid species identification of enterococci. *J. Clin. Microbiol.* **38,** 415–8 (2000).

76. Ross, R. P. & Claiborne, A. Cloning, sequence and overexpression of NADH peroxidase from *Streptococcus faecalis* 10C1. Structural relationship with the flavoprotein disulfide reductases. *J. Mol. Biol.* **221,** 857–71 (1991).

77. Rincé, A., Giard, J. C., Pichereau, V., Flahaut, S. & Auffray, Y. Identification and characterization of gsp65, an organic hydroperoxide resistance (ohr) gene encoding a general stress protein in *Enterococcus faecalis*. *J. Bacteriol.* **183,** 1482–8 (2001).

78. Laplace, J. M., Hartke, A., Giard, J. C. & Auffray, Y. Cloning, characterization and expression of an *Enterococcus faecalis* gene responsive to heavy metals. *Appl. Microbiol. Biotechnol.* **53,** 685–689 (2000).

79. Verneuil, N. *et al.* Implication of (Mn)superoxide dismutase of *Enterococcus faecalis* in oxidative stress responses and survival inside macrophages. *Microbiology* **152,** 2579–89 (2006).

80. Britton, L., Malinowski, D. P. & Fridovich, I. Superoxide dismutase and oxygen metabolism in *Streptococcus faecalis* and comparisons with other organisms. *Microbiology* **134,** 229–236 (1978).

81. Winyard, P. G., Moody, C. J. & Jacob, C. Oxidative activation of antioxidant defence. *Trends Biochem. Sci.* **30,** 453–61 (2005).

82. Janowiak, B. E. & Griffith, O. W. Glutathione synthesis in *Streptococcus agalactiae*. One protein accounts for gamma-glutamylcysteine synthetase and glutathione synthetase activities. *J. Biol. Chem.* **280,** 11829–39 (2005).

83. Patel, M. P., Marcinkeviciene, J. & Blanchard, J. S. *Enterococcus faecalis* glutathione reductase: purification, characterization and expression under normal and hyperbaric O2 conditions. **166,** 155–163 (1998).

84. Carbona, S. La *et al.* Comparative study of the physiological roles of three peroxidases (NADH peroxidase , Alkyl hydroperoxide reductase and Thiol peroxidase) in oxidative stress response , survival inside macrophages and virulence of *Enterococcus faecalis*. **66,** 1148–1163 (2007).

85. Kitano, H. Systems biology: a brief overview. *Science* **295,** 1662–4 (2002).

86. Noble, D. Modeling the heart--from genes to cells to the whole organ. *Science* **295,** 1678–82 (2002).

87. Schneider, H.-C. & Klabunde, T. Understanding drugs and diseases by systems biology? *Bioorg. Med. Chem. Lett.* **23,** 1168–76 (2013).

88. Kreeger, P. K. & Lauffenburger, D. a. Cancer systems biology: a network modeling perspective. *Carcinogenesis* **31,** 2–8 (2010).

89. Pujol, A., Mosca, R., Farrés, J. & Aloy, P. Unveiling the role of network and systems biology in drug discovery. *Trends Pharmacol. Sci.* **31,** 115–23 (2010).

90. Ideker, T., Galitski, T. & Hood, L. A new approach to decodinh life: Systems biology. (2001).

91. Nikiforova, V. J. *et al.* Towards dissecting nutrient metabolism in plants: a systems biology case study on sulphur metabolism. *J. Exp. Bot.* **55,** 1861–70 (2004).

92. Shasha, D. E., Coruzzi, G. M. & Gutie, R. A. Systems Biology for the Virtual Plant. **138,** 550–554 (2005).

93. Peter V. Minorsky. Achieving the *in silico* plant. Systems biology and the future of plant biological research. *Plant Physiol* **132,** 404–409 (2003).

94. Patil, K. R., Akesson, M. & Nielsen, J. Use of genome-scale microbial models for metabolic engineering. *Curr. Opin. Biotechnol.* **15,** 64–9 (2004).

95. Oberhardt, M. A., Palsson, B. Ø. & Papin, J. A. Applications of genome-scale metabolic reconstructions. *Mol. Syst. Biol.* **5,** 320 (2009).

96. Förster, J., Famili, I., Fu, P., Palsson, B. Ø. & Nielsen, J. Genome-scale reconstruction of the *Saccharomyces cerevisiae* metabolic network. *Genome Res.* **13,** 244–53 (2003).

97. Oliveira, A. P., Nielsen, J. & Förster, J. Modeling *Lactococcus lactis* using a genome-scale flux model. *BMC Microbiol.* **5,** 39 (2005).

98. Barrett, C. L., Kim, T. Y., Kim, H. U., Palsson, B. Ø. & Lee, S. Y. Systems biology as a foundation for genome-scale synthetic biology. *Curr. Opin. Biotechnol.* **17,** 488–92 (2006).

99. Saeidi, N. *et al.* Engineering microbes to sense and eradicate *Pseudomonas aeruginosa*, a human pathogen. *Mol. Syst. Biol.* **7,** 521 (2011).

100. Purnick, P. E. M. & Weiss, R. The second wave of synthetic biology: from modules to systems. *Nat. Rev. Mol. Cell Biol.* **10,** 410–22 (2009).

101. Feist, A. M., Herrgård, M. J., Thiele, I., Reed, J. L. & Palsson, B. Ø. Reconstruction of biochemical networks in microorganisms. *Nat. Rev. Microbiol.* **7,** 129–43 (2009).

102. Papoutsakis, E. T. & Meyer, C. L. Fermentation equations for propionic-acid bacteria and production of assorted oxychemicals from various sugars. *Biotechnol. Bioeng.* **27,** 67–80 (1985).

103. Papoutsakis, E. T. & Meyer, C. L. Equations and calculations of product yields and preferred pathways for butanediol and mixed-acid fermentations. *Biotechnol. Bioeng.* **27,** 50–66 (1985).

104. Kim, H. U., Kim, T. Y. & Lee, S. Y. Genome-scale metabolic network analysis and drug targeting of multi-drug resistant pathogen *Acinetobacter baumannii* AYE. *Mol. Biosyst.* **6,** 339 (2010).

105. Henry, C. S., Zinner, J. F., Cohoon, M. P. & Stevens, R. L. iBsu1103: a new genome-scale metabolic model of *Bacillus subtilis* based on SEED annotations. *Genome Biol.* **10,** R69 (2009).

106. Raghunathan, A., Shin, S. & Daefler, S. Systems approach to investigating host-pathogen interactions in infections with the biothreat agent Francisella. Constraints-based model of *Francisella tularensis*. *BMC Syst. Biol.* **4,** 118 (2010).

107. Edwards, J. S. Systems Properties of the *Haemophilus influenzae* Rd Metabolic Genotype. *J. Biol. Chem.* **274,** 17410–17416 (1999).

108. Schilling, C. H. & Palsson, B. O. Assessment of the metabolic capabilities of *Haemophilus influenzae* Rd through a genome-scale pathway analysis. *J. Theor. Biol.* **203,** 249–83 (2000).

109. Schilling, C. H. *et al.* Genome-Scale Metabolic Model of *Helicobacter pylori* 26695. *Society* **184,** 4582–4593 (2002).

110. Thiele, I., Vo, T. D., Price, N. D. & Palsson, B. O. Expanded Metabolic Reconstruction of *Helicobacter pylori* (iIT341 GSM/GPR): an *In silico* Genome-Scale Characterization of Single- and Double-Deletion Mutants. *J. Bacteriol.* **187,** 5818–5830 (2005).

111. Liao, Y.-C. *et al.* An Experimentally Validated Genome-Scale Metabolic Reconstruction of *Klebsiella pneumoniae* MGH 78578, iYL1228. *J. Bacteriol.* **193,** 1710–1717 (2011).

112. Jamshidi, N. & Palsson, B. Ø. Investigating the metabolic capabilities of *Mycobacterium tuberculosis* H37Rv using the *in silico* strain iNJ661 and proposing alternative drug targets. *BMC Syst. Biol.* **1,** 26 (2007).

113. Beste, D. J. V *et al.* GSMN-TB: a web-based genome-scale network model of *Mycobacterium tuberculosis* metabolism. *Genome Biol.* **8,** R89 (2007).

114. Fang, X., Wallqvist, A. & Reifman, J. Development and analysis of an in vivo-compatible metabolic network of *Mycobacterium tuberculosis*. *BMC Syst. Biol.* **4,** 160 (2010).

115. Suthers, P. F. *et al.* A genome-scale metabolic reconstruction of *Mycoplasma genitalium*, iPS189. *PLoS Comput. Biol.* **5,** e1000285 (2009).

116. Baart, G. J. *et al.* Modeling Neisseria meningitidis metabolism: from genome to metabolic fluxes. *Genome Biol.* **8,** R136 (2007).

117. Mazumdar, V., Snitkin, E. S., Amar, S. & Segrè, D. Metabolic network model of a human oral pathogen. *J. Bacteriol.* **191,** 74–90 (2009).

118. Oberhardt, M. a, Puchałka, J., Fryer, K. E., Martins dos Santos, V. a P. & Papin, J. a. Genome-scale metabolic network analysis of the opportunistic pathogen *Pseudomonas aeruginosa* PAO1. *J. Bacteriol.* **190,** 2790–803 (2008).

119. Raghunathan, A., Reed, J., Shin, S., Palsson, B. & Daefler, S. Constraint-based analysis of metabolic capacity of *Salmonella typhimurium* during host-pathogen interaction. *BMC Syst. Biol.* **3,** 38 (2009).

120. AbuOun, M. *et al.* Genome scale reconstruction of a Salmonella metabolic model: comparison of similarity and differences with a commensal *Escherichia coli* strain. *J. Biol. Chem.* **284,** 29480–8 (2009).

121. Thiele, I. *et al.* A community effort towards a knowledge-base and mathematical model of the human pathogen *Salmonella typhimurium* LT2. *BMC Syst. Biol.* **5,** 8 (2011).

122. Becker, S. A. & Palsson, B. Ø. Genome-scale reconstruction of the metabolic network in *Staphylococcus aureus* N315: an initial draft to the two-dimensional annotation. *BMC Microbiol.* **5,** 8 (2005).

123. Heinemann, M., Kümmel, A., Ruinatscha, R. & Panke, S. *In silico* genome-scale reconstruction and validation of the *Staphylococcus aureus* metabolic network. *Biotechnol. Bioeng.* **92,** 850–64 (2005).

124. Lee, D.-S. *et al.* Comparative genome-scale metabolic reconstruction and flux balance analysis of multiple *Staphylococcus aureus* genomes identify novel antimicrobial drug targets. *J. Bacteriol.* **191,** 4015–24 (2009).

125. Borodina, I., Krabben, P. & Nielsen, J. Genome-scale analysis of *Streptomyces coelicolor* A3(2) metabolism. *Genome Res.* **15,** 820–9 (2005).

126. Alam, M. T. *et al.* Metabolic modeling and analysis of the metabolic switch in *Streptomyces coelicolor*. *BMC Genomics* **11,** 202 (2010).

127. Kim, H. U. *et al.* Integrative genome-scale metabolic analysis of *Vibrio vulnificus* for drug targeting and discovery. *Mol. Syst. Biol.* **7,** 460 (2011).

128. Navid, A. & Almaas, E. Genome-scale reconstruction of the metabolic network in *Yersinia pestis,* strain 91001. *Mol. Biosyst.* **5,** 368 (2009).

129. Charusanti, P. *et al.* An experimentally-supported genome-scale metabolic network reconstruction for *Yersinia pestis* CO92. *BMC Syst. Biol.* **5,** 163 (2011).

130. Morgan, R. W. Hydrogen Peroxide-Inducible Proteins in *Salmonella typhimurium* Overlap with Heat Shock and Other Stress Proteins. *Proc. Natl. Acad. Sci.* **83,** 8059–8063 (1986).

131. Burgard, A. P., Pharkya, P. & Maranas, C. D. Optknock: a bilevel programming framework for identifying gene knockout strategies for microbial strain optimization. *Biotechnol. Bioeng.* **84,** 647–57 (2003).

132. Patil, K. R., Rocha, I., Förster, J. & Nielsen, J. Evolutionary programming as a platform for *in silico* metabolic engineering. *BMC Bioinformatics* **6,** 308 (2005).

133. Rocha, I. *et al.* OptFlux: an open-source software platform for *in silico* metabolic engineering. *BMC Syst. Biol.* **4,** 45 (2010).

134. Thiele, I. & Palsson, B. Ø. A protocol for generating a high-quality genome-scale metabolic reconstruction. *Nat. Protoc.* **5,** 93–121 (2010).

135. Henry, C. S. *et al.* High-throughput generation, optimization and analysis of genome-scale metabolic models. *Nat. Biotechnol.* **28,** 977–82 (2010).

136. Rocha, I., Förster, J. & Nielsen, J. in *Microb. gene essentiality - Protoc. Bioinforma.* **416,** 409–431 (2008).

137. Schilling, C. H. & Palsson, B. O. The underlying pathway structure of biochemical reaction networks. *Proc. Natl. Acad. Sci. U. S. A.* **95,** 4193–8 (1998).

138. Raman, K. & Chandra, N. Flux balance analysis of biological systems: applications and challenges. *Brief. Bioinform.* **10,** 435–49 (2009).

139. Hoskisson, P. a & Hobbs, G. Continuous culture--making a comeback? *Microbiology* **151,** 3153–9 (2005).

140. Herbert, D., Elsworth, R. & Telling, R. C. The continuous culture of bacteria; a theoretical and experimental study. *J. Gen. Microbiol.* **14,** 601–622 (1956).

141. Miller, W. M., Blanch, H. W. & Wilke, C. R. A kinetic analysis of hybridoma growth and metabolism in batch and continuous suspension culture: effect of nutrient concentration, dilution rate, and pH. *Biotechnol. Bioeng.* **32,** 947–65 (1988).

142. Tweeddale, H., Notley-McRobb, L. & Ferenci, T. Effect of Slow Growth on Metabolism of *Escherichia coli*, as Revealed by Global Metabolite Pool "Metabolome" Analysis. *J. Bacteriol.* **180,** 5109–5116 (1998).

143. Shigematsu, T. *et al.* Effect of dilution rate on metabolic pathway shift between aceticlastic and nonaceticlastic methanogenesis in chemostat cultivation. *Appl. Environ. Microbiol.* **70,** 4048–52 (2004).

144. Villas-Bôas, S. G., Roessner, U., Hansen, M. A. E., Smedsgaard, J. & Nielsen, J. *Metabolome analysis - An introduction*. 284 (wiley interscience, 2007).

145. Nielsen, J. & Oliver, S. The next wave in metabolome analysis. *Trends Biotechnol.* **23,** 544–6 (2005).

146. Fiehn, O. Metabolomics-the link between genotypes and phenotypes. *Plant Mol. Biol.* **48,** 155–71 (2002).

147. Phelps, T. J., Palumbo, A. V & Beliaev, A. S. Metabolomics and microarrays for improved understanding of phenotypic characteristics controlled by both genomics and environmental constraints. *Curr. Opin. Biotechnol.* **13,** 20–24 (2002).

148. Van der Werf, M. J., Jellema, R. H. & Hankemeier, T. Microbial metabolomics: replacing trial-and-error by the unbiased selection and ranking of targets. *J. Ind. Microbiol. Biotechnol.* **32,** 234–52 (2005).

149. Devantier, R., Scheithauer, B., Villas-Bôas, S. G., Pedersen, S. & Olsson, L. Metabolite profiling for analysis of yeast stress response during very high gravity ethanol fermentations. *Biotechnol. Bioeng.* **90,** 703–14 (2005).

150. Wishart, D. S. Applications of metabolomics in drug discovery and development. *Drugs R. D.* **9,** 307–22 (2008).

151. Van Gulik, W. M. Fast sampling for quantitative microbial metabolomics. *Curr. Opin. Biotechnol.* **21,** 27–34 (2010).

152. Bolten, C. J., Kiefer, P., Letisse, F., Portais, J.-C. & Wittmann, C. Sampling for metabolome analysis of microorganisms. *Anal. Chem.* **79,** 3843–9 (2007).

153. Koning, W. de & Dam, K. van. A method for the determination of changes of glycolytic metabolites in yeast on a subsecond time scale using extraction at neutral pH. *Anal. Biochem.* **204,** 118–123 (1992).

154. Canelas, A. B. *et al.* Leakage-free rapid quenching technique for yeast metabolomics. *Metabolomics* **4,** 226–239 (2008).

155. Wittmann, C., Krömer, J. O., Kiefer, P., Binz, T. & Heinzle, E. Impact of the cold shock phenomenon on quantification of intracellular metabolites in bacteria. *Anal. Biochem.* **327,** 135–9 (2004).

156. Villas-Bôas, S. G. & Bruheim, P. Cold glycerol-saline: the promising quenching solution for accurate intracellular metabolite analysis of microbial cells. *Anal. Biochem.* **370,** 87–97 (2007).

157. Cook, A. M., Urban, E. & Schlegel, H. G. Measuring the concentrations of metabolites in bacteria. *Anal. Biochem.* **72,** 191–201 (1976).

158. Larsson, G. & Törnkvist, M. Rapid sampling, cell inactivation and evaluation of low extracellular glucose concentrations during fed-batch cultivation. *J. Biotechnol.* **49,** 69–82 (1996).

159. Gonzalez, B., François, J. & Renaud, M. A rapid and reliable method for metabolite extraction in yeast using boiling buffered ethanol. *Yeast* **13,** 1347–55 (1997).

160. Weuster-Botz, D. Sampling Tube Device for Monitoring Intracellular Metabolite Dynamics. *Anal. Biochem.* **246,** 225–233 (1997).

161. Schaefer, U., Boos, W., Takors, R. & Weuster-Botz, D. Automated Sampling Device for Monitoring Intracellular Metabolite Dynamics. *Anal. Biochem.* **270,** 88–96 (1999).

162. Jensen, N. B., Jokumsen, K. V & Villadsen, J. Determination of the phosphorylated sugars of the Embden-Meyerhoff-Parnas pathway in *Lactococcus lactis* using a fast sampling technique and solid phase extraction. *Biotechnol. Bioeng.* **63,** 356–62 (1999).

163. Letisse, F. & Lindley, N. D. An intracellular metabolite quantification technique applicable to polysaccharide-producing bacteria. *Biotechnol. Lett.* **22,** 1673–1677 (2000).

164. Buziol, S. *et al.* New bioreactor-coupled rapid stopped-flow sampling technique for measurements of metabolite dynamics on a subsecond time scale. *Biotechnol. Bioeng.* **80,** 632–6 (2002).

165. Mashego, M. R., van Gulik, W. M., Vinke, J. L. & Heijnen, J. J. Critical evaluation of sampling techniques for residual glucose determination in carbon-limited chemostat culture of *Saccharomyces cerevisiae*. *Biotechnol. Bioeng.* **83,** 395–9 (2003).

166. Villas-Bôas, S. G., Højer-Pedersen, J., Akesson, M., Smedsgaard, J. & Nielsen, J. Global metabolite analysis of yeast: evaluation of sample preparation methods. *Yeast* **22,** 1155–69 (2005).

167. Villas-Bôas, S. G., Moxley, J. F., Akesson, M., Stephanopoulos, G. & Nielsen, J. High-throughput metabolic state analysis: the missing link in integrated functional genomics of yeasts. *Biochem. J.* **388,** 669–77 (2005).

168. Faijes, M., Mars, A. E. & Smid, E. J. Comparison of quenching and extraction methodologies for metabolome analysis of *Lactobacillus plantarum*. *Microb. Cell Fact.* **6,** 27 (2007).

169. Link, H., Anselment, B. & Weuster-Botz, D. Leakage of adenylates during cold methanol/glycerol quenching of *Escherichia coli*. *Metabolomics* **4,** 240–247 (2008).

170. Spura, J. *et al.* A method for enzyme quenching in microbial metabolome analysis successfully applied to gram-positive and gram-negative bacteria and yeast. *Anal. Biochem.* **394,** 192–201 (2009).

171. Smart, K. F., Aggio, R. B. M., Van Houtte, J. R. & Villas-Bôas, S. G. Analytical platform for metabolome analysis of microbial cells using methyl chloroformate derivatisation followed by gas chromatography-mass spectrometry. *Nat. Protoc.* **5,** 1709–29 (2010).

172. Cremin, P., Donnelly, D. M. X., Wolfender, J.-L. & Hostettmann, K. Liquid chromatographic-thermospray mass spectrometric analysis of sesquiterpenes of Armillaria (Eumycota: Basidiomycotina) species. *J. Chromatogr. A* **710,** 273–285 (1995).

173. Smits, H. P., Cohen, A., Buttler, T., Nielsen, J. & Olsson, L. Cleanup and Analysis of Sugar Phosphates in Biological Extracts by Using Solid-Phase Extraction and Anion-Exchange Chromatography with Pulsed Amperometric Detection. *Anal. Biochem.* **261,** 36–42 (1998).

174. Le Belle, J. E., Harris, N. G., Williams, S. R. & Bhakoo, K. K. A comparison of cell and tissue extraction techniques using high-resolution 1H-NMR spectroscopy. *NMR Biomed.* **15,** 37–44 (2002).

175. Prasad Maharjan, R. & Ferenci, T. Global metabolite analysis: the influence of extraction methodology on metabolome profiles of *Escherichia coli*. *Anal. Biochem.* **313,** 145–154 (2003).

176. Álvarez-Sánchez, B., Priego-Capote, F. & Castro, M. D. L. de. Metabolomics analysis II. Preparation of biological samples prior to detection. *TrAC Trends Anal. Chem.* **29,** 120–127 (2010).

177. Meyer, H., Weidmann, H. & Lalk, M. Methodological approaches to help unravel the intracellular metabolome of *Bacillus subtilis*. *Microb. Cell Fact.* **12,** 69 (2013).

178. Kawase, N., Tsugawa, H., Bamba, T. & Fukusaki, E. Different-batch metabolome analysis of *Saccharomyces cerevisiae* based on gas chromatography/mass spectrometry. *J. Biosci. Bioeng.* (2013).

179. Hans, M. A., Heinzle, E. & Wittmann, C. Quantification of intracellular amino acids in batch cultures of *Saccharomyces cerevisiae*. *Appl. Microbiol. Biotechnol.* **56,** 776–779 (2001).

180. Castrillo, J. I., Hayes, A., Mohammed, S., Gaskell, S. J. & Oliver, S. G. An optimized protocol for metabolome analysis in yeast using direct infusion electrospray mass spectrometry. *Phytochemistry* **62,** 929–937 (2003).

181. Meyer, H., Liebeke, M. & Lalk, M. A protocol for the investigation of the intracellular *Staphylococcus aureus* metabolome. *Anal. Biochem.* **401,** 250–259 (2010).

182. Tredwell, G. D., Edwards-Jones, B., Leak, D. J. & Bundy, J. G. The development of metabolomic sampling procedures for *Pichia pastoris*, and baseline metabolome data. *PLoS One* **6,** e16286 (2011).

183. Shryock, J. C., Rubio, R. & Berne, R. M. Extraction of adenine nucleotides from cultured endothelial cells. *Anal. Biochem.* **159,** 73–81 (1986).

184. Tremaroli, V. *et al.* Metabolomic investigation of the bacterial response to a metal challenge. *Appl. Environ. Microbiol.* **75,** 719–28 (2009).

185. Kopka, J., Ohlrogge, J. B. & Jaworski, J. G. Analysis of in Vivo Levels of Acyl-Thioesters with Gas Chromatography/Mass Spectrometry of the Butylamide Derivative. *Anal. Biochem.* **224,** 51–60 (1995).

186. Liebeke, M. *et al.* A metabolomics and proteomics study of the adaptation of *Staphylococcus aureus* to glucose starvation. *Mol. Biosyst.* **7,** 1241–53 (2011).

187. Allwood, J. W., Clarke, A., Goodacre, R. & Mur, L. a J. Dual metabolomics: a novel approach to understanding plant-pathogen interactions. *Phytochemistry* **71,** 590–7 (2010).

188. Henderson, J. P. *et al.* Quantitative metabolomics reveals an epigenetic blueprint for iron acquisition in uropathogenic *Escherichia coli*. *PLoS Pathog.* **5,** e1000305 (2009).

189. Soga, T. *et al.* Quantitative metabolome analysis using capillary electrophoresis mass spectrometry. *J. Proteome Res.* **2,** 488–94 (2003).

190. De Carvalho, L. P. S. *et al.* Metabolomics of *Mycobacterium tuberculosis* Reveals Compartmentalized Co-Catabolism of Carbon Substrates. *Chem. Biol.* **17,** 1122–1131 (2010).

191. Yeom, J., Shin, J.-H., Yang, J.-Y., Kim, J. & Hwang, G.-S. 1H NMR-based metabolite profiling of planktonic and biofilm cells in *Acinetobacter baumannii* 1656-2. *PLoS One* **8,** e57730 (2013).

192. Slupsky, C. M. *et al.* Pneumococcal pneumonia: potential for diagnosis through a urinary metabolic profile. *J. Proteome Res.* **8,** 5550–8 (2009).

193. Cascante, M. & Marin, S. Metabolomics and fluxomics approaches. *Essays Biochem.* **45,** 67–82 (2008).

194. Dettmer, K., Aronov, P. A. & Hammock, B. D. Mass spectrometry-based metabolomics. *Mass Spectrom. Rev.* **26,** 51–78 (2007).

195. Christensen, B., Karoly Gombert, A. & Nielsen, J. Analysis of flux estimates based on 13C-labelling experiments. *Eur. J. Biochem.* **269,** 2795–2800 (2002).

196. Dauner, M., Bailey, J. E. & Sauer, U. Metabolic flux analysis with a comprehensive isotopomer model in *Bacillus subtilis*. *Biotechnol. Bioeng.* **76,** 144–56 (2001).

197. Sauer, U. Metabolic networks in motion: 13C-based flux analysis. *Mol. Syst. Biol.* **2,** 62 (2006).

198. Akashi, H. & Gojobori, T. Metabolic efficiency and amino acid composition in the proteomes of *Escherichia coli* and *Bacillus subtilis*. *Proc. Natl. Acad. Sci. U. S. A.* **99,** 3695–700 (2002).

CHAPTER 3

A METABOLOMICS ANALYSIS OF *ENTEROCOCCUS FAECALIS* RESPONSE TO OXIDATIVE STRESS – THE EFFECT OF HYDROGEN PEROXIDE, OXYGEN AND DILUTION RATE

ABSTRACT

Enterococcus faecalis is a lactic acid bacterium that has emerged as an important opportunistic pathogen, particularly in the nosocomial context, due to its proficient acquisition of resistance to a large repertoire of antibiotics. The aim of this study was to explore the metabolic changes occurring in *E. faecalis* AR01/DGVS when exposed to oxidative stress in the form of hydrogen peroxide (H_2O_2). H_2O_2 is best known for its disinfectant properties since it can rapidly dismute into H_2O and O_2 which is a source of oxidative stress. This study also focused on how this response could be influenced by the dilution rate and aeration. The results demonstrate that the stress response of *E. faecalis* to H_2O_2 is dependent on its growth status and environmental conditions. The role of glutathione and benzoic acid is emphasised and particular focus is placed on the redistribution of the carbohydrate flux as a consequence of the effect exerted by H_2O_2 or oxygen. The flux distribution when cells are under stress is driven in an effort to promote NADPH regeneration. Finally, the role of new metabolites, suggested to play an important role in the response to oxidative stress that have not been previously documented in prokaryotes is explored.

Portela, C., Liu, C-H. T., Ferreira, E.C., Rocha, I., Cook, G. M.,Villas-Bôas, S.G., A metabolomics analysis of *Enterococcus faecalis* response to oxidative stress – the effect of hydrogen peroxide, oxygen and dilution rate (To be submitted).

3.1 *INTRODUCTION*

Best known for its role in causing hospital-acquired infections and diverse diseases namely, urinary tract infections, endocarditis, meningitis and bacteraemia among others [1], *Enterococcus faecalis* is an opportunistic bacterium, which naturally inhabits the human and warm-blooded animals' gastrointestinal tract.

Physiological characteristics include the ability to survive heating to 60 ºC for 30 min in neutral medium and in a wide range of pH (from 3.5 to 11), to cope with relatively high salt concentrations (6.5%) and, more interestingly, to resist adaptation challenges; e.g., it has been observed that inducing the organism to grow in the presence of a "low concentration" stress condition, incremented the resistance ability towards a higher concentration of the same stress [2].

The understanding of how *E. faecalis* is able to cope with oxidative stress has been object of study in the past. The presence of oxygen generates unstable and highly reactive intermediates known as "reactive oxygen species" (ROS). These molecules, comprised of superoxide (O_2^-), hydrogen peroxide (H_2O_2), and hydroxyl radical (OH^-), induce adverse effects if allowed to interact with their cellular targets by causing disruption, damage or even cell death. Reactions of oxidative radicals with DNA generate apurinic and apyrimidic sites as well as strand breakage [3]. Furthermore, oxidation of amino acids converts them into various derivatives that generally, if incorporated, inactivate enzymes [4]. Radical oxidants can directly attack membrane fatty acids to elicit lipid peroxidation, which changes membrane fluidity and interferes with membrane properties and membrane-bound protein functions [5].

E. faecalis is generally perceived as a facultative anaerobe that preferentially carries out anaerobic metabolism *via* homolactic fermentative pathways. The lack of essential components from the tricarboxylic acids (TCA) cycle renders the bacterium to rely mainly on glycolysis and the pentose phosphate pathway for energy production [6]. However, studies have shown that *E. faecalis* has the capacity of undergoing aerobic respiration when grown in the presence of haem, due to expression of a cytochrome *bd* complex at the cell surface [7]. Existence of upstream cytoplasmic electron donors, menaquinone and demethylmenaquinone, in the bacterium suggests a functional

electron transport chain (ETC) that allows respiration in *E. faecalis*. The conceptualized model of *E. faecalis* respiratory system is also composed of a putative transporter of hematin for further incorporation into cytochrome *bd* and a fumarate reductase. Demethylmenaquinone (DMK) is reduced to Demethylmenaquinol ($DMKH_2$) by incorporating the cytosolic reducing equivalents through a putative NADH:quinone oxidase. Cytochrome *bd* and fumarate reductase are the final electron acceptors and reduce succinate to fumarate or O_2 to H_2O, respectively [8]. Interestingly, this system has also been implicated in the ability for *E. faecalis* to generate extracellular ROS which has been proposed to exert damages in host cell DNA and a potential trigger for the onset of colorectal cancer [9,10].

The lethal effect caused by antibiotics in bacterial cells has been associated with oxidative stress [11]. Antibacterial drugs mostly fall in three classes: glycopeptides and β-lactams that inhibit the cell wall biosynthesis, the quinolones that inhibit the DNA replication and aminoglycosides that inhibit protein synthesis [12]. Vancomycin belongs to the glycopeptide class of antibiotics and is considered a last resort antibiotic that is applied when the host is sensitive to β-lactam antibiotics or when the strain is resistant to those compounds. The mode of action of vancomycin relies on weakening the cell wall biosynthesis, more specifically by binding to the D-alanyl-D-alanine peptide and blocking the cross linking that confers rigidity to the cell wall [12] (Figure 3.1). Bactericidal drugs also stimulate the production of lethal doses of the hydroxyl radical. The primary drug-target interactions stimulate oxidation of NADH *via* the electron transport chain. Increased activation of the electron transport chain stimulates superoxide formation. Superoxide damages iron-sulfur clusters, releasing ferrous iron which can be oxidised by the Fenton reaction generating hydroxyl radicals damaging DNA, proteins, and lipids, which ultimately result in cell death [13].

A vancomycin resistant strain, reacts to the presence of the antibiotic by altering the peptidoglycan precursor D-ala-D-ala (vancomycin-susceptible) to D-ala-D-lactate (D-lac) which has 1000 times less affinity for vancomycin or D-ala-D-ser (D-ser) that has a seven fold decrease in affinity, therefore allowing the synthesis of the peptidoglycan cross link [14] (Figure 3.1).

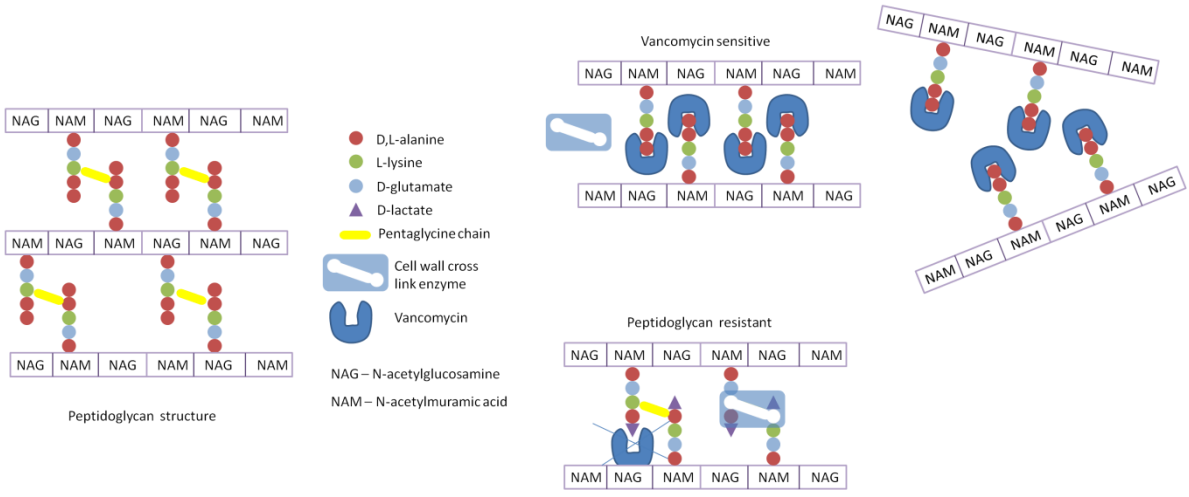

Figure 3.1. Peptidoglycan structure and mechanism of action of vancomycin. The glycan moiety is composed by alternating units of N-acetylglucosamine (NAG) and N-acetylmuramic acid (NAM). Side chain amino acids are connected to the glycan chain. The figure evidences the mechanism by which vancomycin inhibits the peptidoglycan growth by binding the D-alanine moiety on the end of the chain. By doing so, the cross linking is blocked and cell wall synthesis is disrupted. A vancomycin resistant strain, however, is able to synthesise a different moiety than D-alanine (such as D-lactate or D-serine) to which vancomycin is not able to bind due to the different shape and as a consequence, the cross link from may occur.

The antibiotic resistance genes can be found either in the chromosome or harboured in a plasmid. When harboured in a plasmid the transference of the plasmid to other cells can occur *via* conjugation and easily spread antibiotic resistance towards other pathogenic bacteria. These bacteria have the burden of carrying an extra plasmid at the expense of energy consumption, but that confers the organism with antibiotic resistance and therefore, a metabolic advantage towards the others.

In the present study we aim to identify changes in cellular metabolism that occur when an *E. faecalis* vancomycin-sensitive strain is subjected to different forms of oxidative stress that the organism may face, such as hydrogen peroxide, and oxygen with an additional variable imposed by the different dilution rates. Dilution rate *per se* may also constitute a stress factor if considered that at low dilution rates, availability of substrate and vitamins is limited which poses a certain degree of stress, while at high dilution rates the availability of nutrients is higher and thus the cell can freely grow without restrictions. These results will give new insights on the metabolic changes that occur on *E. faecalis* metabolism upon oxidative stress and understand how other variables such

as the dilution rate may contribute to the enhancement of the stress response. This study may contribute to the understanding of how these bacteria can cope with stress conditions and, ultimately, of how they are able to resist to the concomitant action of bactericidal drugs and how to devise new mechanisms to improve the action of these compounds.

3.2 *MATERIAL AND METHODS*

3.2.1 CHEMICALS

Methanol, chloroform, sodium bicarbonate, and sodium hydroxide were obtained from MERCK (Darmstadt, Germany). The internal standard 2,3,3,3-d_4-alanine, the derivatisation reagent methylchloroformate (MCF), pyridine, U-^{13}C glucose, glycerol and vitamin K_2 for menaquinone analysis were purchased from Sigma-Aldrich (St. Louis, USA). Anhydrous sodium sulphate was obtained from Fluka (Steinheim, Germany). All chemicals were of analytical grade.

3.2.2 BACTERIAL STRAIN AND CULTURE CONDITIONS

The bacterial strain used throughout all experiments was *Enterococcus faecalis* AR01/DGVS. The strain is a curated form of a vancomycin resistant strain isolated from a dog with mastitis [15]. The curation involved the removal of the vector, pJM02, which harbours the vancomycin and erythromycin resistance genes, thus rendering a new AR01/DGVS strain vancomycin-sensitive which was used through all experiments.

3.2.3 EXPERIMENTAL DESIGN

E. faecalis was grown under continuous culture supplemented with ^{13}C uniformly labelled (U-^{13}C) glucose with two environmental variables under simultaneous manipulation. The cells were grown either anaerobically (dissolved oxygen of 0 %) or aerobically (20 %) while at the same time at a dilution rate categorised as either low (0.06 h^{-1}) or high (0.11 h^{-1}). Under each of the four conditions, the effect of the H_2O_2 was tested by growing the cells initially in the absence of H_2O_2 and after sampling incorporating 2.4 mM of H_2O_2. The experiments were carried out following the format depicted in Figure 3.2, completed with three biological replicates.

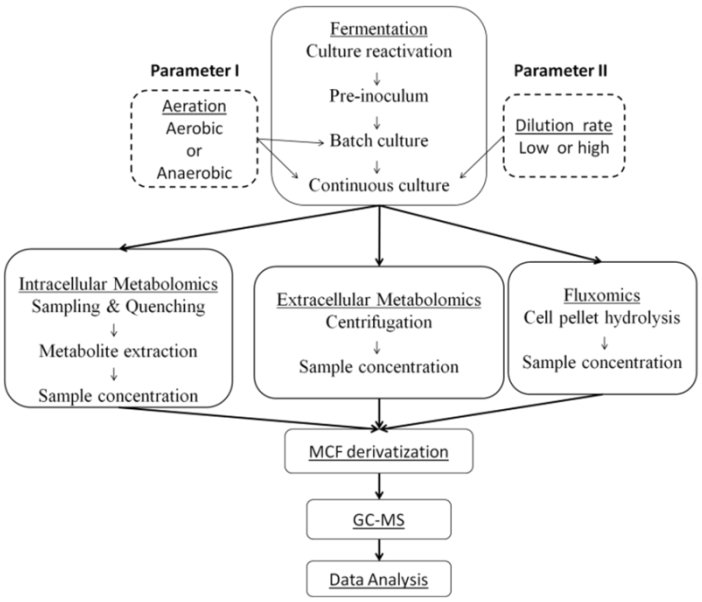

Dilution rate	Anaerobic	Aerobic
Low	3	3
High	3	

Figure 3.2. Overview of the experimental design. Continuous culture was defined by two variables: aeration and dilution rate. Each replicate started with the cells growing in the absence of H_2O_2 and after sampling, H_2O_2 was introduced and sampling process repeated. Samples were taken for intra and extracellular metabolite analysis and carbon labelling experiments.

3.2.4 FERMENTATION

E. faecalis was reactivated from a -80 ºC stock culture immersing a single preservation bead in a microfuge tube containing 200 µL of PBS and mixed vigorously followed by 30 minutes of resting at room temperature. 100 µL of solution was then spread on a tryptone phosphate agar (TPA) plate and grown at 37ºC for 24h. Following this, the cells were re-plated onto new TPA plate under the same conditions to obtain single colonies. TPA agar plates contained peptone (20 g/L), NaCl (5 g/L), glucose (2 g/L), Na_2PO_4 (2.5 g/L), agarose (15 g/L). Pre-inocula were prepared by transferring a single colony of *E. faecalis* growing on TPA plates to TP broth (as described above without agar), followed by overnight aerobic incubation at 37°C and 200 rpm. Subsequently, 50 mL of culture broth were harvested by centrifugation (3000 rpm, 20 min), washed once with 0.9%$_{w/v}$ NaCl solution and re-suspended into batch phase culture medium to be used as the inoculum for the bioreactors. A BioFlo 3000 system (New Brunswick Scientific) was used throughout all experiments with a working volume of 1.5 L. Each fermentation started as a batch phase culture inoculated from the pre-inoculum culture growing at exponential growth phase. The batch phase medium contained: $(NH_4)_2SO_4$

(5 g/L), KH_2PO_4 (6 g/L), $MgSO_4$ (0.5 g/L), hemin chloride (1 mg/L), peptone (2 g/L), glucose (10 g/L), trace metals solution (1 mL/L) comprised of $FeSO_4 \cdot 7H_2O$ (3 g/L), $ZnSO_4 \cdot 7H_2O$ (4.5 g/L), $CaCl_2 \cdot 6H_2O$ (4.5 g/L), $MnCl_2 \cdot 4H_2O$ (l g/L), $CoCl_2 \cdot 6H_2O$ (0.3 g/L), $CuSO_4 \cdot 5H_2O$ (0.3 g/L), $Na_2MoO_4 \cdot 2H_2O$ (0.4 g/L), H_3BO_3 (l g/L), KI (0.l g/L) and Na_2EDTA (15 g/L), and vitamins solution (2 mL/L), which contained riboflavin (0.42 g/L), calcium pantothenate (5.4 g/L), nicotinic acid (6.l g/L), piridoxal ethyl acetal HCl (l.4 g/L), d-biotin (0.06 g/L), folic acid (0.042 g/L), d-thiamine (l g/L) and myo-inositol (12.5 g/L). The working volume of the bioreactors was 1.5 L. Temperature and pH were held constant at 37 °C and 7.0, respectively. The batch phase was carried out until the carbon source (glucose) was exhausted. This was measured using the dinitrosalicylic acid (DNS) reagent [27]. Once the glucose level was depleted, the bioreactor was switched to a continuous culture. Continuous culture was set up using the same medium described for the batch phase except for a glucose concentration of 5 g/L. The continuous culture was left on average for ~2 residence times (time required for the entire volume of the bioreactor to be replaced twice), and then U-^{13}C glucose was fed to the cells at $5\%_{w/w}$ of the total glucose. After a further residence time, samples were then taken for metabolite and ^{13}C-distribution analyses. The bioreactor was then shifted for a further three residence times (with $5\%_{w/w}$ of U-^{13}C glucose being fed to the cells during the final residence time) with a medium containing 2.4 mM H_2O_2 solution ($30\%_{v/v}$). Samples were again harvested under steady state for metabolite and ^{13}C-distribution analyses. Prior to sampling, the OD was monitored to ensure that the cells were in a 'steady state' (constant OD values over three residence times). This procedure was repeated three times (n = 3 chemostats).

3.2.5 SAMPLING AND EXTRACTION PROCEDURE FOR INTRACELLULAR METABOLITE ANALYSIS

The sampling, quenching and intracellular metabolite extraction were based on our previously published protocol [16]. In summary, 50 mL of culture broth, in triplicate, were harvested and quenched from the bioreactors by rapidly mixing the sampled broth with cold glycerol-saline solution (3:2) followed by centrifugation at -20 ^{o}C. The cell pellets were re-suspended in cold glycerol-saline washing solution (1:1) followed by

centrifugation at -20 ^{o}C. Intracellular metabolites were extracted from the cell pellets after addition of cold methanol:water solution (1:1) at -20 ^{o}C and the internal standard (2,3,3,3-d_4-alanine), followed by three freeze-thaw cycles. Samples were then centrifuged (-20 ^{o}C) and the supernatant was collected. The remaining cell pellet was then re-suspended in cold pure methanol (-20 ^{o}C) for a second round of extraction. The mixture was again centrifuged (-20 ^{o}C), the supernatant was collected and pooled to the previous one. The cell pellet was then re-suspended in bi-distilled water, centrifuged and the supernatant collected. 20 mL of cold bi-distilled water (4 ^{o}C) was added to the metabolite extracts, the samples were frozen and subsequently freeze dried using a VirTis freeze-dryer (SP Scientific). The remaining cell debris was used for analysis of ^{13}C-labelled distribution in the biomass-derived amino acids. Only one sample/bioreactor was collected during the transition from anaerobic to aerobic condition every three minutes, with five samples in total per chemostat (n = 3 chemostats).

3.2.6 EXTRACELLULAR METABOLITE ANALYSIS

10 mL of culture was taken from the bioreactor and centrifuged. The supernatant was collected and membrane filtered (0.22 μm pore size). The filtrate was then separated into three aliquots (3 mL) and internal standard (2,3,3,3-d_4-alanine) was added to each of them before they were frozen and subsequently freeze dried on a VirTis freeze-dryer (SP Scientific).

3.2.7 HYDROLYSIS OF PROTEIN BIOMASS FOR AMINO ACID COMPOSITION ANALYSIS

This procedure has been adapted from the Christensen & Nielsen protocol [17]. Following extraction of intracellular metabolites, the remaining cell debris were re-suspended in 100% methanol (l mL) and evaporated to dryness. The cell debris were then hydrolysed using 6 M HCl (1 mL), incubated at 100 °C for 24 h, and then evaporated to dryness using a SpeedVac system (Eppendorf) coupled to a cold trap.

3.2.8 CHEMICAL DERIVATISATION OF METABOLITES AND GC-MS ANALYSIS

Intracellular and extracellular metabolites, and amino acids derived from biomass hydrolysates were made volatile for GC-MS analysis by re-suspending the dry samples in 200 µL of 1M NaOH and derivatised using a methylchloroformate (MCF) method according to our standard laboratorial procedure described previously [16]. The derivatised samples were analysed by GC-MS according to the parameters established previously [18] using a gas chromatograph GC7890 (Agilent Technologies) coupled to a quadrupole mass spectrometer MSD5975 (Agilent Technologies). The GC-capillary column was a Zebron ZB-1701 (Phenomenex) with 30 m × 250 µm (id) × 0.15 µm dimensions, 290 ºC injection temperature, ion source at 70 eV and 230 ºC; and the quadrupole temperature was set to 200 ºC. The carrier gas was helium with a flow of 1 mL/min.

3.2.9 METABOLITE IDENTIFICATION AND DATA ANALYSIS

The metabolite-derivatives detected by GC-MS were identified using the Automated Mass Spectral Deconvolution and Identification System (AMDIS) software. This software was used for deconvolution and identification of chromatographic peaks. To normalise the data, the intensity of each metabolite peak was divided by the intensity of the standard peak (2,3,3,3-d_4-alanine) and also by the amount of biomass in each sample. The statistical analysis was performed using an R package also developed in house [20]. For general pattern identification and to consider the reproducibility of the methods and sample replicates, the software GeneSpring (Agilent Gene Spring MS Proteomics & Metabolomics Analysis 1.1.1 (www.chem.agilent.com) was used based on raw GC-MS data rather than analysis of only identified metabolites.

The data obtained was subjected to multivariate analysis to explore the correlation between the samples and metabolites and which metabolites could better explain the separation of the samples. The multivariate analysis included the determination of biplot principal component analysis (biplot PCA) as a first approach and hierarchical clustering (hclust) analysis to group the data according to its homogeneity or heterogeneity. To fulfil that task, R programming language was used with recourse to packages freely available online.

Also, the statistical significance was accessed by determining the student (t-test) and the results that are significant are presented.

3.2.10 ^{13}C-LABELLING DISTRIBUTION ANALYSIS

^{13}C-labelling patterns in the amino acids derived from the cell pellet hydrolysates were determined by analysing the ratio of ^{13}C to ^{12}C in the major mass fragments generated by MS fragmentation of the respective MCF derivatives. The ratios were compared to those found in natural metabolites (from cells grown in ^{12}C-glucose). Evidence for labelling was determined by an increase in the relative level of ^{13}C-labelling in the metabolites from samples grown in ^{13}C-glucose. The labelling patterns of the amino acids were used to infer changes in the metabolic flux throughout the central carbon metabolism. The labelling pattern analysis was also extended to include an examination of the patterns found within some key intracellular metabolites.

3.3 *RESULTS*

3.3.1 MULTIVARIATE ANALYSIS

Large datasets such as metabolomic datasets, include the measurement of numerous variables. The use of principal component analysis (PCA) may be applied to reduce the dimensionality of the dataset while still retaining much of the information from the original set [21]. The obtained results give a descriptive/exploratory overview of the best two (or three) dimensions that best explain the dataset [22]. A plot of the components can be enhanced by plotting the variables that most influence the PCA distribution in what is known by biplot principal component analysis (biplot PCA) [23]. PCA and biplot PCA are often used as the first step to reduce the data dimensionality before undertaking another multivariate technique such as cluster analysis. A cluster analysis aims to group the data that exhibit high cluster homogeneity (similarity) and high cluster heterogeneity (dissimilarity).

Biplot PCAs for both the intracellular and extracellular data were analysed in order to understand how the samples distribution from a multivariate analysis deviated from the expected distribution of the dataset considering the experimental procedure.

Figure 3.3 and Figure 3.4 evidence a biplot PCA with the two main principal components that assess the similarities and differences between samples.

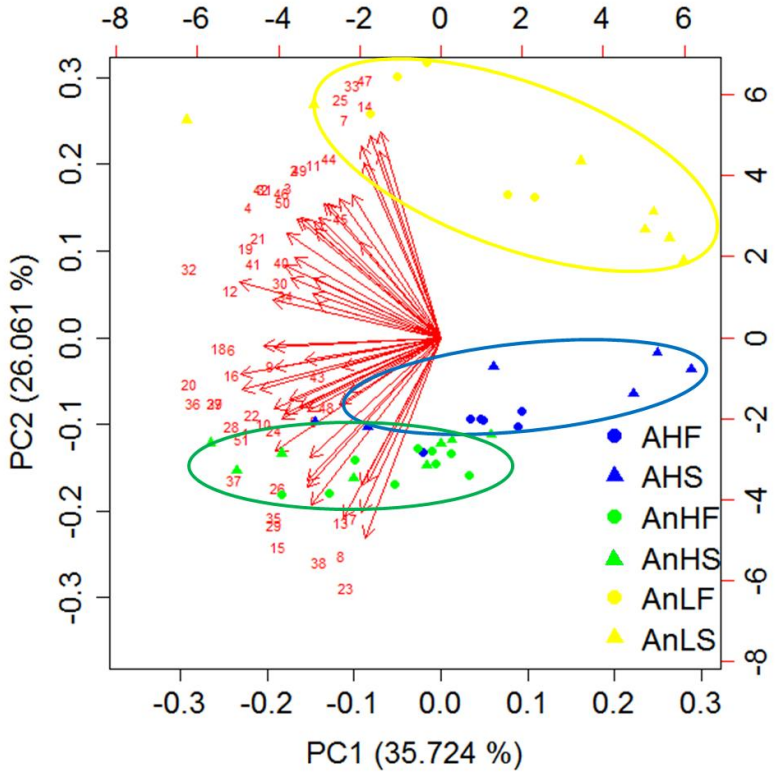

Figure 3.3. Biplot principal component analysis of the intracellular metabolites dataset. Abbreviation list: AHF = Aerobic, High dilution rate, H_2O_2 negative; AHS = Aerobic, High dilution rate, H_2O_2 positive; AnHF = Anaerobic, High dilution rate, H_2O_2 negative; AnHS = Anaerobic, High dilution rate, H_2O_2 positive; AnLF = Anaerobic, Low dilution rate, H_2O_2 negative; AnLS = Anaerobic, Low dilution rate, H_2O_2 positive; 1 = 2-Phosphoenolpyruvic acid; 2 = Alanine; 3 = Asparagine; 4 = Aspartic acid; 5 = Benzoic acid; 6 = Citraconic acid; 7 = Citric acid; 8 = Creatinine; 9 = Cysteine; 10 = Fumaric acid; 11 = Glutamic acid; 12 = Glutathione; 13 = Glycine; 14 = Glyoxylic acid; 15 = Histidine; 16 = Isoleucine; 17 = Lactic acid; 18 = Leucine; 19 = Levulinic acid; 20 = Lysine; 21 = Malonic acid; 22 = N-Acetylglutamic acid; 23 = N-alpha-Acetyllysine; 24 = NADP(H); 25 = Nicotinamide; 26 = Nicotinic acid; 27 = Norvaline; 28 = Ornithine; 29 = Oxalic acid; 30 = para-Toluic acid; 31 = Phenylalanine; 32 = Proline; 33 = Pyroglutamic acid; 34 = Suberic acid; 35 = Succinic acid; 36 = Threonine; 37 = Tryptophan; 38 = Tyrosine; 39 = Valine; 40 = Decanoic acid; 41 = Dodecanoic acid; 42 = Hexanoic acid; 43 = Margaric acid; 44 = Myristic acid; 45 = Myristoleic acid; 46 = Octanoic acid; 47 = Oleic acid; 48 = Palmitic acid; 49 = Palmitoleic acid; 50 = Pentadecanoic acid; 51 = Stearic acid

It can be observed from Figure 3.3 that the sum of the principal component 1 and 2, can only explain 61.7% of the data variability. However, when the third principal component was also plotted, an increment of only about 9% of the data variance could

be explained due to the addition of the third component. Therefore, the biplot represents solely the PC1 and PC2 components since the two still explain the majority of the data variability.

The biplot PCA indicates that there is a high variance of the data over the PC1 but this component is not able to discriminate the different group samples. PC2, on the other hand, explains the differences between the group samples and separates them. The separation brings closer together the samples Aerobic, HDR (AH) and Anaerobic, HDR (AnH) and separates these two from the Anaerobic, LDR (AnL) samples, indicating that the dilution rate is the condition that most influences the variance between the groups. For each group of samples (blue, green and yellow), PC1 seems to be able to distinguish the samples that were under the influence of H_2O_2 (triangles) from those that were not (circles).

The variables that mostly influence the separation of the samples under aerobic condition and high dilution rate (AH, in blue) from the others, evidence a negative correlation, which is observed by the arrows that point in the opposite direction of the samples, thus indicating that these variables influence negatively this group data, causing them to be plotted in the opposite direction along the PC1. The variables that displayed this behaviour are mainly amino acids: 9 = Cysteine; 16 = Isoleucine; 18 = Leucine; 20 = Lysine; 28 = Ornithine; 36 = Threonine; 39 = Valine.

The samples grown under anaerobic conditions at a high dilution rate (AnH, in green) are separated from the others by PC2, with the variables that mostly influence the separation being the amino acids: 13 = Glycine; 15 = Histidine; 37 = Tryptophan; 38 = Tyrosine and also the compounds: 8 = Creatinine; 17 = Lactic acid; 23 = N-alpha-Acetyllysine; 29 = Oxalic acid; 26 = Nicotinic acid; 35 = Succinic acid; 48 = Palmitic acid. Although PC1 evidences the variability within this group, it is not clear the distinction between samples under the presence or absence of H_2O_2.

Samples submitted to an anaerobic environment but at a low dilution rate (AnL, in yellow) are clearly separated from the other groups by PC2, although the variance within the group is diffused along PC1. The samples under H_2O_2 cluster together towards the positive axis of PC1, while the samples that were not submitted to H_2O_2 cluster together towards the negative axis of PC1. The variables that appear to have mainly contributed to the distance of that group were the amino acids: 3 = Asparagine; 4

= Aspartic acid; 11 = Glutamic acid; 33 = Pyroglutamic acid and the fatty acids: 40 = Decanoic acid; 44 = Myristic acid; 47 = Oleic acid; 49 = Palmitoleic acid and 50 = Pentadecanoic acid. Additionally, nicotinamide, glyoxylic acid and citric acid were also responsible for the group division.

For the extracellular analysis, a clear distribution is more evident, with the sum of PC1 and PC2 being able to explain 89.3% of the data variability (Figure 3.4). From the biplot PCA of the extracellular dataset, it is evident that PC1 discriminates the samples that are under oxygen conditions (Aerobic, HDR - AH) from the other groups that were obtained in the absence of oxygen (Anaerobic, HDR - AnH and Anaerobic, LDR - AnL). PC2 is able to further separate the Anaerobic, HDR (AnH) and Anaerobic, LDR (AnL) samples, indicating that the dilution rate is the perturbation that further differentiates these two groups.

For the H_2O_2 factor, however, it does not seem to exist a significant separation. Particularly, for the Anaerobic, HDR (AnH) dataset, despite the fact that, samples cluster closer together, the samples obtained in the presence and absence of H_2O_2 are not distinguishable, i.e., they do not present high variability. The Anaerobic, LDR (AnL) samples present a higher variability described by PC2 but samples subjected to the influence of H_2O_2 are not clearly separated.

Apparently, the variables that best describe the Aerobic, HDR (AH) samples seem to be strongly overlapped in a slightly more distinct group in the overall biplot PCA. This samples point in the direction of the samples separation indicating that these variables have a positive correlation with the Aerobic, HDR (AH) samples, which means they contribute to the separation of these samples. Additionally, these same variables also influence the separation of the Anaerobic, LDR (AnL) samples but with a negative correlation as the arrows (metabolites that contribute to the separation of the samples), point in the opposite direction of the group sample in analysis, i.e., Anaerobic, LDR (AnL).

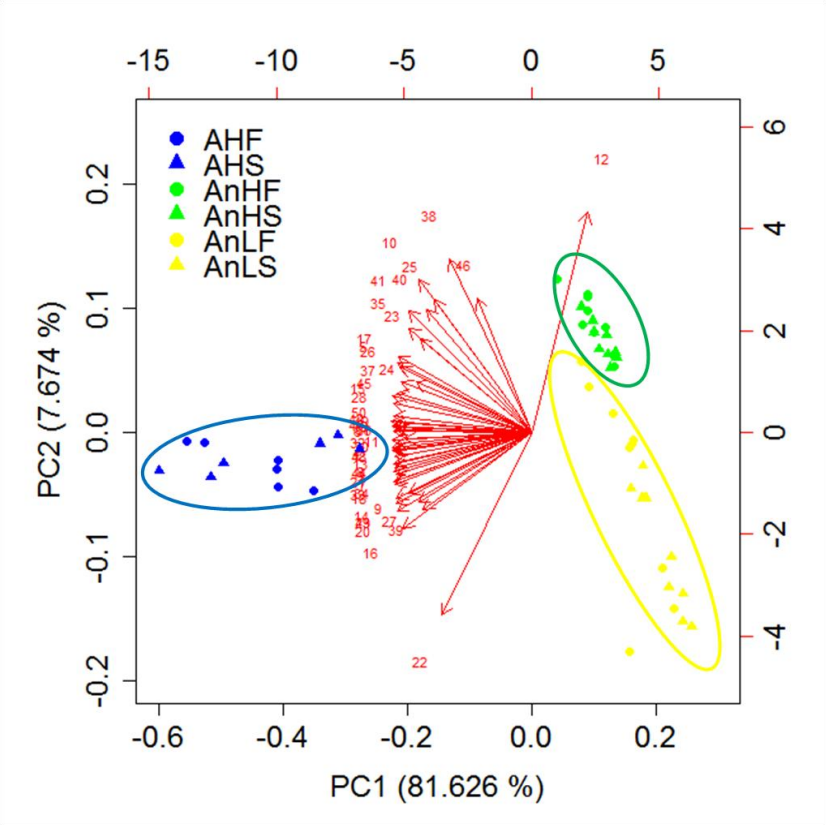

Figure 3.4. Biplot principal component analysis of the extracellular metabolites dataset. Abbreviation list: AHF = Aerobic, High dilution rate, H_2O_2 negative; AHS = Aerobic, High dilution rate, H_2O_2 positive; AnHF = Anaerobic, High dilution rate, H_2O_2 negative; AnHS = Anaerobic, High dilution rate, H_2O_2 positive; AnLF = Anaerobic, Low dilution rate, H_2O_2 negative; AnLS = Anaerobic, Low dilution rate, H_2O_2 positive; 1 = 2-Phosphoenolpyruvic acid; 2 = 3-hydroxybenzoic acid; 3 = 4-aminobutyric acid (gaba); 4 = Alanine; 5 = Asparagine; 6 = Aspartic acid; 7 = Benzoic acid; 8 = Citraconic acid; 9 = citramalic acid; 10 = Citric acid; 11 = Creatinine; 12 = Cysteine; 13 = Glutamic acid; 14 = Glutathione; 15 = Glycine; 16 = Glyoxylic acid; 17 = Histidine; 18 = Isoleucine; 19 = Lactic acid; 20 = Leucine; 21 = Lysine; 22 = Malic acid; 23 = Malonic acid; 24 = Methionine; 25 = N-Acetylglutamic acid; 26 = N-alpha-Acetyllysine; 27 = Nicotinamide; 28 = Nicotinic acid; 29 = Norvaline; 30 = Ornithine; 31 = Oxalic acid; 32 = para-Toluic acid; 33 = Phenylalanine; 34 = Proline; 35 = Pyroglutamic acid; 36 = Pyruvic acid; 37 = Serine; 38 = Succinic acid; 39 = Threonine; 40 = Trans-cinnamic acid; 41 = Tryptophan; 42 = Tyrosine; 43 = Valine; 44 = Decanoic acid; 45 = Dodecanoic acid; 46 = Hexanoic acid; 47 = Myristic acid; 48 = Octanoic acid; 49 = Palmitic acid; 50 = Stearic acid.

Although the biplot PCA allow us to understand if the data can actually be separated in different groups not due to chance but due to specific variables conditioning the separation, this analysis is rather descriptive and exploratory and should be complemented with other multivariate analysis such as cluster analysis to discriminate the group of compounds according to their homogeneity and heterogeneity.

Therefore, a hierarchical clustering (hclust) analysis was performed, which sought to build a clustering representation of the differences and similarities among the variables in the present study. Additionally, it also allows establishing correlations of the metabolites' behaviour between the biplot PCA and the dendrogram generated from hclust.

The dendrogram for intracellular metabolites is depicted in Figure 3.5. The methodology utilised the Pearson correlation coefficient to determine the distance matrix (which quantifies the dissimilarities between samples) and considered a cut off of 0.8 and a cut tree of 5 clusters.

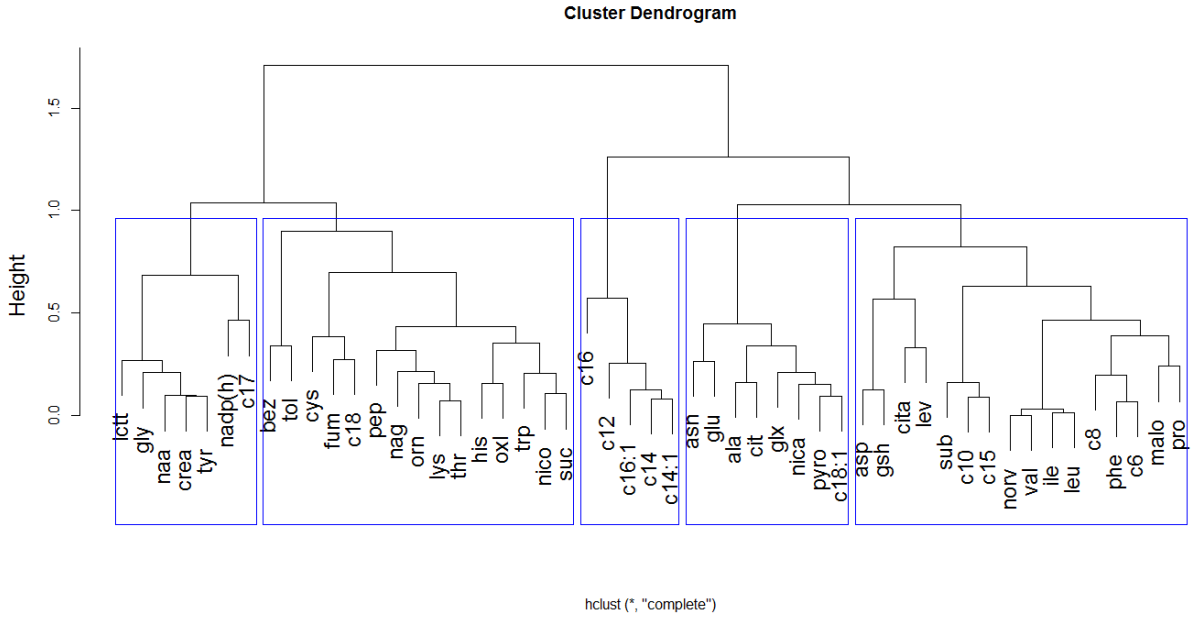

Figure 3.5. Hierarchical cluster (hclust) of the intracellular dataset with a cut-off of 0.8 and a cut tree of 5 clusters. Abbreviation list: ala = Alanine; asn = Asparagine; asp = Aspartic acid; bez = Benzoic acid; c10 = Decanoic acid; c12 = Dodecanoic acid; c14 = Myristic acid; c14:1 = Myristoleic acid; c15 = Pentadecanoic acid ; c16 = Palmitic acid; c16:1 = Palmitoleic acid; c17 = Margaric acid; c18 = Stearic acid; c18:1 = Oleic acid; c6 = Hexanoic acid; c8 = Octanoic acid; cit = Citric acid; cita = Citraconic acid; crea = Creatinine; cys = Cysteine; fum = Fumaric acid; glu = Glutamic acid; glx = Glyoxylic acid; gly = Glycine; gsh = Glutathione; his = Histidine; ile = Isoleucine; lctt = Lactic acid; leu = Leucine; lev = Levulinic acid; lys = Lysine; mal = Malonic acid; naa = N-alpha-Acetyllysine; nadp(h) = NADP_NADPH; nag = N-Acetylglutamic acid; nica = Nicotinamide; nico = Nicotinic acid; norv = Norvaline; orn = Ornithine; oxl = Oxalic acid; pep = 2-Phosphoenolpyruvic acid; phe = Phenylalanine; pro = Proline; pyro = Pyroglutamic acid; sub = Suberic acid; suc = Succinic acid; thr = Threonine; tol = para-Toluic acid; trp = Tryptophan; tyr = Tyrosine; val = Valine.

The picture evidences five main clusters. The information complements the previous biplot PCA by discriminating the variables that are responsible for the separation of the

different groups of samples. The metabolite correlation between the biplot PCA and the hclust is evident when analysing each subset from Figure 3.5, where the displayed variables were also differentiated in the biplot PCA (Figure 3.3). Such an example is given by the first cluster of the hclust (on the left side) where the variables, lactic acid, glycine, N-alpha-acetyllysine, creatinine, tyrosine, NADP(H) and margaric acid are clustered together. However, there is a link that also separates NADP(H) and margaric acid from the other branches of the cluster. When analysing their distribution in the biplot PCA (Figure 3.3), NADP(H) and margaric acid (metabolites nr. 24 and 43) group together but away from the other variables that were also grouped together (metabolites no.: 17, 13, 23, 8 and 38, respectively). These variables are clustered together and are mainly responsible for the separation of the Anaerobic, HDR (AnH) samples (in green). This information is rather relevant as it indicates that, despite these metabolites being all responsible for separating the Anaerobic, HDR (AnH) group, the last two metabolites are more closely related to each other than to the rest of the metabolites in the cluster, which are, on their side, also closely related. Also responsible for the separation of the Anaerobic, HDR (AnH) samples, but with a behaviour different from the previously mentioned group, are the variables that cluster together in the last branch of the second cluster presented in Figure 3.5: histidine (15), oxalic acid (29), tryptophan (37), nicotinic acid (26) and succinic acid (35). This metabolite behaviour is observed along the analysis of the other clusters.

A similar cluster analysis was performed for the extracellular data. Visible in Figure 3.6, the main five clusters were defined for this group of samples, but the division is rather interesting. As depicted in the dendrogram for the extracellular dataset, the cluster division separates the metabolites cysteine (cys) and hexanoic acid (c6) from the remaining compounds. The relevance of these metabolites is supported by the biplot PCA (Figure 3.4), where it is evident a clear distinction of cysteine (no.: 12 in the biplot PCA) from the other variables. This metabolite is responsible for the separation of the samples under the influence of a high dilution rate (AnH) from the samples with a low dilution rate (AnL). On the other hand, hexanoic acid (no.: 46 in the biplot PCA) that, according to the biplot PCA, has a similar discriminating role as succinic acid (allocated to the third cluster), seems to also influence the separation of the Anaerobic, HDR (AnH) samples, as well as a mixture of Anaerobic, LDR, H_2O_2 absence (AnLF) and Anaerobic, LDR, H_2O_2 presence (AnLS) samples (yellow samples).

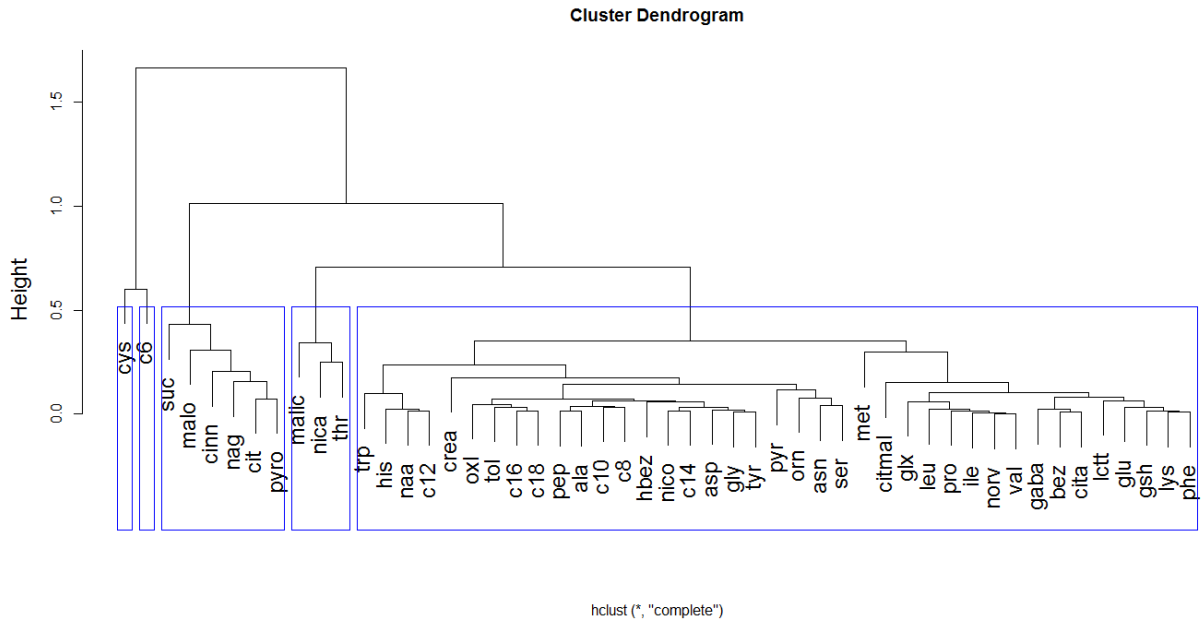

Figure 3.6. Hierarchical cluster (hclust) of the extracellular dataset with a cut-off of 0.8 and a cut tree of 5 clusters. Abbreviation list: ala = Alanine; asn = Asparagine; asp = Aspartic acid; bez = Benzoic acid; c10 = Decanoic acid (C10_0); c12 = Dodecanoic acid (C12_0); c14 = Myristic acid (C14_0); c16 = Palmitic acid (C16_0); c18 = Stearic acid (C18_0); c6 = Hexanoic acid (C6_0); c8 = Octanoic acid (C8_0); cinn = trans-cinnamic acid; cit = Citric acid; cita = Citraconic acid; citmal = citramalic acid; crea = Creatinine; cys = Cysteine; gaba = 4-aminobutyric acid (gaba); glu = Glutamic acid; glx = Glyoxylic acid; gly = Glycine; gsh = Glutathione; hbez = 3-hydroxybenzoic acid; his = Histidine; ile = Isoleucine; lctt = Lactic acid; leu = Leucine; lys = Lysine; malic = malic acid; malo = Malonic acid; met = methionine; naa = N-alpha-Acetyllysine; nag = N-Acetylglutamic acid; nica = Nicotinamide; nico = Nicotinic acid; norv = Norvaline; orn = Ornithine; oxl = Oxalic acid; pep = 2-Phosphoenolpyruvic acid; phe = Phenylalanine; pro = Proline; pyr = pyruvic acid; pyro = Pyroglutamic acid; ser = serine; suc = Succinic acid; thr = Threonine; tol = para-Toluic acid; trp = Tryptophan; tyr = Tyrosine; val = Valine.

The third cluster defined in the dendrogram is composed by the metabolites malonic acid (malo), trans-cinnamic acid (cinn), N-acetylglutamic acid (nag), citric acid (cit) and pyroglutamic acid (pyro), which are also clearly grouped in the biplot PCA, with the respective numbers: 23, 40, 25, 10, and 35. This group seems to be contributing to the separation of the samples further apart in the Anaerobic, LDR (AnL) group (i.e., those samples closer to the positive axis of PC1) but with a negative correlation. In practise, that would correspond to a lower presence of these metabolites in these samples, which would cause the group to be plotted separately from the others that are positively affected by the same variables.

The largest cluster (the fifth) includes many metabolites that do not directly correspond to the groups identified as discriminating in PCA. However, it is possible to understand that the metabolites in this cluster strongly contribute to the separation of the samples obtained in the presence of oxygen (AH) from those that were not. These include creatinine (11), oxalic acid (31), toluic acid (32), palmitic acid (49), stearic acid (50), 2-phosphoenolpyruvic acid (1), alanine(4), decanoic acid (44), octanoic acid (48), 3-hydroxybenzoic acid (2), myristic acid (47), aspartic acid (6), pyruvic acid (36), ornithine (30).

Besides, it was also noticed that a group plotted together in the biplot PCA, composed by the variables: citramalic acid (9), nicotinamide (27), threonine (39), glyoxylic acid (16), leucine (20) and apparently glutathione (14) and valine (43) would be expected to cluster together, as they apparently have a negative correlation with the AnL samples but do contribute to their separation. However, in the dendrogram, it can be noticed that nicotinamide (27) and threonine (39) are clustered together in the fourth cluster in the dendrogram while the others cluster together further away on the fifth cluster. That probably means that, although these compounds contribute to the separation of groups of samples, they do not exhibit a similar behaviour along the conditions tested.

Following the understanding of how and which metabolites have a strong effect on the different datasets and also how they had similar or dissimilar profiles along the conditions tested, the intracellular and extracellular profiles were analysed in deeper detail and the different conditions compared, namely the impact of H_2O_2, O_2 and dilution rate (DR) on *E. faecalis* cells.

3.3.2 INTRACELLULAR METABOLOMICS

Intracellular metabolite samples were taken during two stages of the fermentation that reflected the metabolic state of *E. faecalis* during the absence and presence of H_2O_2 treatment. In addition, the fermentations were further defined by two environmental parameters: aeration and dilution rate. Thus, the experimental design on a grand scale would further allow to study how these variables could influence the oxidative stress response of *E. faecalis*.

After conducting data mining (removal of false positives, internal standard and biomass normalization) on the raw datasets obtained from GC-MS, 51 metabolites were

identified across the three metabolic states (high dilution rate + aerobic; high dilution rate + anaerobic, low dilution rate + anaerobic). These encompass a significant coverage of the central carbon metabolism, constituents of the carbohydrate metabolism, amino acids, fatty acids and carboxylic acids. The list also contains intermediates from various other pathways, including sulphur metabolism, benzoate metabolism and glutamate metabolism.

3.3.2.1 Intracellular response of E. faecalis to H_2O_2

In order to understand how *E. faecalis* responds to H_2O_2 at a metabolic level, comparisons of intracellular metabolite profiles between the two steady states (with and without H_2O_2 in the medium) were made and the main differences induced by the H_2O_2 treatment were pinpointed. To determine how the intracellular metabolome of *E. faecalis* changes due to H_2O_2, the datasets were grouped according to aeration and dilution rate parameters. The results revealed that *E. faecalis* responds to H_2O_2 treatment more prominently when the cells are under anaerobic conditions with a high dilution rate. A lack of major changes in the intracellular metabolite profile was observed under aerobic growth conditions at a high dilution rate (Figure 3.7A) and under an anaerobic environment and the influence of a lower dilution rate (Figure 3.7B). Only two metabolites showed a significant difference in levels due to H_2O_2 presence in those comparisons.

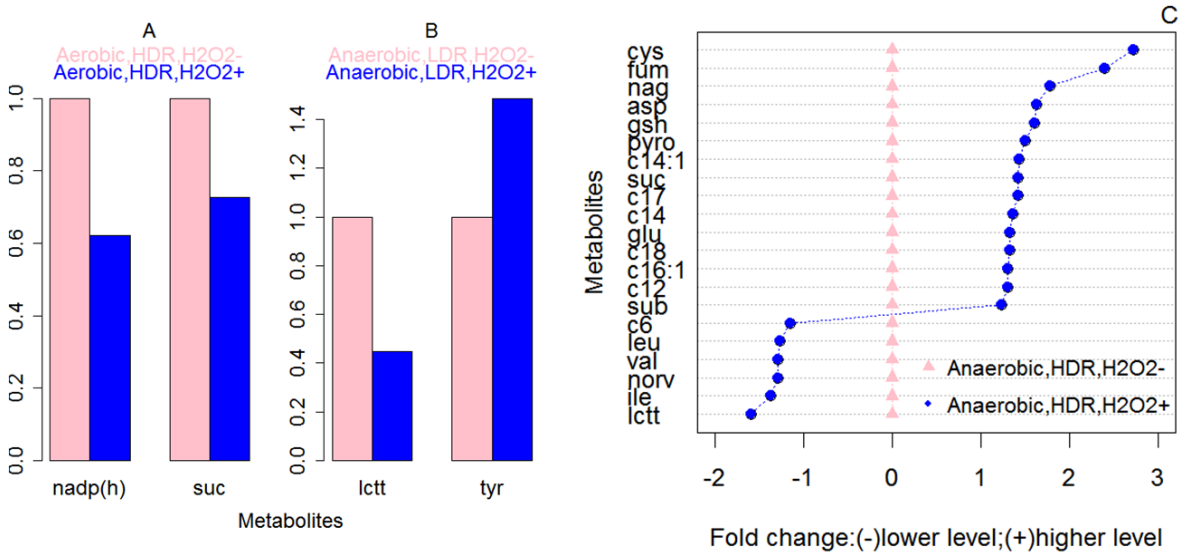

Figure 3.7. Intracellular response of *E. faecalis* to H_2O_2. A – effect of H_2O_2 under aerobic conditions, high dilution rate; B - effect of H_2O_2 under anaerobic conditions, low dilution rate; C - effect of H_2O_2 under anaerobic conditions, high dilution rate. The levels of metabolites were normalised against the internal standard (DL-Alanine-2,3,3,3-d_4) and biomass and adjusted against relative levels under absence of H_2O_2. For figure C, the fold change was displayed differently for ease of visualization. Only metabolites with a statistically significant difference (*p-value* < 0.05) are shown. Abbreviations: asp = Aspartic acid, c6 = Hexanoic acid, c12 = Dodecanoic acid, c14 = Myristic acid, c14:1 = Myristoleic acid, c16:1 = Palmitoleic acid, c17 = Margaric acid, c18 = Stearic acid, cys = Cysteine, fum = Fumaric acid, glu = Glutamic acid, gsh = Glutathione, ile = Isoleucine, lctt = Lactic acid, leu = Leucine, nadp(h) = NADP(H), nag = N-Acetylglutamic acid, norv = Norvaline, pyro = Pyroglutamic acid, sub = Suberic acid, suc = Succinic acid, tyr = Tyrosine, val = Valine.

A reduction on the intracellular levels of cofactors (NADP, NADPH) and succinic acid was observed during H_2O_2 treatment in aerobic conditions at a high dilution rate (Figure 3.7A). Lactic acid and tyrosine, were identified to have altered abundance, with the former having decreased in level and the latter increased due to H_2O_2 treatment in anaerobic conditions and at low a dilution rate (Figure 3.7B).

When grown under anaerobic conditions with a high dilution rate, 21 metabolites were identified to be at statistically different levels between the absence and presence of H_2O_2 (Figure 3.7C). 15 metabolites, including glutathione, fumaric acid, succinic acid, amino acids (cysteine, aspartic acid, valine, pyroglutamic acid) and fatty acids (myristic acid, dodecanoic acid, stearic acid, margaric acid, palmitoleic acid, myristoleic acid) were present at a significantly higher level when *E. faecalis* grew in the presence of H_2O_2. On the other hand, lactic acid, the major product from fermentation by lactic acid bacteria, was at lower levels under H_2O_2 treatment. Three amino acids (valine, leucine, and isoleucine) also had their levels decreased.

3.3.2.2 Intracellular response of E. faecalis to aeration

The effect of aeration on the metabolism of *E. faecalis* was next analysed. Under a high dilution rate and absence of H_2O_2, 30 metabolites were identified to have had their levels significantly affected by the presence of 20 % dissolved oxygen during cultivation (Figure 3.8A).

Among those, margaric acid levels appeared to have been the most affected, with an increase of over 2-fold. An increase in level was also observed for the amino acids aspartic acid and glycine, and fatty acids, myristic, myristoleic and palmitoleic acid. In

addition, glutathione, citric acid and fumaric acid, evidenced a similar behaviour. The remaining metabolites, on the other hand, showed reduced levels.

The list encompasses succinic acid, ten amino acids and two metabolites associated with glutamate metabolism (ornithine and N-acetyl-L-glutamate). Nicotinic acid, a derivative of pyrimidines, the building blocks for DNA and RNA synthesis were also part of this group. Finally, benzoate showed the most dramatic reduction in levels in response to oxygen.

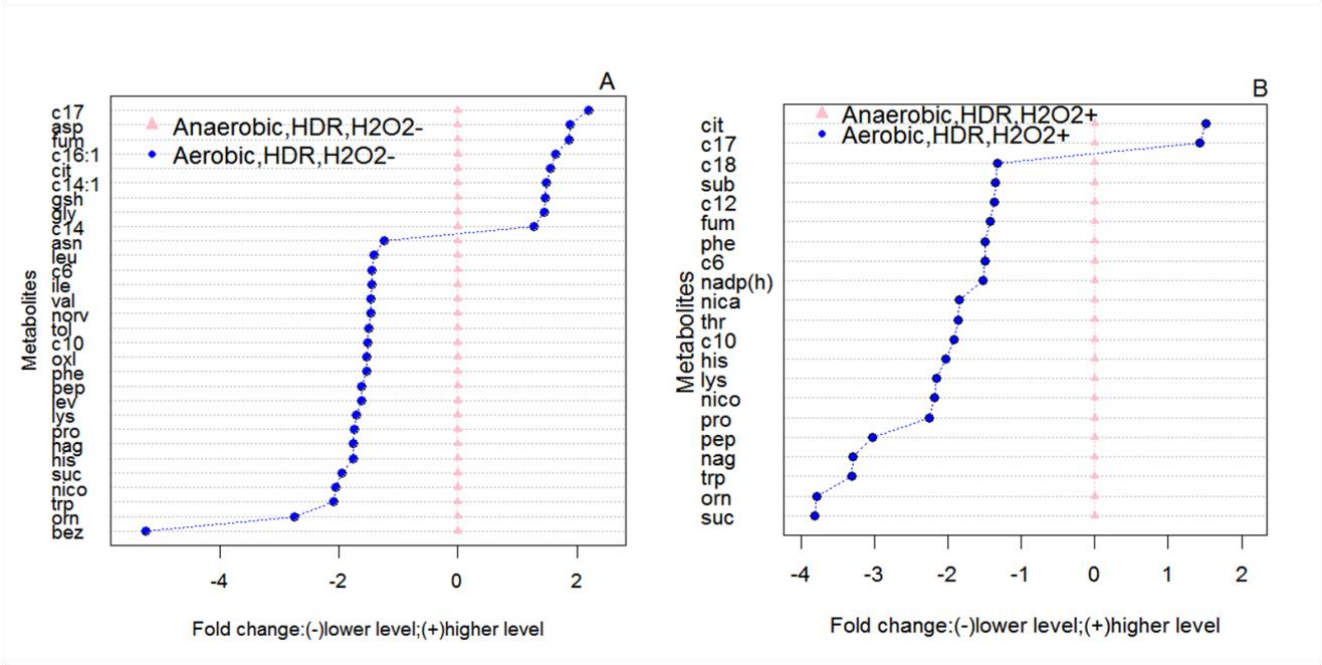

Figure 3.8. Intracellular response of *E. faecalis* to O_2. A – effect of O_2 under a high dilution rate and absence of H_2O_2; B – effect of O_2 under a high dilution rate and presence of H_2O_2. The levels of the metabolites were normalised against the internal standard (DL-Alanine-2,3,3,3-d_4) and biomass and adjusted against relative levels under anaerobic conditions. Only metabolites with statistically significant differences (p-*value* < 0.05) are shown. Abbreviation list: pep = 2-Phosphoenolpyruvic acid, asn = Asparagine, asp = Aspartic acid, bem = Benzoic acid, cit = Citric acid, c10 = Decanoic acid, fum = Fumaric acid, gsh = Glutathione, gly = Glycine, c6 = Hexanoic acid, his = Histidine, ile = Isoleucine, leu = Leucine, lev = Levulinic acid, lys = Lysine, c17 = Margaric acid, c14 = Myristic acid, c14:1 = Myristoleic acid, nag = N-Acetylglutamic acid, nico = Nicotinic acid, norv = Norvaline, orn = Ornithine, oxl = Oxalic acid, c16:1 = Palmitoleic acid, tol = para-Toluic acid, phe = Phenylalanine, pro = Proline, suc = Succinic acid, trp = Tryptophan, val = Valine, nadp(h) = NADP(H), nica = Nicotinamide, sub = Suberic acid, thr = Threonine.

Conversely, when examining the effects of aeration while the cells were under stress exerted by H_2O_2, 21 metabolites were identified to have significant different levels

(Figure 3.8B). However, the number of metabolites that has showed an increase in their levels was reduced (only two) and were margaric acid and citric acid. It is interesting to note that the inclusion of an H_2O_2 perturbation has generated small changes in metabolite levels due to aeration. Also interesting to note, was that both citric acid and margaric acid (c17) increased their levels intracellularly both in the presence and absence of H_2O_2.

3.3.2.3 Intracellular response of E. faecalis to the dilution rate.

Similarly, we investigated how *E. faecalis* responded metabolically to different growth rates. Under anaerobic conditions with no H_2O_2, the levels for 28 metabolites appeared to be at statistically different levels when comparing growth at low and high dilution rates (Figure 3.9A). 22 metabolites showed an increase in level when the cells were growing at a high dilution rate. Among these, half were amino acids. N-acetylglutamic acid and histidine showed the highest increase in levels in response to the dilution rate. On the other hand, pyroglutamic acid, nicotinamide, oleic acid, citric acid, glyoxylic acid and myristic acid had their levels reduced at a high dilution rate.

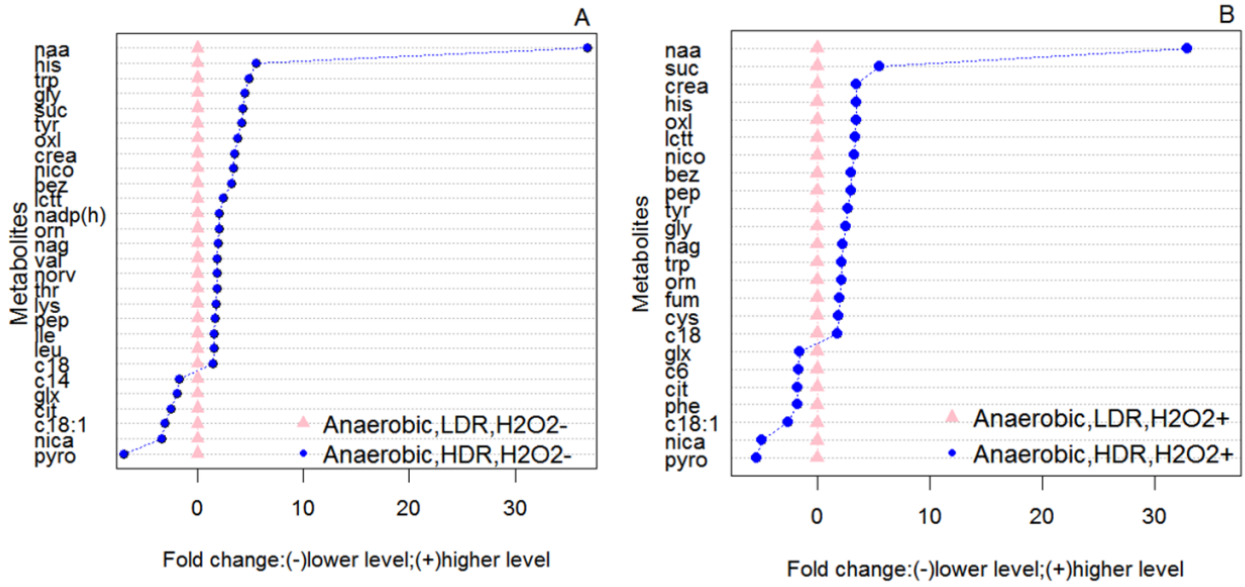

Figure 3.9. Intracellular response of *E. faecalis* to the dilution rate. A – effect of the dilution rate under anaerobic conditions and absence of H_2O_2; B - effect of the dilution rate under anaerobic conditions and presence of H_2O_2. The levels of metabolites were normalised against the internal standard (DL-Alanine-2,3,3,3-d_4) and biomass and adjusted against relative levels of LDR

conditions. Only metabolites with statistically significant differences (*p-value* < 0.05) are shown. Abbrevation list: pep = 2-Phosphoenolpyruvic acid, bez = Benzoic acid, cit = Citric acid, crea = Creatinine, gly = Glycine, glx = Glyoxylic acid, his = Histidine, ile = Isoleucine, lctt = Lactic acid, leu = Leucine, lys = Lysine, nag = N-Acetylglutamic acid, naa = N-alpha-Acetyllysine, nadp(h) = NADP_NADPH, nica = Nicotinamide, nico = Nicotinic acid, norv = Norvaline, orn = Ornithine, oxl = Oxalic acid, pyro = Pyroglutamic acid, suc = Succinic acid, thr = Threonine, trp = Tryptophan, tyr = Tyrosine, val = Valine, c14 = Myristic acid, c18:1 = Oleic acid, c18 = Stearic acid, cys = Cysteine, fum = Fumaric acid, gly = Glycine, glx = Glyoxylic acid, his = Histidine, lctt = Lactic acid, phe = Phenylalanine, c6 = Hexanoic acid.

The intracellular metabolite profiles of cells grown anaerobically under high and low dilution rates, but in the presence of H_2O_2 were compared next. Again, the results suggest dilution rate has a noticeable impact on cellular metabolism (Figure 3.9B). Out of the 24 metabolites identified to be at statistically significant different levels, 17 have shown to be more abundant under a high dilution rate.

The overall behaviour of cells under a high dilution rate seems to be an up regulation of all pathways and therefore higher production of the majority of the compounds identified with statistical significance. It suggests that, more than a response to an imposed stress condition exerted by H_2O_2, an evident change in the metabolism may be caused by increased growth rates.

3.3.3 EXTRACELLULAR METABOLOMICS

Extracellular samples were also taken during the two metabolic steady states. Changes in the exometabolome occur slower and less pronounced than in the endometabolome and could hence represent valuable information to sustain intracellular data. After conducting data mining on the raw data, 50 metabolites were identified across all datasets (high dilution rate + aerobic; high dilution rate + anaerobic, low dilution rate + anaerobic). It is however important to realise that interpretation of extracellular metabolomic data is not straightforward. This is because changes in extracellular metabolite levels may be attributed to either the enzymatic breakdown of complex macromolecules in the medium (e.g., peptone), or the consumption or secretion by the cells. Nevertheless, they would offer support to complement the intracellular information presented previously.

3.3.3.1 Extracellular response of E. faecalis to H_2O_2

Similarly to the intracellular metabolic profiles, we first examined the changes in the metabolic profile obtained from extracellular samples that can be attributed to the effect of H_2O_2 treatment. Again, we could see the response of *E. faecalis* to H_2O_2 is highly influenced by the two environmental variables (oxygen and dilution rate). Under aerobic conditions at a high dilution rate, only three metabolites were detected at significantly different levels in response to H_2O_2, namely citramalic acid, methionine and malonic acid. Both citramalic acid and methionine lowered their secretion levels while malonic acid evidenced an increase in the secretion levels.

Greater changes in extracellular profiles due to the presence of H_2O_2 were observed under anaerobic growth at a high dilution rate (Figure 3.10B). The amino acids cysteine, glutamic acid, methionine, histidine and tryptophan have seen their secretion levels decrease. Tyrosine and 2-phosphoenolpyruvic acid requirements seem to have increased due to H_2O_2 presence, as these metabolites were consumed from the medium. Other metabolites that evidenced a decrease in their levels were 4-aminobutyric acid (gaba), lactic acid, malonic acid, pyruvic acid and hexanoic acid. The metabolites N-acetylglutamic acid, oxalic acid and 3-hydroxybenzoic acid were the only metabolites that exhibited increased levels due to the presence of H_2O_2.

A rather similar behaviour was noticed under the effect of H_2O_2 on *E. faecalis* cells grown at a low dilution rate (Figure 3.10C). Ten out of fifteen identified metabolites in this condition were common to the previous condition (anaerobic, high dilution rate) and also exhibited a similar trend. In particular, the metabolites, 4-aminobutyric acid (gaba), cysteine, glutamic acid, lactic acid, methionine, hexanoic acid and histidine had their levels decreased while 3-hydroxybenzoic had its level increased. The effect of H_2O_2 was more evident for tryptophan that was secreted to the medium in the absence of H_2O_2 while, in the presence of the stress condition, it was consumed (with a 7 fold change difference), suggesting the consumption of this amino acid may be a response towards the effect exerted by H_2O_2. Additionally, oxalic acid, was consumed both in the presence and absence of the stress imposed by H_2O_2.

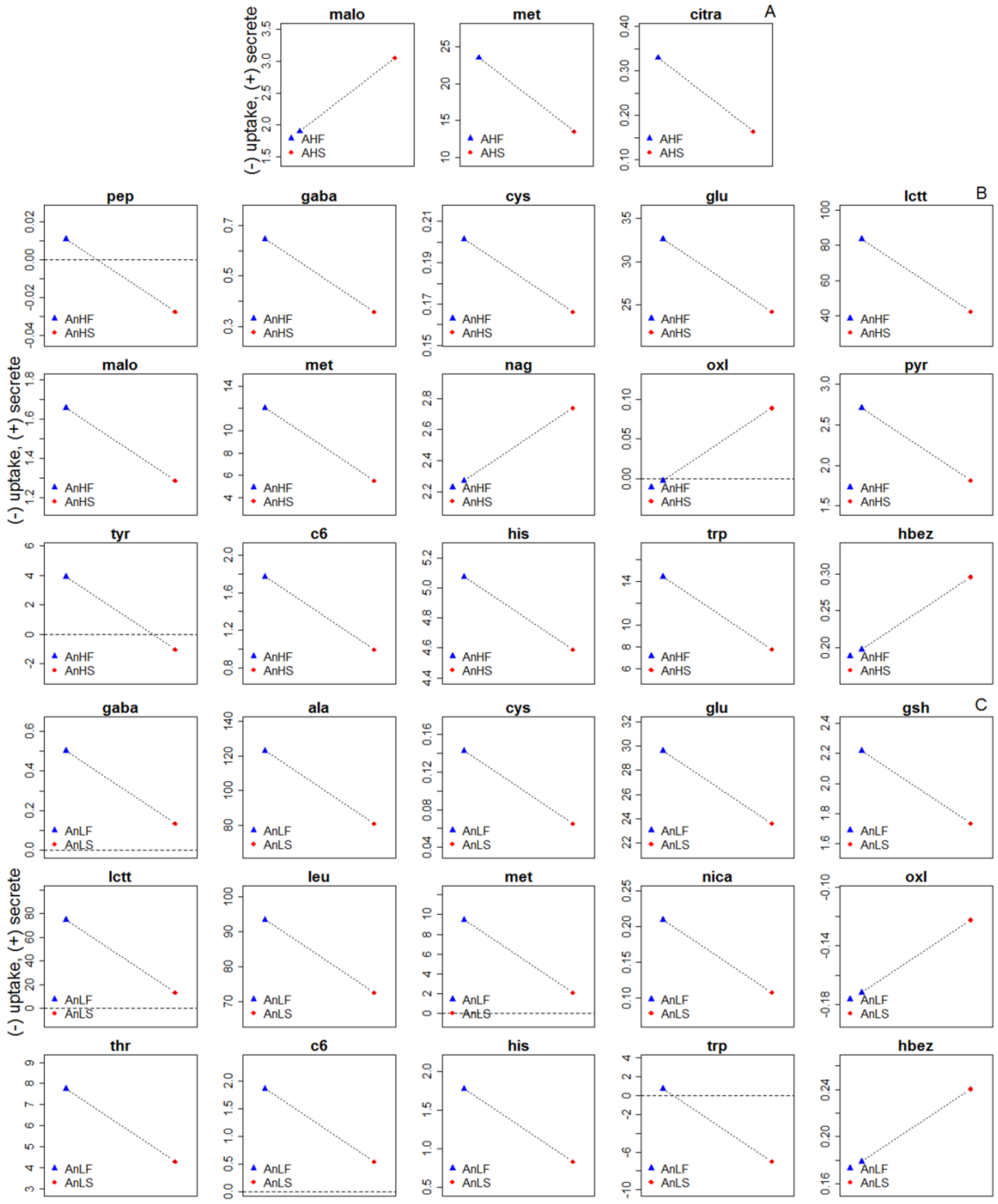

Figure 3.10. Extracellular response of *E. faecalis* to H_2O_2. A – effect of H_2O_2 under aerobic conditions, high dilution rate; B - effect of H_2O_2 under anaerobic conditions, high dilution rate; C - effect of H_2O_2 when under anaerobic conditions, low dilution rate. The levels of metabolites were subtracted to the non-inoculated medium and normalised against the internal standard (DL-Alanine-2,3,3,3-d_4) and biomass. Only metabolites with statistically significant differences (*p-value* < 0.05) are shown. Abbreviation list: AHF = Aerobic, High dilution rate, H_2O_2 negative; AHS = Aerobic, High dilution rate, H_2O_2 positive; AnHF = Anaerobic, High dilution rate, H_2O_2 negative; AnHS = Anaerobic, High dilution rate, H_2O_2 positive; AnLF = Anaerobic, Low dilution rate, H_2O_2 negative; AnLS = Anaerobic, Low dilution rate, H_2O_2 positive; pep = 2-Phosphoenolpyruvic acid; hbez = 3-Hydroxybenzoic acid; gaba = 4-Aminobutyric acid; ala = Alanine; asn = Asparagine; asp = Aspartic acid; bez = Benzoic acid; cita = Citraconic acid;

citra = Citramalic acid; cit = Citric acid; crea = Creatinine; cys = Cysteine; glu = Glutamic acid; gsh = Glutathione; gly = Glycine; glx = Glyoxylic acid; his = Histidine; ile = Isoleucine; lctt = Lactic acid; leu = Leucine; lys = Lysine; malic = Malic acid; malo = Malonic acid; met = Methionine; nag = N-Acetylglutamic acid; nica = Nicotinamide; nico = Nicotinic acid; norv = Norvaline; orn = Ornithine; oxl = Oxalic acid; tol = para-Toluic acid; phe = Phenylalanine; pro = Proline; pyro = Pyroglutamic acid; pyr = Pyruvic acid; ser = Serine; suc = Succinic acid; thr = Threonine; cinn = trans-Cinnamic acid; trp = Tryptophan; tyr = Tyrosine; val = Valine; c10 = Decanoic acid; c12 = Dodecanoic acid; c6 = Hexanoic acid; c14 = Myristic acid; c8 = Octanoic acid; c16 = Palmitic acid; c18 = Stearic acid.

3.3.3.2 Extracellular response of E. faecalis to aeration

From the analysis of the extracellular data, we observed that the presence of H_2O_2 did not have an impact on the extracellular profile of *E. faecalis* since the metabolite profile under the presence or absence of H_2O_2 is highly similar (Figure 3.11). That indicates that an additional stress condition did not exert supplementary pressure on the cells. The effect of oxygen, *per se*, on the other hand, had a significant impact on the extracellular profile of the cells. From a total amount of 52 metabolites detected, 48 were detected to have their levels changed with statistical significance. From the list, 18 compounds were amino acids, and 7 were fatty acids. All amino acids, other than cysteine, behaved similarly, with an increase in the secreted levels as a consequence of oxygen tension. Also, from the list of identified metabolites, all other metabolites were detected in higher levels due to the influence of the dissolved oxygen. Interestingly, the presence of H_2O_2 in addition to oxygen caused subtle changes in the detected metabolites. The additional presence of hexanoic acid and malonic acid and absence of trans-cinnamic acid mark the difference between the two sets. The presence and absence of oxygen has also caused some different metabolite profiles that were either consumed or secreted according to the condition exposed. Secretion of serine and malic acid occurred in the absence of H_2O_2 and presence of oxygen while in the absence of both H_2O_2 and oxygen these compounds were consumed. In the presence of H_2O_2 and under oxygen influence, additionally to serine and malic acid, glyoxylic acid was also secreted. These compounds were all being consumed when in the absence of oxygen tension.

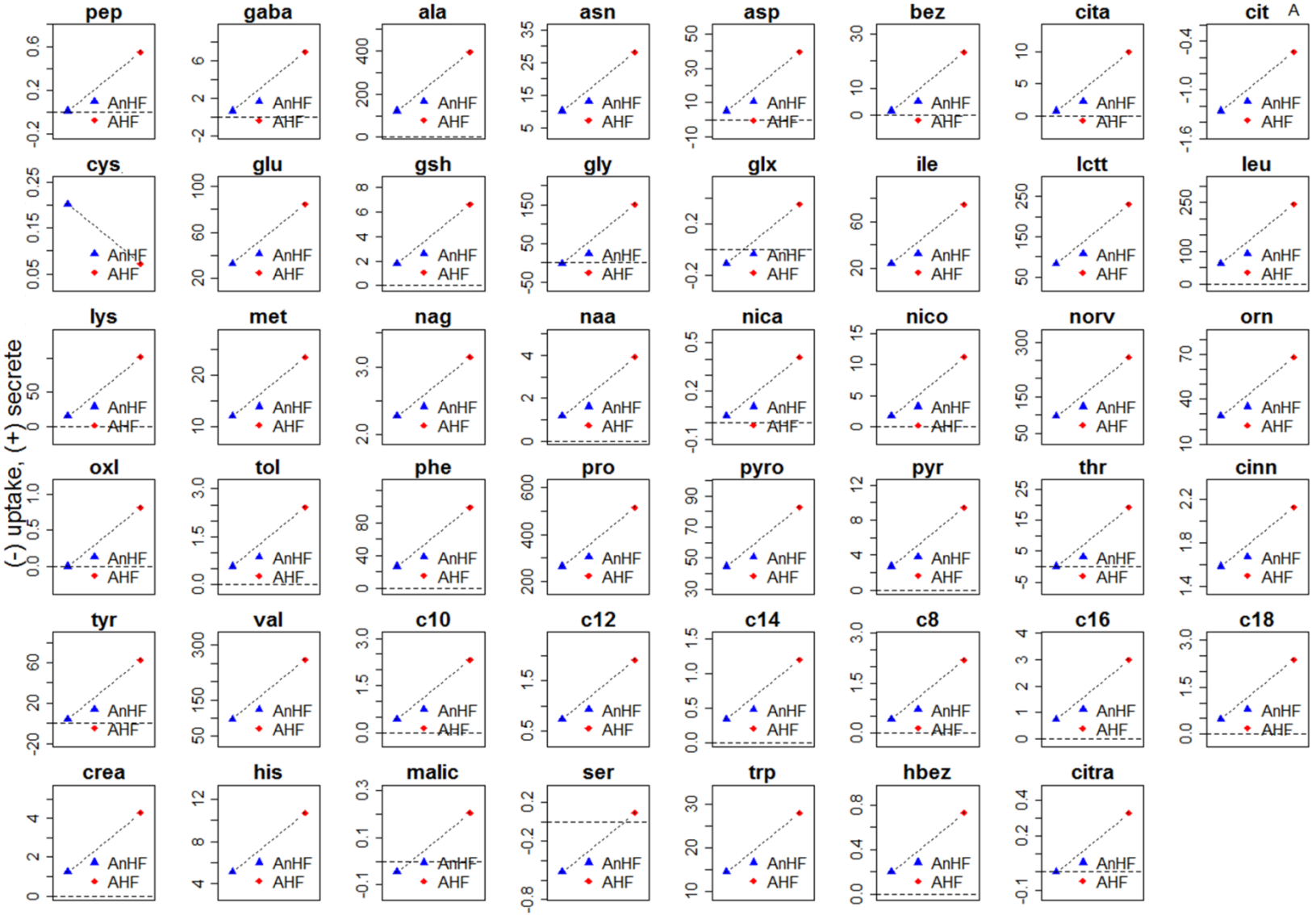
pep
gaba
ala
asn
asp
bez
cita
cit
cys
glu
gsh
gly
glx
ile
lctt
leu
lys
met
nag
naa
nica
nico
norv
orn
oxl
tol
phe
pro
pyro
pyr
thr
cinn
tyr
val
c10
c12
c14
c8
c16
c18
crea
his
malic
ser
trp
hbez
citra
AnHF
AHF
(-) uptake, (+) secrete

Figure 3.11. Extracellular response of *E. faecalis* to O_2. A – effect of O_2 under a high dilution rate and absence of H_2O_2; B - effect of O_2 under a high dilution rate and presence of H_2O_2. The levels of metabolites were subtracted to the non-inoculated medium and normalised against the internal standard (DL-Alanine-2,3,3,3-d_4) and biomass. Only metabolites with statistically significant differences (*p-value* < 0.05) are shown.Abbreviation list: AnHF = Anaerobic, High dilution rate, H_2O_2 negative; AHF = Aerobic, High dilution rate, H_2O_2 negative; AnHS = Anaerobic, High dilution rate, H_2O_2 positive; AHS = Aerobic, High dilution rate, H_2O_2 positive; pep = 2-Phosphoenolpyruvic acid; hbez = 3-Hydroxybenzoic acid; gaba = 4-Aminobutyric acid; ala = Alanine; asn = Asparagine; asp = Aspartic acid; bez = Benzoic acid; cinn = trans-cinnamic acid; cita = Citraconic acid; citra = Citramalic acid; cit = Citric acid; crea = Creatinine; cys = Cysteine; glu = Glutamic acid; gsh = Glutathione; gly = Glycine; glx = Glyoxylic acid; his = Histidine; ile = Isoleucine; lctt = Lactic acid; leu = Leucine; lys = Lysine; mali = Malic acid; mal = Malonic acid; met = Methionine; nag = N-Acetylglutamic acid; naa = N-alpha-Acetyllysine; nica = Nicotinamide; nico = Nicotinic acid; norv = Norvaline; orn = Ornithine; oxl = Oxalic acid; tol = para-Toluic acid; phe = Phenylalanine; pro = Proline; pyro = Pyroglutamic acid; pyr = Pyruvic acid; ser = Serine; thr = Threonine; trp = Tryptophan; tyr = Tyrosine; val = Valine; c10 = Decanoic acid; c12 = Dodecanoic acid; c6 = Hexanoic acid; c14 = Myristic acid; c8 = Octanoic acid; c16 = Palmitic acid; c18 = Stearic acid.

3.3.3.3 Extracellular response of E. faecalis to the dilution rate

Under anaerobic growth conditions in the absence of H_2O_2 perturbation, 30 extracellular metabolites were identified to be statistically different when comparing different growth rates triggered by altering the dilution rate (Figure 3.12A).

Eleven out of thirty metabolites showed an elevated secretion level when the cells were grown at a high dilution rate. Among those, six were amino acids and four fatty acids. On the other hand, Leucine, nicotinamide and threonine were all secreted to the medium, however, at lower levels in response to increased dilution rate.

A group of metabolites have also exhibited a different profile when in the different conditions by either being consumed or secreted. From that list, 2-phosphoenolpyruvic acid, N-alpha-acetyllysine (naa), nicotinic acid (nico) and stearic acid (c18), aspartate and tyrosine were consumed from the medium when in a low dilution rate, but secreted to the medium when at a high dilution rate. On the other hand, glyoxylic and malic acids exhibited the opposite pattern by being secreted under a low dilution rate, but consumed when under a high dilution rate.

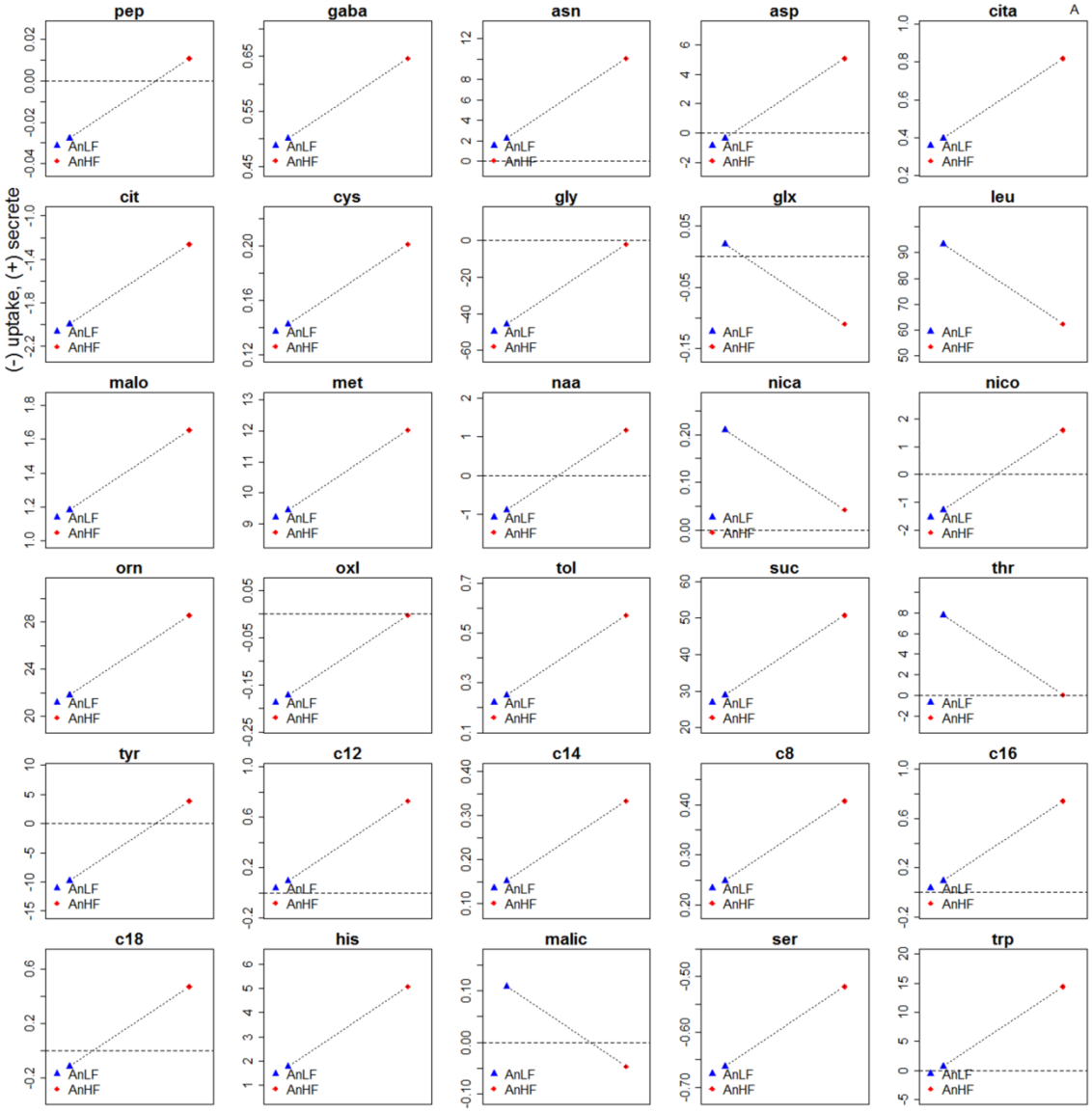
A
(-) uptake, (+) secrete
pep
gaba
asn
asp
cita
cit
cys
gly
glx
leu
malo
met
naa
nica
nico
orn
oxl
tol
suc
thr
tyr
c12
c14
c8
c16
c18
his
malic
ser
trp
AnLF
AnHF

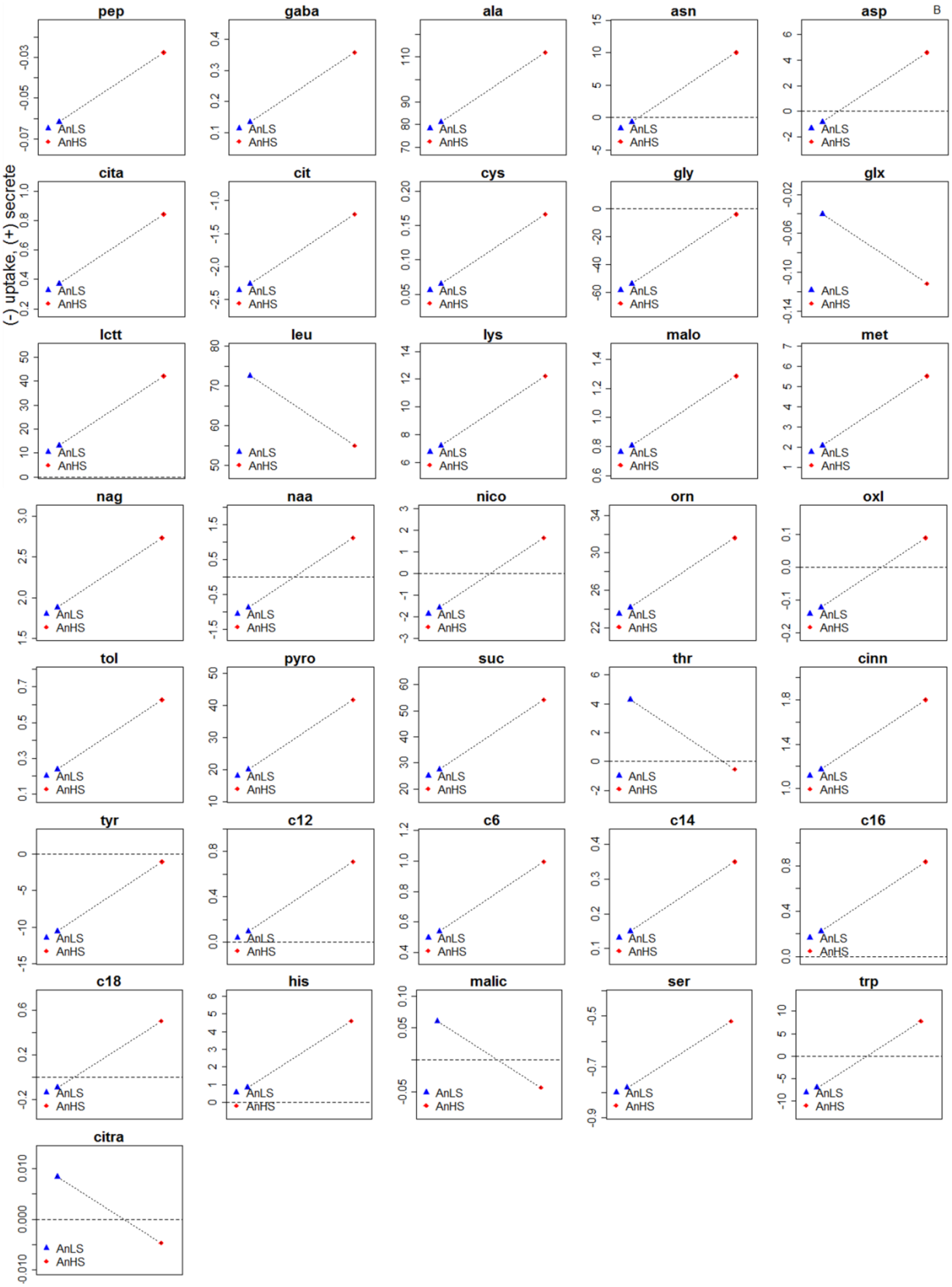

Figure 3.12. Extracellular response of *E. faecalis* to the dilution rate. A – effect of the dilution rate under anaerobic conditions and absence of H_2O_2; B - effect of the dilution rate under anaerobic condition and

presence of H_2O_2. The levels of metabolites were subtracted to the non-inoculated medium and normalised against the internal standard (DL-Alanine-2,3,3,3-d_4) and biomass. Only metabolites with statistically significant differences (*p-value* < 0.05) are shown. Abbreviation list: AnLF = Anaerobic, Low dilution rate, H_2O_2 negative; AnHF = Anaerobic, High dilution rate, H_2O_2 negative; AnLS = Anaerobic, Low dilution rate, H_2O_2 positive; AnHS = Anaerobic, High dilution rate, H_2O_2 positive; pep = 2-Phosphoenolpyruvic acid, gaba = 4-Aminobutyric acid, ala = Alanine, asn = Asparagine, asp = Aspartic acid, cita = Citraconic acid, citra = Citramalic acid, cit = Citric acid, cys = Cysteine, gly = Glycine, glx = Glyoxylic acid, his = Histidine, lctt = Lactic acid, leu = Leucine, lys = Lysine, mali = Malic acid, mal = Malonic acid, met = Methionine, nag = N-Acetylglutamic acid, naa = N-alpha-Acetyllysine, nico = Nicotinic acid, orn = Ornithine, oxl = Oxalic acid, tol = para-Toluic acid, pyro = Pyroglutamic acid, ser = Serine, suc = Succinic acid, thr = Threonine, cinn = trans-Cinnamic acid, trp = Tryptophan, tyr = Tyrosine, c12 = Dodecanoic acid, c6 = Hexanoic acid, c14 = Myristic acid, c16 = Palmitic acid, c18 = Stearic acid.

Interestingly, some metabolites were consumed in both conditions (whether at high or low dilution rates) and comprised the metabolites citric acid, glycine, serine and oxalic acid.

When H_2O_2 was added into the culture medium, more than half of the metabolites detected in the extracellular samples (36 out of 50) were shown to have statistically significant changes in their levels (Figure 3.12B). Furthermore, out of the 36 metabolites, 20 appeared to be secreted at higher levels in response to an increment of the dilution rate. The list encompasses 7 amino acids and four fatty acids.

As observed before, some metabolites have had their profile altered when in the presence of high or low dilution rates. The metabolites, aspartate, asparagine, nicotinic acid (nico), N-alpha-acetyllysine (naa), oxalic acid, stearic acid (c18) and tryptophan were secreted to the medium when at a high dilution rate but were being consumed in a low dilution rate environment. As evidenced before, some metabolites are systematically consumed independently of the dilution rate the cells are growing at, namely citric acid, glycine and serine. Tyrosine replaces oxalic acid in this dataset by also being consumed in both environmental conditions.

3.3.4 ^{13}C LABELLING EXPERIMENTS

To complete the study on how *E. faecalis* responds metabolically to different stress conditions, the metabolic flux distribution based on ^{13}C-labelled substrate was analysed.

Following the analytical techniques described above, we were able to recover a total number of 15 amino acids from the hydrolysed biomass. During acid hydrolysis, cysteine, glutamine, asparagine and tryptophan were lost due to chemical oxidation and degradation. In addition, arginine is not detectable by GC-MS. Afterwards, data mining was performed and ^{13}C-labelling fractions of amino acids for each sample were obtained.

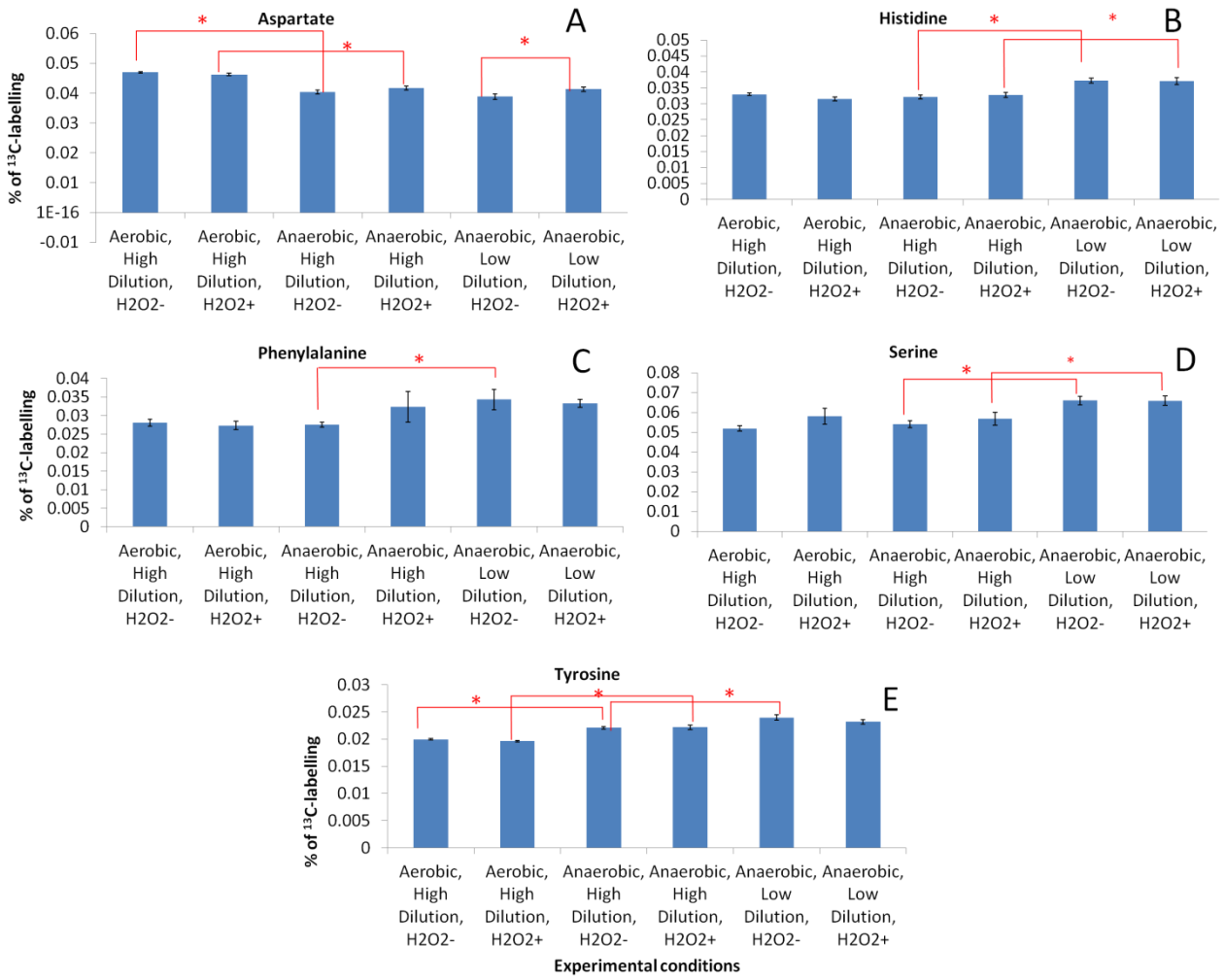

Figure 3.13 Fraction of ^{13}C-labelling in amino acids derived from hydrolysed biomass in each of the conditions analysed. Only amino acids that presented statistically significant differences (* symbol indicates *p-value* < 0.05) in at least one set of the comparisons are shown. Values have been corrected for natural ^{13}C-labelling.

Labelling fractions between experimental conditions were compared in an attempt to gain some insights into how biosynthesis of amino acids from glucose may be affected

by the environmental perturbations examined in this study. Figure 3.13 depicts the five amino acids which were identified to have significant different degrees of labelling in at least one of these comparisons.

The two amino acids which appeared to have their biosynthetic activities altered in response to aeration were aspartic acid and tyrosine (Figure 3.13A and Figure 3.13E), which respectively showed an increase and a decrease in the biosynthetic flux under aerobic conditions. Furthermore, looking at the effects of the dilution rate, we observed an increase in the labelled fraction of histidine, phenylalanine, serine, and tyrosine (Figure 3.13B, Figure 3.13C, Figure 3.13D and Figure 3.13E) when grown at lower dilution rates. Only the biosynthesis of aspartic acid (Figure 3.13A) displayed a significant change while responding to H_2O_2 when *E. faecalis* was growing under anaerobic conditions at a low dilution rate.

As a member of the lactic acid bacteria, one of the major end products generated by *E. faecalis* from glucose metabolism would have been lactate. Therefore, we went on to investigate the labelling patterns found in lactic acid. Here, we examined the fraction labelling of the MS-ion fragment of the MCF-lactic acid derivative corresponding to the fragment containing all three carbons (C1-C3) of lactic acid. Therefore, the increase in m+1 abundance of this fragment would indicate labelling in 1 carbon of lactic acid. Similarly, increase in abundance of m+2 indicate labelling in 2 carbons, and m+3 means in all 3 carbons. Since we have cultured the cells with U-^{13}C glucose, m+3 ion fragment would reflect the amount of lactic acid produced from pyruvic acid synthesised from glycolysis; while m+1 and m+2 ion fragments would correspond to lactic acid produced from pyruvic acid generated from an alternative pathway (i.e. the pentose phosphate pathway) (Figure 3.14). Under anaerobic conditions at a high dilution rate, we observed a significant increase in the percentage of the m+2 ion while the cells were growing in the presence of H_2O_2, but no significant change was verified in the m+1 and m+3 ions (Figure 3.15).

This strongly suggests the cells have increased the amount of glucose going to the pentose phosphate pathway while the amount going through glycolysis was maintained constant. Conversely, when looking at the influence of aeration at a high dilution rate with no H_2O_2 treatment (Figure 3.16), we observed a significant increase in the

percentage of m+3 and m+2 ions found in the aerobic samples compared to the anaerobic samples. This indicates the amount of glucose directing towards glycolysis and the pentose phosphate pathway have both been elevated.

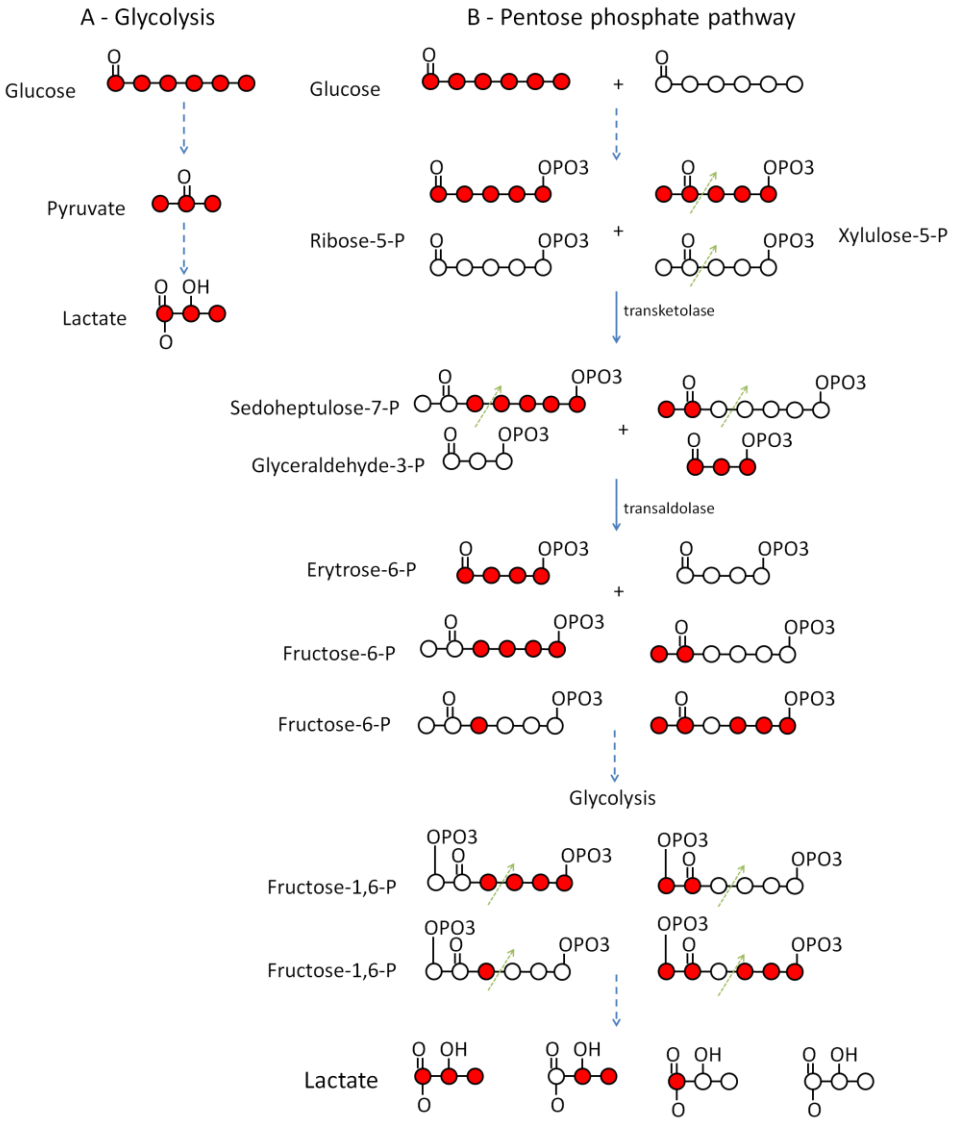

Figure 3.14. Tracking of ^{13}C atom from U-^{13}C glucose to ^{13}C-lactate through glycolysis (A) and the pentose phosphate pathway (B). A: direct flow of ^{13}C through glycolysis. B: flow of ^{13}C through pentose phosphate pathway and then glycolysis. The red dots represent labelled carbons and white dots unlabelled carbons. Full arrows indicate a direct reaction while dashed arrows indicate an omission of steps for easy of visualisation. The distribution presented assumes a mixture of labelled and unlabelled glucose and the possible labelling combinations of the resultant molecules. Fructose-6-phosphate formed during the pentose phosphate pathway further enters the glycolysis to be converted into pyruvate and lactate. Adapted from Fan *et al*. (2010) [24].

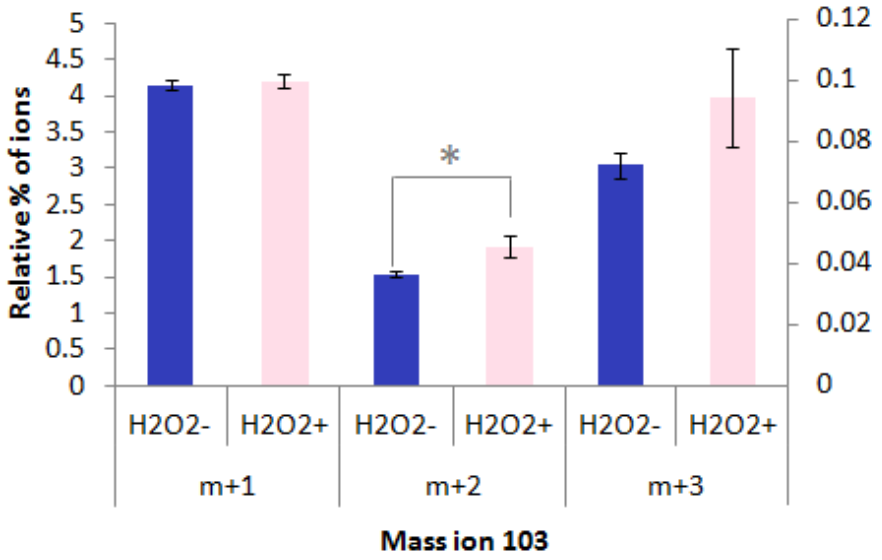

Figure 3.15 Isotope labelling patterns of lactic acid when grown under anaerobic conditions and high dilution rate. The bars indicate relative abundance of ^{13}C found in mass ion fragment 103 after cultured in medium with U-^{13}C glucose. * symbol indicates *p-value* < 0.05.

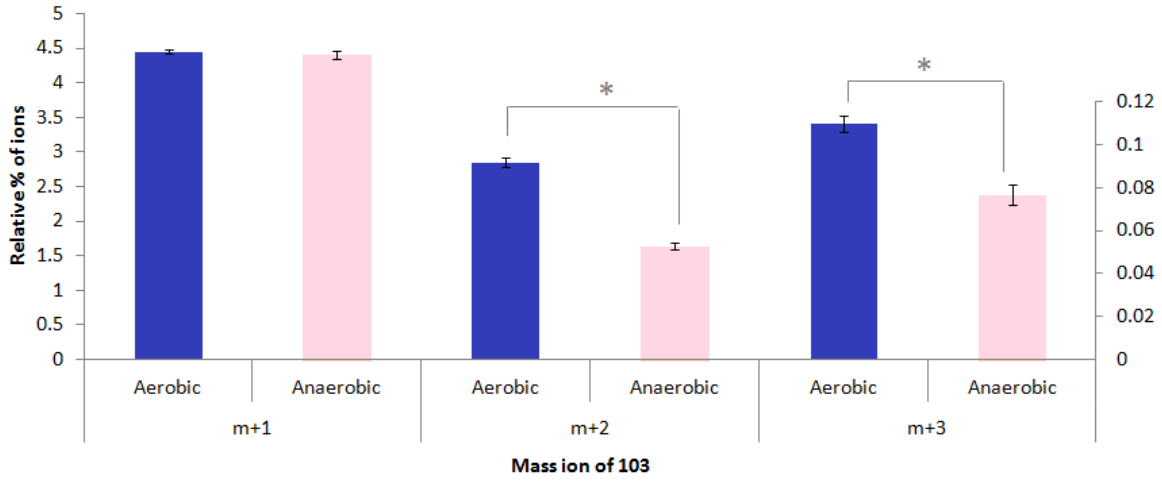

Figure 3.16 Isotope labelling patterns of lactic acid when grown under a high dilution rate in the absence of H_2O_2 treatment. The bars indicate relative abundance of ^{13}C found in the mass ion fragment after cultured in medium with U-^{13}C glucose. * *p-value* < 0.05.

3.4 *DISCUSSION*

3.4.1 OVERALL IMPACT OBSERVED FROM THE MULTIVARIATE ANALYSIS

The multivariate analysis allowed globally analysing the data and inferring about the degree of variability of the data and how different variables explain the distribution of the samples.

It could be observed from all the graphical representations that the two main components (PC1 and PC2) were able to explain the variability of the presented data and the separation of the groups in function of the oxygen and dilution rate.

In fact, the overall impact that H_2O_2 had in the samples was not very significant. Only the samples Anaerobic, HDR (AH) and Anaerobic, LDR (AnL) evidenced a distinct separation between the samples with and without the presence of H_2O_2.

However, H_2O_2 did have an impact on the metabolism of the cells but mostly on one particular condition (Anaerobic, LDR – AnL) which might have caused that overall the H_2O_2 influence not to be significant. Yet, oxygen and dilution rate clearly contribute to the separation of the different group samples. When analysing the hierarchical clustering data however, five main clusters were defined that would reflect the variables relatedness. When analysing deeply the metabolomic data together with the clustering data it is interesting to note that the metabolites that were detected with statistical significance, mainly group between one or two clusters.

In fact, the intracellular metabolic response of the cells to O_2 in the absence of H_2O_2 Figure 3.8A) encompass a list of the statistically significant metabolites that were up or down regulated due to the O_2 effect. The down regulated metabolites all belong to either the second or the fifth cluster (of the intracellular data) and similar results are also true for the metabolic response to O_2 in the presence of H_2O_2 Figure 3.8B).

Moreover, in response to dilution rate (Figure 3.9), it can be seen that the metabolites that appeared up-regulated in response to this condition all grouped together in the first and second cluster with a small group of valine, norvaline, isoleucine and leucine grouped on the fifth cluster.

Although no special relation between the metabolites was found within each cluster, with exception of the third cluster that only contains fatty acids, it is still interesting to point that these metabolites effectively share an important role in the separation of the samples and as a response to a stress condition. The data analysis and interpretation is further explored in the following sections.

3.4.2 METABOLIC RESPONSE OF *E. FAECALIS* TO H_2O_2

Metabolite profiles have revealed how *E. faecalis* responds to the stress exerted by H_2O_2 and its response is highly dependent on the conditions of its surrounding environment. When cultured at a low dilution rate or in the presence of oxygen, the observed shifting of intracellular profiles in response to H_2O_2 perturbation has been minimal. This was not surprising, as both low growth rate and aeration poses metabolic stress on *E. faecalis*. This is because the nutrient limitation and potential oxidative damage would both exert adverse challenges upon cell metabolism and survival. Thus, by being pre-exposed to these conditions, cells were in fact already responding to a stress condition and would subsequently present more tolerance to H_2O_2. Other studies have previously observed the apparent overlapping of cellular responses to different environmental stresses [25,26].

On the other hand, a considerable amount of metabolic information regarding *E. faecalis'* response to H_2O_2 was gathered when the cells were grown under anaerobic conditions at a high dilution rate.

A number of intracellular metabolites have had their levels increased under the influence of H_2O_2 pressure, namely glutamate, pyroglutamic acid, cysteine, glutathione and among others. Pyroglutamic acid, a glutamate related compound, plays a key role in the defence against oxidative stress [27] while cysteine is a key building block for the biosynthesis for glutathione. Glutathione, a tripeptide known to play a significant role in protecting cells from oxidative damage by scavenging and reacting with free radicals, also evidenced a higher level due to H_2O_2 effect [28]. The reaction of glutathione with H_2O_2 is catalysed by glutathione peroxidise with the products being water and glutathione disulphide. This reaction is highly-dependent on the availability of NADPH, thus suggesting the need for *E. faecalis* to up-regulate NADPH forming reactions. This

cofactor is mostly produced via the pentose phosphate pathway and analysis of ^{13}C-labelling experiments suggested that the conversion of glucose to lactic acid could occur through both pentose phosphate pathway and glycolysis, with evidence of an increase in the labelled fractions generated from the former but not the latter pathway in response to H_2O_2 (Figure 3.15). This finding suggests reconfiguration of the central carbohydrate metabolism in response to reactive oxygen species. An earlier study has shown that, after exposing *Saccharomyces cerevisiae* to H_2O_2, expression of enzymes associated with glycolysis and the TCA cycle were simultaneously repressed while the pentose phosphate pathway was induced. The authors proposed that under oxidative challenge, the yeast preferentially redirect carbons to benefit the generation of NADPH, which would provide the necessary reducing power to counterpart free radicals, at the expense of glycolysis [29]. Similar redistribution of metabolic fluxes were subsequently identified in bacteria [30] and in more complex organisms, including *Arabidopsis thaliana* [31] and *Caenorhabditis elegans* [32], suggesting the mechanism has been highly conserved along the course of evolution and is very likely to also occur in *E. faecalis*.

When analysing the extracellular metabolite profile, methionine has been detected across all datasets during H_2O_2 perturbation (Figure 3.10). However, the secreted values are always lower (i.e., less secreted) when in the presence of H_2O_2 than in the absence of it. This suggests the cells demand for this amino acid increased and therefore, it was less secreted suggesting its relevancy in terms of antioxidant defence. Methionine is a sulphur-containing amino acid that readily reacts with reactive oxygen species to form methionine sulfoxide. The reaction is important in scavenging free radicals encountered by the cells. A study has shown that the methionine residues in proteins play a significant role in defence against oxidative stress [33]. The conversion of methionine sulfoxide back to methionine is a vital step in repairing oxidative damage and is performed by the enzymes methionine sulfoxide reductases. *E. faecalis* is able to synthesise two copies of methionine sulfoxide reductase, MsrA and MsrB, thus it is capable of utilising this system in the presence of H_2O_2. Interestingly, this reaction also relies on the availability of NADPH, thus further demonstrating the need for *E. faecalis* to be adept at regulating NADPH generation under an oxidative environment and further suggesting an up regulation of the pentose phosphate pathway. In addition, Zhao *et al.* (2010), have recently shown that *E. faecalis* mutants that were deficient in either

mrsA or *mrsB* genes have reduced virulence and were more susceptible to killing by macrophages [34].

The redox chemistry of other amino acids such as cysteine, tyrosine and tryptophan, has been shown to have a major role in cellular redox sensing and the antioxidant response [35]. Changes in these metabolites are also observed across the datasets supporting their role as antioxidants.

Although no studies relating the antioxidant effect of tryptophan on bacteria have been found, various studies on tryptophan and its derivatives on higher organisms have demonstrated such a phenomenon. Several tryptophan derivatives function as free radical scavengers and antioxidants. These derivatives stimulate a number of antioxidative enzymes and stabilize cell membranes conferring them with higher tolerance towards free radical damage [36]. Although it is not proven that bacteria also possess a similar mechanism, the uptake of this amino acid suggests it may play a role against oxidative stress.

Interestingly, 4-aminobutyric acid was also detected in the metabolite profiles of *E. faecalis*. This metabolite is known to be closely linked with the glutathione metabolism and oxidative stress response, but has so far only been documented in higher organisms such as plants and animals [37,38]. This metabolite has been detected in the extracellular profile, suggesting there may be a yet unknown involvement in the response of *E. faecalis* to oxidative stress.

Little is known about the synthesis of 4-aminobutyric acid in bacteria. A study in recombinant *E. coli* engineered a biochemical pathway relying on transamination reactions from threonine and aspartic acid to synthesise 4-aminobutyrate [39]. The enzymes involved were tyrosine aminotransferase, threonine deaminase and α-acetolactate synthase which, with the exception of α-acetolactate synthase, have not been identified in the genome of *E. faecalis*. Thus, a yet unknown pathway to synthesise this compound would be part of *E. faecalis'* metabolism.

3.4.3 METABOLIC RESPONSE OF *E. FAECALIS* TO O_2

The response of the cells to oxygen tension has been coupled with a high dilution rate and therefore an up regulation of the metabolism would be expected, due to a faster cell growth. The changes are more notorious in the extracellular profile than in the intracellular profile. Nevertheless, metabolites such as glutathione, as previously mentioned, fundamental in protecting cells from oxidative damage was detected in response to oxygen. Additionally, the fatty acids myristic acid (c14), myristoleic acid (c14:1), palmitoleic acid (c16:1) and margaric acid (c17) have been detected at higher levels. In particular, margaric acid has been suggested to be relevant as a resistance-related metabolite in other organisms [40]. Although this mechanism has only been described for eukaryotic organisms, the increased levels detected both in the presence and absence of H_2O_2 suggests a similar effect might occur on *E. faecalis'* membrane. The overall saturation of the membrane however, seems to be maintained. While two saturated fatty acids increased their levels (myristic and margaric acids), two unsaturated fatty acids, also had their levels increased (myristoleic and palmitoleic acids).

One of the key observations produced from this work was that *E. faecalis* responded to oxygen tension by increasing the metabolic flux through glycolysis [27]. This concept is strongly supported by our ^{13}C-labelling analysis (Figure 3.16) which not only showed an increase in the levels of ^{13}C-labelled ions generated by glycolysis, but also through the pentose phosphate pathway. Data suggests that cells have increased their glucose uptake during aerobic growth. However, unlike H_2O_2, cells reacted to the presence of oxygen by distributing the carbon source to both glycolysis and the pentose phosphate pathway. The amino acid aspartate was one of the metabolites that evidenced an increased level (2 fold-change) due to the presence of oxygen (Figure 3.8). Additionally, the ^{13}C-labelling experiments also show that aspartate increased its labelling of the carbons when in the presence of oxygen. Aspartate is synthesised by the transamination reaction: oxaloacetate + glutamate -> aspartate + 2-oxoglutarate catalysed by aspartate aminotransferase (2.6.1.1). Given that oxaloacetate's precursor is pyruvate, this further suggests an increment in the flux through glycolysis.

Interestingly, citric acid was found to be consumed from the medium both in the absence and presence of oxygen. This is interesting, particularly because the intracellular levels of citric acid in response to oxygen also increased both in the presence and absence of H_2O_2.

Metabolism of citric acid is known to occur in *E. faecalis* which yields pyruvate as an intermediary to produce other compounds relevant in the production of flavoured compounds as well as lactic acid [41]. However, citrate metabolism only occurs after the sugar source (such as glucose) is exhausted [42]. Since the experimental design involves continuous fermentation, the glucose availability is constant and it is unlikely that citrate is being metabolised to end products.

Citrate is also a chelating agent, or a binding agent that suppresses chemical activities by forming chelates. It is known that the generation of oxygen-free radicals from the reaction of H_2O_2 with various Co(II) complexes leads to the generation of the superoxide radical, which is inhibited when Co(II) is chelated with adenosine 5-diphosphate or citrate [43]. It has also been suggested that iron regulation ensures that there is no free intracellular iron that could participate in the Fenton reaction, generating highly reactive hydroxyl radical (OH^-); however, under stress conditions, an excess of superoxide releases "free iron" from iron-containing molecules [44]. The chelating agent citrate acts on iron ions thus preventing the Fenton reaction.

Furthermore, we have also recorded an increase in the extracellular level of benzoic acid in the presence of oxygen that was further documented in the next chapter [27]. Combining this observation with the significant lowering of intracellular levels of this compound, suggests that *E. faecalis* may be actively secreting this metabolite. Under aerobic conditions, a decrease in the metabolism of aromatic amino acids, where benzoic acid can be generated, and an increased glucose metabolism suggest that *E. faecalis* would exert a tighter regulation on the intracellular benzoic acid levels.

Moreover, this event seems to be oxygen dependent only, as the effect observed due to H_2O_2 on the cells did not cause any statistically significant change in benzoate levels.

The data suggest that cells were actively removing benzoic acid from the cytosol due to its toxic effects under aerobic conditions. Benzoic acid and related compounds have been widely utilised in food preservation due to their bacteriostatic properties. Activated under low pH, the chemical works by inhibiting the carbohydrate metabolism [45] and it has been shown to be effective against *E. faecalis* [46]. As a consequence, cells may tend to secrete the metabolite to preserve their integrity.

3.4.4 METABOLIC RESPONSE OF *E. FAECALIS* TO THE DILUTION RATE

One general trend observed in the intracellular data in response to the dilution rate was an overall increased level of intracellular amino acids. A higher dilution rate implies a high availability of substrates and all metabolic pathways are also more active. Some studies have also made positive correlations between growth rates and a more effective incorporation of free amino acids from the medium into biomass [47,48]. *E. faecalis* preferentially obtains most of its amino acids from exogenous sources [49]; however, previous studies conducted in our lab (data not shown) have evidenced that *E. faecalis'* cells always required a small amount of a rich nutrient (such as peptone) to trigger growth. Attempts were made at that time to develop a defined medium but those efforts were unsuccessful and therefore peptone was used throughout the experiments. As a consequence, the presence of peptone (whose main composition are dipeptides and some free amino acids) [50] would have caused the cell to uptake it and catabolise it into free amino acids, increasing the pool intracellularly. Additionally, when analysing the extracellular profile we observed that amino acids are being secreted. Considering that peptone is used as substrate, the breakdown of the dipeptides inside the cell (after uptake) would increase the amino acid pool and cause the excess to be secreted (Figure 3.12). ^{13}C-labelling results show increased labelling fractions for histidine, phenylalanine and tyrosine when grown at a low dilution rate (Figure 3.13B, C, D and E). The decreased percentage of labelling when a high dilution rate is imposed to the system suggests that a source like peptone in the medium would be contributing more to these intracellular pools.

We have also demonstrated that the metabolic response of *E. faecalis* to H_2O_2 is greatly influenced by the dilution rate during continuous cultures (Figure 3.7). When *E. faecalis* was grown at a low dilution rate, differences in metabolite profiles in response to the

H_2O_2 perturbation were found to be small. From this, we proposed that the slow growth rate may have triggered a certain degree of cellular stress response as the metabolism approximates the state observed during stationary growth phases, where nutrients are limited. Subsequently, this enables them to become more tolerant to the subsequent stress imposed by H_2O_2. This theory is supported by findings from a study from Notley and Ferenci (1996), which showed that *E. coli* grown under glucose-limited continuous cultures at a low dilution rate induces expression of the stress protein, RpoS, and its associated stress markers [51].

Finally, a study by Ostrowski *et al* (2001) directly investigated the effect of the specific growth rate on H_2O_2 tolerance of the marine bacterium, *Shingomonas alaskensis*, and has also shedded some light on the subject. The authors were able to show that cells grown at low dilution rates in the presence of 25 mM H_2O_2 for 60 minutes obtained a greater percentage of survival than at high dilution rates. As they found no correlation between catalase activity and growth rate, the authors have concluded that the neutralisation of H_2O_2 was due to a first adaptation caused by a low dilution rate [52].

3.5 *CONCLUSIONS*

The present work aimed to utilise metabolomics and ^{13}C-labelling experiments in an attempt to understand how different forms of oxidative stress influence the metabolic response and which mechanisms enable *E. faecalis* to cope with oxidative stress.

Multivariate analysis have shown to be a good initial approach in order to understand the variability of the data while also suggesting interesting group of metabolites that could be further explored with other statistical tools.

The stress response of *E. faecalis* to the different perturbations studied indicated different mechanisms of action. In fact, H_2O_2 did not show a significant effect on the metabolic response which could be caused by the fact that other stress conditions (such as O_2 and low dilution rate) were also exerting some form of stress and therefore the response to H_2O_2 would be minimal; or it could also be due to the efficient activity of catalase that rapidly dismutes H_2O_2 into O_2 and H_2O.

Nevertheless, it was possible to observe a significant impact when the cells were grown under an anaerobic and high dilution rate environment. Metabolites such as pyroglutamic acid, glutathione, methionine and cysteine had a statistical significant change in response to H_2O_2. All these metabolites were shown to be related to different mechanisms to cope with oxidative stress.

Focus was also placed on the important role of redistribution of carbohydrate flux that has been shown to exist in a wide range of organisms in an effort to drive NADPH generation.

Furthermore, the study has underlined the link between oxygen as a source of oxidative stress by showing that aerobic cultures displayed more tolerance to H_2O_2. We have also demonstrated the response to oxygen tension resulted in a redistribution of carbohydrate fluxes in *E. faecalis* that differs from the one obtained with H_2O_2.

The response to oxygen also highlighted the particular action of citric acid as a player in the defence mechanism by chelating iron and avoiding it to undergo Fenton reaction and increase hydroxyl radical pool. Furthermore, benzoic acid levels suggest this compound may play a role in the response to oxidative stress and will be further explored in the next chapter.

This work also highlights the overall upregulation of *E. faecalis* metabolism during response to a higher dilution rate. Apparently, more than a stress response, the overall upregulation of the metabolism seems to be related to the higher availability of nutrients. The bacterium demonstrated to be particularly reluctant to perform *de novo* synthesis of the amino acids and relied heavily on exogenous sources.

The utilisation of an untargeted approach has also allowed us to identify a metabolite (4-aminobutyrate) that has not been previously documented in prokaryotes. Its participation during cellular response to oxidative stress in eukaryotes may suggest similar roles in *E. faecalis*.

We were able to show that when *E. faecalis* attained a slower growth rate it also exhibited an enhanced tolerance to H_2O_2 perturbation mainly because the cells growing

in a low dilution rate have a lower amount of nutrients and therefore are already under some form of stress and with their stress response mechanisms already activated.

Finally, our observations also emphasised the apparent role of benzoic acid in cells exposed to oxygen which should be further explored.

Overall, O_2 seems to be the source of oxidative stress that causes the cells to have a more significant stress response when compared with H_2O_2, while the dilution rate increment did not indicate that cells could be exhibiting any form of stress.

3.6 *REFERENCES*

1. Poh, C. H., Oh, H. M. L. & Tan, A. L. Epidemiology and clinical outcome of enterococcal bacteraemia in an acute care hospital. *J. Infect.* **52,** 383–6 (2006).

2. Flahaut, S. *et al.* Relationship between stress response towards bile salts , acid and heat treatment in *Enterococcus faecalis*. **138,** 49–54 (1996).

3. Dizdaroglu, M., Jaruga, P., Birincioglu, M. & Rodriguez, H. Free radical-induced damage to DNA: mechanisms and measurement. *Free Radic. Biol. Med.* **32,** 1102–1115 (2002).

4. Dean, R. T., Fu, S., Stocker, R. & Davies, M. J. Biochemistry and pathology of radical-mediated protein oxidation. *Biochem. J.* **324 (Pt 1,** 1–18 (1997).

5. Cabiscol, E., Tamarit, J. & Ros, J. Oxidative stress in bacteria and protein damage by reactive oxygen species. *Int. Microbiol.* **3,** 3–8 (2000).

6. Paulsen, I. T. *et al.* Role of mobile DNA in the evolution of vancomycin-resistant *Enterococcus faecalis*. *Science (80-.).* **299,** 2071–4 (2003).

7. Winstedt, L., Frankenberg, L., Hederstedt, L. & von Wachenfeldt, C. *Enterococcus faecalis* V583 contains a cytochrome bd-type respiratory oxidase. *J. Bacteriol.* **182,** 3863–6 (2000).

8. Gilmore, M. S. *The Enterococci: pathogenesis, molecular biology, and antiobiotic resistance*. *ASM Press* 133–175 (ASM Press, 2002).

9. Wang, X. *et al. Enterococcus faecalis* induces aneuploidy and tetraploidy in colonic epithelial cells through a bystander effect. *Cancer Res.* **68,** 9909–17 (2008).

10. Balamurugan, R., Rajendiran, E., George, S., Samuel, G. V. & Ramakrishna, B. S. Real-time polymerase chain reaction quantification of specific butyrate-producing bacteria, *Desulfovibrio* and *Enterococcus faecalis* in the feces of patients with colorectal cancer. *J. Gastroenterol. Hepatol.* **23,** 1298–1303 (2008).

11. Becerra, M. C., Batt, P. C. & P, P. L. Oxidative stress involved in the antibacterial action of different antibiotics. *Biochem. Biophys. Res. Commun.* **317,** 605–609 (2004).

12. Kohanski, M. A., Dwyer, D. J. & Collins, J. J. How antibiotics kill bacteria : from targets to networks. *Nat. Publ. Gr.* **8,** 423–435 (2010).

13. Kohanski, M. A., Dwyer, D. J., Hayete, B., Lawrence, C. A. & Collins, J. J. A common mechanism of cellular death induced by bactericidal antibiotics. *Cell* **130,** 797–810 (2007).

14. Fisher, K. & Phillips, C. The ecology, epidemiology and virulence of Enterococcus. *Microbiology* **155,** 1749–57 (2009).

15. Manson, J. M., Smith, J. M. B. & Cook, G. M. Persistence of vancomycin-resistant enterococci in New Zealand broilers after discontinuation of avoparcin use. *Appl. Environ. Microbiol.* **70,** 5764–8 (2004).

16. Smart, K. F., Aggio, R. B. M., Van Houtte, J. R. & Villas-Bôas, S. G. Analytical platform for metabolome analysis of microbial cells using methyl chloroformate derivatisation followed by gas chromatography-mass spectrometry. *Nat. Protoc.* **5,** 1709–29 (2010).

17. Bjarke Christensen, J. N. Isotopomer analysis using GC-MS. *Metab. Eng.* 282–290 (1999).

18. Villas-Bôas, S. G. & Bruheim, P. Cold glycerol-saline: the promising quenching solution for accurate intracellular metabolite analysis of microbial cells. *Anal. Biochem.* **370,** 87–97 (2007).

19. Aggio, R. B. M., Ruggiero, K. & Villas-Bôas, S. G. Pathway Activity Profiling (PAPi): from the metabolite profile to the metabolic pathway activity. *Bioinformatics* **26,** 2969–76 (2010).

20. Aggio, R., Villas-Bôas, S. G. & Ruggiero, K. Metab: an R package for high-throughput analysis of metabolomics data generated by GC-MS. *Bioinformatics* **27,** 2316–8 (2011).

21. Ringnér, M. What is principal component analysis ? **26,** 303–304 (2008).

22. Everitt, B. S. & Howell, D. C. in *Encycl. Stat. Behav. Sci.* **3,** 1580–1584 (2005).

23. Ter Braak, C. J. F. Principal Components Biplots and Alpha and Beta Diversity. *Ecology* **64,** 454 (1983).

24. Fan, T. W.-M., Lane, A. N., Higashi, R. M. & Yan, J. Stable isotope resolved metabolomics of lung cancer in a SCID mouse model. *Metabolomics* **7,** 257–269 (2010).

25. Morgan, R. W. Hydrogen Peroxide-Inducible Proteins in *Salmonella typhimurium* Overlap with Heat Shock and Other Stress Proteins. *Proc. Natl. Acad. Sci.* **83,** 8059–8063 (1986).

26. McDougald, D. *et al.* Defences against oxidative stress during starvation in bacteria. *Antonie Van Leeuwenhoek* **81,** 3–13 (2002).

27. Portela, C. A. F., Smart, K. F., Tumanov, S., Gregory M. Cook, S. & Villas-Bôas, S. G. The global metabolic response of a vancomycin-resistant *Enterococcus faecalis* strain to oxygen. *Journal of Bacteriology.* (2013). (Submitted).

28. Carmel-harel, O. & Storz, G. Roles of the glutathione and thioredoxin-dependent reduction systems in the *Escherichia coli* and *Saccharomyces cerevisiae* responses to oxidative stress. *Annu. Rev. Microbiol.* **54,** 439–61 (2000).

29. Godon, C. The H2O2 Stimulon in *Saccharomyces cerevisiae*. *J. Biol. Chem.* **273,** 22480–22489 (1998).

30. Rui, B. *et al.* A systematic investigation of *Escherichia coli* central carbon metabolism in response to superoxide stress. *BMC Syst. Biol.* **4,** 122 (2010).

31. Baxter, C. J. *et al.* The metabolic response of heterotrophic *Arabidopsis* cells to oxidative stress. *Plant Physiol.* **143,** 312–25 (2007).

32. Ralser, M. *et al.* Dynamic rerouting of the carbohydrate flux is key to counteracting oxidative stress. *J. Biol.* **6,** 10 (2007).

33. Luo, S. & Levine, R. L. Methionine in proteins defends against oxidative stress. *Fed. Am. Soc. Exp. Biol.* **23,** 464–72 (2009).

34. Zhao, C. *et al.* Role of methionine sulfoxide reductases A and B of *Enterococcus faecalis* in oxidative stress and virulence. *Infect. Immun.* **78,** 3889–97 (2010).

35. Winyard, P. G., Moody, C. J. & Jacob, C. Oxidative activation of antioxidant defence. *Trends Biochem. Sci.* **30,** 453–61 (2005).

36. Reiter, R. J., Tan, D., Cabrera, J. & D'Arpa, D. in *Tryptophan, Serotonin, and Melatonin* (Huether, G., Kochen, W., Simat, T. J. & Steinhart, H.) **467,** pp 379–387 (Springer US, 1999).

37. Landaas, S. The formation of 2-hydroxybutyric acid in experimental animals. *Clin. Chim. Acta* **58,** 23–32 (2009).

38. Gall, W. E. *et al.* alpha-hydroxybutyrate is an early biomarker of insulin resistance and glucose intolerance in a nondiabetic population. *PLoS One* **5,** e10883 (2010).

39. Fotheringham, I. G., Grinter, N., Pantaleone, D. P., Senkpeil, R. F. & Taylor, P. P. Engineering of a novel biochemical pathway for the biosynthesis of L-2-aminobutyric acid in *Escherichia coli* K12. *Bioorg. Med. Chem.* **7,** 2209–13 (1999).

40. Hamzehzarghani, H. *et al.* Metabolite profiling coupled with statistical analyses for potential high-throughput screening of quantitative resistance to fusarium head blight in wheat. *Can. J. Plant Pathol.* **30,** 24–36 (2008).

41. Sarantinopoulos, P., Kalantzopoulos, G. & Tsakalidou, E. Citrate Metabolism by *Enterococcus faecalis* FAIR-E 229. **67,** 5482–5487 (2001).

42. Rea, M. C. & Cogan, T. M. Glucose prevents citrate metabolism by enterococci. *Int. J. Food Microbiol.* **88,** 201–206 (2003).

43. Hanna, P. M., Kadiiska, M. B. & Mason, R. P. Oxygen-derived free-radical and active oxygen complex formation from cobalt(II) chelates in vitro. *Chem. Res. Toxicol.* **5,** 109–115 (1992).

44. Valko, M., Rhodes, C. J., Moncol, J., Izakovic, M. & Mazur, M. Free radicals, metals and antioxidants in oxidative stress-induced cancer. *Chem. Biol. Interact.* **160,** 1–40 (2006).

45. Krebs, H. A., Wiggins, D., Stubbs, M., Sols, A. & Bedoya, F. Studies on the mechanism of the antifungal action of benzoate. *Biochem. J.* **214,** 657–63 (1983).

46. Karabay, O., Kocoglu, E., Ince, N., Sahan, T. & Ozdemir, D. In vitro activity of sodium benzoate against clinically relevant *Enterococcus faecalis* and *Enterococcus faecium* isolates. *J. Microbiol.* **44,** 129–31 (2006).

47. Lahtvee, P.-J. *et al.* Multi-omics approach to study the growth efficiency and amino acid metabolism in *Lactococcus lactis* at various specific growth rates. *Microb. Cell Fact.* 10:12 (2011).

48. Dressaire, C. *et al.* Growth rate regulated genes and their wide involvement in the *Lactococcus lactis* stress responses. *BMC Genomics* **9,** 343 (2008).

49. Fernández, M. & Zúñiga, M. Amino acid catabolic pathways of lactic acid bacteria. *Crit. Rev. Microbiol.* **32,** 155–83 (2006).

50. Amezaga, M. R. & Booth, I. R. Osmoprotection of *Escherichia coli* by peptone is mediated by the uptake and accumulation of free proline but not of proline-containing peptides. *Appl. Environ. Microbiol.* **65,** 5272–8 (1999).

51. Notley, L. & Ferenci, T. Induction of RpoS-dependent functions in glucose-limited continuous culture: what level of nutrient limitation induces the stationary phase of *Escherichia coli*? *J. Bacteriol.* **178,** 1465–1468 (1996).

52. Ostrowski, M., Cavicchioli, R., Blaauw, M. & Gottschal, J. C. Specific growth rate plays a critical role in hydrogen peroxide resistance of the marine oligotrophic ultramicrobacterium Sphingomonas alaskensis strain RB2256. *Appl. Environ. Microbiol.* **67,** 1292–9 (2001).

CHAPTER 4

THE GLOBAL METABOLIC RESPONSE OF A VANCOMYCIN-RESISTANT *ENTEROCOCCUS FAECALIS* STRAIN TO OXYGEN

ABSTRACT

Oxygen and oxidative stress have become central components in explaining the mode of action of bactericidal antibiotics. Given the importance of oxidative stress in antimicrobial action, it is important to understand how bacteria respond to this stress at a metabolic level. The aim of this study was to determine the impact of oxygen on the metabolism of the facultative anaerobe *Enterococcus faecalis* (vancomycin-resistant isolate) using continuous cultures, metabolomics and ^{13}C-enrichment of metabolic intermediates and also to compare the changes with the results from a sensitive strain (previous chapter). When *E. faecalis* was rapidly transitioned from anaerobic to aerobic growth, cellular metabolism was directed towards intracellular glutathione production and glycolysis was upregulated two-fold, which increased the supply of critical metabolite precursors (e.g., glycine and glutamate) for sulfur metabolism and glutathione biosynthesis as well as reducing power for cellular respiration in the presence of haemin. The ultimate metabolic response of *E. faecalis* to an aerobic environment was the upregulation of fatty acid metabolism and benzoate degradation, which was linked to important changes in the bacterial membrane composition as evidenced by changes in membrane fatty acid composition and the reduction of membrane-associated demethylmenaquinone. Overall it seemed that the response between the sensitive and resistant strains were similar in various mechanisms of action which raised the question if vancomycin mode of action relied in fact, on oxidative stress.

Portela, C., Smart, K.F., Tumanov, S., Cook, G. M.,Villas-Bôas, S.G., The global metabolic response of a vancomycin-resistant *Enterococcus faecalis* strain to oxygen. Journal of Bacteriology. (Submitted).

4.1 *INTRODUCTION*

Enterococcus faecalis is a Gram-positive facultative anaerobe that features prominently as an opportunistic pathogen in hospital-acquired infections. It is responsible for a number of infections including surgical site infections, urinary tract infections, endocarditis, visceral infections and bloodstream infections [1–5]. In addition, it has a number of characteristics that make it an ideal agent for nosocomial infections: it is resistant to high temperatures, many harsh chemicals, drying conditions [4] and is able to survive in various hospital surfaces [4,6]. *E. faecalis* strains exhibit intrinsic and acquired resistance to many antibiotics [4,5], with an increasing occurrence of multidrug resistant strains [e.g., vancomycin resistant enterococci (VRE)]. VRE poses a serious health threat as vancomycin is considered a last resort antibiotic. In addition, widespread use of vancomycin, especially via oral route, was responsible, at least in part, for the development of VRE [2]. *E. faecalis* is also involved in the transmission of resistant genes to other medically relevant bacterial species such as *Staphylococcus aureus* [7].

More recently, attention within the investigation of antibiotic resistant microbes has focused on the link between oxidative stress and anti-bactericidal activity [8]. It has been proposed that a number of antibiotics mediate bacterial cell death by inducing changes in bacterial metabolism to increase the production of reactive oxygen species (ROS) which ultimately prove bactericidal [9,10]. However, *E. faecalis* is able to not only eliminate ROS but also to generate some. This characteristic is essential for its survival and virulence [8]. It has also been observed that the extracellular production of ROS by *E. faecalis* may cause deleterious effects on the surrounding cells and ultimately cause some forms of colorectal cancer in rats [11]. The arsenal of *E. faecalis* enzymes related to oxidative stress response have been described previously [12,13] demonstrating that *E. faecalis* provides an interesting framework for the analysis of the innate and acquired resistance to antibiotics as well as the adaptations to survive in an aerobic environment and hence resist to oxidative stress. Although *E. faecalis* does not present typical oxygen-dependent metabolic pathways, it is able to respire aerobically when grown in the presence of hemin [14]. In addition, proteomic studies have shown that *E. faecalis* produces approximately 200 different stress proteins [15]. Many of these proteins are

enzymes induced in response to oxygen, such as catalase, NADH peroxidase, NADH oxidase, superoxide dismutase and glutathione reductase [16]. However, there have been no previous studies examining the impact of oxygen on the central carbon metabolism of *E. faecalis.* Therefore, we here present the study of an endemic vancomycin resistant strain of *E. faecalis* (5A-13) in New Zealand and its response to oxidative stress induced by aerobiosis. In this study we combined metabolomics and ^{13}C enrichment experiments with continuous cultures of a vancomycin resistant strain to enable an *in vivo* assessment of the metabolic state of the cells under a stress condition. The metabolites are downstream to other 'omics' technologies and, as a result, offer definitive responses of cellular systems to environmental perturbations [17]. The understanding of *E. faecalis* response to oxidative stress may provide new insights on the role of oxidative stress and its relation to vancomycin as well as providing vital clues into the survival of *E. faecalis* in the environment.

4.2 *MATERIAL AND METHODS*

4.2.1 CHEMICALS

Methanol, chloroform, sodium bicarbonate, and sodium hydroxide were obtained from MERCK (Darmstadt, Germany). The internal standard 2,3,3,3-d_4-alanine, the derivatisation reagent methylchloroformate (MCF), pyridine, U-^{13}C glucose, glycerol and vitamin K_2 for menaquinone analysis were purchased from Sigma-Aldrich (St. Louis, USA). Anhydrous sodium sulphate was obtained from Fluka (Steinheim, Germany). All chemicals were of analytical grade.

4.2.2 BACTERIAL STRAIN AND CULTURE CONDITIONS

The bacterial strain used throughout all experiments was *Enterococcus faecalis* 5A-13. This bacterium was maintained on TPA agar plates, which contained peptone (20 g/L), NaCl (5 g/L), glucose (2 g/L), Na_2PO_4 (2.5 g/L), agarose (15 g/L) and vancomycin hydrochloride (40 mg/L), incubated at 37°C. Pre-inocula were prepared by transferring a single colony of *E. faecalis* growing on TPA plates to TP broth (as described above without agar), followed by overnight aerobic incubation at 37°C and 200 rpm.

Subsequently, 50 mL of culture broth were harvested by centrifugation (3000 rpm, 20 min), washed once with 0.9%$_{w/v}$ NaCl solution and re-suspended into batch phase culture medium to be used as the inoculum for the bioreactors. A BioFlo 3000 system (New Brunswick Scientific) was used throughout all experiments with a working volume of 1.5 L. Each fermentation started as a batch phase culture inoculated from the pre-inoculum culture growing at exponential growth phase. The batch phase medium contained: $(NH_4)_2SO_4$ (5 g/L), KH_2PO_4 (6 g/L), $MgSO_4$ (0.5 g/L), vancomycin hydrochloride (40 mg/L), hemin chloride (1 mg/L), peptone (2 g/L), glucose (10 g/L), trace metals solution (1 mL/L) comprised of $FeSO_4 \cdot 7H_2O$ (3 g/L), $ZnSO_4 \cdot 7H_2O$ (4.5 g/L), $CaCl_2 \cdot 6H_2O$ (4.5 g/L), $MnCl_2 \cdot 4H_2O$ (l g/L), $CoCl_2 \cdot 6H_2O$ (0.3 g/L), $CuSO_4 \cdot 5H_2O$ (0.3 g/L), $Na_2MoO_4 \cdot 2H_2O$ (0.4 g/L), H_3BO_3 (l g/L), KI (0.l g/L) and Na_2EDTA (15 g/L), and vitamins solution (2 mL/L), which contained riboflavin (0.42 g/L), calcium pantothenate (5.4 g/L), nicotinic acid (6.l g/L), piridoxal ethyl acetal HCl (l.4 g/L), d-biotin (0.06 g/L), folic acid (0.042 g/L), d-thiamine (l g/L) and myo-inositol (12.5 g/L). The working volume of the bioreactors was 1.5 L. Temperature, pH and oxygen saturation were held constant at 37 °C, 7.0 and 0% respectively, under a nitrogen atmosphere. The batch phase was carried out until the carbon source (glucose) was exhausted. This was measured using dinitrosalicylic acid (DNS) reagent[27]. Once the glucose level was depleted, the bioreactor was switched to continuous culture. Continuous culture was set up using the same medium described for the batch phase except with a glucose concentration of 5 g/L. The dilution rate was set at 0.06 h^{-1} (low dilution rate that resembles growth in host). Continuous culture was left on average for ~2 residence times (time required for the entire volume of the bioreactor to be replaced twice), and then U-^{13}C glucose was fed to the cells at 5%$_{w/w}$ of the total glucose. After a further residence time, samples were then taken for protein, metabolite and ^{13}C-distribution analyses. Oxygen was then introduced into the bioreactor until 20% oxygen saturation was reached. During the addition of oxygen, samples were taken for intracellular metabolite analysis at 3 min intervals over a 15 min period. The bioreactor was then left for a further three residence times (with 5%$_{w/w}$ of U-^{13}C glucose being fed to the cells during the final residence time). Samples were harvested under aerobic

steady state for protein, metabolite and ^{13}C-distribution analyses. Prior to sampling, the OD was monitored to ensure that the cells were in a 'steady state' (constant OD values over three residence times). This procedure was repeated three times (n = 3 chemostats).

4.2.3 SAMPLING AND EXTRACTION PROCEDURE FOR INTRACELLULAR METABOLITE ANALYSIS

The sampling, quenching and intracellular metabolite extraction were based on our previously published protocol [18]. In summary, 50 mL of culture broth, in triplicate, were harvested and quenched from the bioreactors by rapidly mixing the sampled broth with cold glycerol-saline solution (3:2) followed by centrifugation at -20^{o}C. The cell pellets were re-suspended in cold glycerol-saline washing solution (1:1) followed by centrifugation at -20^{o}C. Intracellular metabolites were extracted from the cell pellets after addition of cold methanol:water solution (1:1) at -20^{o}C and the internal standard (2,3,3,3-d_4-alanine), followed by three freeze-thaw cycles. Samples were then centrifuged (-20^{o}C) and the supernatant was collected. The remaining cell pellet was then resuspended in cold pure methanol (-20 ^{o}C) for a second round of extraction. The mixture was again centrifuged (-20 ^{o}C), the supernatant was collected and pooled to previous one. The cell pellet was then re-suspended in bi-distilled water, centrifuged and supernatant collected. 20mL of cold bi-distilled water (4^{o}C) was added to the metabolite extracts, frozen and subsequently freeze dried using a VirTis freeze-dryer (SP Scientific). The remaining cell debris was used for analysis of ^{13}C-labelled distribution in the biomass-derived amino acids. Only one sample/bioreactor was collected during the transition from anaerobic to aerobic condition every three minutes, with five samples in total per chemostat (n = 3 chemostats).

4.2.4 EXTRACELLULAR METABOLITE ANALYSIS

10 mL of culture were taken from the bioreactor and centrifuged. The supernatant was collected and membrane filtered (0.22 μm pore size). The filtrate was then separated into three aliquots (3 mL) and internal standard (2,3,3,3-d_4-alanine) was added to each of them before they were frozen and subsequently freeze dried on a VirTis freeze-dryer (SP Scientific).

4.2.5 HYDROLYSIS OF PROTEIN BIOMASS FOR AMINO ACID COMPOSITION ANALYSIS

This procedure has been adapted from the Christensen & Nielsen protocol[19]. Following extraction of intracellular metabolites, the remaining cell debris were re-suspended in 100% methanol (l mL) and evaporated to dryness. The cell debris were then hydrolysed using 6 M HCl (1 mL), incubated at 100 °C for 24 h, and then evaporated to dryness using a SpeedVac system (Eppendorf) coupled to a cold trap.

4.2.6 CHEMICAL DERIVATISATION OF METABOLITES AND GC-MS ANALYSIS

Intracellular and extracellular metabolites, and amino acids derived from biomass hydrolysates were made volatile for GC-MS analysis by re-suspending the dry samples in 200 µL of 1M NaOH and derivatised using a methylchloroformate (MCF) method according to our standard laboratorial procedure described previously[18]. The derivatised samples were analysed by GC-MS according to the parameters established previously [20] using a gas chromatograph GC7890 (Agilent Technologies) coupled to a quadrupole mass spectrometer MSD5975 (Agilent Technologies). The GC-capillary column was a Zebron ZB-1701 (Phenomenex) with 30 m × 250 µm (id) × 0.15 µm dimensions, 290ºC injection temperature, ion source at 70 eV and 230ºC; and the quadrupole temperature was set to 200ºC. The carrier gas was helium with a flow of 1 mL/min.

4.2.7 ACETATE QUANTIFICATION

Acetate levels in the spent culture media were assayed using the commercial Enzymatic BioAnalysis/Food Analysis UV method (R-Biopharm AG, Darmstadt, Germany) following manufacturer's instructions.

4.2.8 DEMETHYLMENAQUINONE EXTRACTION AND QUANTIFICATION

Approximately 10 mL of culture broth (OD_{600} ~1.0) were freeze dried, and the residue was extracted with 25 mL of chloroform:methanol ($2{:}1_{v/v}$) for 15 min under vigorous

stirring over a magnetic stirrer. The mixture was then centrifuged for 15 min at 4ºC (4000 rpm) and the supernatant collected and dried under a stream of N_2 gas. The lipid fraction was resuspended into 2 mL of hexane and passed through a solid phase extraction (SPE) column (Strata SI-1 Silica, 55 µm, 70A, Phenomenex) in order to isolate menaquinone fraction. The analytes were eluted from the cartridges using a mixture of hexane:diethylether ($96:4_{v/v}$). The eluents were collected and dried under a N_2 stream and later resuspended in 20 µL of acetone prior to HPLC analysis. The separation and quantification of menaquinones was performed using a System Gold© Complete HPLC system coupled to a Gemini-NX C18 column (250x4.6 mm, 5µ) from Phenomenex and UV detection at 245 nm following the methodology proposed by Suvarna *et al.* (1998)[21]. Sample was eluted under isocratic conditions with methanol-diethylether solution ($3:1_{v/v}$) as mobile phase at 0.7 mL/min for 20 min. Vitamin K_2 (menaquinone-4) from Sigma was used as a standard to build up the calibration curve.

4.2.9 FATTY ACID COMPOSITION OF CELL ENVELOPES

Approximately 5 mg of freeze-dried bacterial biomass were used for determining the profile of membrane-associated fatty acids. Dried biomass samples were transferred to GC-MS amber vials for saponification with an excess amount of base (KOH in methanol) and butylated hydroxytoluene (BHT) solution. BHT is a powerful antioxidant that preserves unsaturated and polyunsaturated fatty acids from oxidation. The mixture was homogenised by 1h incubation at 55ºC. Then, the hydrolysate was transferred into silanised glass tubes and derivatised by MCF as previously described[18]. After the derivatisation step, the samples were analysed by GC-MS as described above.

4.2.10 METABOLITE IDENTIFICATION AND DATA ANALYSIS

The metabolite-derivatives detected by GC-MS were identified using the Automated Mass Spectral Deconvolution and Identification System (AMDIS) software. This software is very useful for deconvolution and identification of chromatographic peaks. To normalise the data, the intensity of each metabolite peak was divided by the intensity of the standard peak (2,3,3,3-d_4-alanine) and also by the amount of biomass in each sample. A comparative metabolite profile was determined using PAPi (Pathway

Activity Profiling) [22] and the statistical analysis was performed using an R package also developed in house [23]. For general pattern identification and to consider the reproducibility of the methods and sample replicates, the software GeneSpring (Agilent Gene Spring MS Proteomics & Metabolomics Analysis 1.1.1, www.chem.agilent.com) was used based on raw GC-MS data rather than analysis of only identified metabolites. In order to determine the statistical significance of our findings, analysis of variance (ANOVA) and student (t-test) were used.

4.2.11 ^{13}C-LABELLING DISTRIBUTION ANALYSIS

^{13}C-labelling patterns in the amino acids derived from the cell pellet hydrolysates were determined by analysing the ratio of ^{13}C to ^{12}C in the major mass fragments generated by MS fragmentation of the respective MCF derivatives. The ratios were compared to those found in natural metabolites (from cells grown in ^{12}C-glucose). Evidence for labelling was determined by an increase in the relative level of ^{13}C-labelling in the metabolites from samples grown in U-^{13}C glucose. The labelling patterns of the amino acids were used to infer changes in the metabolic flux throughout the central carbon metabolism. The labelling pattern analysis was also extended to include an examination of the patterns found within some key intracellular metabolites.

4.3 *RESULTS*

4.3.1 GROWTH OF *E. FAECALIS* IN CONTINUOUS CULTURE

Growth experiments were carried out in continuous cultures, which means that cells are constantly metabolising and actively growing, that is, the primary (central carbon) metabolism is highly active. Continuous culture in a bioreactor is a highly advantageous system where growth rates can be controlled and all other variables are constant. Under anaerobic conditions, a steady state was achieved at a dilution rate of 0.06 h^{-1} (which resembles the human gut) and an optical density with an average of 1.7. Analysis of the fermentation end-products lactate and acetate showed that lactate levels were not markedly different between aerobic and anaerobic growth, whilst acetate levels decreased by 2-fold during aerobic growth (16.7 mM *vs.* 33 mM).

4.3.2 METABOLITE PROFILE DURING THE TRANSITION BETWEEN ANAEROBIC AND AEROBIC GROWTH CONDITIONS

Given that metabolite levels are altered rapidly in response to environmental changes, we expected to observe some changes during the transition state (as the oxygen saturation changed from 0% to 20% over a 15 min period), which would provide important insights into the immediate metabolic response of *E. faecalis* to oxygen. The levels of pyroglutamate and glutamate showed the most pronounced change from steady state to transition and back to steady state as a response to oxygen (Figure 4.1).

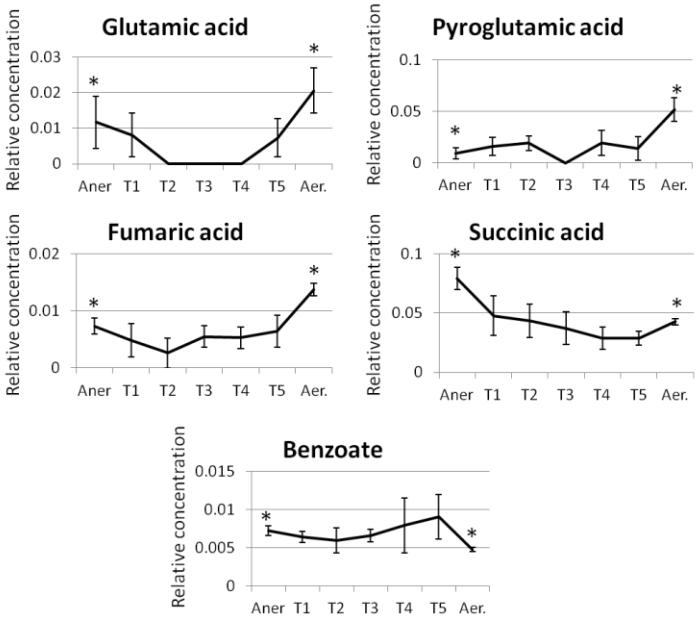

Figure 4.1. Changes in metabolite levels over time during transition from anaerobic-to-aerobic steady-states (Aner = anaerobic steady state, T1, T2, T3, T4, T5 = Transition states 1,2,3,4,5, Aer = aerobic steady state). The relative metabolite levels have been normalized by the level of internal standard (2,3,3,3-d_4-alanine) and biomass concentration. The error bars show the standard error between three biological replicates. The star symbol (*) indicates the steady state levels of the different metabolites before and after the transition state.

Interestingly, these two metabolites are precursors for glutathione biosynthesis, which is an important antioxidant molecule in the cell. The depletion of glutamate during the transition state suggests an increased demand for this metabolite as the oxygen tension increased. Augment of pyroglutamate levels under aerobic conditions suggests that this metabolite could be a key signature metabolite in *E. faecalis* oxidative stress response.

Opposite transition profiles were observed for fumarate and succinate, as fumarate shows an increase in levels aerobically, while succinate levels decreased. The conversion of fumarate to succinate occurs via fumarate reductase which is known to be irreversible in *E. faecalis* as it does not express succinate dehydrogenase [24,25], hence aerobically the cell appears to reduce or even stop the flux through this reaction, which results in fumarate accumulation.

4.3.3 METABOLITE PROFILES AT STEADY-STATE

A total of 44 metabolites were identified among intra and extracellular samples showing differential levels between the two environmental conditions with statistical significance ($p < 0.05$). Ten metabolites were commonly detected in all samples. Those include important central carbon metabolism intermediates. Figure 4.2 andFigure 4.3 show statistically significant fold changes in metabolite levels (extra and intracellular) between aerobic and anaerobic conditions, indicating that oxygen had a significant impact on *E. faecalis* metabolism. Overall, the level of extracellular metabolites increased under aerobic growth (Figure 4.2). The majority of the amino acids showed significant differences between aerobic and anaerobic growth and twelve of them showed an increase in levels aerobically, with exceptions being serine and cysteine. Our results suggest that serine was transported from the medium at a greater extent under aerobic growth, which indicates a higher demand for this metabolite. Serine is the precursor of glycine, which is also a precursor for glutathione. Indeed, extracellular glutathione levels increased significantly aerobically.

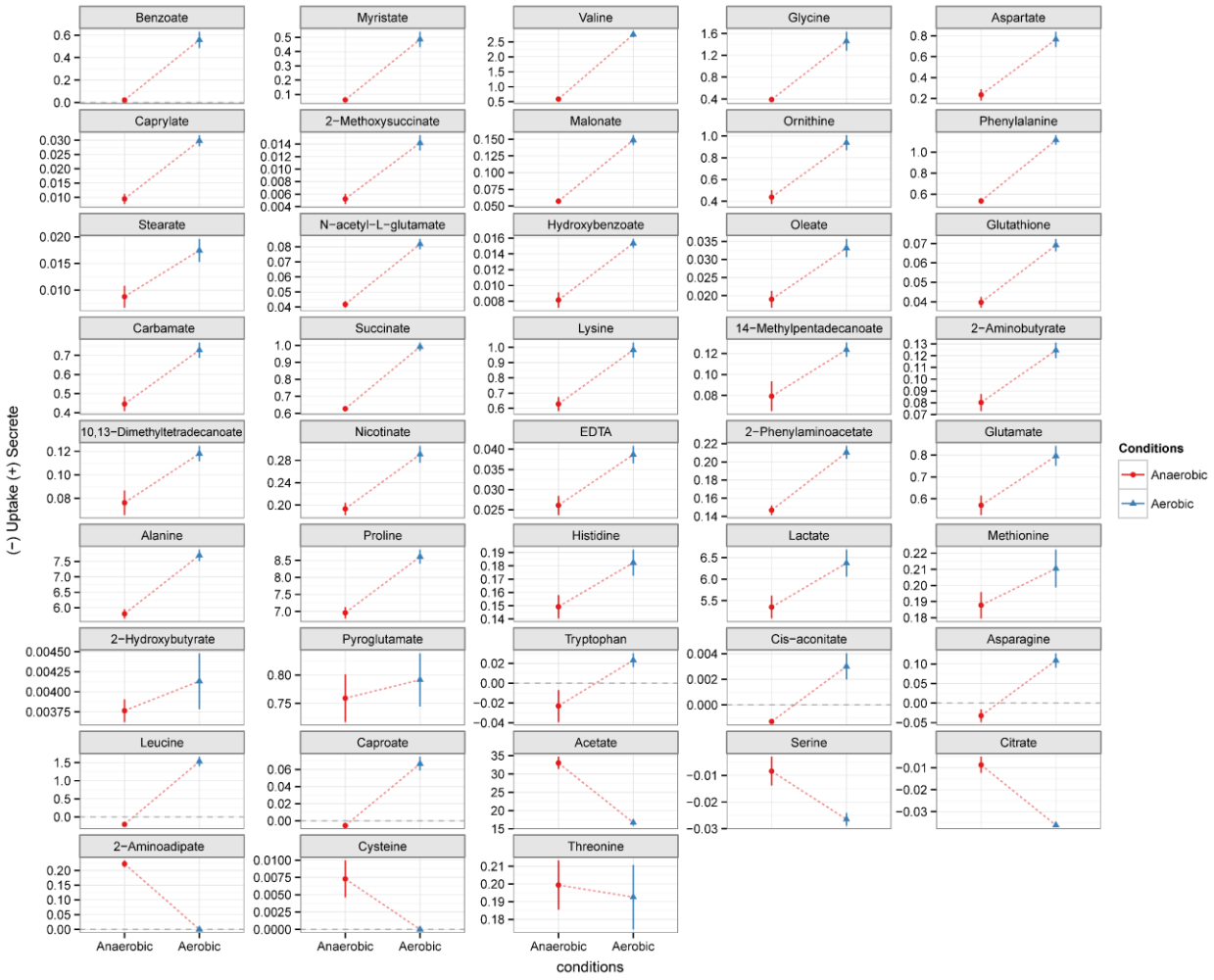

Figure 4.2. Extracellular metabolite levels of *E. faecalis* cultures grown under anaerobic and aerobic conditions. These metabolite levels were normalized by internal standard (2,3,3,3-d_4-alanine), subtracted from the non-inoculated medium and normalized by biomass. All metabolites were detected at statistically significant levels (p<0.05).

On the other hand, cysteine levels appeared depleted under aerobic conditions compared to anaerobic growth, which also indicates a higher demand for this amino acid intracellularly in response to oxygen. Thus, changes in sulphur metabolism could be closely associated with *E. faecalis* adaptation to an aerobic environment. Interestingly, extracellular benzoate levels (and hydroxybenzoate) significantly increased under aerobic growth, in parallel to a significant decrease in intracellular benzoate levels. Benzoate is an intermediate metabolite involved in the synthesis and catabolism of aromatic amino acids [26]. It is also a toxic intermediate to the cell and therefore usually excreted [27]. The same behaviour was observed for myristic acid. Along with myristic

acid, other intermediates from fatty acids metabolism showed increased levels under aerobic conditions.

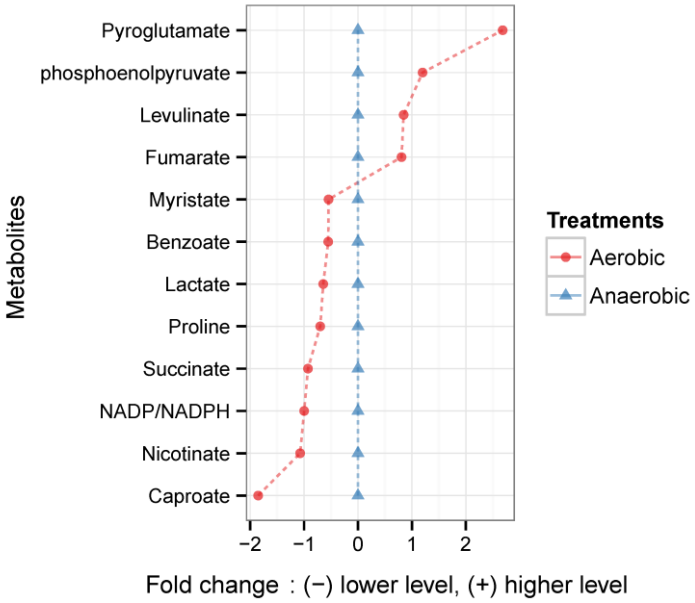

Figure 4.3. Intracellular metabolite levels of *E. faecalis* cells detected at significant different levels (p<0.05) when comparing anaerobic and aerobic growth conditions. Metabolites levels were normalized by internal standard (2,3,3,3-d_4-alanine), and biomass concentration and fold change adjusted against relative levels under anaerobic condition.

4.3.4 RESPONSE OF METABOLIC PATHWAYS TO OXYGEN TENSION

Based on the metabolites identified in the different samples, it was possible to determine which metabolic pathways were more likely to be up and down regulated when comparing the two experimental conditions. Figure 4.4 and Figure 4.5 show the pathway activity profile (PAPi) based on our extracellular and intracellular data, respectively.

Based on the profile of extracellular metabolites (Figure 4.4), there were five major metabolic pathways that could have been responsible for the greatest difference in extracellular metabolite profile when comparing anaerobic and aerobic growth: benzoate degradation, sulphur metabolism, valine, leucine & isoleucine degradation, fatty acid biosynthesis, and glycine, serine and threonine metabolism.

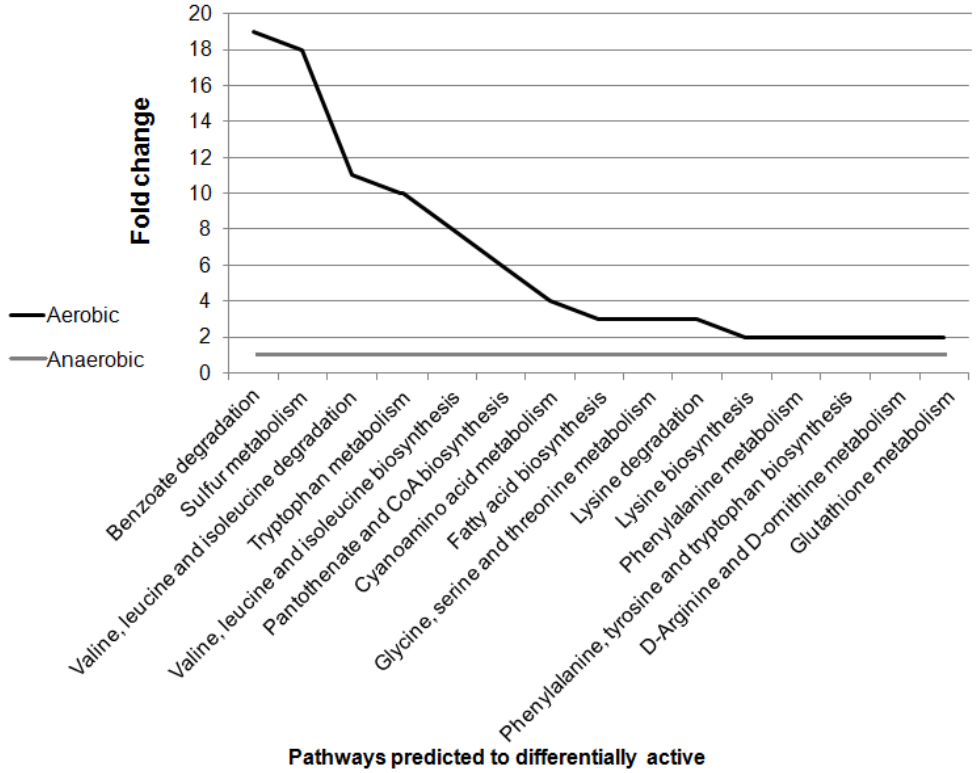

Figure 4.4. Pathway activity profiling (PAPi) analysis based on extracellular metabolite data from *E. faecalis* grown under different environmental conditions (anaerobic and aerobic). Only pathways with statistical significance (p <0.05 using ANOVA) and with more than 2 fold change are shown. The activity of pathways under anaerobic conditions has been set to one and compared to their activity under aerobic conditions.

Prediction of an up regulation of benzoate degradation aerobically in parallel with an up-regulation of phenylalanine, tyrosine and tryptophan metabolism is a further indication of a possible interconversion of aromatic amino acids into benzoate and its derivatives, such as hydroxybutyrate. Valine, leucine and isoleucine degradation and in particular isoleucine degradation yields propanoyl-CoA and acetyl-CoA, compounds involved in fatty acid biosynthesis. This could be linked to the observed changes in fatty acid metabolism.

Additionally, sulphur metabolism and glycine, serine and threonine metabolism are important in the production of precursors for glutathione biosynthesis, which seems to be the first line-response of *E. faecalis* to oxidative stress. Moreover, glycolysis, benzoate degradation and biosynthesis of phenylpropanoids are metabolic pathways that

appear to be up-regulated aerobically when compared to anaerobic conditions based on intracellular metabolite profile (Figure 4.5)

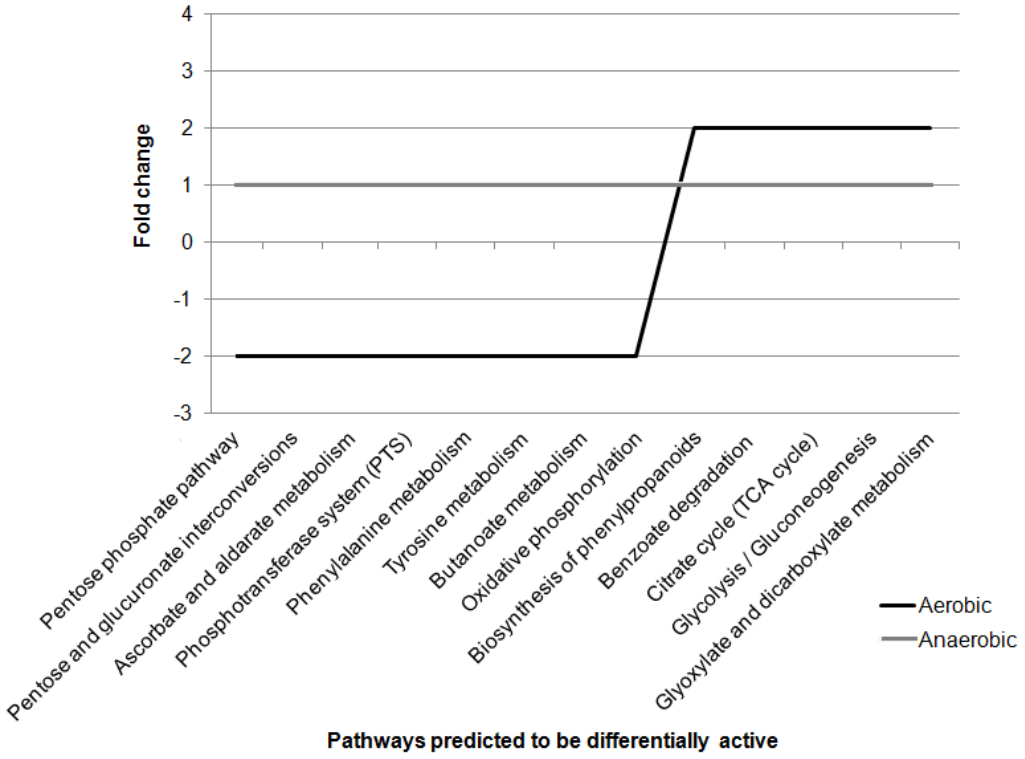

Figure 4.5. Pathway activity profiling (PAPi) analysis based on intracellular metabolite data from *E. faecalis* grown under different environmental conditions (anaerobic and aerobic). Only pathways with statistical significance (p <0.05 using ANOVA) and with more than 2 fold change are shown. The activity of pathways under anaerobic conditions has been set to one and compared to their activity under aerobic conditions.

4.3.5 ^{13}C-LABELLED DISTRIBUTION

To determine the ^{13}C flux distribution we chose to analyse the labelling patterns in both the amino acids derived from the hydrolysed biomass and free intracellular metabolites. ^{13}C-enrichments provides an insightful compliment to metabolomics data given that the level of ^{13}C incorporation give us clues to the activity of the different metabolic pathways operating within the cell rather than a static snapshot of relative metabolite concentrations. Four metabolites showed significant ^{13}C-labelling enrichment as summarised in Figure 4.6. Lactate and pyroglutamate showed statistical different levels

of ^{13}C enrichment between anaerobic and aerobic conditions (Figure 4.6A and Figure 4.6C).

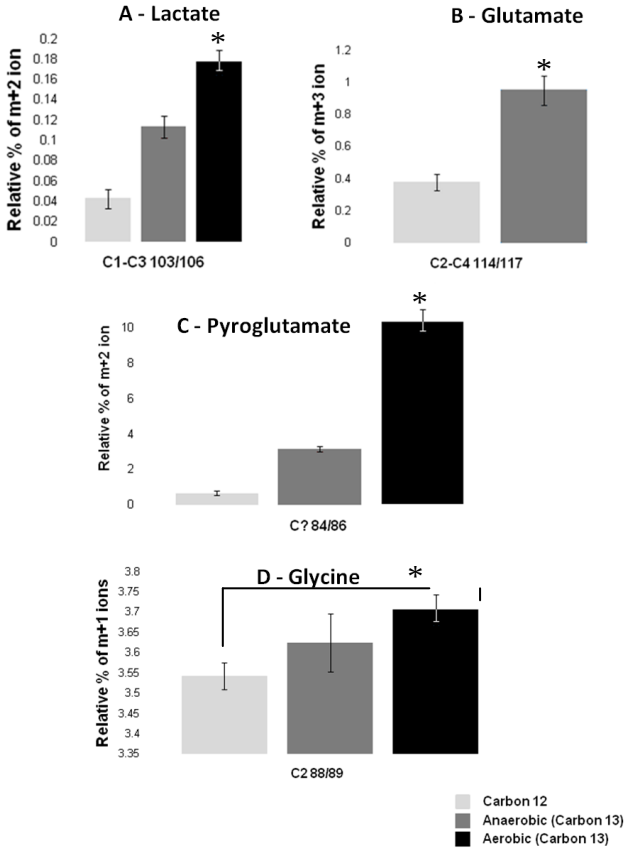

Figure 4.6. Isotope labelling patterns of A – lactate, B – glutamate, C – pyroglutamate, D – glycine. Light grey bar describes the natural level of ^{13}C expected in the mass ions of each compound. Light grey and black bars indicate the relative concentration of ^{13}C found in the MS fragments after culture in the U-^{13}C glucose medium. * symbol indicates $p<0.05$.

Interestingly, we have observed ^{13}C-enrichment in free glutamate from aerobic samples, indicating that under aerobic conditions glutamate was (at least in part) *de novo* synthesised from glucose (Figure 4.6B) despite the fact that *E. faecalis* lacks citrate dehydrogenase and isocitrate dehydrogenase. Similarly, ^{13}C-enrichment was also observed in pyroglutamate, with increased enrichment under aerobic growth (Figure 4.6C).

Glycine showed significant ^{13}C-enrichment only in samples derived from aerobic growth (Figure 4.6D). Glycine precursor is 3-phosphoglycerate, a glycolysis

intermediate. This is further evidence that aerobiosis up-regulates glycolysis as predicted by our PAPi analysis (Figure 4.5). However, we have not found ^{13}C-labelling enrichment in the amino acids proline, valine, isoleucine and leucine under either growth condition, which demonstrates that these amino acids were primarily derived from the peptone in the medium rather than synthesised *de novo* from glucose.

4.3.6 DEMETHYLMENAQUINONE LEVELS IN *E. FAECALIS* MEMBRANE

The membrane-associated electron carrier demethylmenaquinone (DMK) is important in the survival process of *E. faecalis* towards oxidative stress [11,28,29]. The concentration of demethylmenaquinone determined in bacterial cells grown anaerobically was 5 times higher than in cells grown aerobically (Figure 4.8). This has been previously observed for *Lactococcus lactis* [30]. An unexpected consequence of demethylmenaquinone expression by *E. faecalis* is the production of extracellular O_2^-. If, on one hand, this strategy could mean a potential threat to the host, on the other hand it can also be suicidal to the bacterial cell due to the accumulation of toxic free radicals when grown in a chemostat, which may justify the down-regulation of its biosynthesis under aerobic conditions as confirmed by its lower level aerobically.

4.3.7 FATTY ACID COMPOSITION OF *E. FAECALIS* CELLS

As presented previously, the metabolomic data suggested that oxidative stress must have a marked impact on the fatty acid/lipid metabolism, which could ultimately affect the cell membrane composition. To confirm this hypothesis we also determined the fatty acid composition of membrane-associated lipids when *E. faecalis* cells were grown aerobically versus anaerobically as well as in the presence and absence of vancomycin (Figure 4.7). Figure 4.7A evidences the fatty acid modulation profile in response to oxygen while Figure 4.7B evidences the fatty acids changes in the presence of both oxygen and vancomycin.

Indeed the results showed a statistically significant change in the fatty acid composition of membrane-associated lipids, with increased levels of unsaturated fatty acids such as oleic, heptadecenoic, myristoleic and palmitoleic acids under aerobic conditions (Figure 4.7A). Nonetheless, the levels of some saturated fatty acids such as lauric, myristic and pentadecanoic acids also had their levels increased in response to oxygen.

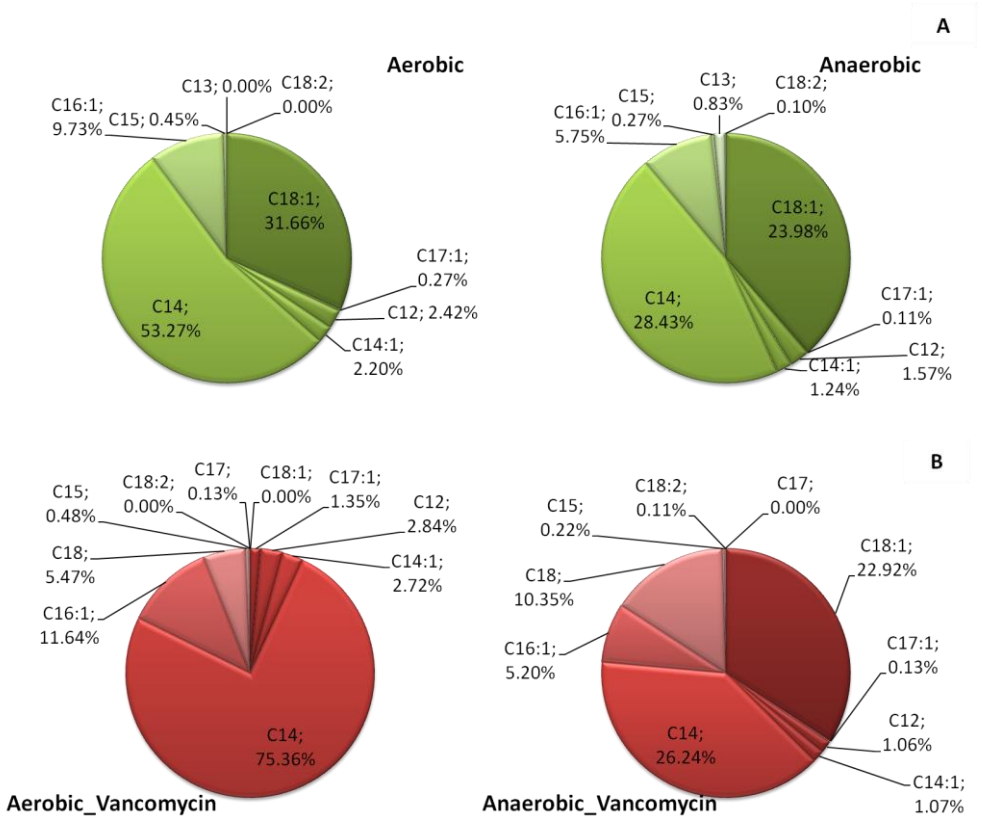

Figure 4.7. Membrane fatty acid composition of *E. faecalis* cells grown under different environment conditions. (A) Aerobic versus anaerobic growth; (B) Aerobic versus anaerobic growth in the presence of vancomycin. C12, Lauric acid; C13, Tridecanoic acid; C14, Myristic acid; C14:1, Myristoleic acid; C15, Pentadecanoic acid; C16:1, Palmitoleic acid; C17, Margaric acid = heptadecanoic; C17:1, cis-10-Heptadecenoic acid; C18, Stearic acid; C18:1, Oleic acid; C18:2, Linoleic acid.

Interestingly, the presence of the antibiotic vancomycin induced similar changes on the composition of membrane lipids when compared to aerobiosis. Particularly, the levels of myristoleic, palmitoleic, heptadecenoic, lauric, myristic, and pentadecanoic acids had their levels increased in response of both oxygen and vancomycin (Figure 4.7B). On the other hand, margaric acid was only detected in cells grown aerobically in the presence of vancomycin, and linoleic acid was only detected anaerobically (in the presence or not of vancomycin).

4.4 *DISCUSSION*

Oxidative stress is defined as an imbalance between the production of free radicals and antioxidative mechanisms. Free radicals have a deleterious effect on the cell by damaging lipids, proteins and DNA [39]. Various studies have been published around this topic [8,9,15,16] but the present study is the first to combine metabolomic and ^{13}C-isotope distribution approaches to address metabolic changes under aerobic versus anaerobic environments and provide a comprehensive analysis of the global metabolic response of *E. faecalis* to oxygen. Our metabolomics data clearly showed that oxygen has a significant impact on *E. faecalis* metabolism. Continuous culture was used in these experiments as it enables the assessment of the changes in the metabolome without confounding variables such as growth rate and other environmental conditions as they remain constant and only the oxygen concentrations varied. Furthermore, continuous culture provides an *in vivo* model of *E. faecalis* metabolism as it is an approximate model of the natural habitat of this bacterium within the gastro-intestinal tract of animals where nutrients are constantly flowing in and out. Our study yielded three key insights into *E. faecalis* response to oxidative stress: 1) up-regulation of sulphur metabolism and glutathione biosynthesis, which seems to be the fastest response of *E. faecalis* to oxidative stress; 2) increased glycolytic flux to supply metabolic demand for critical metabolite precursors and reducing power; and 3) up-regulation of fatty acid metabolism and benzoate degradation, which seems to be linked to important changes in the bacterial membrane composition. These results are summarised in Figure 4.8.

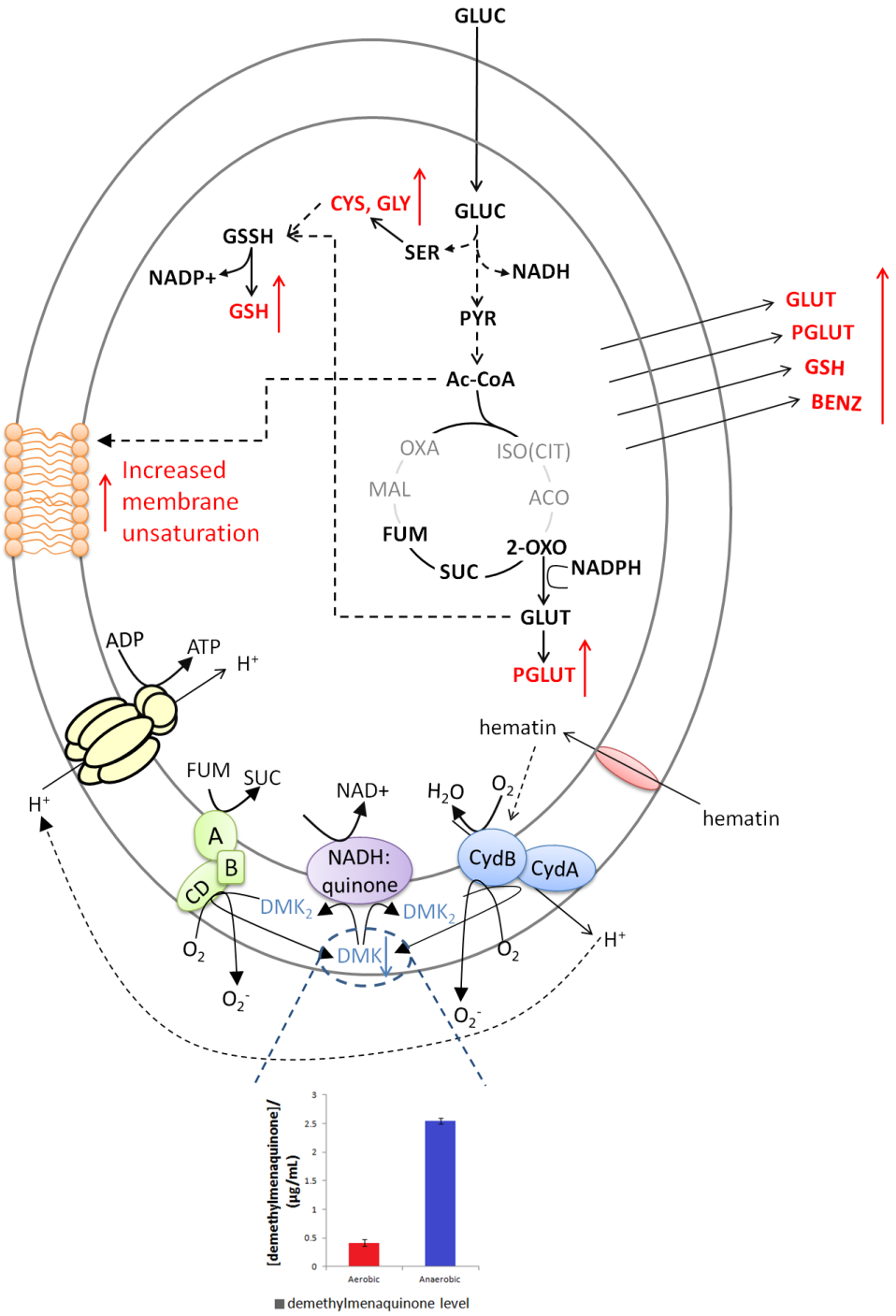

Figure 4.8. Overall metabolic response of *E. faecalis* to oxygen. A first line defence drives the cellular metabolism towards glutathione production. Consequently, an increase in the glycolytic flux is necessary to assure the demand for reducing equivalents. Downstream response of the cells is related to changes in the lipid membrane and demethylmenaquinone levels of the cell membrane.

4.4.1 SULPHUR + GLUTATHIONE METABOLISM

Changes in sulphur metabolism appear to be a key motif that changes in response to oxygen. This is evidenced across our experimental data. We therefore hypothesised that the major response of *E. faecalis* cells following the introduction of oxygen is the up-regulation of glutathione biosynthesis, particularly because glutathione plays an important role in protecting cells against oxidative stress [31]. Glutathione is a small peptide composed of cysteine, glycine and glutamate. It exists in two forms within the cell, the reduced form (GSH) and the oxidised form (GSSH). The inter-conversion between these two forms allows glutathione to donate reducing equivalents (H^+/e^-) to unstable ROS in order to neutralise oxidative stress agents [32]. The increase in glutathione activity under aerated conditions in *E. faecalis* has been previously suggested using proteomics data where the level of glutathione reductase increased in response to oxygen [33]. Our metabolome data suggest that up regulation of GSH biosynthesis is the first response of *E. faecalis* against oxidative stress evidenced by the coordinated up regulation of glutamate metabolism and increased levels of pyroglutamate and glutathione. Depletion of glutamate in the transition between anaerobic to aerobic growth and a significant increase of intracellular pyroglutamate levels and extracellular glutathione levels are key indications that glutathione biosynthesis should be up regulated in response to oxygen (Figure 4.8).

The increase uptake of serine and depletion in cysteine levels observed under aerobic condition (Figure 4.2) also corroborate with the conclusion of an upregulation of glutathione biosynthesis. Cysteine is a key precursor for glutathione and serine can be converted into cysteine through the activity of the enzymes serine *O*-acetylacetylase (*cysE*) and cysteine synthase (*cysK*) coupled with release of acetate [34]. Cysteine is also a key metabolite in the synthesis of other sulphur containing compounds including thiamine, coenzyme A and biotin which have all been implicated in oxidative stress response in other organisms such as *E. coli* and *B. subtilis* [35,36]. In addition, there are many cysteine-rich proteins that are crucial for oxidative stress responses including thioredoxin [37]. Thioredoxin (*trxB*) are small heat-stable oxidoreductases that contain two conserved cysteine residues in their active sites [38]. This protein is involved in many roles including different cellular processes, such as protein folding and regulation, repair of oxidatively damaged proteins and sulphur metabolism. The effect of ROS in

the cell metabolism and the defence systems activated to protect the cells against them require an increased demand in reducing equivalents to maintain their activity. A number of reports have highlighted the importance of thioredoxin systems in maintaining the redox homeostasis of the cell [31,37–39]. *E. faecalis* expresses this system in order to regenerate the pools of NADPH. In addition, Liu *et al.*(2008) developed a genome-scale metabolic model for *Lactobacillus reuteri* which predicted that the demand for intracellular levels of cysteine should be considerably higher under aerobic compared to anaerobic conditions [34].

Increased labelling in glycine under aerobic condition is another indication of an increased flux through pathways that lead to the formation of compounds related to glutathione metabolism, such as cysteine and glycine. Similarly, ^{13}C-labelling in glutamate and increased labelling in pyroglutamate further corroborates to the increased cellular demand for these metabolites under aerobic conditions (Figure 4.6A). Pyroglutamate and glutamate are also key metabolites for biosynthesis of glutathione which explains the need of the cell to *de novo* synthesise glutamate.

4.4.2 INCREASED GLYCOLYTIC FLUX

Up-regulation of glycolysis under oxidative stress is in line with the overall results obtained. The lack of a typical oxygen-dependent pathways means that *E. faecalis* must rely on other mechanisms to survive and grow in the presence of oxygen. Analysis of *E. faecalis* metabolism shows that it does not display typical oxygen dependent pathways such as a tricarboxylic acid cycle (TCA) and oxidative phosphorylation as it lacks key enzymes such as fumarase and aconitase**.** However, there is evidence that it is able to respire aerobically using a cytochrome *bd* terminal oxidase, when grown in the presence of haemin [14]. A conceptualized model of an adapted functional electron transport chain (ETC) has been proposed and involves a putative haemin transporter, a *cytochrome bd* and a fumarate reductase (Figure 4.8). DMK is reduced to demethylmenaquinol (DMK_2) by accepting the cytosolic equivalents through a putative NADH:quinone oxidase. The previously haemin-activated *cytochrome bd* and fumarate reductase are the final electron acceptors and reduce succinate to fumarate and O_2 to H_2O [40]. It seems that an increased glycolytic flux compensates the lack of a tricarboxylic acid cycle by overproducing NADH to be further regenerated in the adapted ETC. Additionally, a

higher glycolytic flux allows for increased availability of important metabolites involved in key defence mechanisms (Figure 4.8). As mentioned in the previous section, a number of metabolites are important for the synthesis of glutathione. Cysteine and glycine are metabolites synthesised from precursors produced during glycolysis, namely, 3-phosphoglycerate. The higher demand for these metabolites in addition to the detection of ^{13}C-labelling in glycine, glutamate and pyroglutamate aerobically and increased levels of fully labelled lactate aerobically (Figure 4.6A) further suggest that a higher flux through glycolysis is a key response of *E. faecalis* to oxygen. Overall, it was clearly shown that an increased glycolytic flux is required to supply metabolites that will have a significant role against oxidative stress and are involved in regeneration of cofactor pools, essential for the cell survival.

4.4.3 BENZOATE METABOLISM

Another major feature of the extracellular metabolite profile is the detection of high levels of benzoate and hydroxybenzoate secreted to the medium under aerobic conditions (Figure 4.2). Benzoate is an aromatic compound usually involved in the biosynthesis or catabolism of aromatic compounds including aromatic amino acids [26,41]. Oxidative phosphorylation requires ubiquinones (UQ) which are phenolic compounds that act as essential redox carriers for the aerobic respiratory chains [40]. UQ are involved in protection against oxidative stress in addition to their role in the electron transport chain [42]. They form an essential part of the cell membrane. In bacteria, quinones are derivatives of either ubiquinone (2,3-dimethoxy-5-methyl-6-(prenyl)n-1,4-benzoquinone) or menaquinone (2-methyl3-(prenyl)n-1,4-naphthoquinones). *E.coli* synthesises ubiquinone-8 and therefore requires benzoate, hydroxybenzoate and other related compounds [43]. In *E. faecalis*, many elements of the UQ operon have been identified, such as Men F, D, E, B enzymes [28] and the membrane-associated electron carrier is a modified menaquinone as it lacks the 2-methyl group. The derivative is termed demethylmenaquinone (DMK) and it appears to be constitutively expressed [40]. Isochorismate is the precursor for DMK biosynthesis in *E. faecalis* as well as aromatic amino acids such as phenylalanine, tyrosine and tryptophan. We have observed a decrease in DMK levels aerobically while the levels of the aromatic amino acids were higher (Figure 4.4), which could be explained by a re-direction of the common precursor towards the aromatic amino acid biosynthesis in detriment of DMK.

On the other hand, *E. faecalis* evolved respiratory mechanism consists of DMK, and two quinol oxidases: cytochrome *bd* (*cydA* and *cydB*) and fumarate reductase (frdA). Quinol oxidases maintain oxidized quinone for electron transport and also regulate superoxide production from DMK aerobically, depending on the availability of nutrients required for the quinol oxidases to operate freely, namely haemin and fumarate [28]. As observed in our intracellular metabolite profile data, fumarate levels were higher aerobically and haemin was supplied in the growth medium, hence both quinol oxidases where actively working minimising the action of DMK and consequently superoxide production which could explain the lower levels of demethylmenaquinone aerobically.

In a different, but interesting perspective, DMK and benzoate are related phenolic compounds that share, in some organisms, common pathways, such as, DMK biosynthesis. Aerobic gram-negative bacteria and eukaryotes contain the benzoquinone and ubiquinone, as the sole quinone, while the facultative anaerobic bacteria such as *E. coli* contain the naphthoquinones, DMK and menaquinone (MK) in addition to ubiquinone [44]. *E. coli* and other gram-negative bacteria are able to synthesise ubiquinone from 4-hydroxybenzoate that derives directly from chorismate. Aromatic compounds form a large group of diverse compounds that include amino and organic acids, quinones and flavonoids. The metabolism of aromatic compounds is also important for instance, to supply growth substrates for microorganisms. A review from Harwood *et al.* analysed the different pathways involved in the degradation of aromatic compounds and observed that the transformation of some aromatic growth substrates all lead to the formation of a central intermediate, benzoyl-CoA [45]. This compound can be further converted to benzoate through enzymes such as, benzoyl-CoA thioesterase. Although the mechanism in gram positive bacteria remains unknown we hypothesise that a pathway sharing some similarities may also occur in *E. faecalis* if eventually an excessive amount of DMK was being produced. That hypothesis would likewise explain the lower levels observed aerobically. Additionally, DMK are located in the lipid membrane of *E. faecalis* and thus, changes in the synthesis or degradation of DMK in parallel to modulation of membrane lipid composition due to a stress condition would be the ultimate response of *E. faecalis* to oxidative stress [28].

4.4.4 FATTY ACID METABOLISM

Our metabolomic results indicate that lipid metabolism and changes in the membrane composition would be key long term changes induced by *E. faecalis* exposure to aerobic conditions as discussed above. Acetate level decreased by 2-fold under aerobic condition. Mixed acid fermentation in *E. faecalis* yields acetate coupled with ATP production. Although *E. faecalis* does not possess typical respiration pathways it expresses an electron transport chain that couples fermentation to oxidative phosphorylation with a net energy gain for the cell [46–48]. Acetate is formed from acetyl-CoA that is also the main precursor for the synthesis of fatty acids. We hypothesise that under aerobic conditions there is a reduction in acetate formation and a redirection of flux towards acetyl-CoA and fatty acids biosynthesis hence explaining the reduction of acetate in 2-fold aerobically. Increased levels of unsaturated and saturated fatty acids (Figure 4.7) indicate a modulation of the lipid membrane under oxidative stress. These data complement the extracellular metabolomic profile where similar results were observed (Figure 4.2). The effect of a stress condition on the membrane lipid composition is usually dependent on the imposed stress. Marr *et al.* showed that an increase in temperature or glucose limitation was coupled to an increased content of unsaturated fatty acids, while a limitation of ammonium salts was coupled with increase content in saturated fatty acids [49]. When *Lactobacillus helveticus* was exposed to a varied combination of stress conditions such as NaCl, H_2O_2, temperature and pH; the main consequence was an increase desaturation of the fatty acids in the membrane [50]. Although no previous studies have been reported for *E. faecalis*, our data suggest that under oxidative stress the fatty acid composition of cell membrane changes with an overall trend of increased unsaturation in response to oxidative stress as well as vancomycin. Studies on other organisms have observed similar results [50–52].

Many antibiotics cause bacterial cell death when acting on its lipid membrane by changing its permeability [53]. Since we have not observed a significant change in the lipid composition of the membrane in response to vancomycin under aerobic conditions, this may indicate that oxygen rather than vancomycin was imposing the stress. Vancomycin on its side, was simply forcing the cell to express its resistance genes and allow peptidoglycan structure to be formed. On a different scenario it could be inferred that *E. faecalis* cells could cope with both vancomycin and oxygen in a similar manner.

It has been previously demonstrated that when an organism is exposed to an initial stress condition, the organism is able to cope more easily to a new stress and also to further increase its resistance towards a stronger stress input [54]. Nonetheless, margaric acid was the main difference in membrane fatty acids composition in the presence of vancomycin under aerobic conditions. Therefore, this fatty acid appears to be directly related to *E. faecalis* response towards vancomycin. Hamzehzarghani *et al.* (2008) analysed the metabolite profile of *Fusarium graminearum* and its resistance towards stresses. They observed that some important resistance-related metabolites were fatty acids and among those, margaric acid was one of them [55]. Although further studies would need to be carried out, it might be possible that margaric acid among other fatty acids also plays an important role in the protection of *E. faecalis* membrane against the deleterious effect of vancomycin.

4.5 *CONCLUSIONS*

In conclusion, oxygen showed to have a significant impact on the cellular metabolism of the vancomycin resistant *E. faecalis* strain. As an aerotolerant microbe *E. faecalis* has developed sophisticated mechanisms to cope with the oxidative stress present in an aerobic environment. This study has sought to provide an insight into the *in vivo* response of this bacterium to changing oxygen tensions. Metabolomics has been a vital endeavour in this approach by building up comparative metabolite profiles under different oxygen conditions. As a result it was possible to understand the global impact of oxygen on the metabolic network of *E. faecalis*. The drive of cellular metabolism towards glutathione production inside the cell was the major impact of oxygen on the cellular system and this is likely the most upstream metabolic response by which *E. faecalis* is able to rapidly neutralise the impact of increased oxidative stress imposed by aerobiosis. Integration of the ^{13}C-isotope distribution and membrane fatty acid composition information to the metabolomic data helped reiterate that under aerobic conditions the metabolic flux was driven towards increasing glycolytic flux in order to produce NADH to be oxidised through the adapted respiratory chain as well as to increase the availability of important key metabolites responsible for different defence mechanisms. Labelling in free glutamate was an interesting finding as it indicates that

glutamate was *de novo* synthesised from glucose despite no previous evidence being found of *E. faecalis* being capable of expressing aconitase or isocitrate dehydrogenase. Therefore, *E. faecalis* is capable of synthesising glutamate, probably via a yet undescribed metabolic pathway.

In addition, differences in benzoate and fatty acid metabolism impacting on the lipid composition and DMK content of cell membrane may represent the final downstream changes induced by exposure to oxygen, which seems to have a similar response observed towards vancomycin.

The overall results clearly showed that oxidative stress was evident even in the presence of vancomycin antibiotic throughout the experiments. That raises the question if vancomycin has a multi-parallel effect involving oxidative stress or if the mode of action relies solely on the inhibition of the cell wall synthesis.

In fact, the resistance to vancomycin is activated by the expression of genes that confer the synthesis of a different moiety in the peptidoglycan chain which blocks vancomycin activity. However, the parallel effect of antibiotics seems to stimulate the oxidation of NADH *via* electron transport chain, hyperactivating the superoxide production. If *E. faecalis* resistance genes to vancomycin only confer a protection to the destruction of the cell wall or if vancomycin presence does not promote oxidative stress is a question that needs further research.

4.6 *REFERENCES*

1. Ferrieri, P. Unique Features of Infective Endocarditis in Childhood. *Circulation* **105,** 2115–2126 (2002).

2. Levine, D. P. Vancomycin: a history. *Clin. Infect. Dis.* **42,** S5–12 (2006).

3. Poh, C. H., Oh, H. M. L. & Tan, A. L. Epidemiology and clinical outcome of enterococcal bacteraemia in an acute care hospital. *J. Infect.* **52,** 383–6 (2006).

4. Fisher, K. & Phillips, C. The ecology, epidemiology and virulence of Enterococcus. *Microbiology* **155,** 1749–57 (2009).

5. Livermore, D. M. Has the era of untreatable infections arrived? *J. Antimicrob. Chemother.* **64,** i29–36 (2009).

6. Neely, A. N. & Maley, M. P. Survival of Enterococci and Staphylococci on Hospital Fabrics and Plastic. *J. Clin. Microbiol.* **38,** 724–726 (2000).

7. Weigel, L. M. *et al.* Genetic analysis of a high-level vancomycin-resistant isolate of *Staphylococcus aureus*. *Science* **302,** 1569–71 (2003).

8. Riboulet, E. *et al.* Relationships between oxidative stress response and virulence in *Enterococcus faecalis*. *J. Mol. Microbiol. Biotechnol.* **13,** 140–6 (2007).

9. Albesa, I., Becerra, M. C., Battán, P. C. & Páez, P. L. Oxidative stress involved in the antibacterial action of different antibiotics. *Biochem. Biophys. Res. Commun.* **317,** 605–9 (2004).

10. Kohanski, M. A., Dwyer, D. J., Hayete, B., Lawrence, C. A. & Collins, J. J. A common mechanism of cellular death induced by bactericidal antibiotics. *Cell* **130,** 797–810 (2007).

11. Huycke, M. M. *Enterococcus faecalis* produces extracellular superoxide and hydrogen peroxide that damages colonic epithelial cell DNA. *Carcinogenesis* **23,** 529–536 (2002).

12. Paulsen, I. T. *et al.* Role of mobile DNA in the evolution of vancomycin-resistant *Enterococcus faecalis*. *Science (80-.).* **299,** 2071–4 (2003).

13. Bizzini, A., Zhao, C., Auffray, Y. & Hartke, A. The *Enterococcus faecalis* superoxide dismutase is essential for its tolerance to vancomycin and penicillin. *J. Antimicrob. Chemother.* **64,** 1196–202 (2009).

14. Winstedt, L., Frankenberg, L., Hederstedt, L. & von Wachenfeldt, C. *Enterococcus faecalis* V583 contains a cytochrome bd-type respiratory oxidase. *J. Bacteriol.* **182,** 3863–6 (2000).

15. Giard, J. C. *et al.* The stress proteome of *Enterococcus faecalis*. *Electrophoresis* **22,** 2947–54 (2001).

16. Flahaut, S., Laplace, J. M., Frère, J. & Auffray, Y. The oxidative stress response in *Enterococcus faecalis*: relationship between H2O2 tolerance and H2O2 stress proteins. *Lett. Appl. Microbiol.* **26,** 259–64 (1998).

17. Hollywood, K., Brison, D. R. & Goodacre, R. Metabolomics: current technologies and future trends. *Proteomics* **6,** 4716–23 (2006).

18. Smart, K. F., Aggio, R. B. M., Van Houtte, J. R. & Villas-Bôas, S. G. Analytical platform for metabolome analysis of microbial cells using methyl chloroformate derivatisation followed by gas chromatography-mass spectrometry. *Nat. Protoc.* **5,** 1709–29 (2010).

19. Christensen, B. & Nielsen, J. Isotopomer analysis using GC-MS. *Metab. Eng.* 282–290 (1999).

20. Villas-Bôas, S. G. & Bruheim, P. Cold glycerol-saline: the promising quenching solution for accurate intracellular metabolite analysis of microbial cells. *Anal. Biochem.* **370,** 87–97 (2007).

21. Suvarna, K., Stevenson, D., Meganathan, R. & Hudspeth, M. E. S. Menaquinone (Vitamin K2) biosynthesis: localization and characterization of the menA gene from *Escherichia coli*. *J. Bacteriol.* **180,** 2782–2787 (1998).

22. Aggio, R. B. M., Ruggiero, K. & Villas-Bôas, S. G. Pathway Activity Profiling (PAPi): from the metabolite profile to the metabolic pathway activity. *Bioinformatics* **26,** 2969–76 (2010).

23. Aggio, R., Villas-Bôas, S. G. & Ruggiero, K. Metab: an R package for high-throughput analysis of metabolomics data generated by GC-MS. *Bioinformatics* **27,** 2316–8 (2011).

24. Hederstedt, L. Respiration Without O2. *Science (80-.).* **284,** 1941–1942 (1999).

25. Gennis, R. . & Stewart, V. in *Escherichia coli Salmonella Cell. Mol. Biol.* (Neidhardt, F. C.) p 217–261 (ASM Press, 1996, 1996).

26. Fernández, M. & Zúñiga, M. Amino acid catabolic pathways of lactic acid bacteria. *Crit. Rev. Microbiol.* **32,** 155–83 (2006).

27. Seo, J.-S., Keum, Y.-S. & Li, Q. X. Bacterial degradation of aromatic compounds. *Int. J. Environ. Res. Public Health* **6,** 278–309 (2009).

28. Huycke, M. M. *et al.* Extracellular superoxide production by *Enterococcus faecalis* requires demethylmenaquinone and is attenuated by functional terminal quinol oxidases. *Mol. Microbiol.* **42,** 729–40 (2001).

29. Szemes, T. *et al.* On the origin of reactive oxygen species and antioxidative mechanisms in *Enterococcus faecalis*. *Redox Rep. Commun. Free Radic. Res.* **15,** 202–206(5) (2010).

30. Brooijmans, R. *et al.* Haem and menaquinone induced electron transport in lactic acid bacteria. *Microb. Cell Fact.* **8,** 28 (2009).

31. Carmel-harel, O. & Storz, G. Roles of the glutathione and thioredoxin-dependent reduction systems in the *Escherichia coli* and *Saccharomyces cerevisiae* responses to oxidative stress. *Annu. Rev. Microbiol.* **54,** 439–61 (2000).

32. Imlay, J. A. Pathways of oxidative damage. *Annu. Rev. Microbiol.* **57,** 395–418 (2003).

33. Patel, M. P., Marcinkeviciene, J. & Blanchard, J. S. *Enterococcus faecalis* glutathione reductase: purification, characterization and expression under normal and hyperbaric O2 conditions. **166,** 155–163 (1998).

34. Liu, M., Nauta, A., Francke, C. & Siezen, R. J. Comparative genomics of enzymes in flavor-forming pathways from amino acids in lactic acid bacteria. *Appl. Environ. Microbiol.* **74,** 4590–600 (2008).

35. Park, J.-H. *et al.* Biosynthesis of the thiazole moiety of thiamin pyrophosphate (vitamin B1). *Biochemistry* **42,** 12430–8 (2003).

36. Zhang, S. G., Sanyal, I., Bulboaca, G. H., Rich, A. & Flint, D. H. The Gene for Biotin Synthase from *Saccharomyces cerevisiae*: Cloning, Sequencing, and Complementation of *Escherichia coli* Strains Lacking Biotin Synthase. *Arch. Biochem. Biophys.* **309,** 29–35 (1994).

37. Cabiscol, E., Tamarit, J. & Ros, J. Oxidative stress in bacteria and protein damage by reactive oxygen species. *Int. Microbiol.* **3,** 3–8 (2000).

38. Grant, C. M. MicroReview Role of the glutathione / glutaredoxin and thioredoxin systems in yeast growth and response to stress conditions. *Mol. Microbiol.* **39,** 533–541 (2001).

39. Holmgren, A. Thioredoxin and Glutaredoxin System. *J. Biol. Chem.* **264,** 13963–13966 (1989).

40. Gilmore, M. S. *The Enterococci: pathogenesis, molecular biology, and antiobiotic resistance*. *ASM Press* 133–175 (ASM Press, 2002).

41. Evans, W. C. & Fuchs, G. Anaerobic degradation of aromatic compounds. *Annu. Rev. Microbiol.* **42,** 289–317 (1988).

42. Søballe, B. & Poole, R. K. Ubiquinone limits oxidative stress in *Escherichia coli*. *Microbiology* **146,** 787–96 (2000).

43. Knoell, H. E. Isolation of a soluble enzyme complex comprising the ubiquinone-8 synthesis apparatus from the cytoplasmic membrane of *Escherichia coli*. *Biochem. Biophys. Res. Commun.* **91,** 919–925 (1979).

44. Meganathan, R. Ubiquinone biosynthesis in microorganisms. *FEMS Microbiol. Lett.* **203,** 131–9 (2001).

45. Harwood, C. S., Burchhardt, G., Herrmann, H. & Fuchs, G. Anaerobic metabolism of aromatic compounds via the benzoyl-CoA pathway. *FEMS Microbiol. Lett.* **22,** (1999).

46. Road, W. M. Haematin-dependent Oxidative Phosphorylation in *Streptococcus faecalis*. *J. Gen. Microbiol.* 247–260 (1969).

47. Gallin, J. I. & VanDemark, P. J. Evidence for oxidative phosphorylation in *Streptococcus faecalis*. *Biochem. Biophys. Res. Commun.* **17,** 630–635 (1964).

48. Pritchard, G. G. & Wimpenny, J. W. Cytochrome formation, oxygen-induced proton extrusion and respiratory activity in *Streptococcus faecalis* var. *zymogenes* grown in the presence of haematin. *J. Gen. Microbiol.* **104,** 15–22 (1978).

49. Marr, A. G. & Ingraham, J. L. Effect of temperature on the composition of fatty acids in *Escherichia coli*. *J. Bacteriol.* **84,** 1260–7 (1962).

50. Guerzoni, M. E., Lanciotti, R. & Cocconcelli, P. S. Alteration in cellular fatty acid composition as a response to salt, acid, oxidative and thermal stresses in Lactobacillus helveticus. *Microbiology* **147,** 2255–2264 (2001).

51. Quivey, R. G., Faustoferri, R., Monahan, K. & Marquis, R. Shifts in membrane fatty acid profiles associated with acid adaptation of *Streptococcus mutans*. *FEMS Microbiol. Lett.* **189,** 89–92 (2000).

52. Pesakhov, S. *et al.* Effect of hydrogen peroxide production and the Fenton reaction on membrane composition of *Streptococcus pneumoniae*. *Biochim. Biophys. Acta* **1768,** 590–7 (2007).

53. Cetinkaya, Y., Falk, P. & Mayhall, C. G. Vancomycin-Resistant Enterococci. *Clin. Microbiol. Rev.* **13,** 686–707 (2000).

54. Murray, B. E. The life and times of the Enterococcus. *Clin. Microbiol. Rev.* **3,** 46–65 (1990).

55. Hamzehzarghani, H. *et al.* Metabolite profiling coupled with statistical analyses for potential high-throughput screening of quantitative resistance to fusarium head blight in wheat. *Can. J. Plant Pathol.* **30,** 24–36 (2008).

CHAPTER 5

GENOME SCALE METABOLIC MODEL RECONSTRUCTION OF *ENTEROCOCCUS FAECALIS* V583

ABSTRACT

The first genome-scale metabolic network of the pathogen *Enterococcus faecalis* V583, was reconstructed and is presented in this chapter. This opportunistic pathogen is mostly known for its implications in the medical field while some other strains of *E. faecalis* are gaining attention in the dairy and fermented products industries. The genome-scale model reconstruction followed an iterative protocol by collecting all the metabolic reactions catalysed by the organism from different databases and further manually curating the information using literature and other specific data sources. The first version of the model presented herein comprises a total of 665 reactions and 645 metabolites. The annotated genome of *E. faecalis* V583 contains 3500 ORF and from those, 366 are associated with metabolic reactions. The different prediction capabilities of the model were analysed in terms of predicting the shift from a homolactic behaviour of *E: faecalis*, to mixed acid fermentation. Additionally, the shift between anaerobic and aerobic environments was also analysed and further discussed. The present model is able to predict accurately the qualitative behaviour of the organism, by simulating the metabolic changes between different cellular states. Ultimately, this model aims to serve as a tool to better understand the metabolic behaviour under different environmental conditions.

Portela, C., Vilaça, P., Villas-Bôas, S.G., Ferreira, E.C., Rocha, I., Genome-scale metabolic network of the pathogen *Enterococcus faecalis* V583. (To be submitted).

5.1 *INTRODUCTION*

Enterococcus faecalis is a gram positive bacterium from the lactic acid bacteria (LAB) group. With a low G+C content, this organism is normally found in our intestines and is considered to be a commensal organism. However, it is an opportunist bacterium that can cause serious infections in the host organism. From nosocomial to urinary tract infections and endocarditis, this organism presents a serious health threat [1]. On a perfectly opposite panorama, *E. faecalis* has been subject of study in the dairy industry due to its important role in the production of flavour compounds during fermentation processes [2].

Considered to be a facultative anaerobe, *E. faecalis* usually relies on fermentative pathways for energy formation [3]. *E. faecalis*, similarly to all LAB, is nutritionally demanding and therefore, usually inhabits nutrient-rich environments like warm-blooded animals. Amino acid biosynthesis is limited and therefore uptake from the medium is usually preferred, with only a small fraction being *de novo* synthesised from a carbon source. The major part of the carbohydrates consumed are converted into end-products to produce energy and reducing equivalents, with as little as 5% of the sugar consumed being converted into biomass [4]. The limited biosynthetic capacity of *E. faecalis* implies that the growth medium must include not only fermentable sugars but also amino acids, vitamins and mineral salts [5]. As a facultative anaerobe, *E. faecalis* does not possess a typical TCA cycle and a typical oxidative phosphorylation chain. Energy production derives in its majority from substrate level phosphorylation. Nevertheless, this organism has been shown to express a cytochrome *bd* and is therefore able to respire under certain environmental conditions, namely in the presence of haemin [6]. The adapted respiratory system not only yields ATP, but also confers the organism with an extra mechanism to improve survival in environments outside the host, hence increasing its chance to disseminate [7].

The prospect of better understanding its metabolism and further designing metabolic targets became a subject of relevance in the medical and also in the dairy industry fields. A reconstructed genome-scale metabolic model can serve as a tool to predict the phenotypic behaviour under different environmental conditions.

Since the metabolic reconstruction of *Haemophilus influenzae* was published in 1999 [8], many other researchers have focused their attention into the possibilities that the new era of genome-scale metabolic models could bring to the scientific scene. Published models for organisms such as *Mycobacterium tuberculosis* or *Klebsiella pneumoniae* or even *Yersinia pestis* have had their genome-scale models reconstructed precisely because they represent human pathogens that can cause diseases in hospitals or in underdeveloped countries. The main goal of these models is to be able to better understand the metabolism of these organisms and identify potential steps in the metabolism that can lead to the formulation of broad therapeutics [9–11].

The field of genome-scale reconstructions has expanded rapidly over the years and currently counts with more than 60 genome-scale network reconstructions (GENRE) for bacterial species alone. When considering archea and eukaryotes, the total number of GENRE raises up to 90, according to an updated repository maintained by the Systems Biology Research Group at the University of California, San Diego (http://gcrg.ucsd.edu/InSilicoOrganisms/OtherOrganisms) [12].

Constraint based genome-scale reconstructions can be used as modelling tools and use, among others, the flux balance analysis (FBA) [13] approach to explore the capabilities of the network. Metabolic conversions are translated into a stoichiometric matrix that is defined by the metabolites and their participation in each enzymatic reaction occurring in the system. Considering that cells regulate their internal metabolism to keep it, if possible, in steady state, the system becomes linear and can be solved by defining an appropriate objective function. Usually, the objective function is biomass formation, since often microorganisms' main purpose is to maximize their growth. Through the definition of the environmental constraints and applying Flux Balance Analysis (FBA) approaches, it is possible to predict phenotypes, as well as product yields and specific growth rates. Figure 2.6 (chapter 2) elucidates the process of a genome-scale reconstruction. Chapter 2 also gives a deeper insight about methodologies for model reconstruction.

In the present chapter, the reconstruction of the genome-scale metabolic model of *E. faecalis* is presented. The reconstruction started with the information on *E. faecalis* from the KEGG database. Additional information from biochemical and metabolic

pathways from databases and the literature was compiled and analysed deeply to complement or validate the initial data. Once the model was set and debugged, FBA was applied and the network capabilities were explored. Simulations were designed to analyse the effects of different environmental conditions and the phenotypic change caused by switching from anaerobic to aerobic environments and homolactic to heterolactic fermentations. Simulation results were compared with experimental data published. Also, single gene deletions were computed and reactions essentiality analysed. The present model was developed in order to better characterise the metabolism and physiology of *E. faecalis* and to identify new possible targets related to pathogenicity.

5.2 *METHODOLOGY*

5.2.1 NETWORK RECONSTRUCTION

The reconstruction procedure involved an exhaustive search of the available information about the organism. A reaction database, specific for *E. faecalis* V583 and based on the annotated genome, was compiled using Kyoto Encyclopaedia of Genes and Genomes (KEGG database), [14]. Although there is little manual curation of the information in this database, it still contains the most extent repertoire of reactions known from all available databases.

Afterwards, each individual pathway associated with *E. faecalis'* metabolism was manually curated. The Merlin software was used to perform this task [15]. This software aims to semi-automate the process of genome-scale reconstructions and, among other tasks, it allows performing a BLAST search of the sequenced genome against the entire NCBI database. It further allows viewing the information of the possible homologues for each gene, their function and the associated *e-value* score, in a user friendly view and also to perform searches within all the homologues found for a particular organism. The curation methodology involved the analysis of enzymes marked as not present according to the data collected from KEGG but that were required to complete important conversions, known to occur, as observed in the metabolic maps. Each of those EC numbers were searched within Merlin for identifying homologues with the

same function and the corresponding genes in *E. faecalis*. If a homologue was found with a high similarity, the corresponding EC number would be included in the model. As a result, 25 reactions involved in the metabolism of *E. faecalis* were added to the initial database.

Furthermore, all relevant literature information collected on *E. faecalis*' metabolism was analysed and some new functions were added or simply validated. Also, information from the BRENDA database on *E. faecalis* [16] was retrieved and included, as it represents information with experimental validation. The same procedure was applied to all data from SwissProt (data from UniProt database [17] that have been manually curated). Other data sources such as BioCyc [18] or the TrEMBL database (UniProt section where data is not manually curated) were used for consistency checking and validation purposes only.

Finally, additional reactions were added to the model for gap filling purposes. The procedure applied involved the addition of reactions that were necessary to be present such that biomass could be produced. Several simulations were performed with biomass production as the objective function and, while this had a value of zero, each individual biomass component was analysed to check for its connectivity to the network. When necessary, new reactions were added from KEGG (not initially associated with *E. faecalis*) that would solve the gaps found.

5.2.1.1 Mass and charge balance of reactions

Constraint-based approaches assume that the network being analysed is under steady state. Considering that, the sum of influx must equal the sum of efflux for each metabolite. For that premise to be correctly applied, it is necessary to balance all elements in terms of mass and charge on both sides of the reactions. This step is straightforward for many central metabolic reactions, but may become challenging for more complex ones. It should be noted that unbalanced reactions may lead to the synthesis of extra carbons, protons or energy (ATP) out of nothing, misleading the simulation results [19].

The network was balanced in terms of mass and charge for each compound. The chemical formula and the charge of each compound was retrieved from the ChEBI

database for pH 7.4 (close to the intracellular pH [20]), from BiGG (http://bigg.ucsd.edu/bigg/home.pl) [21] or from KEGG, whenever the information about a metabolite was missing in both databases. Afterwards, an automatic validation process to detect inconsistencies on charge and mass balances was used. When the reaction unbalance was caused by a proton, the process automatically corrected the reaction by adding a proton on the reactants' or products' side of the equation. On the other hand, if the charge or mass balance differed greatly, a manual inspection of the chemical formula had to be made in order to balance the equation.

5.2.1.2 Reversibility of reactions

A particular emphasis was given to reactions' reversibility. The reversibility was manually curated for all reactions, with focus on eQuilibrator [22], BioCyc [18] and Brenda [16,23] databases. Reactions, whose reversibility was not defined, were considered to be reversible. All the information is compiled in an excel spreadsheet available as supplementary material.

5.2.1.3 Gene-Protein-Reaction associations (GPR)

GPR associations acquire a relevant role in GEnome-scale Models (GEM) by bridging the connection between genes to the reactions catalysed by the respective enzymes. In particular, when simulating gene knockouts, it is important that the relation between a gene and the reaction (or reactions) catalysed by the enzyme associated with that same gene is well defined. It is therefore important to determine if: enzymatic complexes exist; an enzyme (or complex) can carry out more than one reaction and if more than one protein can carry out the same function (i.e., isozymes). Literature and the KEGG database were used to assist in this step. KEGG database proved quiet useful in this task as it often provides information about the GPR association, i.e., it indicates which gene has what function. Boolean rules (or/and) define the relation between the different genes that code for one or multiple enzymes and that information is available as supplementary material.

5.2.1.4 Biomass assembly

The biomass equation was adapted from the genome-scale reconstruction of *Lactococcus lactis* [24]. The linear combination of seven macromolecules, namely protein,

DNA, RNA, lipoteichoic acids (LTA), lipids (LIP), peptidoglycans (PG) and polysaccharides (POLYS) represent the overall requirements for biomass formation.

The biomass reaction used from the *L. lactis* model was lumped for the PG and LTA reactions. A deep effort to unravel the lumped reactions to incorporate the basic composition was unsuccessful due to the complexity and nature of these reactions. However, we consider that little differences would be observed between the two organisms since both are closely related lactic acid bacteria. The lumped reactions are named: lump_PG2 for peptidoglycan assembly and lump_LTA3 for lipoteichoic acid assembly.

Finally, a demethylmenaquinone lumped reaction was also incorporated for model simplification.

The described procedure culminated in the reconstruction of the first GEM of *E. faecalis*. The model was further tested in terms of its predicting capabilities, as described next.

5.2.1.5 Simulations

All the simulations and analysis of the network were performed using a software developed in house, Optflux [25]. This open-source and user friendly tool allows the researchers to perform multiple analysis, simulations and optimizations of genome-scale models.

The software supports several GEM formats, from flat file formats to the SBML standard. It also incorporates strain optimization tasks, i.e., the identification of metabolic engineering targets, using evolutionary algorithms or simulated annealing metaheuristics. Analysis of the metabolic models include, among others: phenotype simulation of both wild-type and mutant organisms, using the different methods including FBA, determination of flux variability analysis (FVA) given a set of environmental conditions, or optimization of gene over / underexpression [25].

The FBA method is commonly used to analyse biochemical networks, in particular genome-scale metabolic network reconstructions, and allows to calculate the flow of

metabolites through the metabolic network, thereby making it possible to predict the growth rate of an organism or the rate of production of an important metabolite [26].

5.3 *RESULTS*

The iterative process of the *E. faecalis* GEM reconstruction resulted on the first genome-scale model of the organism. The main results of the reconstruction process and analysis of the network are detailed next. The model validation comprised a set of simulations and gene deletion experiments that were compared with data already published in the literature. The model aims to serve researchers to explore the *in silico* metabolism of *E. faecalis* and support the prediction and better understanding of the behaviour of the organism.

5.3.1 BASIC NETWORK CHARACTERISTICS

The present genome-scale reconstruction comprises 665 reaction and 645 metabolites. From the initial set of 1127 reactions from the KEGG database that were associated with *E. faecalis'* metabolism, 554 were kept while the rest were considered not to be relevant for the model, since they were reactions involving co-factors for which no literature evidence was found (it is often the case that KEGG associates more than one co-factor with each reaction), or they were dead end reactions or because there was no pathway associated with those reactions. One hundred and eleven reactions are unique to the model when compared with data from KEGG and were included because new genomic or literature evidence was found, or they represent gap filling, biomass assembly or lumped reactions. A Venn diagram denotes the intersection of information obtained from KEGG and new manually curated information included in the model (Figure 5.1).

Out of the 665 reactions, 579 are intracellular reactions while 86 are transport related reactions. The annotated genome of *E. faecalis* contains 3500 ORF and from those, 366 are associated with metabolic reactions in the present model. That corresponds to 88% of reactions with gene association. The remaining 12% (80 reactions) correspond to membrane transport reactions with no gene identified, reactions without associated EC numbers (non-enzymatic or spontaneous) and reactions added for gap filling purposes.

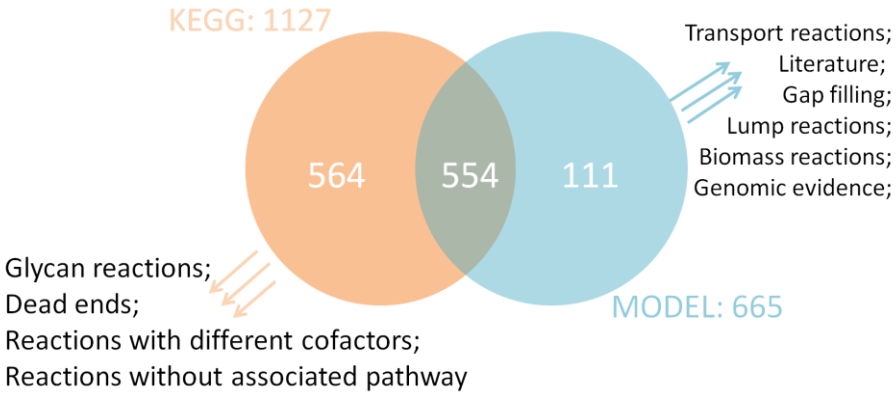

Figure 5.1. Venn diagram where the intersection of information available in the KEGG database and the significant information added to the model is depicted.

The final reaction set with all relevant information such as: reaction id, reaction equation, reversibility, gene(s) coding for the enzyme(s) that catalyse(s) the reaction, the subsystem the reaction belongs to, the compartment where the reaction takes place (either the cytosol or the extracellular environment) and GPR (Gene-Protein-Reaction) associations are available as supplementary material.

Table 5.1 summarizes the basic network information for the reconstructed model of *E. faecalis*.

Table 5.1. Basic network properties of *E. faecalis'* genome-scale model

Genome characteristics	
Genome size	3.2 Mb
Total ORF	3500
ORF with known function	~1166
Average G+C	~37%
Basic model properties	
Metabolic genes	366
Corresponding percentage of genome	10%
Reactions	665
Gene association	589
Gene associated reactions	88%
Non-gene associated reactions	12%
Transport reactions	82
Metabolites	645

Different sources were used to validate the information included in the model. For each reaction in the dataset, a level of confidence was attributed. The highest confidence level, four stars (****) was given to reactions validated with literature or alternatively, present in the Brenda database, which comprises molecular and biochemical experimental information on enzymes. Following the literature evidence, information from manually annotated and reviewed databases such as SwissProt (from UniProt) was given a 3 stars mark (***).

Next, all genomic evidence obtained either from the annotated genome (KEGG) or homology data obtained with Merlin have a confidence score of 2 stars (**). The genome annotated may contain intrinsic errors or may even be incomplete and therefore the information is not considered as reliable as the previous sources. Finally, the reactions with lowest confidence levels (*) are those added for gap filling purposes. Those are reactions that are required for the model to work but the associated enzymes may not have homology to *E. faecalis*. However, those are essential and therefore may not be discarded.

Table 5.2 shows the reactions supported by the different sources of information and their corresponding confidence level. Additionally, the confidence level given to each reaction in the network is available as supplementary material.

As observed from Table 5.2, this genome-scale model relies essentially on the annotated genome and available literature. It is frequent that a reconstructed structure has gaps, whether because there is limited information about a pathway or because it is a still unknown path. The gap filling process is consequently an important step to connect the metabolites to the network for it to be able to produce all the biomass precursors.

Table 5.2. Different sources of information and confidence levels to support the inclusion of the reactions in the metabolic network.

Source of Information	No. of reactions	Confidence Level
Literature (published data; Brenda entries)	174	****
Curated info (SwissProt)	96	***
Genomic evidence (Annotated genome, Homology data)	382	**
Gap filling	12	*

As a consequence, it was necessary to include additional reactions to the model where no homology or low homology was detected in related organisms in order to fill the gaps in the network. A total of 12 new reactions were added to the network to account for biomass production. All the information is available as supplementary material.

5.3.2 SUBSTRATE UTILISATION

As previously mentioned, *E. faecalis* grows in environments where the availability of nutrients prevails, such as the human intestines. Due to that, it is expected that an efficient and varied transport system is available to allow the uptake of numerous amino acids, sugars, vitamins and salts. The limited biosynthetic capacity of *E. faecalis* indicates that most amino acids are uptaken from the growth medium while only a few are *de novo* synthesized from glucose. Therefore, only a small percentage of the metabolised sugar is converted into biomass, while the majority is converted into end-products and energy [4,27]. A wide variety of carbohydrates can be fermented by enterococci. At least 13 sugars are metabolised by all species (glucose, fructose, maltose, mannose, ribose, galactose, N-acetylglucosamine, arbutin, salicin, cellobiose, maltose, lactose and trehalose) [7]. The capability of *E. faecalis* to grow on different carbon sources has been tested elsewhere demonstrating its ability to grow on multiple substrates [28].

The capabilities of the *in silico* model to utilise those 13 different carbon sources were analysed using the FBA method, by comparing the phenotypic response to the same uptake rates. All the above mentioned carbon sources were supplied, one at a time, together with all amino acids and inorganic compounds. For qualitative purposes, the sugar consumption rate was set to 12 mmol/gDW.g. In order to maintain a constant carbon uptake of 72 $mmol_{Carbon}$/gDW.h, the availability of disaccharides, was set to 6 mmol/gDW.h, while for pentoses it was set to 14.4 mmol/gDW.h. Also, for N-acetylglucosamine and salicin it was set to 9 mmol/gDW.h and 5.54 mmol/gDW.h, respectively. All carbon sources were predicted to be consumed and produce biomass with exception to salicin and arbutin. These two carbon sources were not consumed since their consumption was coupled to the production of two metabolites: salicyl alcohol, which did not enter any further reaction and p-Benzenediol for which the following degradation reactions were missing from the network.

All other metabolites with exception of mannitol and mannose, originated a similar net conversion in terms of the main end products produced and biomass formation, indicating that the different substrates can serve as source for carbon and energy.

Analysis of the *in silico* flux distribution of mannose and mannitol consumption showed that no flux was going through glycolysis but rather through the pentose-phosphate pathway and therefore possibly a lower amount of ATP was being generated. Consequently, biomass production was lower with only acetate production as end-product.

5.3.3 AMINO ACIDS REQUIREMENTS

In addition to carbon source utilisation, the minimal growth requirements of *E. faecalis*, were determined by analysing the amino acids essentiality. For that purpose, amino acids were individually omitted from *in silico* the medium and biomass production analysed.

Inorganic compounds such as phosphate, minerals, ammonium and water were freely available, which means that lower and upper bounds were left unconstrained. For qualitative purposes, the glucose flux was set to 12 mmol/gDW.h and individual amino acids were supplied at a rate of 10 mmol/gDW.h.

From literature, it is known that lactic acid bacteria have complex nutritional requirements, as they are usually associated with nutrient rich environments [3]. *E. faecalis* is a fastidious organism that requires a number of amino acids for its survival. Although no studies have been focused on the definition of a minimal growth medium of *E. faecalis*, some authors have developed a chemically defined medium to serve a specific purpose [29,30]. The authors have determined that the amino acid requirements were different in each study, most likely due to the fact that they were working with different bacterial strains. Hence, it is expected that *E. faecalis* V583 might also exhibit different amino acid essentiality.

Table 5.3 resumes the *in vivo* amino acid essentiality for two different strains (OG1RF and KA177) and the *in silico* prediction of amino acid essentiality for V583.

Table 5.3. Essential amino acids for each strain tested in different published studies and *in silico* simulation. * Zhang *et al.*; ** Khan *et al.*; *** *in silico* predictions from the genome-scale model of *E. faecalis* V583 (present study).

Amino acid	IUPAC id	OG1RF and KA177 Zhang et al*	B9510 Khan et al**	V583 *in silico****
Alanine	A	No	No	No
Arginine	N	Yes	Yes	No
Aspartic acid	D	No	No	No
Cysteine	C	No	No	No
Glutamic acid	E	No	No	No
Glutamine	Q	No	No	Yes
Glycine	G	Yes	No	No
Histidine	H	Yes	Yes	Yes
Isoleucine	I	No	Yes	Yes
Leucine	L	Yes	Yes	Yes
Lysine	K	No	No	No
Methionine	M	Yes	Yes	Yes
Phenylalanine	F	No	No	No
Proline	P	No	No	No
Serine	S	No	No	No
Threonine	T	No	No	No
Tryptophan	W	Yes	No	Yes
Tyrosine	Y	No	No	No
Valine	V	Yes	Yes	Yes

From the results presented in Table 5.3, simulations analysing amino acid requirements allowed to infer that glutamine (or glutamate), histidine, isoleucine, leucine, methionine, tryptophan and valine are essential for the *in silico* strain and, in the absence of one of the mentioned essential amino acids, growth is not possible.

Additionally, auxotrophy for histidine, leucine, methionine and valine was common among the different studies.

Histidine, tryptophan, valine, leucine and isoleucine are easily identified as essential, since the biosynthetic pathways to produce these amino acids are incomplete in the model and therefore it is not possible for the organism to synthesise them. The histidine

pathway in KEGG, for instance, does not exhibit a single annotated enzyme for the *E. faecalis* genome. Likewise, for branched chain amino acids, valine, leucine and isoleucine, although they share pyruvate as a common precursor, the absence of both dihydroxyisovalerate dehydrogenase (1.1.1.86) and 2,3-dihydroxyisovalerate dehydratase (4.2.1.9) breaks the pathway towards valine and isoleucine synthesis. Leucine branch is even less detailed than closely related compounds valine and isoleucine, therefore explaining the auxotrophy for these amino acids.

For methonine auxotrophy, the results are in agreement with *in vivo* observations. However, the genome annotation suggests that genes coding for the enzymes necessary for the biosynthesis of this amino acid are present, and the model should therefore be able to synthesise the amino acid, concomitantly that L-cystathionine is produced. However, probably for stoichiometric reasons not yet identified, methionine cannot be produced *in silico* using that pathway.

Both experimental studies indicate that *E. faecalis* OG1RF, KA177 and B9510 are auxotrophic for arginine, while V583 appears to be able to synthesise this amino acid. Despite the fact that the genome sequence of strains KA177 and B9510 are not available, the annotated genome of strain OG1RF is available and also presents the annotated enzyme responsible for the synthesis of arginine from citrulline under arginine deiminase activity (3.5.3.6). Therefore, the auxotrophy for arginine might have been inaccurately determined experimentally or, in contrast, other unclear factors limiting the biosynthesis of arginine not taken into account in the GEM model may be incorrectly predicting the biosynthesis of the amino acid.

On the other hand, glutamine (or glutamate, as they interconvert on one another) was defined as essential for V583 but not for the other strains. The precursor for glutamine (or glutamate) is α-ketoglutarate, which is an intermediary of the TCA cycle. As mentioned previously, *E. faecalis* does not possess a TCA cycle and it is therefore not able to synthesise the direct precursor for this amino acid. However, as previously mentioned in chapter 3, metabolomics and fluxomics data support that glutamate can be *de novo* synthesised by glucose, as evidenced by ^{13}C labelling experiments. Nevertheless, the strain used in the previous chapter was not the V583 strain and

whether the metabolic difference is related to the strains used or to a still unknown pathway to be determined, remains unclear.

5.3.4 PREDICTION OF PHYSIOLOGICAL PARAMETERS

5.3.4.1 Simulation with chemically defined media

With a minimal medium defined for *E. faecalis* V583, biomass formation was maximized using FBA under anaerobic conditions. The minimal medium was designed based on the amino acids essentiality determined above, together with other components known to be essential: inorganic phosphate source, ammonium and orotate. This compound was concluded to be essential in our model but also in experimental analysis [31]. Results show that the maximum specific growth rate obtained with the minimal defined medium was 0.04 h^{-1} (Table 5.4). Such value is apparently low compared to normal *E. faecalis* growth rates. However this value is also influenced by the limiting carbon source (glutamine) to be set to 3 mmol/gDW.h. This value was chosen for qualitative purposes only. If the value was set to 10 mmol/gDW.h an increment in biomass to 0.07 h^{-1} would be evidenced while the end products formed were mostly acetate and ethanol (data not shown). Nevertheless, no reported literature has evidenced the application of a defined minimal medium for *E. faecalis* growth before. Therefore, it is not possible to validate or refute this prediction unless experimentally in the laboratory.

Table 5.4. Simulation A. Minimal medium and the phenotypic response of *E. faecalis*. All fluxes for metabolites are in mmol/gDW.h and for biomass in h^{-1}.

Environmental conditions	Lower bound	Upper bound
Ammonium	-10000	10000
Glutamine	-3	10000
Orotate	-1	10000
Alanine, Arginine, Asparagine, Aspartate, Cysteine, Glutamate, Glycine, Lactate, Lysine, Ornithine, Phenylalanine, Proline, Serine, Threonine, Tyrosine	0	10000
Glucose	-12	10000
Acetaldehyde, Acetate, Acetoin, Ethanol, Formate, Malate, Pyruvate	0	10000
Citrate, Cysteine, Pantothenate, Sulfate	0	10000
Oxygen	0	10000

Net conversion:
16.11 Ammonium + 0.29 Biphosphate + 12 Glucose + 3.00 Glutamine + 0.26 Histidine + 1.04 Isoleucine + 1.48 Leucine + 1.00 Methionine + 0.01 Orotate + 0.29 Tryptophan + 1.23 Valine => 25.77 H2O + 5.54 Ethanol + 2.75 Threonine + 2.35 Formate + 1.59 Alanine + 1.23 Acetate + 0.57 O-Phosphoryl homoserine + 4.9E-03 Pantothenate + 3.0E-06 Proline + 0.04 Biomass

	Yield (**mmol** $_{end\ product}$ /**mmol** $_{glucose}$)
Acetate	0.103
Formate	0.196
Ethanol	0.461

Despite the low growth rate value obtained, which is a consequence of a limitation of substrate and amino acids, the results seem to mimic the behaviour of a mixed acid fermentation with different end products being excreted, such as formate, acetate and ethanol. Additionally, when performing simulations with the minimal medium in the absence of glucose, a decrease in the specific growth rate is observed (0.0088 h^{-1}), indicating that glucose was contributing to generate energy and reducing power.

To further analyse these results, data on a chemically defined medium published by Mehmeti *et al.* (2011) and the corresponding uptake rates [31], was used to simulate a more complete growth medium (as all amino acids are included but the corresponding uptake fluxes are low).

A specific growth rate of 0.0032 h^{-1} was obtained with the computed environmental condition defined in Table 5.5.

The predicted value is underestimating the specific growth rate mentioned in the literature, which is described to be 0.15 h^{-1}. Such low value could be due to limiting amino acids uptake. In fact, if glucose is removed from the environment, the model still predicts growth (data not shown). To our knowledge, no literature evidence was found supporting that *E. faecalis* is not able to grow using amino acids as carbon sources. *Helicobacter pylori*, a pathogenic bacterium that shares with *E. faecalis* the characteristic of being a fastidious organism, has been shown to be able to survive, employing amino acids as the basic nutrients [32].

Table 5.5. Simulation B. Chemically defined medium and the phenotypic response of *E. faecalis*. All fluxes for metabolites are in mmol/gDW.h and for biomass in h^{-1}.

Environmental conditions	Lower bound	Upper bound
Alanine	-0.260	10000
Arginine	-0.069	10000
Asparagine	-0.073	10000
Aspartate	-0.305	10000
Glutamate	-0.328	10000
Glutamine	-0.132	10000
Glycine	-0.225	10000
Histidine	-0.093	10000
Isoleucine	-0.155	10000
Leucine	-0.350	10000
Lysine	-0.291	10000
Methionine	-0.081	10000
Phenylalanine	-0.161	10000
Proline	-0.561	10000
Serine	-0.313	10000
Threonine	-0.182	10000
Tryptophan	-0.023	10000
Tyrosine	-0.133	10000
Valine	-0.268	10000
Ornithine	0	10000
Cysteine	-0.103	10000
Glucose	-12	10000
Lactate, Acetoin, Pyruvate, Malate, Acetaldehyde, Ethanol, Formate, Acetate	0	10000
Ammonium	-0.510	10000
Pantothenate	-10000	10000
Citrate	0	0
Sulfate	0	10000
Orotate	-1	10000
Oxygen	0	10000

Net conversion:
0.33 Ammonium + 0.07 Arginine + 0.07 Asparagine + 0.31 Aspartate + 5.1E04 Biphosphate + 0.05 Cysteine + 0.76 Glucose + 3.7E03 Glutamate + 0.13 Glutamine + 0.23 Glycine + 0.02 Histidine + 0.08 Isoleucine + 0.12 Leucine + 0.10 Lysine + 0.03 Methionine + 5.6E04 Orotate + 0.05 Phenylalanine + 0.03 Proline + 0.31 Serine + 0.08 Threonine + 0.02 Tryptophan + 0.04 Tyrosine + 0.10 Valine => 1.27 Formate + 0.89 Alanine + 0.86 Acetate + 0.23 Ethanol + 3.9E-04 Pantothenate + 3.2E-03 Biomass

	Yield (mmol $_{end\ product}$ /mmol $_{glucose}$)
Acetate	1.137
Formate	1.670
Ethanol	0.310

Published work related with *E. faecalis* growth usually contains a carbon source in addition to amino acids. If indeed *E. faecalis* is able to survive with only amino acids that would require the organism to be able to activate the gluconeogenesis pathway in order to synthesise carbohydrates to be further utilised for biosynthetic purposes. A study from Snoep *et al.*, 1990 analysed the anaerobic growth of *E. faecalis* on pyruvate and suggested that low levels of fructose 1,6- biphosphate formation resulted from gluconeogenesis occurrence [33].

In simulation B (Table 5.5) glucose was still being consumed in small quantities from the medium (0.76 out of the 5.37 mmol/gDW.h available). It is plausible that, under amino acids limitation (especially essential amino acids), biomass formation is constrained. Glucose degradation is therefore only needed to produce the required ATP that will be used for the biosynthesis of that limited amount of biomass.

Similarly to the results observed in simulation A, mixed acid fermentation behaviour was also observed, with formate, acetate and ethanol being produced. The yields of each end product were 1.670, 1.137, 0.310 mmol $_{end\ product}$ / mmol $_{glucose}$, respectively. That corresponds to a ratio of 2:1.4:0.4 which is not in agreement with the expected ratio of 2:1:1 [31]. The *in silico* preference for acetate production in contrast with ethanol might be related with the production of one extra ATP from the first and the NAD^+ regeneration from the second. The demands for energy supply seem to be higher than the regeneration of cofactors.

Although the model simulations were predicting with accuracy the qualitative behaviour of the cell, another approach was designed to fit the model in terms of coherent values for the expected specific growth rate ($0.15h^{-1}$).

5.3.4.2 Fitting intake fluxes for specific growth rate adjustment

Firstly, for fitting purposes the amino acids availability was set to a maximum of 10 mmol/gDW.h for all amino acids. The net conversion was analysed and the specific

growth rate obtained was 0.227 h^{-1} (Table not shown). This value was now higher than what the expected growth rate should be, reiterating the direct effect of the amino acids on biomass production. Since, under these circumstances, some amino acids were consumed at their maximum rate (i.e. 10 mmol/gDW.h); they were hence the ones limiting the system. Those amino acids were: alanine, asparagine, aspartate, glutamate, glutamine, phenylalanine, proline and serine.

Next, for those amino acids, the availability was set to 5 mmol/gDW.h. As it can be seen in simulation C, biomass decreased to 0.152 h^{-1} which is in accordance with what would be expected (Table 5.6). The main end product now formed was acetate together with the amino acids ornithine, tyrosine and glycine.

Table 5.6. Simulation C. Fitting of the specific growth rate and the phenotypic response of *E. faecalis*. All fluxes for metabolites are in mmol/gDW.h and for biomass in h^{-1}.

Environmental conditions	Lower bound	Upper bound
Arginine, Cysteine, Glycine, Histidine, Isoleucine, Leucine, Lysine, Methionine, Threonine, Tryptophan, Tyrosine, Valine	-10	10000
Alanine, Asparagine, Aspartate, Glutamate, Glutamine, Phenylalanine, Proline, Serine	-5	10000
Ornithine	0	10000
Glucose	-12	10000
Acetoin, Pyruvate, Malate, Acetaldehyde, Ethanol, Formate, Acetate, Lactate	0	10000
Ammonium	-10	10000
Orotate	-1	10000
Pantothenate, Citrate, Sulfate	0	10000
Oxygen	0	10000

Net conversion:
5.00 Alanine + 1.99 Ammonium + 10.00 Arginine + 5.00 Asparagine + 5.00 Aspartate + 0.02 Biphosphate + 2.15 Cysteine + 12 Glucose + 5.00 Glutamate + 5.00 Glutamine + 11.62 H2O + 0.96 Histidine + 3.90 Isoleucine + 5.56 Leucine + 4.62 Lysine + 1.60 Methionine + 0.03 Orotate + 5.00 Phenylalanine + 5.00 Proline + 5.00 Serine + 3.58 Threonine + 1.09 Tryptophan + 4.60 Valine => 33.07 Acetate + 19.14 Glycine + 10.14 Ornithine + 0.85 Tyrosine + 0.02 Pantothenate + 0.15 Biomass

	Yield (mmol $_{end\ product}$ /mmol $_{glucose}$)
Acetate	2.756

Ornithine leaves the cell by antiport with arginine [34]. From flux analysis it was observed that the cell synthesised considerable amounts of ornithine from citrulline to be further secreted with parallel uptake transport of arginine. The conversion of citrulline to ornithine which is coupled with ATP generation occurs through deiminase catabolism. Deiminase catabolism is a pathway that leads to the formation of high energy carbamoyl phosphate that yields ATP production (Figure 5.2). The energy increment in parallel with a possible demand of the cell in terms of arginine supply resulted in a win-win situation. This pathway is expressed in *E. faecalis* and is catalysed by the three enzymes arginine deiminase (*arcA*), ornithine carbamoyltransferase (*arcB*) and carbamate kinase (*arcC*) [35].

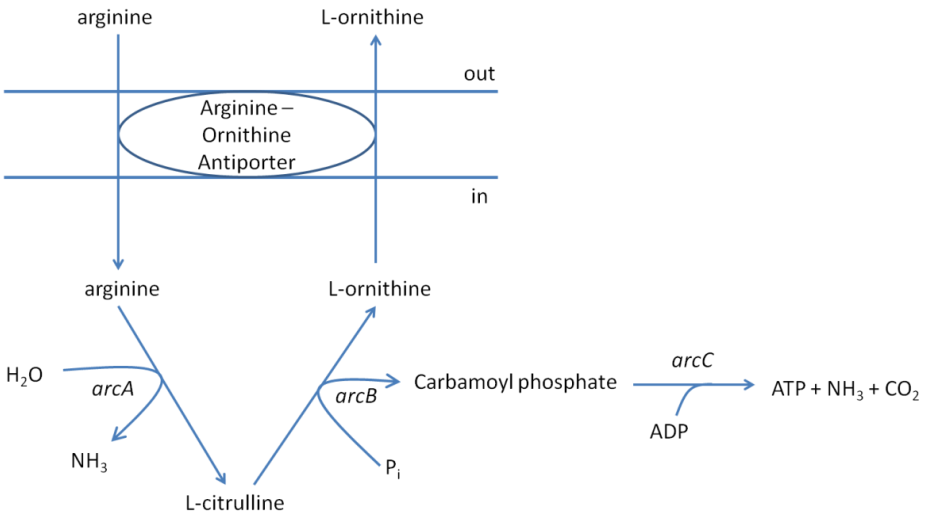

Figure 5.2. Arginine deiminase pathway. An antiporter regulates the antiport movement of arginine and ornithine leading to the formation of the intermediates L-citrulline and carbamoyl phosphate that are further converted to ATP increment. The genes coding for the enzymes involved in this pathway have been characterised for *E. faecalis*. *arcA*, arginine deiminase (3.5.3.6), *arcB*, orninthine carbamoyltransferase (2.1.3.3.) and *arcC*, carbamate kinase (2.7.2.2). Adapted from Gilmore *et al.* (2002) [7].

On the other hand, analysis of tyrosine is less clear since it is being produced solely through 3-(4-Hydroxyphenyl)pyruvate + L-Glutamate <=> L-Tyrosine + 2-Oxoglutarate, and further included in the biomass equation with the remaining being secreted. Most likely, the other participants in the reaction for tyrosine production were required in higher levels and consequently, tyrosine produced in excess was forced to be

secreted into the environment. Similarly, glycine demand is apparently low. The amino acid is being produced in high quantities through Tetrahydrofolate + L-Serine <=> 5,10-Methylenetetrahydrofolate + Glycine + H_2O. Tetrahydrofolate and 5,10-methylenetetrahydrofolate are compounds involved in the pyrimidine metabolism, which is essential to produce building blocks for DNA and RNA synthesis, therefore justifying an elevated flux.

Glucose available was all consumed and had now influence on the phenotypic response of *E. faecalis* to the growing conditions. When glucose was removed from the growth medium, the model was still able to predict growth, however with a much lower specific growth rate (0.08 h^{-1}).

5.3.5 MODELLING THE SHIFT FROM HOMOLACTIC TO HETEROLACTIC FERMENTATION

To further evaluate the capabilities of the genome-scale model, the shift from homolactic to mixed acid fermentation metabolism was simulated. *In vivo*, lactic acid bacteria can carry both types of fermentation, depending on the concentration of the fermentable sugar available or the dilution rate [4,36].

In silico simulations were performed using the environmental conditions described in Mehmeti's *et al*. (2011) work [31]. As it can be seen from simulation D (Table 5.7), when an increase in glucose consumption is imposed to the model (using a constraint that imposes full glucose consumption), the net conversion changes from mixed acid fermentation (as observed in simulation B) into a homolactic fermentation with lactate and acetoin as major end products with yields on glucose of 1.829 $mmol_{lactate}$ / $mmol_{glucose}$ and 0.009 $mmol_{acetoin}$ / $mmol_{glucose}$, respectively. *In vivo*, such phenotypic behaviour results from the regulatory effect caused by an increase of the intermediaries of glucose degradation. As demonstrated in Figure 5.3 an increase of glucose concentration leads to an increase of fructose 1,6 biphosphate (FBP), glyceraldehyde 3-phosphate (G3P) and dihydroacetone phosphate (DHAP). While high intracellular levels of FBP induce lactate dehydrogenase activity, high levels of G3P and DHAP inhibit pyruvate formate-lyase and therefore the flux is redirected towards the formation of mainly lactate and acetoin.

Table 5.7. Simulation D. Homolactic fermentation. All fluxes for metabolites are in mmol/gDW.h and for biomass in h^{-1}.

Environmental conditions	Lower bound	Upper bound
Alanine	-0.260	10000
Arginine	-0.069	10000
Asparagine	-0.073	10000
Aspartate	-0.305	10000
Glutamate	-0.328	10000
Glutamine	-0.132	10000
Glycine	-0.225	10000
Histidine	-0.093	10000
Isoleucine	-0.155	10000
Leucine	-0.350	10000
Lysine	-0.291	10000
Methionine	-0.081	10000
Phenylalanine	-0.161	10000
Proline	-0.561	10000
Serine	-0.313	10000
Threonine	-0.182	10000
Tryptophan	-0.023	10000
Tyrosine	-0.133	10000
Valine	-0.268	10000
Ornithine	0	10000
Cysteine	-0.103	10000
Glucose (mixed acid fermentation)	**-12**	**10000**
Glucose (homolactic fermentation)	**-12**	**-12**
Lactate, Acetoin, Pyruvate, Malate, Acetaldehyde, Ethanol, Formate, Acetate	0	10000
Ammonium	-0.510	10000
Pantothenate	-10000	10000
Citrate	0	0
Sulfate	0	10000
Orotate	-1	10000
Oxygen	0	10000

Net conversion (Mixed Acid Fermentation):
0.33 Ammonium + 0.07 Arginine + 0.07 Asparagine + 0.31 Aspartate + 5.1E04 Biphosphate + 0.05 Cysteine + 0.76 Glucose + 3.7E03 Glutamate + 0.13 Glutamine + 0.23 Glycine + 0.02 Histidine + 0.08 Isoleucine + 0.12 Leucine + 0.10 Lysine + 0.03 Methionine + 5.6E04 Orotate + 0.05 Phenylalanine + 0.03 Proline + 0.31 Serine + 0.08 Threonine + 0.02 Tryptophan + 0.04 Tyrosine + 0.10 Valine => 1.27 Formate + 0.89 Alanine + 0.86 Acetate + 0.23 Ethanol + 3.9E-04 Pantothenate + 3.2E-03 Biomass

Net conversion (Homolactic Fermentation):
0.51 Ammonium + 0.07 Arginine + 0.07 Asparagine + 0.31 Aspartate + 0.00 Biphosphate + 0.05 Cysteine + 12 Glucose + 0.11 Glutamate + 0.13 Glutamine + 0.12 Glycine + 0.02 Histidine + 0.08 Isoleucine + 0.12 Leucine + 0.10 Lysine + 0.03 Methionine + 5.6E-04 Orotate + 0.02 Tryptophan + 0.10 Valine => 21.95 Lactate + 1.72 H2O + 1.04 Pyruvate + 0.51 Hydrogen + 0.49 Threonine + 0.11 Acetoin + 0.07 Proline + 3.9E-04 Pantothenate + 3.2E-03 Biomass.

	Yield (mmol $_{end\ product}$ /mmol $_{glucose}$)	
	Mixed Acid	**Homolactic**
Lactate	-	1.829
Acetate	0.103	0.009
Formate	0.196	-
Ethanol	0.461	-

Lactate is the preferred end product since it regenerates with high efficiency NAD^+ pools to be used in the next round of glucose degradation [37]. *In silico*, the redirection of fluxes to lactate is probably also related with the higher efficiency in terms of NADH regeneration. Although the formation of ethanol could also be neutral in terms of NADH (if the path with formate formation is chosen by the cells), the enzymes involved in the route from pyruvate to ethanol are two instead of one in the case of lactate. Acetate, although energetically more favourable given the fact that ATP is also formed, does not allow to recycle any NADH and therefore is not an option as by-product, unless this is compensated by an equimolar production of acetate and ethanol (this time not producing formate and therefore sinking twice as NADH as lactate) [38]. However, it only makes sense for the cells to exhibit this profile if they are energy limited, i.e., if the bottleneck for biomass formation is the availability of ATP (which would be the case with glucose limitation). When other biosynthetic constituents such as amino acids are limiting (glucose excess), it does not make sense anymore to use longer paths for product excretion [37]. Lactate becomes then the major or only by-product.

It should be emphasised that these conclusions are only valid in strict anaerobic conditions and considering that there are few requirements in terms of reducing equivalents in biosynthesis, i.e., that catabolism and anabolism are to some extent decoupled.

Additionally, experimental observations reported in the literature, also show that *E. faecalis* exhibits an homolactic fermentation by growing cells at a low-culture pH [37]. Since the model considers that metabolites are charge balanced for pH at 7.4, it is not possible to simulate changes in metabolism by varying the pH.

Although the shift between mixed acid fermentation to homolactic fermentation is evident, the biomass value predicted did not change in result of glucose increase. As mentioned previously, amino acids are the limiting factor, therefore conditioning the value of biomass.

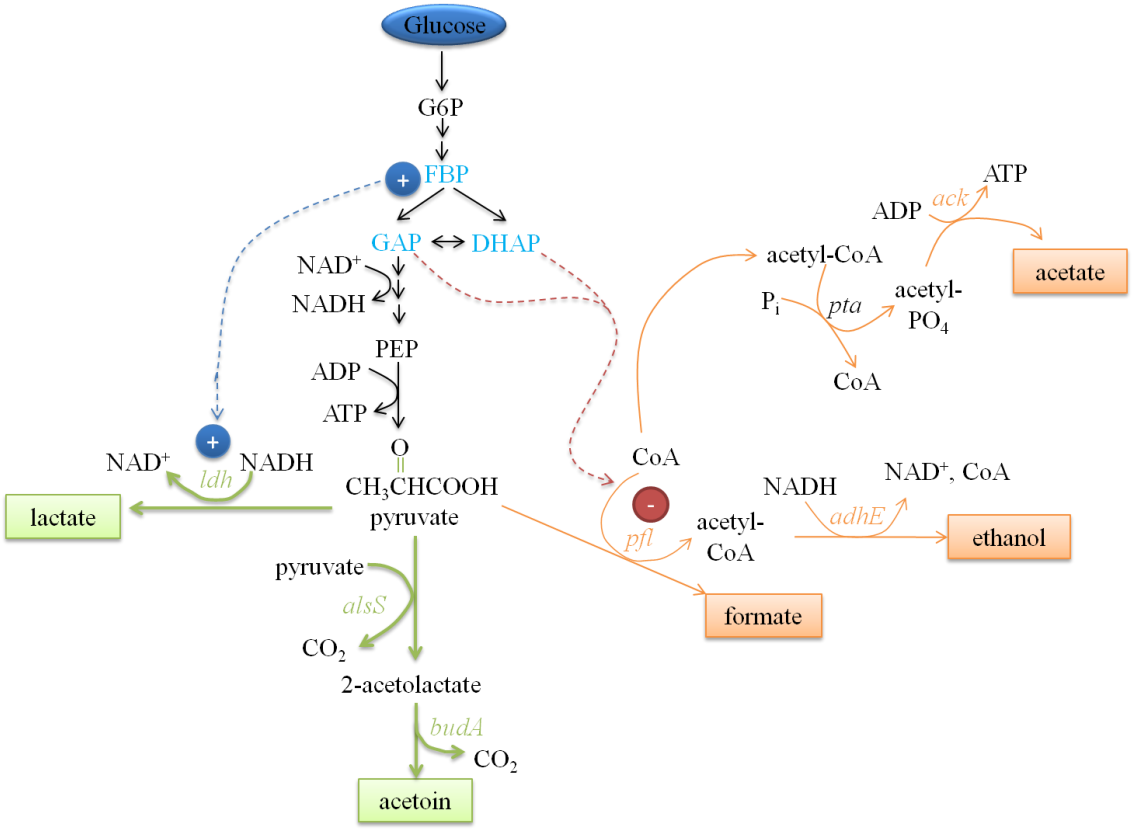

Figure 5.3. Effect of increased glucose concentration on the metabolism of *E. faecalis*. The increased concentration of the intermediates fructose 1,6-biphosphate (FBP) causes an activation of the lactate dehydrogenase (*ldh*) while simultaneous increased levels of glyceraldehyde 3 phosphate (GAP) and dihydroxyacetone phosphate (DHAP) promote the inhibition of formate lyase (*pfl*). G6P, glucose 6 phosphate.

However, if glucose was the limiting factor, an increase of glucose availability would lead to an increase in biomass until a point where amino acids would be the limiting

factor and, as a consequence, glucose would be channelled towards the expected end products again. Interestingly, forcing the model to consume all the glucose available causes an increased consumption of amino acids, but a decreased consumption of the total number of amino acids from the medium. 19 out of 20 amino acids were consumed in the mixed acid fermentation, while only 14 out of 20 amino acids were consumed in homolactic fermentation. The amino acids that were not consumed from the medium were: threonine, proline, serine, tyrosine and phenylalanine. Tyrosine and phenylalanine share a common precursor, chorismate, which is synthesised via the pentose phosphate pathway (PPP). *De novo* synthesis of these metabolites suggests an increase in the flux through the PPP in parallel with the increased glycolytic flux.

On the other hand, the amino acids threonine and proline not only have not been consumed from the medium, but were even secreted to the environment, together with the end products. That observation may be related to the precursors for these two amino acids. Aspartate is the precursor for threonine while glutamate the precursor of proline. Since these two amino acids were consumed (and in the case of glutamate) 30 times more than in mixed acid fermentation, the synthesis of the derivatives amino acids (threonine and proline) is a consequence of the increased consumption of precursors. Thus, if those amino acids were not being incorporated into biomass, they had to be secreted.

Serine precursor is a glycolytic intermediate, 3-phosphoglycerate (3PG). As the glucose consumption increased, the precursors' concentration also increased and consequently, it became energetically more favourable for the cell to synthesise serine from the excess precursor than to consume it from the medium.

Finally, it should be remarked that, although the overall behaviour is predicted, biomass production in this case does not match the experimentally observed values (as mentioned before). If the simulation is performed in conditions C, where the biomass prediction is accurate, the same profile for the by-products would not be obtained (as observed for simulation C, only acetate is formed). This fact is probably related with the need to impose strict constrains for amino acids uptake in simulation C, which is corroborated by the fact that simulation D (where amino acids uptake is defined) originates more consistent results in terms of by-products. However, at this stage and

with no accurate experimental data available, it is not possible to further validate the predictions.

5.3.6 MODELLING THE SHIFT FROM ANAEROBIC TO AEROBIC ENVIRONMENT

As previously mentioned, *E. faecalis* is a facultative anaerobe that normally carries anaerobic fermentation for carbon and energy supply. However, when in the presence of haemin, it expresses a cytochrome *bd* respiratory oxidase capable of carrying aerobic respiration [6].

A conceptualized respiratory system has been described for *E. faecalis* and depends on essential components such as: demethylmenaquinone, cytochrome *bd*, fumarate reductase and F_0F_1-ATPase [7]. The metabolic reactions that mimic the adapted respiratory chain of *E. faecalis* were added to the model based on the predicted respiratory electron transport chain (Table 5.8) [7]:

Table 5.8. Reactions involved in the adapted respiratory system of *E. faecalis*

2-Demethylmenaquinone + NADH + H^+ => 2-Demethylmenaquinol + NAD^+	(a)
Fumarate + 2-Demethylmenaquinol => Succinate + 2-Demethylmenaquinone	(b)
2-Demethylmenaquinol + 0.5 O_2 => 2-Demethylmenaquinone + H_2O	(c)
H^+ ext + ADP + Orthophosphate <=> ATP + H^+ + H_2O	(d)

As shown in Table 5.8, reducing equivalents produced during glycolysis are transferred to demethylmenaquinone through a putative NADH:quinone oxireductase (a). Fumarate reductase and cytochrome *bd* are the terminal demethylmenaquinol oxidases that generate succinate from fumarate (b) and water from oxygen (c), respectively. Cytochrome *bd* translocates one proton per electron to establish a proton motive force and F_0F_1-ATPase couples the proton movement into the cell with ATP formation (d).

Compared to fermentation, respiration provides more ATP and therefore more energy for growth. As it can be observed in simulation E (Table 5.9), analyses were performed

considering the conditions from simulation C (Table 5.6) where the effect of the absence *vs.* presence of oxygen had an evident impact on biomass formation.

The net conversion obtained when the model is in the absence of oxygen and the amino acids requirements are adjusted, leads to a specific growth rate of 0.15 h^{-1}.

When the system is simulated in the presence of oxygen, an increase in the growth rate is observed (0.24 h^{-1}) as expected.

Table 5.9. Simulation E. The effect of oxygen in the phenotypic response of *E. faecalis*. All fluxes for metabolites are in mmol/gDW.h and for biomass in h^{-1}.

Environmental conditions (No Oxygen)	Lower bound	Upper bound
Arginine, Cysteine, Glycine, Histidine, Isoleucine, Leucine, Lysine, Methionine, Threonine, Tryptophan, Tyrosine, Valine	-10	10000
Alanine, Asparagine, Aspartate, Glutamate, Glutamine, Phenylalanine, Proline, Serine	-5	10000
Ornithine	0	10000
Glucose	-12	10000
Acetoin, Pyruvate, Malate, Acetaldehyde, Ethanol, Formate, Acetate, Lactate	0	10000
Ammonium	-10	10000
Orotate	-1	10000
Pantothenate, Citrate, Sulfate	0	10000
Oxygen	0	10000
Environmental conditions (Oxygen)	**Lower bound**	**Upper bound**
Arginine, Cysteine, Glycine, Histidine, Isoleucine, Leucine, Lysine, Methionine, Threonine, Tryptophan, Tyrosine, Valine	-10	10000
Alanine, Asparagine, Aspartate, Glutamate, Glutamine, Phenylalanine, Proline, Serine	-5	10000
Ornithine	0	10000
Glucose	-12	10000
Acetoin, Pyruvate, Malate, Acetaldehyde, Ethanol, Formate, Acetate, Lactate	0	10000
Ammonium	-10	10000
Orotate	-1	10000
Pantothenate, Citrate, Sulfate	0	10000
Oxygen	-10000	10000
Formate	0	0

Net conversion (No Oxygen):
5.00 Alanine + 1.99 Ammonium + 10.00 Arginine + 5.00 Asparagine + 5.00 Aspartate + 0.02 Biphosphate + 2.15 Cysteine + 12 Glucose + 5.00 Glutamate + 5.00 Glutamine + 11.62 H2O

+ 0.96 Histidine + 3.90 Isoleucine + 5.56 Leucine + 4.62 Lysine + 1.60 Methionine + 0.03 Orotate + 5.00 Phenylalanine + 5.00 Proline + 5.00 Serine + 3.58 Threonine + 1.09 Tryptophan + 4.60 Valine => 33.07 Acetate + 19.14 Glycine + 10.14 Ornithine + 0.85 Tyrosine + 0.02 Pantothenate + 0.15 Biomass

Net conversion (Oxygen):
5.00 Aspartate + 5.58 Threonine + 0.04 Biphosphate + 6.08 Isoleucine + 5.00 Glutamine + 1.50 Histidine + 5.00 Serine + 1.85 Proline + 12 Glucose + 3.36 Cysteine + 29.91 O2 + 1.48 Tyrosine + 0.04 Orotate + 7.18 Valine + 10.00 Ammonium + 5.00 Asparagine + 5.73 Arginine + 7.21 Lysine + 2.49 Methionine + 5.00 Glutamate + 5.00 Phenylalanine + 1.70 Tryptophan + 8.68 Leucine + 5.00 Alanine => 43.81 H2O + 0.54 Glycine + 9.90 Acetate + 0.03 Pantothenate + 24.57 Carbon Dioxide + 0.24 Biomass.

	Yield (mmol *end product* /mmol *glucose*)	
	Anaerobic	**Aerobic**
Acetate	2.756	0.825
CO_2	-	2.048

It should be emphasised that, under aerobic conditions, the balance of NADH no longer requires the formation of lactate and ethanol, since the redox balance is obtained from NADH oxidase and NADH peroxidase reactions, and additionally one extra molecule of ATP due to acetate generation is formed.

On the other hand, the flux distribution of this model under anaerobic conditions does not reflect the expected behaviour. Under anaerobic conditions and a high glucose uptake rate a homolactic fermentation pattern would have been expected. However, the major end product obtained was acetate along with the secretion of some amino acids. The reason for this was analysed in deeper detail. Following the flux distribution it was evident that glycolysis was not being used but rather, the pentose phosphate pathway. The reason for this might be related to the enhanced nucleotide precursors biosynthesis required for biomass maximization. Since the production of energy was not coming from the glycolytic pathway, the production of high levels of acetate (from glyceraldehyde 3-phosphate, also produced in pentose phosphate pathway) could compensate that limitation, while NADH pools were being regenerated in different reactions other from the network that also utilise the cofactor.

5.3.7 ESSENTIALITY ANALYSIS

The determination of gene/reactions essentiality was performed using Optflux. The algorithm simulates iterative singe gene deletions to predict which reactions are essential in the system, giving an insight of the impact of the different pathways in the metabolism of the organism.

The *in silico* essentiality prediction is presented on Table 5.10. A complete list of essential reactions is provided in the supplementary material.

Table 5.10. *In silico* prediction of essential reactions for model viability in terms of the pathways involved.

Functional classification	*In silico* prediction
Amino acids	44
Nucleotides	24
Vitamins and cofactors	14
Carbohydrates	9
Cell wall	16
Transport	8
Other	17

As observed, the amino acids, nucleotides, and vitamins and cofactors are the most relevant functional groups in terms of essentiality. That fact is in accordance with *in vivo* experiments since this bacterium is known to be fastidious for amino acids and vitamins [28,29,39]. However, to our knowledge there is no available literature analysing *in vivo* single gene deletions of *E. faecalis* that could be used to verify gene essentiality predictions.

5.4 *CONCLUSIONS*

The first genome-scale model of *E. faecalis* has been reconstructed and aims to serve as a valuable tool for researchers in the medical field and its related applications.

The process of reconstruction is extremely time-consuming and improvement of the information incorporated in the model is an iterative process that relies on new publications allied with this pathogen.

Initially, the draft model consisted of a set of metabolic reactions based on the annotated genome sequence, supplemented with all the available information from online databases and published literature with relevant biochemical and physiological information.

The model was continuously improved for filling gaps, analysing the network for biomass production and further validated by comparison against published data.

The final model consists of a set of 665 reactions, 645 metabolites and 366 ORF, which sums up to a total of just 10% of the whole genome with metabolic properties accounted for in the model.

The capability of *E. faecalis* to grow on different carbon sources *in silico* was confirmed against data published, demonstrating its ability to grow on multiple substrates.

In addition to carbon source utilisation, the minimal growth medium (in terms of amino acids) was defined and should be tested in the laboratory to validate the predictions. Glutamine (or glutamate), histidine, isoleucine, leucine, methionine, tryptophan, and valine were found to be essential and, in the absence of each one of them, *in silico* growth was not possible.

Further validation of the system capabilities included the analysis of the shift from mixed acid fermentation to homolactic fermentation under anaerobic conditions, as well as the shift between aerobic and anaerobic environments.

Table 5.11 – Growth yields of each end product for *E. faecalis* in each of the conditions analysed. The table summarises the overall end products yields in function of the substrate utilised (glucose) in the different conditions analysed.

Table 5.11 – Growth yields of each end product for *E. faecalis* in each of the conditions analysed.

	Aerobic	Anaerobic (Mixed Acid)	Anaerobic (Homolactic)
Lactate	-	-	1.829
Formate	-	1.670	-
Acetate	0.825	1.137	0.009
Ethanol	-	0.310	-
CO_2	2.048	-	-

As observed from the table, the model predicts with accuracy the expected end products. When grown in anaerobic conditions with a low glucose concentration, a typical mixed acid fermentation is observed where formate, acetate, ethanol (and also lactate) are expected. On the other hand, if oxygen is supplied, a shift towards acetate and CO_2 is expected. This shift is due to the existence of an adapted respiratory system that can be activated to balance the cofactors levels. In alternative, specialized reactions such as NADH oxidase (oxygen dependent) are capable of NADH regeneration. On the other hand, when under anaerobic conditions with a high concentration of glucose, the metabolism is switched into a homolactic fermentation, as this is the most efficient pathway for cofactor regeneration. Under those conditions, the extra ATP obtained in acetate formation is no longer needed as the growth rate is being limited by amino acids uptake.

The capabilities of the first genome-scale model have been demonstrated and, as expected, further improvements and refinements should be carried out in order to increase the accuracy of the predictions.

A genome-scale model reconstruction is a continuous process that can lead to an even more powerful tool in terms of predictions. In particular, improvement of the reactions reversibility is in line. Also, the limitation in terms of biomass maximization (when simulating with a chemically defined medium) needs to be further explored. Moreover, accurate measurements concerning the uptake of amino acids need to be performed in order to further validate the predictions in terms of biomass production and product formation.

The present model already predicts the qualitative behaviour of *E. faecalis'* metabolism with some accuracy when the appropriate constrains are included in the model.

From the analysis of the metabolomic data from the previous chapters, relevant information was considered to be added to the model. In particular, some metabolites were detected in our metabolomic data which supported / validated the inclusion of new reactions to feed the genome-scale model. Namely, the presence of glutathione, diverse amino acids such as glutamate, cysteine, pyroglutamate and fatty acids.

When analysing in depth the metabolomics data from the previous chapter, an interesting case was found that, however, could not be contemplated in the metabolic model. The metabolite 2-oxoglutarate, which is known to be an intermediary formed in the TCA cycle and involved in multiple reactions such as amino acid biosynthesis, was found recurrently throughout the datasets. Since *E. faecalis* does not possess a typical TCA cycle it was not expected that 2-oxoglutarate would be identified. However, the detection of this metabolite gave further confirmation of the synthesis of this compound through a yet unknown pathway. Also, ^{13}C labelling experiments showed labelling in glutamate. Considering that this amino acid precursor is precisely 2-oxoglutarate gave even deeper support that *E. faecalis* should somehow synthesise the different intermediates and be able to produce glutamate directly from glucose. However, the identification of the enzymes responsible for the production of 2-oxoglutarate from genome analysis was not possible and therefore decided not to include the reactions that include the synthesis of 2-oxoglutarate from glucose until new laboratory experiments can confirm that capability.

5.5 *REFERENCES*

1. Fisher, K. & Phillips, C. The ecology, epidemiology and virulence of Enterococcus. *Microbiology* **155,** 1749–57 (2009).

2. Liu, M., Nauta, A., Francke, C. & Siezen, R. J. Comparative genomics of enzymes in flavor-forming pathways from amino acids in lactic acid bacteria. *Appl. Environ. Microbiol.* **74,** 4590–600 (2008).

3. Fernández, M. & Zúñiga, M. Amino acid catabolic pathways of lactic acid bacteria. *Crit. Rev. Microbiol.* **32,** 155–83 (2006).

4. Moat, A. G., Foster, J. W. & Spector, M. P. in *Microb. Physiol.* 412–433 (2002).

5. Mccoy, T. A. & Wender, S. H. Some factors affecting the nutrional requirements of *Streptococcus faecalis*. *J. Biol. Chem.* **65,** 660–665 (1953).

6. Winstedt, L., Frankenberg, L., Hederstedt, L. & von Wachenfeldt, C. *Enterococcus faecalis* V583 contains a cytochrome bd-type respiratory oxidase. *J. Bacteriol.* **182,** 3863–6 (2000).

7. Gilmore, M. S. *The Enterococci: pathogenesis, molecular biology, and antiobiotic resistance*. *ASM Press* 133–175 (ASM Press, 2002).

8. Edwards, J. S. Systems Properties of the *Haemophilus influenzae* Rd Metabolic Genotype. *J. Biol. Chem.* **274,** 17410–17416 (1999).

9. Liao, Y.-C. *et al.* An Experimentally Validated Genome-Scale Metabolic Reconstruction of *Klebsiella pneumoniae* MGH 78578, iYL1228. *J. Bacteriol.* **193,** 1710–1717 (2011).

10. Fang, X., Wallqvist, A. & Reifman, J. Development and analysis of an in vivo-compatible metabolic network of *Mycobacterium tuberculosis*. *BMC Syst. Biol.* **4,** 160 (2010).

11. Charusanti, P. *et al.* An experimentally-supported genome-scale metabolic network reconstruction for *Yersinia pestis* CO92. *BMC Syst. Biol.* **5,** 163 (2011).

12. Feist, A. M., Herrgård, M. J., Thiele, I., Reed, J. L. & Palsson, B. Ø. Reconstruction of biochemical networks in microorganisms. *Nat. Rev. Microbiol.* **7,** 129–43 (2009).

13. Schilling, C. H. & Palsson, B. O. The underlying pathway structure of biochemical reaction networks. *Proc. Natl. Acad. Sci. U. S. A.* **95,** 4193–8 (1998).

14. Kanehisa, M., Goto, S., Kawashima, S., Okuno, Y. & Hattori, M. The KEGG resource for deciphering the genome. *Nucleic Acids Res.* **32,** D277–80 (2004).

15. Dias, O., Rocha, M., Ferreira, E. & Rocha, I. Merlin : Metabolic Models Reconstruction using Genome-Scale Information. 120–125 (2010).

16. Schomburg, I., Chang, A. & Schomburg, D. BRENDA, enzyme data and metabolic information. *Nucleic Acids Res.* **30,** 47–9 (2002).

17. Apweiler, R. *et al.* UniProt: the Universal Protein knowledgebase. *Nucleic Acids Res.* **32,** D115–9 (2004).

18. Caspi, R. *et al.* MetaCyc: a multiorganism database of metabolic pathways and enzymes. *Nucleic Acids Res.* **34,** 511–6 (2006).

19. Thiele, I. & Palsson, B. Ø. A protocol for generating a high-quality genome-scale metabolic reconstruction. *Nat. Protoc.* **5,** 93–121 (2010).

20. Booth, I. R. Regulation of cytoplasmic pH in bacteria. *Microbiol. Rev.* **49,** 359–378 (1985).

21. Schellenberger, J., Park, J. O., Conrad, T. M. & Palsson, B. Ø. BiGG: a Biochemical Genetic and Genomic knowledgebase of large scale metabolic reconstructions. *BMC Bioinformatics* **11,** 213 (2010).

22. Flamholz, A., Noor, E., Bar-Even, A. & Milo, R. eQuilibrator-the biochemical thermodynamics calculator. *Nucleic Acids Res.* **40,** D770–5 (2012).

23. Schomburg, I. *et al.* BRENDA, the enzyme database: updates and major new developments. *Nucleic Acids Res.* **32,** 431–3 (2004).

24. Oliveira, A. P., Nielsen, J. & Förster, J. Modeling *Lactococcus lactis* using a genome-scale flux model. *BMC Microbiol.* **5,** 39 (2005).

25. Rocha, I. *et al.* OptFlux: an open-source software platform for *in silico* metabolic engineering. *BMC Syst. Biol.* **4,** 45 (2010).

26. Orth, J. D., Thiele, I. & Palsson, B. Ø. What is flux balance analysis? *Nat. Biotechnol.* **28,** 245–8 (2010).

27. Greenhut, I. T., Shweigert, B. S. & Elvehjem, C. A. The amino acid requirements of *Streptococcus faecalis* and the use of this organism for the determinations of threonine in the natural products. *J. Biol. Chem.* 69–76 (1946).

28. Aakra, Å., Nyquist, O. L., Snipen, L., Reiersen, T. S. & Nes, I. F. A survey of genomic diversity in *Enterococcus faecalis* by microarray based comparative genomic hybridization. *researchgate.net*

29. Khan, H., Flint, S. H. & Yu, P.-L. Development of a chemically defined medium for the production of enterolysin A from *Enterococcus faecalis* B9510. *J. Appl. Microbiol.* **114,** 1092–102 (2013).

30. Zhang, G., Mills, D. A. & Block, D. E. Development of chemically defined media supporting high-cell-density growth of lactococci, enterococci, and streptococci. *Appl. Environ. Microbiol.* **75,** 1080–7 (2009).

31. Mehmeti, I., Faergestad, E. M., Bekker, M., Nes, I. F. & Holo, H. Growth Rate-Dependent Control in *Enterococcus faecalis* : Effects on the Transcriptome and Proteome, and Strong Regulation of Lactate. (2011).

32. Mendz, G. L. & Hazell, S. L. Amino acid utilisation by *Helicobacter pylori*. *Int. J. Biochem. Cell Biol.* **27,** 1085–93 (1995).

33. Snoep, J. L., Mattos, M. J. T. de, Postma, P. W. & Neijssel, O. M. Involvement of pyruvate dehydrogenase in product formation in pyruvate-limited anaerobic chemostat cultures of *Enterococcus faecalis* NCTC 775. 50–55 (1990).

34. Driessen, A. J. M. & Smid, E. J. Transport of diamines by *Enterococcus faecalis* is mediated by an agmatine-putrescine antiporter. 4522–4527 (1988).

35. Simon, J., Wargnies, B. & Stalon, V. Control of enzyme synthesis in the arginine deiminase pathway of Streptococcus Control of Enzyme Synthesis in the Arginine Deiminase Pathway of *Streptococcus faecalis*. (1982).

36. Snoep, J. L., Graef, mark R. De, Mattos, M. J. T. de & Neijssel, O. M. Pyruvate catabolism during transient state conditions in chemostat cultures of Enterococcus faecali pyruvate concentrations and NADHlNAD ratios. (1992).

37. Snoep, J. L., de Graef, M. R., Teixeira de Mattos, M. J. & Neijssel, O. M. Pyruvate catabolism during transient state conditions in chemostat cultures of *Enterococcus faecalis* NCTC 775: importance of internal pyruvate concentrations and NADH/NAD+ ratios. *J. Gen. Microbiol.* **138,** 2015–20 (1992).

38. Cocaign-bousquet, M., Garrigues, C., Loubiere, P. & Lindley, N. D. Physiology of pyruvate metabolism in *Lactococcus lactis*. *Antonie Van Leeuwenhoek* **70,** 253–267 (1996).

39. Aakra, A., Nyquist, O. L., Snipen, L., Reiersen, T. S. & Nes, I. F. Survey of genomic diversity among *Enterococcus faecalis* strains by microarray-based comparative genomic hybridization. *Appl. Environ. Microbiol.* **73,** 2207–17 (2007).

CHAPTER 6

GENERAL CONCLUSIONS AND FUTURE WORK

The work developed during this PhD project aimed to understand the impact of oxidative stress on the metabolism of *Enterococcus faecalis* cells. Vancomycin resistant and sensitive strains of *E. faecalis* were subjected to different stress conditions such as oxygen, hydrogen peroxide and dilution rate and their metabolic response was analysed using metabolomic approaches. Additionally, during the course of this project the first genome-scale metabolic model of *E. faecalis* was reconstructed to support the integration of the high-throughput data, as well as to serve as a tool that compiled all the metabolic information concerning this pathogen. Hopefully, this will allow the researchers to explore and perform different *in silico* simulations that could support new experimental design or answer a new level of questions concerning *E. faecalis* metabolism.

The mechanisms of resistance towards different sources of oxidative stress give this organism a survival advantage towards other bacteria. The deep understanding of the metabolic modulation of *E. faecalis* is therefore important. The consequences of oxidative stress and their ultimate impact on the cells have been explored along this thesis.

Particularly, in chapter 2, we analysed how different sources of oxidative stress or perturbations such as hydrogen peroxide, oxygen and dilution rate could potentiate the stress response of a vancomycin sensitive strain. Results indicate a different modulation of the network in response to different factors. Summing up, analysis of the oxidative stress response of *E. faecalis* to different factors indicates that:

- The response is highly dependent on its growth status and environmental conditions.
- A redistribution of the carbohydrate flux through the pentose phosphate pathway seemed to be the strategy adopted by *E. faecalis* in an effort to drive NADPH generation as a consequence of the effect exerted by H_2O_2.
- The methionine sulfoxide reductase mechanism, which is highly efficient in scavenging free radicals and is involved in fighting oxidative stress in other organisms, seemed to also be active in *E. faecalis*.
- Interestingly, the overall behaviour observed for citrate led to hypothesise the role of citrate as a chelating agent (that binds to free iron), thus preventing the Fenton reaction. Results suggest that its increased levels intracellularly may be related to this antioxidant mechanism.
- It was also observed that, when *E. faecalis* attained a slower growth rate, it also exhibited an enhanced tolerance to H_2O_2 perturbations. It is known that a lower dilution rate is related to a limitation of nutrients, which *per se,* may be a form of stress. Hence, when another stress was present, such as H_2O_2, its effect was minored.
- Intracellular and extracellular levels of benzoic acid suggested that this compound may play a role in the response to oxygen and was further explored in chapter 4.
- The utilisation of an untargeted approach has also allowed us to identify metabolites that have not been previously documented in prokaryotes such as 4-aminobutyric acid. Their known participation during cellular response to oxidative stress in eukaryotes may suggest a similar, but yet uncharacterised role in *E. faecalis* defence mechanism.

The overall results indicated that both O_2 and H_2O_2 were in fact causing agents of oxidative stress, while the dilution rate response appeared to be a consequence of the increased fluxes in the cells (i.e., due to increased nutrients availability). Although similarities in terms of the metabolic response between the two stress agents were observed, the effect of H_2O_2 was lowered when in the presence of O_2. Given this conclusion, and in order to explore other ways by which *E. faecalis* could cope with

oxidative stress, only O_2 was used as stress agent in the next study. A low dilution rate was chosen as it resembles the natural environment where *E. faecalis* is usually found (i.e., the human gut).

Hence, in chapter 4 we looked at the metabolic changes imposed by oxygen pressure. Also, to understand if the effect of vancomycin would be somehow related to oxidative stress as for its *peers* antibiotics, as well as to understand if a resistant strain is more or less susceptible to oxidative stress, a vancomycin resistant strain was used. For that, we analysed samples from both the long term effect of oxygen (during steady state) and samples taken during the rapid transition from an anaerobic environment to aerobic stress. The consequences of an imposed stress on the lipid membrane were analysed. Being the membrane fatty acids susceptible targets, their modulation in response to the presence and absence of oxygen and vancomycin was determined. Additionally, the demethylmenaquinone levels were measured in the presence and absence of oxygen. As an aerotolerant microbe, *E. faecalis* has developed mechanisms to cope with the oxidative stress present in an aerobic environment.

The main observations from this chapter were:

- A drive of cellular metabolism towards glutathione production was hypothesised as the first line defence in response to oxygen.

- Oxygen input also seemed to cause an up-regulation of sulphur metabolism from where cysteine can be generated. This is a critical compound for the cysteine-rich proteins such as thioredoxin or other compounds such as thiamine and coenzyme A all known to be involved in the fight against oxidative stress.

- In aerobic conditions, an increasing glycolytic flux seemed to occur to drive energy formation through NADH oxidation in the adapted respiratory chain.

- The up-regulation of the glycolytic pathway also served to increase the pools of important intermediates in glutathione production, such as glycine.

- Labelling in free glutamate was an interesting observation, as it indicates that glutamate was *de novo* synthesised from glucose, despite no previous evidence

has been found of *E. faecalis* expressing a TCA cycle, where the precursors for glutamate are produced. Therefore, it is hypothesised that *E. faecalis* is capable of synthesising glutamate, probably via a yet undescribed metabolic pathway.

- Up-regulation of the fatty acids metabolism, with increased production of both unsaturated and saturated fatty acids (all known to have roles as antioxidant compounds) was also observed in response to oxygen.

- A similar response was observed when cells were exposed to vancomycin, raising the question if vancomycin bactericidal effect is indeed also causing oxidative stress or if the oxidative stress was only being caused by the presence of oxygen.

- Benzoate is an intermediate metabolite involved in the synthesis and catabolism of aromatic compounds, including aromatic amino acids which are also involved in the synthesis of ubiquinone (demethylmenaquinone in *E. faecalis*). Its altered levels seem to be related to the demethylmenaquinone altered levels in response to oxygen.

- Both the fatty acid and demethylmenaquinone metabolism may represent the final downstream changes induced by oxygen exposure.

Overall, metabolomics has been a vital endeavour in this approach by building up comparative metabolite profiles under different stress conditions and has proven to be an interesting strategy in unravelling new key aspects of the *E. faecalis* metabolism. The different metabolic responses are of major importance as the shift and inherent mechanisms confer the organism with an ecological advantage towards other bacteria.

On the fifth chapter we aimed at compiling all the obtained knowledge from the wet experiments with the available literature and genome sequence information and use it to build the first genome-scale metabolic model of *E. faecalis*. We expect this mathematical tool may serve the scientific panorama, especially those working in the medical field.

The final model consists of a set of 665 reactions and 645 metabolites catalysed by 366 ORF, which sums up to a total of 10% of the whole genome.

It was possible to test different simulation environments and confirm the model capabilities to

- Predict the changes in metabolism associated with aerobiosis/anaerobiosis.
- Predict the shift in the metabolism caused by excess or limitation of the main carbon source, leading to a homolactic or mixed acid fermentation, respectively.
- The type of by-products formed is related to the needs of the cell in terms of ATP production but also of NADH regeneration.
- A list of the reactions essentiality was determined and could be used to further explore possible interesting targets.
- The metabolomics data gathered gave new insights to be further explored using the generated model particularly in the analysis of the *de novo* biosynthesis of amino acids from glucose such as glutamate. Moreover, several of the identified metabolites in our datasets were used for validation/confirmation of reactions included in the network.

Nevertheless, the capabilities of the generated model should be further explored, improved and refined in order to increase the accuracy of the predictions. As expected, a genome-scale model reconstruction is an endless process that can lead to an even more powerful tool in terms of predictions.

In the near future, the question raised concerning the capabilities of the *de novo* biosynthesis of glutamate will be deeply analysed and further experiments in order to identify possible missing enzymes to link this pathway will be designed.

Additionally, data already generated in our lab comprise experiments where a vancomycin resistant strain (from which the vancomycin sensitive strain was derived) was grown in the absence of the antibiotic but further subjected to external oxidative stress. These data will be analysed and discussed and compared to the vancomycin sensitive strain.

Furthermore, another experiment that could be interesting to run would be to grow the sensitive strain with a lower dose of vancomycin (under the minimal inhibition concentration level) and analyse its metabolic profile and compare it with the response of a vancomycin resistant strain.

The generated data can further clarify if indeed vancomycin also induces oxidative stress as most of the common bactericidal antibiotics do and the mechanisms elicited in the metabolism that could be further used to design adjuvant drug targets.

In terms of the generated model, it will continuously be refined and optimised iteratively, to ensure it can predict more accurately quantitative values of end products formation and simulate with higher accuracy other metabolic phenotypes.

Also, the *in vivo* flux distributions of the central carbon metabolism of *E. faecalis* will be calculated using ^{13}C-labelling experimental data already generated in New Zealand and using software being developed in house. These data will be essential to perform the final steps of model validation.

Finally, the model will be used to perform optimisations that aim for new possible oxidative stress targets.

SCIENTIFIC OUTPUT

Outcome manuscripts from thesis chapters

Portela, C., Smart, K.F., Tumanov, S., Cook, G. M., Villas-Bôas, S.G., The global metabolic response of a vancomycin-resistant *Enterococcus faecalis* strain to oxygen. *Antimicrobial Agents and Chemotherapy*. (Submitted).

Portela, C., Liu, C-H. T., Ferreira, E.C., Rocha, I., Cook, G. M.,Villas-Bôas, S.G., A metabolomics analysis of *Enterococcus faecalis* response to oxidative stress – the effect of hydrogen peroxide, oxygen and dilution rate. (To be submitted).

Portela, C., Vilaça, P., Villas-Bôas, S.G., Ferreira, E.C., Rocha, I., Genome-scale metabolic network of the pathogen *Enterococcus faecalis* V583. (To be submitted).

Oral communications

Portela, C., Villas-Bôas, S.G., Ferreira, E.C., Rocha, I., Metabolic network reconstruction of the pathogen *Enterococcus faecalis*, *Joint meeting of the NZ Microbiological Society and NZ Society for Biochemistry & Molecular Biology: Small things, BIG ideas*, Auckland, New Zealand, 30th November-3rd December 2010.

Portela, C., Villas-Bôas, S.G., Ferreira, E.C., Rocha, I., Metabolic network reconstruction of the pathogen *Enterococcus faecalis*, *NZMS 2011 Annual Conference - Right Here Right Now*, Palmerston North, New Zealand, 22nd November – 24th November 2011.

Portela, C., Villas-Bôas, S.G., Ferreira, E.C., Rocha, I., "Super model of the world" – *Enterococcus faecalis*, *8th International Conference of the Metabolomics Society*, Washington DC, United states; 25th June – 28th June 2012.

Portela, C., Villas-Bôas, S.G., Ferreira, E.C., Rocha, I., Genome scale network reconstruction of the pathogen *Enterococcus faecalis*, *Computer applications in biotechnology*, Mumbai, India; 16th December – 18Th December 2013.

Papers in conference proceedings

Portela, C., Villas-Bôas, S.G., Ferreira, E.C., Rocha, I., "Super model of the world" – *Enterococcus faecalis*, *8th International Conference of the Metabolomics Society*, Washington DC, United states; 25th June – 28th June 2012.

Portela, C., Villas-Bôas, S.G., Ferreira, E.C., Rocha, I., Genome scale network reconstruction of the pathogen *Enterococcus faecalis*, *Computer applications in biotechnology*, Mumbai, India; 16th December – 18th December 2013.

Abstracts in conference proceedings

Portela, C., Villas-Bôas, S.G, Rocha, I., Ferreira, E.C., *In vivo* metabolic pathway analysis of pathogenic bacteria to identify new drug targets, *Semana da Engenharia 2009*, Guimarães, Portugal; 20th-23rd October 2009.

Portela, C., Carneiro, S., Villas-Bôas, Lourenço, A., S.G, Rocha, I., Ferreira, E.C., Metabolic network reconstruction of the pathogen *Enterococcus faecalis*, *Jornadas de Bioinformática 2009*, Lisboa, Portugal, 3rd-6 th November 2009.

Portela, C., Villas-Bôas, S.G, Rocha, I., Ferreira, E.C., Genome-scale metabolic network of the central carbon metabolism of *Enterococcus faecalis*, *2nd Australasian Symposium on Metabolomics*, Melbourne, Australia; 30th September-5th October 2010.

Portela, C., Villas-Bôas, S.G., Ferreira, E.C., Rocha, I., Genome-scale metabolic network of the pathogen *Enterococcus faecalis*, *Fifth annual workshop on the business-Government interface: Workshop in systems and synthetic biology*, Braga, Portugal, 6th June 2011.

Portela, C., Villas-Bôas, S.G., Ferreira, E.C., Rocha, I., Genome-scale metabolic network of the pathogen *Enterococcus faecalis*, *10th Symposium on Lactic acid bacteria – 30 years of LAB research*, Egmond Aan Zee, The Netherlands; 28th August – 1st September 2011

SUPPLEMENTARY MATERIAL

All supplementary material was made available for further consultation.

Under the files:

"S1:GEM *E. faecalis* V583 SupplementaryMaterial.xlsx" – the excel file contains all the reactions included in the GEM of *E. faecalis*, the enzymes that codify for each reaction, the gene association and the subsystem the reaction belongs to, the source of information and the reference when appropriate.

"S2:GEM *E. faecalis* V583.xlm" – SBML file of the GEM of *E. faecalis* for further analysis and simulations.